Use of a human cell model of Tuberous sclerosis complex (TSC) for study of neuroinflammation and neuronal dysfunction in dementia

A thesis presented for the award of

Doctor of Philosophy

Laura Katharina Kleckner

December 2022

Supervisors: Prof. Adrian Harwood, Prof. Andrew Tee
Assessor: Prof. Emyr Lloyd-Evans

Acknowledgements

First, I would like to thank my supervisors Professor Adrian Harwood and Professor Tee for the guidance and advice throughout this project. I have deeply enjoyed working with them in this supportive environment. Next, I would like to thank the Harwood group for their help and support throughout the last four years. Thank you answering my questions, giving me advice, and discussing results as well as helping to troubleshoot. Thank you for making the work environment so enjoyable. I would especially thank Gemma Wilkinson for teaching me cell culture techniques, as I was previously a complete novice to cell work. Thanks to Mouhamed Alsaqati on advising me many times on experiments and trouble shooting. I would like to thank Karolina Dec for teaching me the RT-PCRs and the astrocyte differentiation. I would also like to thank Jamie Wood and Jo Haddon for their insight on troubleshooting as well as their advice. Furthermore, I would like to thank Shane Wainwright for making even the less enjoyable parts of experiments very funny. Also, I would like to thank Professor Emyr Lloyd-Evans for offering me access to the calcium imaging. Additional thanks to Emma Dalton and all the technicians for the smooth running of the lab during these tumultuous times.

I would also like to thank my family and friends, for their support over the last few years. Their support was fantastic during these last few years. Additional thanks to Liz Loveridge, for helping me to stay calm and fight through all obstacles.

A final thanks to the DRI for funding this project and Ph.D.

Table of Contents

List of Figures

List of abbreviations

AA	Amino acids
Aβ	Amyloid beta
AD	Alzheimer´s Disease
ADHD	Attention Deficit-Hyperactivity Disorder
AMPK	AMP-activated protein kinase
ASD	Autism spectrum Disorder
BBB	Blood brain barrier
Ca^{2+}	calcium
Cas	Caspase
CDK5	cyclin-dependent kinase 5
CNS	central nervous system
crRNA	CRISPR RNA
DSBs	DNA double-stranded breaks
ER	Endoplasmic reticulum
ERM	Ezrin, radixin and moesin
GAP	GTPase activating protein
GLT	Glutamate transporters
gRNA	Guide RNA
GSK3	Glycogen synthase-Kinase 3
HDR	Homology directed repair
HGF	Hepatocyte Growth Factor
ID	Intellectual disability
IGF1	insulin like growth factor 1
iPSC	Induced pluripotent stem cells
K^{+}	Kalium
LAM	Lymphangioleiomyomatosis
LTD	long-term depression
LTP	late-phase long-term potentiation
MAP	microtubule-associated protein

mTOR	mammalian target of rapamycin
mTORC1	mammalian target of rapamycin complex 1
mTORC2	mammalian target of rapamycin complex 2
NFkB	Nuclear factor kappa-light-chain-enhancer of activated lls
NFT	neurofibrillary tangles
NHEJ	Non-homologous end joining
NMDAR	N-methyl-D-aspartate receptor
NPCs	Neural progenitor cells
NSCs	Neuronal stem cells
PAI-1	Plasminogen activator inhibitor 1
PAM	Protospacer Adjacent Motif
PKC	protein kinase C
PP5	protein phosphatase 5
Raptor	regulatory-associated protein of mTOR
Rheb	Ras homologue enriched in brain
RAs	renal angiomyolipoma
Rictor	rapamycin-insensitive companion of mTOR
S6K1	Ribosomal protein S6 kinase beta-1
SEGA	subependymal giant cell astrocytoma
SERPIN	Serine Protease Inhibitors
shRNA	Small hairpin RNA
TALEN	transcription activator–like effector nuclease
TFEB	Transcription Factor EB
tPA	tissue plasminogen activator
tracrRNA	trans-activating crRNA
TSC	Tuberous sclerosis complex
TSC1	Tuberous sclerosis complex 1
TSC2	Tuberous sclerosis complex 2
TUB	Tubers
uPA	urokinase-type plasminogen activator
uPAR	urokinase-type plasminogen activator receptor

VOCC	Voltage operated calcium channels
ZFN	zinc-finger nuclease

Abstract

Tuberous sclerosis complex (TSC) is caused by mutations in the genes *TSC1* or *TSC2* and is a rare genetic disorder. These mutations result in loss of function of the respective gene, thus leading mammalian target of rapamycin complex 1 (mTORC1) overactivity. TSC is a multi-organ disorder with known comorbidities such as glia tumours, epilepsy, autism spectrum disorder (ASD) or psychiatric disorders. Despite this, it is still unknown what molecular and developmental changes are occurring in the patient brain. Alzheimer's Disease (AD) is neurodegenerative disease and the most common form of dementia. Literature research suggests that similar molecular pathways are dysregulated in both AD and TSC and this project is aiming to identify commonalities in the developmental, autophagy and inflammation related markers. Human induced pluripotent cells (iPSCs) enable human astrocytes and neurons to be cultured *in vitro*, thereby circumventing developmental and genetic differences of an animal model compared to humans, and they allow the generation of neurons and astrocytes; cell types which are otherwise inaccessible from humans due to major ethical concerns unless post-mortem. By using two CRISPR-based techniques CRISPR-Cas9 and CRISPR-Cas13a systems, both knockout and knockdown models for TSC1 were generated. These cell lines underwent neuronal differentiation to identify changes in developmental and autophagy markers similar to AD and a database analysis of TSC patients identified further target genes/pathways which were common between both disorders. The TSC1 cell models were used to generate neurons to investigate the effect of TSC1 loss on neuronal development. While the knockout model creates a chronic loss of TSC1, the knockdown model enabled controlled reduction of TSC1 mRNA at different timepoints of development for brief periods. Expression of developmental, inflammation, autophagy and urokinase pathway marker genes were tested at different timepoints of the neuronal development. Astrocytes generated from Cas13 cells, where the TSC1 knockdown was induced at different levels, demonstrated excitotoxicity as well as dysregulated calcium signalling. The dysregulation of the analysed marker genes seen in both TSC1 models is consistent to that previously reported in both TSC and AD, strengthening the overlap between both disorders. Overall, both TSC1 cell models displayed significant dysregulation of markers throughout the development, demonstrating the importance of TSC1 expression for neuronal differentiation as acute loss caused significant dysregulation for weeks after the treatment. As these dysregulated markers align with observed AD pathology, this strengthens the hypothesis of that the TSC pathway will be an interesting target for future AD research and potential treatment.

1. General Introduction

1.1. Overview

TSC is a genetic disorder derived from heterozygous and dominant mutations in the causative TSC genes (*TSC1* and *TSC2*). The birth incidence is around 1:6000-1:10000, leading to an estimated number of 1 million affected individuals worldwide, involving all racial and ethnic groups (Franz *et al.* 2010). Characteristically, TSC affects several organs throughout the body, causing abnormalities of the skin, brain, kidney, heart, and lungs (Northrup *et al.* 2018). Since several organs are affected by TSC, the disease has several comorbidities; especially neurological ones. Studies have shown that impaired autophagy is part of the TSC phenotype, a consequence of mTORC1 overactivity (Rosset *et al.* 2021), thus leading to the suggestion to count TSC as a neurodegenerative disease (Di Nardo *et al.* 2014). AD, a common neurodegenerative disease, was found to display altered expression of TSC and mTORC1 overactivity (Caccamo *et al.* 2013; Wang *et al.* 2013; Cai *et al.* 2015), thus identifying TSC1 and TSC2 as potential treatment targets for AD (Ferrando-Miguel *et al.* 2005). Studies have shown abnormal neuronal development of TSC cells, highlighted by the dysregulation of NPC and neuronal markers, several of which are also known to be dysregulated in AD. Therefore, the gene expression of these markers was analysed in both TSC1 CRISPR- Cas9 and CRISPR-Cas13a cells in an attempt to identify both sensitive timepoints in neuronal development as well as the effect TSC1 loss has as the majority of studies focuses on TSC2, since its mutations are more common in patients (Jones *et al.* 1999). Consistent with literature, a database analysis of TSC patients demonstrated a significant upregulation of inflammation related genes, several of which also align with AD. Upregulation of several AD-related genes in the TSC patients was found. The database analysis highlighted two targets, which were then analysed in both TSC1 cell lines during this project: inflammation related genes and SERPING1, a member of the urokinase pathway. The latter was investigated under a collaboration with Prof. Maija Castren from the University of Helsinki.

Furthermore, as glutamate excitotoxicity has been established in both TSC and AD, the aim was to identify if acute TSC1 loss in astrocytes would also demonstrate that phenotype or if TSC loss needs to occur during the development of the cells (Wong *et al.* 2003; Zeng *et al.* 2007; González-Reyes *et al.* 2017).

1.2. Genetic background of Tuberous Sclerosis Complex (TSC)

TSC occurs due to a dominant inactivating mutation in either the *TSC1* gene (coding for the protein Hamartin, identified in 1997) (Van Slegtenhorst *et al.* 1997) or the *TSC2* gene (coding for Tuberin, identified in 1993) (Consortium 1993). Both the Hamartin and Tuberin protein were renamed to TSC1 and TSC2, respectively. Both TSC1 and TSC2 protein interact to form a complex responsible for inhibiting the small GTPase protein, Ras homologue enriched in brain (Rheb), to control the activity of mTORC1 (Zhang *et al.* 2003). mTOR is a highly conserved protein kinase regulating protein synthesis, cellular metabolism, cell differentiation and growth as well as cell migration. There are two different mTOR complexes which differ in function. mTORC1 has a cofactor known as regulatory-associated protein of mTOR (Raptor) which activates the protein kinase domain of mTOR leading to an increased mRNA transcription and protein synthesis (Franz *et al.* 2010). The other mTOR complex is called mTORC2 and its cofactor rapamycin-insensitive companion of mTOR (Rictor). The activity of the mTORC2 kinase complex is unaffected by Rheb, and regulates protein synthesis separately from mTORC1 (Zhang *et al.* 2003). TSC1/TSC2 functions as a GTPase activating protein (GAP) towards Rheb to convert active GTP-bound Rheb to an inactive GDP-bound Rheb. Rheb-GTP is necessary for activation of mTORC1. Therefore, in the absence of TSC1/TSC2, Rheb becomes GTP-bound, driving mTORC1 hyper-activation, thus causing abnormal cellular proliferation and differentiation, thereby producing the hamartomatous lesions of TSC. Absence of TSC complex causes hyperactivation of mTORC1 which when turns insensitive to growth factor stimulation while remaining responsive to changes in amino acids (AA) levels (Menon *et al.* 2014).

1.3. Comorbidities of Tuberous Sclerosis Complex

Since several organs throughout the body are affected by TSC, the disease has several comorbidities; especially neurological ones. The first, most frequent comorbidity is epilepsy (in over 80% of the affected TSC individuals), a common chronic neurological disorder characterized by recurrent unpredictable seizures (Chong *et al.* 2010). The mTOR signalling pathway is implicated in TSC epilepsy. Mutations of *TSC1* and *TSC2* that act upstream of the mTOR lead to a high incidence of the neurological disorder (Waltereit *et al.* 2006). Rapamycin treatment that inhibits the mTOR pathway alleviates structural abnormalities and reduces seizures in TSC mouse models (Zeng *et al.* 2008), suggesting that the overactive mTOR expression interferes with normal brain development and leads to epilepsy. Another comorbidity of TSC is ASD, affecting up to 25% of patients (Gipson *et al.* 2013). However, the risk factors for ASD in the TSC population are still controversial. Epilepsy is considered as a potential risk factor for ASD in TSC patients, especially when epilepsy starts early and with infantile spasms (Gipson *et al.* 2013). Several reports have indicated infantile spasms as indicators for developing autism in children with TSC (Gutierrez *et al.* 1998; Kaczorowska *et al.* 2011). The localization of cortical tubers was identified as another risk factor for developing ASD in TSC patients, as tubers in the frontal and temporal cortex were associated with ASD (Numis *et al.* 2011). Finally, intellectual disability (ID) is considered a comorbidity for ASD in patients with TSC (Gutierrez *et al.* 1998; Van Eeghen *et al.* 2013). Noteworthy, studies about potential ASD genes have shown that *TSC2* mutations seem to be frequently associated with ASD, regardless the mutation type (Numis *et al.* 2011). Other psychiatric disorders like Anxiety Disorders (PTSD, panic disorder or Anxiety), ADHD or behavioural disorders (like self-harm or obsessive-compulsive behaviour) are also common among TSC patients (Chung *et al.* 2011). Furthermore, there have been reports that patients with TSC have a phenotypic overlay with frontotemporal dementia (Liu et al. 2020) while a cohort study of TSC patients in Taiwan found dementia as a reoccurring comorbidity (Hong et al. 2016). Thus, an increased risk for neurodegenerative diseases in TSC patients could be assumed.

1.4. Effect of TSC on neurons and their development

As described previously, TSC demonstrates a variability of neuronal and cognitive deficits in patients. Patients with mutations in either *TSC1* or *TSC2* experience neurological comorbidities such as epilepsy, autism spectrum disorder, intellectual disability, or psychiatric disorders such as ADHD or behavioural disorders like obsessive-compulsive behaviour. Tubers (TUBs) are detectable in ~80–90% of TSC patients and their pathology seems to correlate with neurocognitive deficits and autistic symptomatology (Ruppe *et al.* 2014). TUBs are malformations and are classified as a major feature for TSC diagnosis and most frequently found within the cerebral cortex (Feliciano 2020). They are regions of cortical dysplasia with abnormal neurons that have either adapted the wrong identity, are enlarged, and can be dysmorphic. Abnormal neurons are intermixed with seemingly normal-looking neurons and there can also be the occurrence of giant-cells (Feliciano 2020). The dysplastic neurons in the TUBs still express exclusively neuronal markers, form functional synaptic contacts, and can generate action potentials. In contrast, giant cells have an undifferentiated neural progenitor phenotype, expressing both neuronal and glial markers, do not form synaptic contacts, and are unable to generate action potentials (Cepeda *et al.* 2003; Ruppe *et al.* 2014). Other types of TSC brain lesions are subependymal giant cell astrocytoma (SEN/SEGAs), the occurrence of SEN/SEGAs and TUBs as well as epilepsy among other factors are significantly associated with mental retardation in the patient (Gül Mert et al. 2019). The histopathology of SEGAs consists of spindle cells, gemistocytic-like cells, and giant cells and they belong to the astrocytic neoplasms, despite showing both glial and neuronal expression patterns (Bongaarts et al. 2017). SEGAs develop from SENs (Hulshof et al. 2022), and there are still many questions about the molecular mechanisms underlying their progressive growth (Bongaarts et al. 2017).

The loss of either TSC1 or TSC2 leads to overactivation of mTORC1 which downstream effects include activation of the translational apparatus through inactivation of 4E-BP1 and activation of p70S6K and its downstream target S6K1. Additionally, mTORC1 signalling is required for normal neuronal development and function, and dysregulation of this pathway impairs the development of neural circuits at multiple levels. Animal models demonstrated that upregulated mTORC1 signalling due to loss of TSC1/TSC2 activity leads to changes in the neuronal phenotype including increased neuronal size, altered dendritic arborizations and spine formation, enhanced glutamatergic neurotransmission (Goto *et al.* 2011), altered axonal pathfinding and growth (Choi *et al.* 2008), as well as impaired synaptic plasticity (Bateup *et al.* 2011; Ruppe *et al.* 2014).

The degree of mTORC1 pathway hyperactivation seems to correlate with the severity of neurologic dysfunction especially regarding epilepsy and the behavioural abnormalities. Studies have shown that the use of the mTORC1 inhibitor rapamycin improves seizures and cognitive deficits in TSC mouse models (Ehninger *et al.* 2008; Goto *et al.* 2011). While mTORC1 activity increases in TSC, mTORC2 activity decreases though there are still uncertainties about its specific role in the disease pathogenesis. Inactivation of mTORC2 signalling occurs via the deletion of Rictor (rapamycin insensitive component of mTOR), and the group of Carson *et al.* demonstrated that a loss of mTORC2 via conditional Rictor deletion results in significant hypomyelination in their TSC mouse model as well as TSC reminiscent behavioural abnormalities, despite the lack of brain abnormalities or altered cortical layering (Carson et al. 2013). The mice demonstrated disorganized axonal projections and an overall increase in axonal connectivity in the TSC brain, especially within cortical tubers. Additionally, the mice presented an excitatory phenotype and the capability to form abundant synaptic contacts, suggesting an increased local excitatory innervation similar to the studies reporting increased synaptic excitation in human TSC (Cepeda *et al.* 2010; Ruppe *et al.* 2014).

1.5. Alzheimer´s Disease (AD)

Dementia is a chronic neurodegenerative disease leading to a constant decline of cognitive function and memory, interfering with the ability to perform activities of daily living (Merck *et al.* 1899). Dementia mainly affects elderly people above 60 years. Dementia is diagnosed when a cognitive decline occurs unexplainable by delirium or major psychiatric disorder. The cognitive or behavioural impairment involves at least two of the following criteria: impaired ability to acquire and remember new information. In addition, impaired reasoning and handling of complex tasks and poor judgment of, for example, safety risks or finances are also major symptoms of dementia. Further symptoms are impaired language functions (speaking, reading, writing) and changes in personality and behaviour (agitation, apathy; loss of empathy and compulsive or obsessive behaviours) (McKhann et al. 2011).

AD is a progressive, incurable disease leading to the loss of cognitive function and memory. Hallmarks of AD are extracellular senile plaques and intracellular neurofibrillary tangles (NFTs) (Merck *et al.* 1899). AD is the most common form of dementia (80% of all dementia cases), affecting more than 50 million people (Date: 2019) with a continuous increase of cases expected in the upcoming decades (Net 2019). AD is separated into two categories: early onset which is often familial (mostly caused by genetic mutations of either APP, Presenilin 1 or 2 (PSEN1/2)) (Chávez-Gutiérrez et al. 2012) or late-onset dementia which is mostly spontaneous and for which apolipoprotein E (APOE) mutations are a risk factor (Rabinovici 2019). Senile plaques, one of the major pathological lesions in AD brains, are extracellular deposits of amyloid β (Aβ), making amyloid a hallmark for AD. Aβ is generated by the cleavage of amyloid beta precursor protein (AβPP) by β and γ-secretases, the generated monomers rapidly form soluble prefibrillar and fibrillar oligomers prior to further aggregation, leading to insoluble plaques (Zhang *et al.* 2010). The second hallmark of AD is hyperphosphorylated TAU which aggregates to neurofibrillary tangles (NFTs). TAU protein is part of the microtubule-associated proteins (MAPs) family, and it is thereby an essential molecule for the assembly and stabilization of microtubular cytoskeleton (Weingarten *et al.* 1975). TAU was identified as a component of paired helical filaments (PHFs) which comprise NFTs in AD (Guillozet *et al.* 2003). NFTs in AD brains better correlate with neurodegenerative changes, cognitive decline and disease duration (Guillozet *et al.* 2003), and the tangles have long be considered toxic (Ballatore *et al.* 2007). TAU toxicity includes the phosphorylation-induced loss of function of TAU (i.e. impaired microtubule binding), as well as the gain of function (i.e. an increased tendency for oligomerization), reducing the levels of functional TAU and thus disrupts normal microtubule-based functions (Johnson and Stoothoff 2004).

Neuropathological diagnosis of AD is conventionally preformed postmortem via the assessment of the spatial occurrence of NFTs described by the Braak stages. Braak stage 0 contains all pathology free cases; Braak 1-2 has mild tau pathology but are not classified as AD, this level of tau is currently believed to be the result of aging (see Figure 1-1). Intermediate cases are described in the stages 3-4, and severe degrees of AD are included in the stages 5-6 (Braak and Braak 1995; Thal et al. 2010). Important to remark are the differences in location of origin and progression of tau and amyloid beta. Soluble oligomeric Aβ was found to induce selective neurodegeneration in the brain. *In vivo* and *in vitro* studies demonstrated that oligomeric soluble Aβ is toxic towards central nervous system (CNS) neuronal cells in both in comparison to fibrillary Aβ (Lambert *et al.* 1998; Walsh *et al.* 2002; Kim *et al.* 2003). Other studies found that soluble forms of Aβ exhibited strong neurotoxicity and that increased soluble Aβ can block long-term potentiation which may underlie the failure of memory in AD (Lambert *et al.* 1998; Walsh *et al.* 2002). Synapses, specifically the postsynaptic compartment, are the prime targets of Aβ toxicity (Selkoe 2002). Accordingly, acute Aβ exposure leads to synapse and spine loss, inducing long-term depression (LTD) and impairs long-term potentiation (LTP) (Shankar *et al.* 2008).

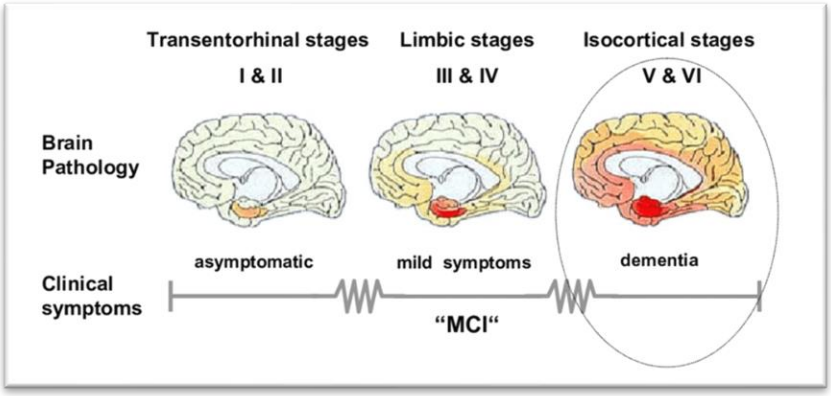

Figure 1-1: Plaque and tangle distribution at different stages of AD progression (Braak staging) (Wolf 2007); the yellow/orange shades describe the distribution of the proteins with darker colours indicating a stronger pathology in the brain regions

1.6. Consequence of TSC loss: mTOR overactivity

In the absence of TSC1/TSC2, Rheb becomes GTP-bound thus driving mTORC1 hyper-activation (Menon *et al.* 2014). mTOR has several functions in the cell, among them protein degradation. Normally, misfolded, or unnecessary proteins are degraded via two major pathways: (i) the ubiquitin-proteasome pathway, in which proteins bind with a ubiquitin chain and are rapidly degraded by a proteasome, or (ii) the lysosomal pathway, in which the protein is enveloped by a protease containing lysosome. Under nutrient and energy starvation conditions autophagy is induced, targeting cellular components to be broken down and recycled to regenerate the building blocks for new rounds of protein synthesis. One of the primary known functions of mTORC1 is the suppression of autophagy (B. Jahrling and Laberge 2015). Loss of function of the TSC1/2 tumour suppressor complex inhibits autophagy (see Figure 1-2) in neurons, due to the increased activity of mTORC1 and thus supressing the autophagy initiating kinase ULK1 via phosphorylation. Previous studies have indicated that loss of TSC1/2 in neurons results in increased stress detrimental for neuronal homeostasis: higher susceptibility to endoplasmic reticulum and oxidative stress as TSC1/2-dependent inhibition of mTORC1 is required to regulate autophagy in response to reactive oxygen species. TSC has never been classified as a neurodegenerative disease, though the increased stress response together with the accumulation of autophagic organelles could hint that uncleared protein aggregates and cellular debris may contribute to the altered neuronal morphology and survival (Di Nardo *et al.* 2014). M. Taneike *et al.* indicate that autophagy via the TSC1-mTORC1 signalling pathway plays an important role in maintenance of cardiac function and mitochondrial quantity and size in the heart (Taneike *et al.* 2016). Indication of autophagy impairment in post-mortem brain tissue also occurs in various neurodegenerative diseases wherein autophagosomes are inadequately cleared (B Jahrling and Laberge 2015).

mTOR overactivity is also found in AD. Several factors ranging from lifestyle e.g., diet and exercise to diseases such as diabetes or vascular disease can result in increased mTORC1 activity (see Figure 1-1). While this would lead to increased cell survival and proliferation in healthy conditions and patients, the increased mTORC1 activity in AD has different consequences. In AD, the mTOR pathway is disrupted in lymphocytes, correlating associated cognitive decline and reduced responsiveness to rapamycin (Paccalin *et al.* 2006; Yates *et al.* 2013). Additionally, mTOR activity was found to closely correlate with Aβ build-up, increased Aβ presence led to increased mTOR signalling, whereas decreased mTOR signalling reduced Aβ levels (Caccamo *et al.* 2010).

Furthermore, Caccamo *et al.* demonstrated that mTOR regulates TAU phosphorylation and degradation and mTOR overactivity in mice elevates TAU levels and phosphorylation, thus highlighting the importance of mTOR in AD (Caccamo *et al.* 2013) and other tauopathies among TSC is included as an infantile tauopathy (Sarnat and Flores-Sarnat 2015). Further studies demonstrated the up regulation of various components of the mTORC1 pathway in AD (An *et al.* 2003; Götz *et al.* 2004) as well as its link to disrupted removal of Aβ and phosphorylated TAU, leading thereby to synaptic loss and cognitive decline in AD due to a feedback inhibition of insulin and insulin like growth factor (IGF1) responses (Heras-Sandoval *et al.* 2014). These studies demonstrated the possible therapeutic approach of using mTOR inhibitors (such as rapamycin) for treating AD by reducing the tauopathies and amyloid build-up (Caccamo *et al.* 2011; Caccamo *et al.* 2013), thus resulting in the suggestion that TSC would be a suitable therapeutic target for AD (Ferrando-Miguel *et al.* 2005). Part of AD pathology is cognitive decline and memory loss, both of which were found to be affected by mTORC1 activity. Several studies demonstrated the importance of mTORC1 for late-phase long-term potentiation (LTP) (Swiech *et al.* 2008), while the *mTOR* inhibitor rapamycin can impair long-term consolidation of rodent fear memory (Parsons *et al.* 2006). mTOR activity appears necessary to memory, however hyperactive mTOR is disrupting memory formation (B Jahrling and Laberge 2015). The investigation of a TSC mice model demonstrated that the animals exhibited both overactive mTORC1 and memory impairment, both were treatable by rapamycin (Ehninger *et al.* 2008); human patients with either TSC1 or TSC2 mutations exhibit similar symptoms.

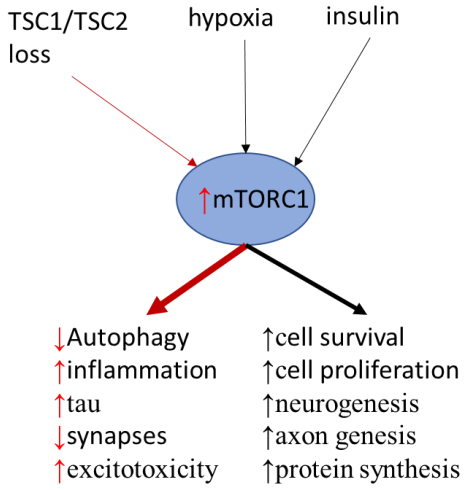

Figure 1-2: Model of mTOR pathway effect in the human brain in TSC and AD (marked in red) and under healthy conditions (marked in black). TSC loss leads to mTORC1 overactivity and consequently decreased autophagy and synaptic connections while inflammation, excitotoxicity, and phospho-TAU increase. Under healthy conditions, insulin and hypoxia are among several factors inducing mTORC1 activity to increase cell survival and proliferation.

1.7. Common mechanisms between TSC and AD

1.7.1. Neuroinflammation

One mechanism through which TSC activity might affect dementia, next to autophagy, would be inflammation. Microglia make up 5-12% of all glia cell in the human adult CNS (Mammana *et al.* 2018). Inflammatory conditions are mainly characterized by activation of macrophages and monocytes leading to an increased release of pro-inflammatory markers such as IL6 or IL1β. In AD, it was demonstrated that microglia can support disease progression (Mammana *et al.* 2018). Aβ-40 and Aβ-42 cause neuronal damage when microglia are present (Giulian 1999). Microglia react to Aβ peptides and promote their clearance through the release of cytotoxic factors, which initiate the phagocytosis of these peptides (Koenigsknecht and Landreth 2004). In the early disease stages of AD, microglia activation promotes Aβ clearance via their scavenger receptors, though continuous microglia activation is known to lead to the release of pro-inflammatory cytokines, thus resulting in neuronal death (Wang *et al.* 2015). The inhibition of Aβ-induced microglial activation can reduce the inflammatory cytokines production and lower Aβ deposition (Liu and Bian 2010); suggesting that Aβ indirectly contribute to activation of inflammatory systems, leading to AD progression (Wang *et al.* 2015). Aβ binding to the microglial cells induces the expression of pro-inflammatory genes resulting in the elevation of pro-inflammatory cytokine levels such as of TNFa, or IL1ß which lead to TAU hyper-phosphorylation and neuronal loss (Wang *et al.* 2015).

Studies suggest that continuous inflammation can lead to proinflammatory cytokines in the CNS by crossing the blood brain barrier (BBB), thereby contributing to cognitive decline in AD patients (Perry *et al.* 2007; Holmes *et al.* 2009). In TSC, microglia exhibit an increased secretion of proinflammatory cytokines and an impaired rate of M2 polarization (Byles *et al.* 2013). Evidence suggests an important role for mTORC1-mediated feedback inhibition of Akt signalling in TSC1 deficient bone marrow-derived macrophages because treatment with rapamycin and myc-Akt expression restored the Akt activation as well as rescuing the M2 gene expression (Byles *et al.* 2013). The group of Thomas Weichhart investigated whether mTOR influences cytokine expression and if rapamycin would affect that pathway. They demonstrated that rapamycin regulates the balance of IL-12 and IL-10 after mTOR hyper-activation due to bacterial stimulation.

Also, other cytokines were affected, IL-12p40 and TNF-production were reduced; IL6 production was partly inhibited in TSC2-silenced cells, whereas IL10 was increased. NF-kB, a crucial regulator of proinflammatory responses, has enhanced activation in primary human monocytes after treatment with rapamycin, indicating that mTOR negatively regulates NF-kB (Weichhart *et al.* 2008). Additionally, mTOR inhibition seems to prevent BBB breakdown by cytokines in several models of age-associated neurological disorders, suggesting an important role of mTOR in BBB dysfunction in age-related brain disease states (Van Skike and Galvan 2018).

1.7.2. Neuroinflammation and Autophagy

Impaired autophagy can affect neuroinflammation, as impaired TAU clearance can trigger inflammation responses from microglia (Bellucci *et al.* 2004; Yoshiyama *et al.* 2007; Laurent *et al.* 2017), thus being another commonality between TSC and AD. In AD, reactive astrocytes are essential in neuroinflammation due to their release of pro-inflammatory mediators and cytotoxic molecules (Heneka *et al.* 2015). Additionally, astrocytes also play a role in phagocytosis, which may attenuate pathology through uptake and clearance of protein aggregates (Cahoy *et al.* 2008) as it had been shown for Aβ in several studies (Wyss-Coray *et al.* 2003; Basak *et al.* 2012), but there are still many open questions about the ability of astrocytes to modulate TAU pathology (Martini-Stoica *et al.* 2018). The uptake of hyperphosphorylated TAU by astrocytes during synapse degeneration was shown in a TAU model (De Calignon *et al.* 2012). The possibility of TAU spreading from neuron to astrocyte or even glia to glia has been suggested in some tauopathies such as progressive supranuclear palsy (PSP) and corticobasal degeneration (CBD) (Narasimhan *et al.* 2017). Defects in the lysosomal pathway can occur with aging (Wolfe *et al.* 2013) and lysosomal dysfunction alone results in the accumulation of aberrant TAU (Nixon 2004). Transcription Factor EB (TFEB) is a ubiquitously expressed transcription factor whose activation leads to stimulation of lysosomal biogenesis and autophagy, resulting in the breakdown of proteins and lipids for nutrients (Settembre *et al.* 2011; Martini-Stoica *et al.* 2018). Furthermore, TFEB promotes clearance of aberrant storage material in lysosomal storage disorders (Medina *et al.* 2011; Palmieri *et al.* 2017). CNS expression of TFEB results in clearance of aberrant TAU species in TAU transgenic mice, though this was primarily attributed to an intraneuronal/cell autonomous mechanism (Polito *et al.* 2014). Martini-Stoica *et al.* demonstrated a functional role for astroglial TFEB for stimulating uptake and clearance of aberrant extracellular TAU thereby preventing neuronal spreading of TAU pathology in a mouse model of tauopathy.

They found that enhancement of the lysosomal pathway in astrocytes through TFEB overexpression could mitigate disease progression and reduce TAU spreading, but it had mixed results in TAU pathology in their mice models. TFEB activation has been linked to lysosomal stress and the accumulation of aberrant protein aggregates (Martini-Stoica *et al.* 2018). Its activation is a known consequence of lysosomal stress/dysfunction (Sardiello *et al.* 2009), whether due to normal aging or AD–related mutations (Wolfe *et al.* 2013). TFEB seems to be activated in tauopathies since transcriptional up-regulation of TFEB and several of its lysosomal target genes in astrocytes from whole brain samples has been demonstrated (Martini-Stoica *et al.* 2018). Several factors such as the presence of aberrant extracellular TAU, as well as signals from a stressed neuron, or secreted inflammatory molecules could cause astroglial TFEB activation. Martini-Stoica *et al.* also suggested that astroglial TFEB overexpression may also indirectly impact disease pathogenesis via neuron-astrocyte interaction or neuroinflammation modulation although this hasn't been investigated yet (Martini-Stoica *et al.* 2018). Autophagy plays crucial roles during neurodevelopment and neurogenesis, as well as in the synaptic zone; autophagy seems to be implicated in axonal dystrophy following excitotoxic damage and axotomy but also in dysfunctional axons in diseases like Huntington Disease (HD) or AD. Neuronal autophagy plays a protective role in the CNS, by being involved in protein turnover and removal of damaged proteins through lysosomal degradation. Also, neuronal autophagy has been implicated to play a role in neuronal death as observed in several pathological conditions (Muller *et al.* 2017).

1.7.3. Disrupted autophagy in TSC and AD

As discussed previously, disrupted autophagy is a commonality between TSC and AD. Both disorders also share several altered gene expressions related to autophagy due to their connection to mTOR. RB1CC1 (a tumour repressor gene) is functionally connected to TSC1 and can cause neuronal atrophy by insufficient expression through mTORC1 signalling alteration and there is the evidence that it is also involved in the pathology of AD (Chano *et al.* 2007). RBC1CC1 is a known interactor with ULK1 (Hara *et al.* 2008) and it was demonstrated that knockdown of RBC1CC1 reduces mTORC1 activity (Chano *et al.* 2007). Additionally, researchers suggested the targeting of the TSC1/TSC2 complex signalling pathway as a potential future treatment for AD, since post-mortem AD patient brains had reduced levels of TSC resulting in mTORC1 over activity (Ferrando-Miguel *et al.* 2005). Activity alterations of mTOR influences various protein pathways next to cytokine expression or autophagy.

ULK1 is a serine/threonine kinase promoting autophagy signalling and it has been shown that mTORC1 associates with the ULK1-ATG13- RB1CC1 complex through Raptor-ULK1 binding. Through the interaction with the ULK1-ATG13-RB1CC1 complex, phosphorylation of both ULK1 and ATG13 through mTORC1 occurs, which represses ULK1 kinase activity to inhibit autophagy. A signalling feedback-loop was demonstrated, showing that ULK1 can directly phosphorylate Raptor on multiple sites to inhibit mTORC1 signalling (see Figure 1-3) by impeding substrate binding during nutrient limitation, thereby repressing protein synthesis and cell growth (Dunlop *et al.* 2011; Wong *et al.* 2013). It was further shown that overexpression of ULK1 increased mTORC1 catalytic activity, demonstrated by increased phosphorylation of mTOR Ser2481 and Raptor Ser863. This occurred simultaneously with a decrease in phosphorylation of mTORC1 substrates, suggesting that inhibition of substrate access to mTORC1 by ULK1 is preventing mTORC1 signalling, despite its heightened kinase activity (Dunlop *et al.* 2011). A study working on neurons with TSC2 knockdown thanks to shRNA interference has shown a surprising autophagy dysfunction associated with loss of TSC1*/2* and the molecular mechanism underlying these defects. In contrast to the expected inhibition of autophagy arising from mTOR overactivity due to the loss of TSC1/2, the group showed evidence that TSC2-knockdown neurons display increased accumulation of autolysosomes and autophagic activity through AMPK-dependent activation of ULK1 (Di Nardo *et al.* 2014).

Glycogen is a critical source of energy supply in cells. Glycogen homeostasis is regulated by opposing pathways governing glycogen synthesis and degradation, the homeostasis is disrupted in multiple diseases (Vilchez *et al.* 2007; Zois *et al.* 2014). Altered glycogen homeostasis in astrocytes is linked to several seizure disorders. Impaired glycogen metabolism is also a critical component of tumour formation. Insulin triggers inhibitory phosphorylation of glycogen synthase kinase-3 (GSK3α/ß), leading to dephosphorylation and activation of GSK3 (Zhang *et al.* 2006; Bouskila *et al.* 2010). In the absence of a functional TSC complex, GSK3ß is phosphorylated and inactivated by S6K1, evidence of aberrant phosphorylation of GSK3ß in human and animal tissues with deficient TSC has been demonstrated (Pal *et al.* 2019). This leads to dysregulation of GSK3 substrates and the contribution of the continuous proliferation of TSC-deficient cells despite the absence of growth factors (Zhang *et al.* 2006). mTORC1 hyperactivity leads to decreased autophagosome formation and autophagic impairment by ULK1 inhibition. Glycogen accumulates in patients and models with TSC via impaired clearance of glycogen by the autophagy-lysosome pathway.

That aberrant glycogen storage in TSC is caused by impairment of mTORC1-GSK3ß-dependent and -independent pathways, depending on the specific mutation in the TSC-encoding gene. Research suggests that GSK3 phosphorylation, performed by S6K1, is independent of PI3K, but a downstream target of mTORC1 in TSC-deficient cells (Zhang *et al.* 2006). GSK3 activity changes have been associated with several neurodegenerative or psychiatric diseases, such as AD, and ASD. Therefore, GSK3 is now targeted as a potential future common therapeutic target for drugs (Beaulieu 2007; Beaulieu *et al.* 2009). Aβ oligomers in AD brains can bind to specific cell receptors and behave as an antagonist to insulin, preventing the activation of the PI3 kinase resulting in an activity increase of GSK3 (Townsend *et al.* 2007). GSK3 phosphorylates TAU in the regions of the microtubule binding domain, resulting in a disturbance of the TAU-microtubule interaction, TAU detachment and self-aggregation (Hernández *et al.* 2010). Thus, GSK3 can be a link between Aβ and TAU. Additionally, Aβ formation in APP transgenic mice causes hyper-phosphorylation of TAU, while there is no increased amyloid-β plaque pathology in TAU transgenic mice (Götz *et al.* 2004).

Studies demonstrated that GSK3 might be a player in Aβ pathology as its inhibition restored lysosomal acidification leading to clearance of Aβ burden (Cohen and Goedert 2004; Avrahami *et al.* 2013). Furthermore, GSK3α has been shown to have a regulating function on APP cleavage resulting in an increased production of Aβ (Hooper *et al.* 2008) which then enhances GSK3 activity in a feedback loop. Impaired mTORC1-GSK3ß signalling stimulates glycogen synthesis (Pal *et al.* 2019). Molecular mechanisms which are linked to autophagy have been demonstrated to be altered in AD. Presinilin-1, which is involved in the regulation of lysosome acidification to be impaired in AD. In the autophagosomes, which accumulate in cellular and animal models of AD, an excess of amyloid precursor protein converts these autophagic vesicles into an endogenous reservoir of this pathogenic product. Furthermore, Beclin-1 seems also to be impaired in AD since its mRNA and protein levels are decreased in brain regions of AD human and mouse models and its overexpression in AD mice was shown to reduce intracellular accumulation of Aβ and extracellular deposition of Aβ plaques (Muller *et al.* 2017).

S6K1 (also known as p70 S6 kinase) is a downstream target of mTORC1, which is stimulated by both nutrients and growth factors (Manning 2004). S6K1 modifies accordingly the level of input from growth factors, such as insulin and IGF-*I* as a critical component of the negative feedback loop. When mTORC1 is chronically activated, S6K1 will constitutively shut down the responsiveness of certain cells to insulin (Manning 2004). Aβ deposition in plaques seems to activate S6K1 resulting in TAU phosphorylation and microtubule disruption (Pei *et al.* 2008). NFT staining demonstrated positive results for S6K1; the localization of S6K1-immunoreactive structures in involvement in TAU pathology (Sonoda *et al.* 2016).

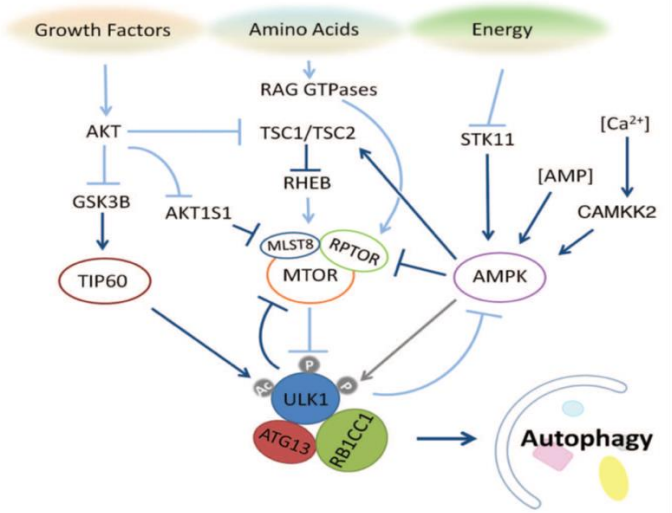

Figure 1-3: Pathway of TSC-mTOR-ULK1 autophagy control (O'Brien and Wong 2011)

1.7.4. Calcium signalling in the brain.

Calcium functions as a major trigger for neurotransmitter release in the brain and both AD and TSC have demonstrated an altered calcium homeostasis. Calcium is essential for neuronal excitability, synaptic plasticity, dendritic development and programmed cell death amongst other functions (Marambaud *et al.* 2009; Nikoletopoulou and Tavernarakis 2012). Therefore, calcium homeostasis is tightly regulated for normal function of the previously mentioned cell processes. There are two main types of calcium channels: voltage regulated channels and ligand binding regulated channels; the most prominent ligand of the latter type is L-glutamate which activates both ionotropic and metabotropic receptors, thereby mediating direct influx of extracellular calcium into the cells. The ER is a site of intracellular calcium storage and it is the source of calcium waves which have been functionally linked to synaptic plasticity (Nikoletopoulou and Tavernarakis 2012).

Aging neurons show increased calcium influx into the cell due to increased VOCCs activity (Voltage operated calcium channels), as well as reduced calcium export via PMCA (ATP-driven plasma membrane pump) and increased calcium release from the ER. Additionally, calcium buffering and mitochondrial ability as calcium sinks also decrease with age. This changes overall lead to an increased calcium load in neurons, disturbing neuronal excitability. Calcium is also involved in memory formation, more specifically it plays a major role in LTP (long-term potentiation) and LTD (long-term depression). The thresholds for LTP and LTD rise/fall respectively with age and LTP maintenance is disrupted. Furthermore, the calcium source of synapses changes with age: NMDAR receptors as a source decrease while L-type VOCCs increase; hypothesized reasons for this change are changes in gene or protein expression or changes of the phosphorylation state of the channels. Consistently increased intracellular calcium levels in neurons can lead to phenotypes such as neuronal death and degeneration as calcium contributes to the activation of cell death by stimulating ROS production as mitochondria dysfunction and overload with calcium. Studies have shown that disturbed ER calcium homeostasis significantly contributes to dysfunction and degeneration in AD. AD models for example showed impaired calcium uptake in mitochondria (Nikoletopoulou and Tavernarakis 2012), especially after oxidative stress (Kumar *et al.* 1994) and AD neurons showed increased levels of mitochondrial DNA and proteins in cytoplasm and lysosomes (Hirai *et al.* 2001). Reduced expression of calcium buffers such as calmodulin or calbindin in AD brains has been demonstrated, disturbing calcium homeostasis.

Excessive glutamate receptor activation leading to excessive calcium influx, thereby impairing synaptic activation, neuronal plasticity and synthesis of NO which will cause cell death, have been identified in AD (Sattler and Tymianski 2000; Marambaud *et al.* 2009). Aβ increases NMDAR receptor vulnerability towards excitotoxicity (Mattson *et al.* 1992; Mattson 2004) and it seems that its oligomers may induce mitochondrial calcium overload resulting in massive calcium influx in toxicity in neurons (Caspersen *et al.* 2005). Disruptions in the calcium homeostasis have also been found in TSC: neurons showed an increase of spontaneous calcium transients (Nadadhur *et al.* 2019), while iPSC derived TSC2 -/- neurons demonstrated elevated neuronal activity with highly synchronized calcium spikes, enhanced calcium influx via L-type calcium channels resulting in abnormal neurite extension and sustained CREB (critical mediator of synaptic plasticity) activation.

Furthermore, the expression of Cav1.3 LTCC was increased and Hisatsune *et al.* suggested that it is a downstream target of the mTOR pathway. Additionally, the paper also stated a changed morphology on the homozygous TSC2 cell line with abnormal morphology including a larger soma and longer neurites (Hisatsune *et al.* 2021). At last, Kimberley Raab-Graham *et al.* showed an increase of dendrites in TSC2 -/- mice, reduction of branch specific potentiation and increased expression of the calcium channels Kv1.1, CaV2.2 and the auxiliary subunit $\alpha 2\delta 1$ in synapses with CaV2.2 being mislocalised and thereby causing the disruption of branch specific potentiation (Raab-Graham 2021).

1.7.5. Glutamate in TSC and AD

Glutamate is essential for synaptic transmission as a major excitatory neurotransmitter in the mammalian CNS; however the balance of the signal is crucial (Lauderback *et al.* 2001). Overactive neuronal stimulation by glutamate (known as excitotoxicity) can induce neuronal damage and death (Maragakis and Rothstein 2001). Therefore, clearance of glutamate from the synapse is critical for neuronal health. Cellular uptake by glutamate transport is the primary mechanism in maintaining synaptic glutamate concentrations (Anderson and Swanson 2000), mediated by astrocytes (Lauderback *et al.* 2001). In TSC, glutamate excitotoxicity seems to occur. Knock-out mouse model of TSC (TSC1GFAPCKO mice) demonstrated decreased expression and function of the glutamate transporters (GLT) GLT-*1* and GLAST, leading to an increase in extracellular glutamate levels and excitotoxic neuronal death (Wong *et al.* 2003; Zeng *et al.* 2007). Abnormal glutamate homeostasis and neuronal death could lead to neurological deficits and promote neuronal hyper excitability and seizures as consequence (Zeng *et al.* 2010). There is the evidence that abnormal glutamate homeostasis due to impaired astrocyte glutamate transport could be a contributing factor to epilepsy and other neurological deficits in TSC (Wu *et al.* 2005; Zeng *et al.* 2007). Modulation of astrocyte glutamate transporter expression improves neuronal survival and neurological deficits in animal models (Zeng *et al.* 2010). Recent studies showed glutamate receptor alterations in the tubers, common for TSC (Boer *et al.* 2008c); alterations in ionotropic glutamate and GABA receptor subunit mRNA expression have been observed (White *et al.* 2001).

Glutamate receptors are divided in different groups based on their function. Group I include receptors which are responsible for mediating postsynaptic excitatory effects in neurons. Group II and group III receptors regulate presynaptic inhibitory effects on synaptic transmission and neurotransmitter release. The first two receptor groups are expressed in human astrocytes (Boer *et al.* 2008c), playing an important role in regulating the extracellular levels of glutamate (Aronica *et al.* 2003). Group I metabotropic glutamate (mGlu) receptors seems to regulate proliferation, differentiation, and survival of neural stem/ progenitor cells, suggesting a role in brain development and developmental disorders (Catania *et al.* 2007). Recently, activation of the mTOR pathway has been reported after stimulation of group I mGluRs, suggesting a link between mGluR activation and the major pathway disrupted in TSC (Boer *et al.* 2008c).

mTORC1/*2* have been shown to regulate the synthesis and turnover of glutamate receptors of neurons and alter the morphology of dendritic spines, thereby affecting processes of long-term potentiation that are crucial for epileptogenesis, learning, and memory (B Jahrling and Laberge 2015). Cell death caused by excitotoxicity have been implicated in AD (Maragakis and Rothstein 2001). Glutamate transport is inhibited in AD brain by oxidation while oxidative damage is elevated in the AD brain (Lauderback *et al.* 2001). As mentioned earlier, glial GLT proteins are crucial for cell health. Decreasing glial GLT proteins increases neuronal sensitivity to glutamate and induces neurodegeneration and death (Lauderback *et al.* 2001). Aβ-42 mediates decreased GLT *in vivo* by generating HNE (a lipid peroxidation product); unifying several neurodegenerative mechanisms in AD like altered APP processing, oxidative damage, decreased GLT, excitotoxicity and altered calcium homeostasis (Lauderback *et al.* 2001). G. Shankar *et al.* demonstrated that Aβ oligomers induce progressive loss of hippocampal synapses by using NMDA-type glutamate receptors (NMDARs) (Shankar *et al.* 2007).

1.7.6. Urokinase Pathway

Another altered pathway found in both TSC, and AD is the urokinase pathway. The urokinase-type plasminogen activator (uPA), a serine protease with an implicated role in tumour growth, migration, and tissue invasion, is expressed in overall low levels in non-dividing cells but shows significant expression increases in most malignant tumours (Stepanova *et al.* 2017). Upon binding to its receptor uPAR, uPA catalyses plasminogen activation and plasmin generation as initiation of the proteolysis cascade (Peteri *et al.* 2021). uPA also is involved in the activation of cell signalling pathways regulating differentiation, cellular adhesion, migration, and proliferation through non-plasminogenic mechanisms (Peteri *et al.* 2021). Sumi *et al.* demonstrated high levels of uPA expression as well as its proteolytic regulation of axonal growth in rat neuronal tissue. They hypothesised that intracellular proteolytic degradation is regulating axoplasmic traffic and suggested a role of uPA in neuronal plasticity (Sumi *et al.* 1992).

uPA activity is regulated by plasminogen activator inhibitors PAI-1 (Plasminogen activator inhibitor 1), PAI-2, and PN-1, belonging to the SERPIN (serine protease inhibitors) family and therefore also called SERPINE1/2 (Stepanova *et al.* 2017). Stepanova *et al.* investigated Lymphangioleiomyomatosis (LAM), a fatal lung disease associated with TSC1 or TSC2 inactivating mutations, which occurs in 30% of adult women with TSC. They have shown that loss of TSC induces overexpression of uPA in homozygous TSC1 LAM cells. TSC1 -/- and TSC2 -/- MEFs expressed higher levels of uPA than their WT counterparts and silencing of TSC2 in WT MEFs resulted in an increase of uPA expression. Additionally, rapamycin enhanced up-regulated expression of uPA in human TSC1 and TSC2 -/- cells. Several other genes implicated in the progression of LAM such as PARP1 and members of Wnt signalling cascade, were upregulated upon the loss of TSC function, but none are negatively regulated by rapamycin. Inhibition of AMPK was able to partially inhibit the rapamycin-induced increase in uPA expression in TSC2-null cells, suggesting a contribution of AMPK to the uPA expression upregulation in TSC2-negative cells. Parallel to the uPA expression, FOXO3 was also upregulated in the TSC2 cells which is consistent with previously reported observations that FOXO3 expression is upregulated upon mTORC1 inactivation. Dexamethasone, a FOXO1/3 inhibitor, and an inhibitor of uPA catalytic activity by UK122 prevented the acceleration of *TSC1*-null cell migration and invasion by rapamycin (Stepanova *et al.* 2017). Research identified a role of uPA in dendritic spine recovery as it induces the expression of ezrin in dendritic spines.

Ezrin, radixin and moesin (ERM) belong to a conserved protein group regulating the reorganization of the actin cytoskeleton in different cell systems (Merino and Yepes 2018). Merino *et al.* revealed that uPA/uPAR binding induces the synthesis of ezrin as well as its recruitment to the post-synaptic density and its subsequent activation by phosphorylation. uPA- induced synthesis and activation of ezrin promotes the reorganization of the actin cytoskeleton in the injured dendritic spine, leading to recovery and to the formation of proximal dendritic branches (Merino and Yepes 2018). uPA-uPAR interactions can result in increased cleavage of cell-associated plasminogen with the production of the protease processing plasmin, the latter's production aids in the process of inflammatory and neoplastic cell invasion through its ability to degrade extracellular matrix proteins (Walker *et al.* 2002). Studies have demonstrated increased uPAR expression in macrophage/ microglia cells in the brains of cases with acute multiple sclerosis lesions and in cases with traumatic brain injury. The plasminogen activation system seems to play a significant role in phagocytic cell migration to sites of inflammation. A prominent feature of AD pathology is the accumulation of microglia around aggregated Aβ plaques and neurofibrillary tangles in brain tissue, a process where both microglial proliferation or microglial chemotaxis and adhesion to these structures can be involved. uPAR is a central coordinator in these processes through its interactions with uPA and CD11b, the latter is expressed by human brain microglia, and is upregulated in AD brains. Studies have furthermore observed that uPA is localized to a subset of plaques in AD brains. In addition, an important regulator of uPA, SERPINE2 demonstrated increased expression microglia in AD brains and Vitronectin, an alternative high-affinity ligand of uPAR, has also been localized to AD plaques and tangles (Walker *et al.* 2002). Additionally, uPAR has been shown to be involved in physiological events such as inflammation (Bruneau and Szepetowski 2011).

It has been established that uPAR is involved in the interneuron development via HGF (hepatocyte growth factor) which is a target of uPAR activity, promoting migration of interneurons during cortical development (Powell *et al.* 2001). A study has demonstrated increased expression of the different components of the urokinase pathway in cortical tubers of TSC patients (Iyer *et al.* 2010). Enhanced HGF expression was demonstrated in a TSC1 mice model. It must be remarked that recent studies suggest that HGF and other growth factors influence mTOR activity (Parker *et al.* 2011). Additionally, increased HGF expression has been found in AD (Yamada *et al.* 1994; Fenton *et al.* 1998; Zhu *et al.* 2018); HGF has been found to be involved in axon outgrowth, neuronal survival, synaptic function and plasticity (Ebens *et al.* 1996; Nakamura and Mizuno 2010; Wright and Harding 2015).

SERPINE1 function is the inhibition of tissue plasminogen activator (tPA) and uPA (see Figure 1-3) to maintain clot formation and thus plays a significant role in non-neoplastic disorders, such as deep vein thrombosis, myocardial infarction, atherosclerosis, and stroke (Furuya *et al.* 2020). SERPINE1 expression is regulated by intrinsic factors such as cytokines and growth factors and extrinsic factors like cellular stress. A study focusing on bladder cancer identified SERPING1 as a potential missing factor that regulate SERPINE2 overexpression. SERPING1 is a protease inhibitor belonging to the serpin superfamily (Furuya *et al.* 2020). Analysis of a TSC database has demonstrated a significant expression change of SERPING1 in TSC patients and literature has identified an involvement of SERPING1 in AD and TSC.

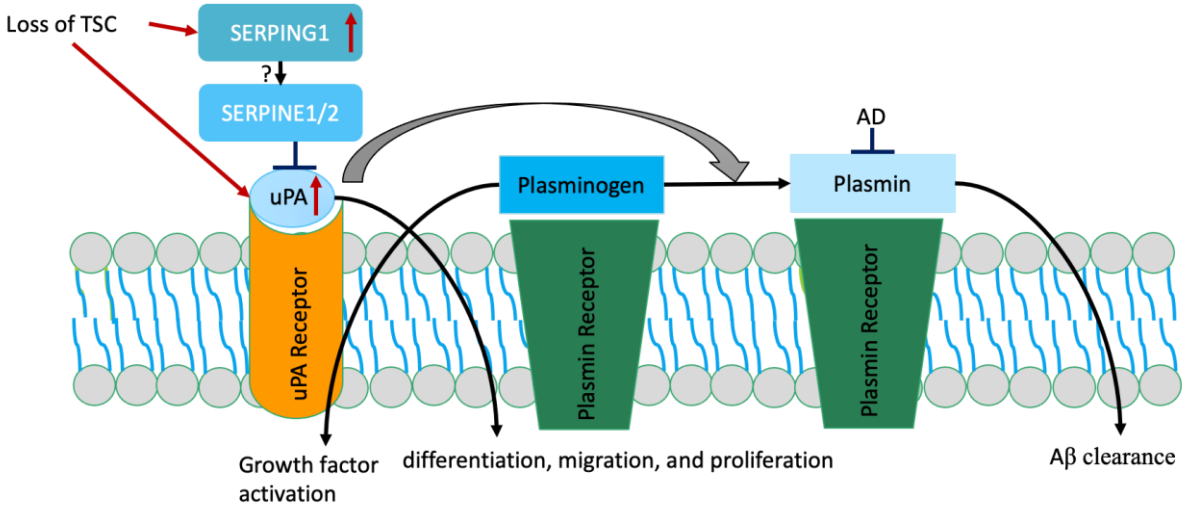

Figure 1-4: Scheme of TSC-urokinase-SERPINE1-SERPING1 Interaction, the interaction between SERPING1 and SERPINE1 is currently unknown despite the indication that SERPING1 has some effect on SERPINE1 activity.

1.8. Astrocytes

TSC expression changes have an effect on all cell types in the human brain which consists of neurons, astrocytes, microglia and oligodendrocytes, each with their distinct origins and turnover dynamics (Frisén 2016). The hippocampal dentate gyrus and the subventricular zone in adult mammal brains continuously generate new neurons from neural stem or progenitor cells. While the neurogenic cells of the adult brain cells display the stem cell properties of multipotency and self-renewal *in vitro*, they often act as unipotent cells *in vivo*, giving rise to only one distinct subset of neurons (Lledo *et al.* 2008). During CNS development, neurogenesis precedes gliogenesis, where radial glial support both migration and the neural stem cell substrate for both astrocytes and neurons (Chaboub and Deneen 2013). During early development, morphogens such as Shh, BMPs and Wnts design patterns throughout the dorso-ventral axis of the neural tube, regulating the expression of transcription factors that further form domains from which different sub-types of neurons will appear. This domain pattern is conserved during gliogenesis and regulates the generation of astrocyte sub-types. Astrocytes populate all areas of the CNS and they must therefore migrate to colonise their final destination (Chaboub and Deneen 2013).

There is little generation of new astrocytes in the brain parenchyma as new astrocytes seem to derive from proliferating mature astrocytes. Astrocytes are well known to have an important influence on neural transmission (Frisén 2016). Microglia derive from a hematopoietic lineage in the yolk sac and populate the nervous system in early fetal life, after which they are a self-sustaining population (Frisén 2016). Markers such as GFAP, S100B1, Aldh1L1, AldoC, Ascgb1, Glt1, and aquaporin 4 label mature astrocytes. However, none of these markers labels all astrocyte populations; for example, GFAP preferentially labels white matter astrocytes, whereas S100 marks grey matter astrocytes and some oligodendrocyte populations (Chaboub and Deneen 2013).The function of astrocytes is quite diverse and differs among their population. One major role of astrocytes is among the blood brain barrier (BBB). The BBB is a highly specialized brain microvascular structure made up of endothelial cells coupled to astrocytes (Wang and Bordey 2008; Zlokovic 2008). The main function of the BBB is preventing harmful or toxic substances circulating in the blood stream from entering the brain. Additionally, the BBB maintains ion gradients, which are essential for neurotransmission. Astrocytes contribute to BBB formation and function by making physical contact with endothelial cells and secreting diffusible molecules (bFGF, GDNF and TGFβ) that regulate formation of tight junctions (Hayashi *et al.* 1997; Sobue *et al.* 1999; Abbott *et al.* 2006). Furthermore, astrocytes are required for synaptogenesis.

It had been demonstrated that astrocyte-free cultures of retinal ganglion cells form synapses but fail to generate spontaneous synaptic activity and demonstrated impaired neurotransmission but in the presence of astrocytes, the normal synaptic functions were restored as well as number of synapses of those neurons were being increased. This is the basis of the "tripartite synapse" model, stating that pre- and post-synaptic connections are surrounded by astrocytes that participate in neurotransmission. (Chaboub and Deneen 2013).

Another role of astrocytes lies in communication, while astrocytes are not equipped with adequate ion channels to fire action potentials like neurons, calcium (Ca^{2+}) concentration of astrocytes undergo changes in response to the release of neurotransmitters. Also, one of earliest known functional role for astrocytes is the regulation of ionic concentration in extracellular space. The firing of action potentials by neurons results in the accumulation of K^+ extracellularly and astrocytes that enwrap the synapse take up excess amount of K^+ then dilute it by passing it to other astrocytes. Failure of removing excess amount of K^+ would result in neuronal hyperexcitability and seizures, which is why this role is important in regional and global networking (Chaboub and Deneen 2013). Glutamate is the major neurotransmitter in the nervous system and maintenance of its concentration in the extracellular space is crucial for neuronal homeostasis and physiology. Astrocytes are essential in glutamate uptake and metabolism in the brain, and thus are essential for neuronal function. The up-take of glutamate in astrocytes is mainly accomplished by glutamate transporters GLAST or/and GLT-1, which are specifically expressed on astrocytes and their precursors. Glutamate is then converted into glutamine before transporting it back to neurons for re-synthesis of glutamate. In addition to glutamate metabolism, astrocytes also function as reservoir of energy substrates such as lactate for neurons (Chaboub and Deneen 2013).

1.8.1. TSC in astrocytes

Pathologic examination of brains from TSC patients has demonstrated various abnormalities based on dysregulated cell growth, differentiation, and migration processes. The brain tissue demonstrated abnormal cortical lamination associated with dysplastic astrocytes and giant cells which have been shown to express both astroglia and neuronal markers. Abnormal expression of neuronal differentiation and proliferation makers have been identified in tubers and subependymal giant cell astrocytoma (SEGA) from TSC patients in molecular studies.

During development,TSC1 and TSC2 are expressed in astrocytes and neurons (Gutmann *et al.* 2000), both function as negative growth regulators through mTORC1 (Tee *et al.* 2002). As homozygous loss of either TSC1 or TSC2 is lethal in embryos, the generation of murine models has been proven difficult. Animals heterozygous for mutations in either the TSC1 or TSC2 gene e.g., several TSC animal models have a high incidence of liver and renal abnormalities, but do not develop the neurologic features seen in human TSC (with the exception of Eker rats which do display neurological abnormalities). Some of the giant cells in the tubers express proteins associated with astrocytes such as GFAP, Vimentin, and S-100 protein. The expression of neuronal and glial cell markers in TSC tubers has been supported by molecular studies. Ess *et. al* generated mice with selectively inactivated TSC1 in astrocytes using the GFAP promoter to express Cre recombinase. These mice developed abnormalities in hippocampal neuronal organisation, increased astrocyte size and growth, and epilepsy. They stated that much of the CNS pathology in TSC can be modelled in mice by astroglial cell TSC1 inactivation (Ess *et al.* 2004).

Sosunov *et al.* pointed out significant differences between subpopulations of astrocytes based on morphology in tubers (Sosunov *et al.* 2008). They hypothesized that the development of astrogliosis in tubers related to loss TSC1 or TSC2 and involved in lesion formation. Their investigation showed that astrogliosis in tubers was consist of several astrocyte subpopulations that were similar to ‘‘reactive’’ astrocytes that were Vimentin positive and exhibited mTOR activation. Their research also supported the hypothesis that astrocytosis could reflect the effects of mTOR pathway activation as phosphorylated S6 protein has been detected in tuber astrocytes (Sosunov *et al.* 2008). Additionally, expression of proinflammatory cytokines in tuber astrocytes has been demonstrated suggesting that their expression increase might be a response to regional changes in the tuber tissue arising as consequences from seizures or alteration in the BBB (Maldonado *et al.* 2003).

Examples of increasingly expressed proinflammatory cytokines are TNFa, NFkB and IL1B (Boer *et al.* 2008a; Boer *et al.* 2008b). It is suggested that the occurrence of proinflammatory cytokines may further activate astrocytes within tubers and may even contribute to neurobehavioral abnormalities in TSC as SENs are present in about 80% of TSC patients and are seen as not related to cognitive deficits or epilepsy in TSC. On the other hand, SEGAs occur in only about 10%–15% of TSC patients and can be associated with rapid neurological decline and death (Wong and Crino 2012). Homozygous mutations for TSC2 in a human embryonic stem cell line show a hyperactive mTORC1 pathway, increased soma size, neuronal hyperactivity, and increased dendritic branching (Costa *et al.* 2016), while a heterozygous loss causes mild neuronal phenotypic defects. iPSC studies of TSC patients cells demonstrated increased astrocyte proliferation, soma size and decreased neurite length in iPSC derived neuronal cultures (Li *et al*. 2017) as well as delayed neuronal differentiation (Zucco *et al.* 2018). Additionally, an increase in neural stem cell and astrocyte proliferation, hypertrophy, and neurite abnormalities in patient cultures had been found by Li *et al.* (Li *et al.* 2017), another research group (Nadadhur *et al.* 2019) found no increase in soma size in neuron cultures of TSC derived iPS cells but could confirm the increase in the number of basal dendrites.

1.8.2. AD in astrocytes

The presence of Aβ results in an immune response by glia cells due to its interaction with glia cell receptors. Therefore, components of the innate immunity cascade are seen as risk factors for AD and have been associated with abnormal Aβ clearing or deposition. Furthermore, Aβ species, like Aβ 1-42, can induce the expression of proinflammatory cytokines like IL1B, IL6, and TNFa (Minter *et al.* 2016). The precise mechanism behind the proinflammatory response in neurons and glia cells is still unknown, although it has been demonstrated that the NFkB pathway is involved (Shi *et al.* 2016). As the role of astrocytes is essential in the CNS, interruptions of their function and therefore of glia transmission may result in different neuropsychiatric disorders as well as neurodegenerative diseases like AD (González-Reyes *et al.* 2017). One example of a functional change in glia cells after a pathological increase of Aβ is calcium dysregulation. Microglia and astrocytes close to senile plaques are activated in order to break down Aβ, this response may result in an inflammatory response, thereby showing both detrimental and neuroprotective results in AD pathophysiology (González-Reyes *et al.* 2017).

It has been demonstrated that Aβ binds to calcium receptors in astrocytes, thereby activating intracellular signalling, inducing the generation of phosphorylated TAU (Chiarini *et al.* 2017), as well as disrupting gliotransmission by enhancing calcium signalling in astrocytes resulting in abnormal calcium levels in AD models (González-Reyes *et al.* 2017). Additionally, studies have found that Aβ can interrupt glutamate uptake capacity (Matos *et al.* 2012), and that expression increase of astrocytic TAU leads to a decline in GLT activity. Also, amyloid species like Aβ 1-42 decrease the expression of GLT-1 and GLAST, two major GLTs in astroglia (De Vivo *et al.* 2010; Matos *et al.* 2012). Therefore, it is predicted that the disruption in the clearance of excitatory neurotransmitters and increased levels of Aβ and TAU from astrocytes are involved in the neuronal excitotoxicity seen in AD (González-Reyes *et al.* 2017). Next to the calcium receptors, the involvement of glutamate NMDA and AMPA receptors in AD physiopathology has been identified (Parameshwaran *et al.* 2008). Several studies have identified the involvement of functional astrocyte NMDA receptor expression in synaptic transmission, and neuronal–glial signalling (Verkhratsky and Kirchhoff 2007; Palygin *et al.* 2010; Parfenova *et al.* 2012). Hence, the Aβ -induced dysfunction of glutamate receptors in astrocytic NMDA receptors, can interfere with neuronal–glial communication (Mota *et al.* 2014) and cause cellular excitotoxicity (Lee *et al.* 2010).

Astrocytes are capable of degrading Aβ enzymatically, and Aβ-containing astrocytes were observed in AD cases. The accumulation of Aβ in astrocytes suggests a failure in the clearance of Aβ in AD and that astrocytes play an important role for the clearance of Aβ. Alterations induced by AD impair the function of the astrocytes, for example by the cells entering their reactive stage to clear Aβ or phosphorylated TAU instead of providing metabolic support of neurons, recycling transmitters, or clearing proteins including Aβ from extra cellular space. Therefore, it is predicted that the Aβ clearance competes with the normal function of astrocytes such as neuronal support (Thal 2012). Research by Mulder *et al.* strengthens the hypothesis that Aβ clearance by astrocytes is not entirely beneficial as well as that fibrillar Aβ influences astrocytic NEP and SCARB1 gene expression and its binding to amyloid-associated proteins such as ApoE and SAP–C1q are required for these effects (Mulder *et al.* 2012). Astrocytes from AD cases did not respond to Aβ–ApoE complexes with an increased NEP and SCARB1 gene expression, as did astrocytes from non-AD subjects. These findings confirm other studies showing that ApoE is required for Aβ uptake by astrocytes (Koistinaho *et al.* 2004) and that astroglial expression of EAAT-*2* can be reduced in AD (Thal *et al.* 2010). Therefore, it can be proposed that astrocytes are functionally altered in AD cases.

The initial reduction of Aβ by astrocytes may be beneficial but a chronically increased Aβ clearance will compete with supporting functions of astrocytes, and reduced numbers of physiologically active astrocytes might lead to the decreased metabolic supply of neurons, reduced protein clearance and, thereby, support Aβ-related neurodegeneration. Research has demonstrated the reduced morphological appearance of astrocytes in animal AD models by using antibodies against GFAP, GS and S100B, but the total number of astrocytes did not change with AD progression (Rodríguez-Arellano *et al.* 2016). The morphological atrophy of astroglial cells likely indicates a reduction in the astroglial coverage of neurons and synapses. Astroglial atrophy might be directly linked to a reduction of astroglial homeostatic support, resulting in severe consequences for performance and survival of neurons as well as functional activity of synapses (Rodríguez-Arellano *et al.* 2016).

1.9. iPSC models

Induced pluripotent stem cells (iPSCs) arise from reprogrammed differentiated somatic cells by expressing four transcription factors (Oct3/4, Sox2, Myc and Klf4), as demonstrated by Takahashi *et al.* (Takahashi *et al.* 2007). iPSCs as pluripotent cells can be differentiated into several cell types by adding the necessary growth/differentiation proteins and co-factors to the cell culture medium. For example, fibroblasts or peripheral blood mononuclear cells (PBMC) from patients with neurodegenerative diseases are reprogrammed and differentiated into neurons to study disease pathology (McKinney 2017). iPSC models have several advantages over animal models such as murine models. Despite being a useful model for research, mouse models have some considerable limitations, especially concerning the genome as around 1% of human genes have no identifiable mouse homologs. Although most of the genes play conserved roles in mice and humans, obvious species-specific differences exist in morphology for example or regulation of gene expression during embryonic development. Consequently, mouse models do not always fully replicate the features of human diseases (Zhu and Huangfu 2013). iPSC derived cell models are extremely useful when no appropriate animal model is available, and they offer the chance to model neuron subtypes like glia and astrocytes (McKinney 2017). Two characteristics of iPSCs make them well suited for studies of human development. First, their pluripotency offers the possibility to examine human development. The *in vitro* culture system also provides a rapid, cost-effective way to interrogate the function of a gene during a specific developmental process. Secondly, iPSCs have unlimited self-renewal capacity, providing abundant material for high-throughput screening (Zhu and Huangfu 2013).

The development of iPSC-based disease models allows the examination of the roles of a specific gene in cell development and the physiological functions of disease-relevant cells (Zhu and Huangfu 2013). The field in which iPSCs have had a major impact was neurobiology/ neurodevelopmental research. Neurodevelopmental and psychiatric disorders are challenging to study, caused by the lack of suitable models due to the essential differences between humans and animal models such as rodents (Dolmetsch and Geschwind 2011). The lack of preclinical models for investigating the pathophysiology of diseases or identifying their therapeutic targets as well as testing potential therapies makes the development of treatments a challenge. Although post-mortem tissue allows to investigate changes in brain structure at cellular and molecular level, the study of neurodevelopmental or neurodegenerative diseases is difficult with this model. With the iPSC pluripotency and therefore the possibility to generate neurons and glial cells from patient cells, it is possible to study cell types with genetic information from patients with, for example, a neuropsychiatric disease.

With the genetic diversity of iPSC from the patient population, the model allows to study how mutations lead to disease, which can be difficult to replicate in genetically modified animals (Dolmetsch and Geschwind 2011). Numerous studies have examined iPSC-derived neurons from patients, including those with schizophrenia, autism, and AD. These cells express characteristics of a fully functional neuron, including cytoskeletal and synaptic proteins, the ability to generate action potentials, and calcium transients. So far, studies have used iPSC-derived neurons to investigate changes in morphology, protein expression, and developmental alterations in disease compared to healthy controls. Additionally, neuronal models can be used for studying mechanisms of psychotropic drug action (Kim *et al.* 2018).

1.10. CRISPR-Cas9 systems

CRISPR-Cas systems have been identified as bacterial adaptive immune systems (Barrangou *et al.* 2007). Bacteria use various CRISPR systems that can be classified into different classes and types based on their characteristics. RNA-guided CRISPR-Cas nuclease system are counted among the genome editing technologies like zinc-finger nucleases (ZFNs), transcription activator–like effector nucleases (TALENs) (Beumer et al. 2013). ZFNs and TALENs use endonuclease catalytic domains to induce targeted DNA double-stranded breaks (DSBs) at specific genomic loci. In CRISPR-Cas9 systems, the nuclease Cas9 is guided by small RNAs to bind to the target DNA, simplifying the process of designing the system and improving its efficiency and specificity. Cas9 edits the genome by stimulating DSB at the target genomic locus. During the cleavage by Cas9, the target area follows one of two major pathways for DNA damage repair: non-homologous end joining (NHEJ), or Homology directed repair (HDR) pathway. In the absence of a repair template, DSBs are repaired through the NHEJ pathway, an error-prone process that can induce insertion/deletion (indel) mutations. Indels occurring within a coding exon, can lead to frameshift mutations and loss of function (Bibikova *et al.* 2002). The HDR process on the other hand occurs at more variable frequencies than NHEJ; it generates precise modifications at a target locus in the presence of a repair template. Multiple DSBs can additionally be used to initiate larger deletions in the genome (Rudin *et al.* 1989; Rouet *et al.* 1994). There are three types (I–III) of CRISPR systems that have been identified, each system includes Cas genes, noncoding RNAs and an array of repetitive elements (direct repeats). These repeats have intervals of short variable sequences known as protospacers, and together they generate the CRISPR RNA array. Within the DNA target, each protospacer is associated with a protospacer adjacent motif (PAM); variation of the PAMs exists between the CRISPR systems (Bae *et al.* 2019).

Different organisms have different CRISPR systems, the CRISPR type II system in *Streptococcus pyogenes* is the simplest. Cas9 in this system is critical for CRISPR RNA (crRNA) maturation, the Cas9 DNA cleavage is triggered by the presence of transactivating crRNA (tracrRNA). The two essential functions of the tracrRNA are the initiation of pre-crRNA processing by RNase III enzymes and the activation of crRNA-guided DNA cleavage by Cas9 (Quiroz and Ryan 2019) (See Figure 1-5). Our group uses the Type II CRISPR system, one of the best characterized systems consisting of Cas9, the guide RNAs and a required auxiliary trans-activating crRNA (tracrRNA) (Cho *et al.* 2014). Analyses show that CRISPR-Cas9–mediated editing can reach efficiency levels up to 80% or more depending on the target (Doudna and Charpentier 2014).

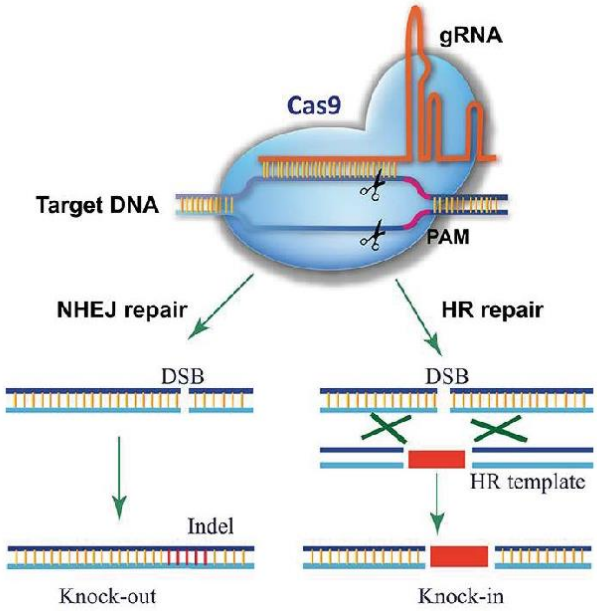

Figure 1-5: Scheme of CRISPR/CAs 9 System of Genome Editing; Type 2 CRISPR System. Cas9 is active when it binds with sgRNA, a complex of Cas9 and sgRNA forms which binds to the target DNA sequence as its sequence is complementary to the sgRNA sequence and PAM sequence. When sgRNA binds with the target sequence, the target sequence strands are cleaved and DSBs are formed (Razzaq and Masood 2018).

1.11. CRISPR-Cas13a system

CRISPR-Cas systems have been identified as bacterial adaptive immune systems (Barrangou *et al.* 2007) and are classified into different classes and types based on their characteristics. Shmakov *et al.* identified a group of bacterial species that contain CRISPR systems called C2c2 (or CRISPR-Cas13), that target RNA instead of DNA (Abudayyeh *et al.* 2016). Cas13 enzymes have two nucleotide-binding (HEPN) endoRNase domains that control precise RNA cleavage (Cox *et al.* 2017) (see Figure 1-6). Abudayyeh *et al.* showed that CRISPR-Cas13 from *Leptotrichia wadei* (LwaCas13a) can induce knockdown effect by targeting and degrading the mRNA in human and plant cells. They demonstrated programmable RNA cleavage with a crRNA encoding a 28-nucleotide spacer in *in vitro* cleavage reactions with LwaCas13a. They monitored the Cas13a-mediated cleavage of the ß-lactamase (ampicillin resistance) transcript by quantifying the number of surviving bacteria colonies (Abudayyeh *et al.* 2017). Unlike the CRISPR Cas 9 system where off target changes (such as deletions, inversions or translocations) are common (Cho *et al.* 2014), tests in mammalian and plant cells have shown no off-target knockdown. Thereby, the Cas 13 system has a lower variability as shRNA libraries due to their significant off-targets (Abudayyeh *et al.* 2017; Cox *et al.* 2017). The Cas 13 system has several advantages over the traditional DNA editing systems such as CRISPR/Cas 9. For example, RNA editing is independent from the HDR machinery which is why it can be used in non-dividing cells such as neurons. Furthermore, Cas13 enzymes are also independent from a PAM sequence at the target locus, making them more flexible than Cas9/Cpf1. Cas13 enzymes do not contain the RuvC and HNH domains responsible for DNA cleavage, so they cannot directly edit the genome and therefore, genomic off-targets or indels introduced through NHEJ are avoided (Cox *et al.* 2017).

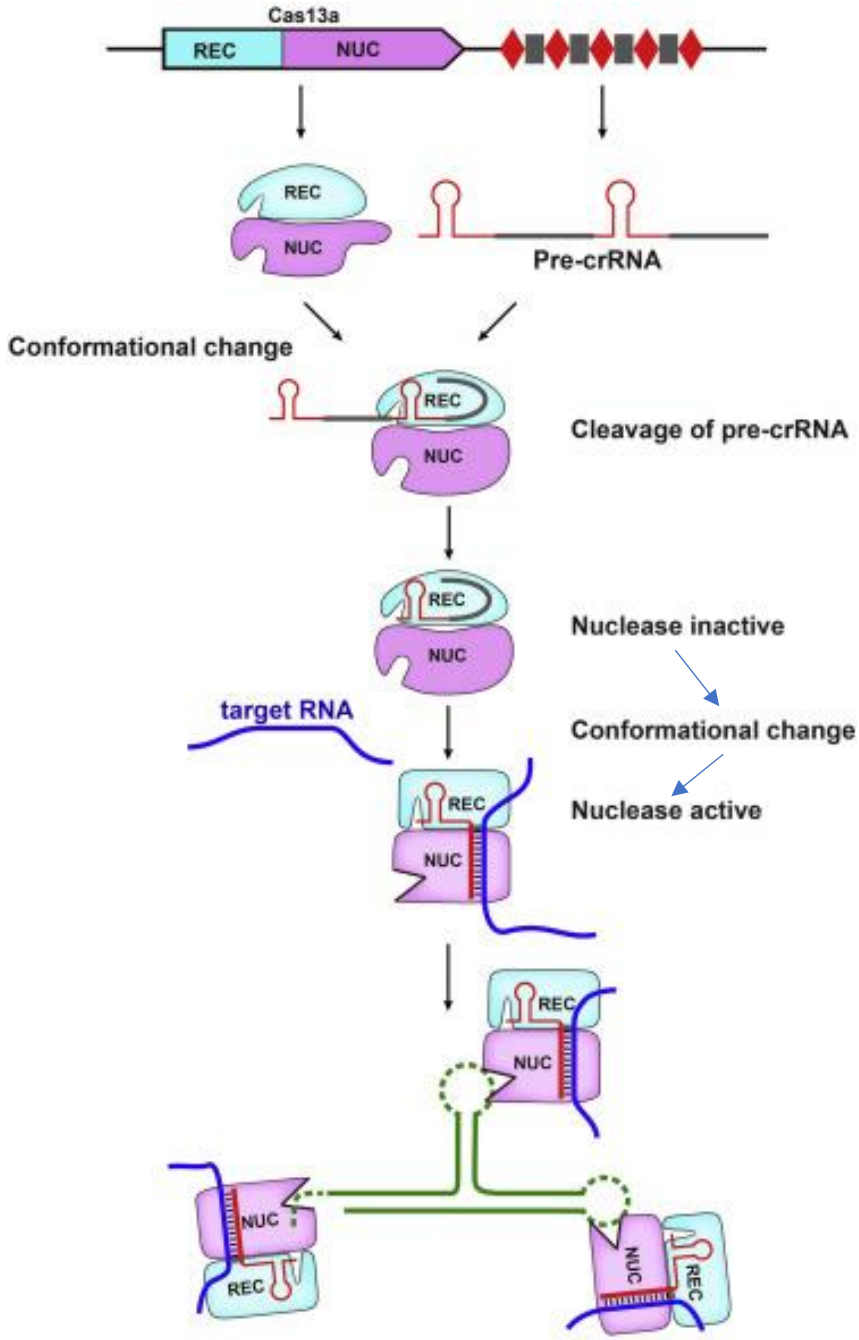

Figure 1-6: Scheme of CRISPR-Cas13a RNA editing (Liu et al. 2017): Cas13a consists of REC (recognition lobe) (cyan) and a NUC (nuclease lobe) (magenta). Cas13a cleaves the pre-crRNA, thus generating an inactive crRNA-guided complex. Cas13a undergoes conformational changes upon target RNA (blue) binding, and the formation of guide-target RNA duplex activates the HEPN catalytic site. The activated Cas13a cleave any single-stranded (ssRNAs) (green). The free RNAs in solution and the bound target RNA beyond the guide complementary region can be the RNA substrate of activated Cas13a.

1.12. Currently available AD models

Although the understanding of AD genetics and pathology has progressed over the last decades, these advances have not yet resulted in the development of therapeutics that either slow or reverse cognitive decline (Scearce-Levie *et al.* 2020). Several AD models, mostly murine, had been developed to define disease related mechanisms and to test potential treatments. Most AD cases are sporadic, and their causes remain unknown as of now. As their cause is still unclear, animal models are based on genetic mutations associated with familial AD. While these models have given important insights into the mechanisms underlying AD by enabling the identification of molecular and cellular pathways that contribute to the production of Aβ and the formation of amyloid plaques, these genetic models only mimic certain characteristics of the disease but none of them display all aspects of AD, unfortunately. For example, APP transgenic mice display Aβ plaques but no NFTs despite TAU hyperphosphorylation, which is a major difference to the human pathology. This led to the hypotheses that (a) rodent TAU has a different structure and therefore might be less prone to aggregation; (b) the life span of mice is too short to lead to enough aggregation as NFT development in humans occurs over decades; or (c) a combination of these (LaFerla and Green 2012). In addition to the previous discrepancies, APP-based models do not display the obvious neuronal atrophy observed over time in AD patients, despite displaying synaptic dysfunction and neuronal loss. Though this lack of massive neuronal death might be due to the lack of a clear TAU pathology as amyloid plaques correlates poorly with cognitive decline in AD unlike TAU (Scearce-Levie *et al.* 2020). As previously discussed, studies indicate that Aβ plaques induce an inflammation response (Koenigsknecht and Landreth 2004; Wang *et al.* 2015).

In conclusion, AD models which would display a closer likeness to the human pathology are clearly needed to establish new treatments. While post-mortem samples from AD patients allow the investigation of the human pathology, they only display the late stages of the disease development and are limited in showcasing the disease progression. In the recent years, iPSC models entered the focus of AD research, especially iPS cells derived from AD patients as they might capture the early disease stage (Julia 2019). Also, large scale genomic studies helped identify risk genes of spontaneous AD, which would allow AD iPSC models designed by genome editing such as CRISPR. Unfortunately, iPSC models have the same disadvantage as murine models: time. iPSC -derived neurons can be easily developed and kept for a few months, but this would still represent a foetal developmental stage and not the neurons of a senior AD patients (Julia 2019).

While some studies attempted to artificially age the cells by inducing telomere shortening for example (Vera *et al.* 2016), they do not mimic the decades an AD patient lived before displaying the disease. Additionally, variations among iPSC lines can easily occur (Volpato *et al.* 2018) from their treatment and care, next to the expected differences between the patients derived-iPSCs due to different genetic backgrounds and lifestyles. Bassil *et al.* designed an AD co-culture model consisting of neurons, astrocytes and microglia derived from iPSCs and exposed to soluble Aβ (Bassil *et al.* 2021). They observed synaptic loss, initiation of an inflammation response, positive staining for phospho-TAU and subsequent neuronal loss. All these characteristics align with the human pathology observed in AD patients, demonstrating the suitability of iPSC -derived models for AD research. Despite utilizing mature neurons for their study (Bassil *et al.* 2021), these neurons will not resemble several decades old neurons from AD patients but their alignment to many AD characteristics still make them a useful model.

1.13. General Aims and Objectives

This project has 4 aims, each with several objectives:

1. Aim 1: The effect complete loss of TSC1 has on brain development is still unclear. The aim of this thesis was to gain an understanding how TSC1 loss in iPS cells affect their neuronal development. The influence of TSC1 loss on a range of developmental and autophagy markers during neuronal development was investigated to ascertain if the genetic mutation would inhibit or alter the neuronal development as homozygous mutations do not occur in patients except in cases of double hit mutation during life.
    i. Design of a TSC1 iPSC line utilising CRISPR-Cas9 systems for genome editing
    ii. Neuronal development of the TSC1 iPSC line and sample collection throughout development
    iii. RT-PCRs for gene expression analysis of developmental and autophagy markers

2. Aim 2: There is uncertainty of the effect on brief and acute TSC1 loss on neuronal development. This thesis aimed to gain an understanding how acute TSC1 loss in iPS cells affects neuronal development and which time points of the development are the most sensitive to acute TSC1 loss. The influence of TSC1 loss on a range of developmental and autophagy markers during neuronal development was investigated to ascertain if the acute loss would alter the neuronal development and if it would mimic the TSC1 knockout cell line. Additionally, the effect of acute TSC1 loss was also tested in astrocytes with focus on their calcium signalling and their reaction to glutamate as previous studies suggested an increased rate of glutamate toxicity in TSC models.
    i. Design of a TSC1 iPSC line utilising CRISPR-Cas13a systems for genome editing
    ii. Neuronal development of the TSC1 iPSC line and sample collection throughout development
    iii. RT-PCRs for gene expression analysis of developmental and autophagy markers
    iv. Astrocytic differentiation of the TSC1 iPSC line and acute induction of TSC1 loss for 48 h

v. Calcium imaging of the TSC1 astrocytes with glutamate induced calcium waves.
vi. Staining for apoptosis after brief glutamate treatment of the astrocytes

3. Aim 3: To gain a better understanding about the effect of TSC1 loss has on cells, this project aimed to find additional potentially altered pathways in TSC to test their expression in the previously designed TSC1 cell lines. As studies have shown a strong involvement of inflammation in TSC, the expression of inflammation markers during the neuronal development was also investigated.
    i. Performing a database analysis of TSC patients with focus on inflammation and AD
    ii. RT-PCRs for gene expression of inflammation and urokinase markers

4. Aim 4: Comparing the expression pattern of the tested markers in TSC with AD studies to establish any potential commonalities.

2. General Material and Methods

2.1. Cell line and Maintenance

The Cas9 (generated by Dr. Mouhamed Alsaqati and Dr. Ian Tully) (Tully 2020) and Cas13 (generated by Dr. Gemma Wilkinson) cell lines that were used in this project to generate TSC1 cell lines were designed from the IBJ4 IPs cell line, originally gifted from Josh Chenoweth from the Lieber Institute for Brain Development, MD, USA. The cell lines insert either the Cas9 or the Cas13 gene into the AAVS1 locus under a tetracycline inducible promoter. This locus allows stable, long-term gene expression for the Cas systems in the cells (Oceguera-Yanez *et al.* 2016) and enables therefore an easier application of CRISPR. All iPS cells were maintained as feeder-free cultures in Essential 8^{TM} Medium (Thermo Fisher, #A1517001; prepared according to the manufactures instructions) and on a matrix layer of Matrigel (Corning, #354234) or Cultrex (Biotechne, #3434-010-02). To prepare plates for the iPS cells, frozen 100% Matrigel or Cultrex aliquots were slowly thawed and diluted 1:85 in DMEM/F12 1:1 (Thermo Fisher, #12634-010) and plated onto the plastic ware at 1 mL/9.6 cm2. Coated plates were incubated for at least 1 h at 37˚C, after which plates were washed with Gibco DPBS without Magnesium and Calcium (Thermo Fisher, #12559069) and maintained with DPBS until use. Used diluted Matrigel was reused once on a further plate for coating before being discarded, while Cultrex can only be used once.

2.2. Defrosting iPS cells

Frozen 1 mL vials of iPS cells were rapidly thawed at 37˚C, before being added into 5 mL of E8 medium and centrifuged at 200rcf for 3 mins. After aspirating all the medium, cells were re-suspended in 3 mL of E8 with Rock/Rho pathway inhibitor Y27632 (1:500, referred to herein as Y27; Stem Cell technologies, #72302) and plated into 2 wells of a 6 well plate pre-coated with Matrigel or Cultrex as described. Y27 has been shown to improve the survival of human pluripotent stem cells after thawing and single cell dissociation (Watanabe *et al.* 2007; Li *et al.* 2008). After 24 h, the medium was aspirated; cells were washed with DPBS to remove dead cells and 2 mL of fresh E8 without Y27 were added to each well. iPS cells were maintained in E8 with media changes every day until 70-80% confluency, at which point cells were passaged using Gentle Cell Dissociation Reagent (Stem Cell Technologies, #07174).

2.3. iPSC growth and maintenance

For standard passaging, following aspiration of medium and washing with DPBS, 1 mL Gentle cell dissociation reagent was added per well of cells (for 6 well plate, for plates with a higher well number a lower volume of Gentle cell was used respectively) and incubated at 37˚C for 3 mins. The reagent was then carefully aspirated, and the cells were covered with 1 mL E8. Cells were then lifted from the culture surface by scratching with a 1000 µL pipette and were collected into a 15 mL universal centrifuge tube. For routine maintenance of the line, cells were passaged and diluted with E8 based on the number of wells being passaged and the number of wells required (usually a 1:6 dilution in case of the six well plate).

2.4. iPSC freezing

For freezing iPS cells for storage, Y27 (1:500) or RevitaCell (1:100, Thermo Fisher, #A2644501) was first added to the cells for at least 1 h before freezing (cells needed at least 70% confluence prior freezing). Cells were frozen in a cryoprotection medium of E8 containing a concentration of 10% dimethyl sulfoxide (v/v) (DMSO; Sigma-Aldrich, #D2650). Cells were dissociated for freezing following the same protocol as that described for standard cell passaging with gentle cell dissociation reagent. Once collected, cells were then centrifuged at 200rcf for 3 mins. After aspiration of medium, cells were gently re-suspended in cryoprotection medium (1 ml for each well of a 6-well plate). In this way, pooled wells of cells were frozen according to the number of wells being frozen. 1 mL of re-suspended cells were added per cryovial, and vials were placed in a CoolCell freezing box “Mr. Frosty” (freezing box needed to be at RT (room temperature) prior use) (Biocision) and transferred to a -80 °C freezer for at least 3 h. Cells were transferred to liquid nitrogen for long terms storage within 48 h. As the generation of the Cas13 TSC1 cell line required first the generation of the Cas13 cell line itself (performed by Dr. Gemma Wilkinson) and then the electroporation of the cell line with the TSC1 plasmid, the result is a higher passage number of around 60. Similarly, the generation of the TSC1 -/- cell line required intense time and genome testing and resulted in a high passage number of around 60. This was partly due to using a currently in use IBJ4 Cas9 line which had accumulated a few passages since defrost.

2.5. CRISPR Lipofection and Sub-cloning

The nuclease transfection of the stem cells was performed according to the protocol from Thermo Fisher (Lipofectamine CRISPRMAX Cas9 Transfection Reagent Protocol, Thermo Fisher, CMAX00008). Prior that protocol, the gRNA (guide sequences were a gift from Prof. Bateup from the US and were successfully used in their lab (Blair *et al.* 2018) needed to be added to the tracer RNA and duplexed via PCR. The cells were treated for 48 h altogether with doxycycline (when cells reached ~70% confluency), starting with 24h prior the transfection for the induction of Cas 9 expression in the cells. The Lipofection took place one day after passaging the stem cells, leading to the Lipofection of many smaller colonies and therefore an increased surface of cells. The transfection was repeated the next day to increase the chance of a successful Lipofection. As soon as the colonies reached 80-90% confluency, they were treated for one hour with Y27 and then single celled by incubating them with Accutase (Thermo Fisher, #A1110501) for 10 min at 37˚C. The cells suspended in the Accutase were collected in a 15mL Tube and 5 mL of E8 were added for neutralizing the Accutase. Once collected, cells were then centrifuged at 200rcf for 3 mins. After aspiration of medium, cells were gently re-suspended in E8 (1 mL for each well of a 6-well plate). The cells were then added in the dilution of 1:500 and 1:1000 into a previously coated petri dish containing E8 and Y27. After 5-7 days, when the single cells reached a bigger colony size, the petri dishes were treated for 1h with Y27 and the cell colonies were picked under the Evos XL core microscope and added into separate wells of a 96 well plate (precoated with Matrigel and filled with 100uL of E8 with Y27). These colonies are kept until they reach confluency before being passaged into either a 24- or 48- well plate.

2.6. Sequencing Preparation

For sequencing the cell cultures to identify which have the desired mutation, DNA was extracted from cells using QuickExtract DNA Extraction Solution (Lucigen). The cells were dissociated from plates using Gentle cell as described previously when they reached >70% confluency. While half the cells were passaged into a new plate, the second half of the cells was added to 30-100mL of QuickExtract solution. This solution was vortexed for 30 seconds and then incubated at 65°C for 6 minutes. After another mix via vortex, the solution was incubated at 98°C for 2 minutes. Samples were then placed on ice or stored at -20°C until required for PCR.

2.7. PCR amplification for Sequencing

Genomic DNA was amplified by PCR using the GoTaq G2 Mastermix (Promega). The PCR Protocol of the lab was designed to contain the Mastermix at 1X concentration (12.5mL), 10mM forward primer, 10mM reverse primer (1mL for each Primer), <100ng genomic DNA (4mL) and nuclease-free water (5.5mL) resulting in a total volume of 25mL.

The PCR reaction was then amplified in a thermocycler using the following programme:

Initial Denaturation	98°C	30 s,	
Initial Denaturation	98°C	30 s	
30 Cycles of:		98°C	10 s
		30 s	*(Annealing temperature was primer dependent)*
	72°C	30 s/kb	
Final Extension	72°C	2 min	
Hold	4°C		

PCR reactions were then run on a 2% (w/v) agarose gel with TBE Buffer to verify specific amplification of the DNA.

The Primers were designed on Benchling (an online platform for biotech research) to amplify Exon 17 of TSC1, including the guide cut sites. Primers used for sequencing had M13 tags added to the 5'-end. The annealing temperature for both these sets which allow the attachment of the barcode primers in the second PCR was 58°C. DNA that was amplified using M13 tag primers for sequencing was then diluted 1:100 before being reamplified by PCR using barcoded primers (see Table 1). These primers allowed the PCR product of up to 96 samples from subcloned cells to be pooled together for sequencing, as the barcodes were used to identify individual samples.

Table 1: Primers for amplification of TSC1 Exon 17 and sequencing barcodes

Primer	**Sequence (5' to 3')**
TSC1 Exon17 Fwd	AGACTTCCTGCCAGGCTTCCCT
TSC1 Exon 17 Rev	CTGACTGGCTTCACACCCGCTG
M13 *TSC1* Exon 17 Fwd	GTAAAACGACGGCCAAGACTTCCTGCCAGGCTTCCCT
M13 *TSC1* Exon 17 Rev	GGAAACAGCTATGACCATGCTGACTGGCTTCACACCCGCTG
Barcode Fwd 1	AAGAAAGTTGTCGGTGTCTTTGTGGTAAAACGACGGCCA
Barcode Fwd 2	TCGATTCCGTTTGTAGTCGTCTGTGTAAAACGACGGCCA
Barcode Fwd 3	GAGTCTTGTGTCCCAGTTACCAGGGTAAAACGACGGCCA
Barcode Fwd 4	TTCGGATTCTATCGTGTTTCCCTAGTAAAACGACGGCCA
Barcode Fwd 5	CTTGTCCAGGGTTTGTGTAACCTTGTAAAACGACGGCCA
Barcode Fwd 6	TTCTCGCAAAGGCAGAAAGTAGTCGTAAAACGACGGCCA
Barcode Fwd 7	GTGTTACCGTGGGAATGAATCCTTGTAAAACGACGGCCA
Barcode Fwd 8	TTCAGGGAACAAACCAAGTTACGTGTAAAACGACGGCCA
Barcode Fwd 9	AACTAGGCACAGCGAGTCTTGGTTGTAAAACGACGGCCA
Barcode Fwd 10	AAGCGTTGAAACCTTTGTCCTCTCGTAAAACGACGGCCA
Barcode Fwd 11	GTTTCATCTATCGGAGGGAATGGAGTAAAACGACGGCCA
Barcode Fwd 12	CAGGTAGAAAGAAGCAGAATCGGAGTAAAACGACGGCCA
Barcode Rev A	AGAACGACTTCCATACTCGTGTGAGGAAACAGCTATGACCATG
Barcode Rev B	AACGAGTCTCTTGGGACCCATAGAGGAAACAGCTATGACCATG
Barcode Rev C	AGGTCTACCTCGCTAACACCACTGGGAAACAGCTATGACCATG
Barcode Rev D	CGTCAACTGACAGTGGTTCGTACTGGAAACAGCTATGACCATG
Barcode Rev E	ACCCTCCAGGAAAGTACCTCTGATGGAAACAGCTATGACCATG
Barcode Rev F	CCAAACCCAACAACCTAGATAGGCGGAAACAGCTATGACCATG
Barcode Rev G	GTTCCTCGTGCAGTGTCAAGAGATGGAAACAGCTATGACCATG
Barcode Rev H	TTGCGTCCTGTTACGAGAACTCATGGAAACAGCTATGACCATG

2.8. MinION sequencing

2.8.1. Library preparation

Barcoded PCR products were pooled together and purified using the Wizard® SV Gel and PCR Clean-Up System and its protocol (Promega, #A9281). Membrane binding solution was added to the PCR products in an SV Minicolumn. After incubation for one min the mixture was centrifuged at 16,000 RCF for 1 min. The flow through was discarded and the Minicolumn was washed twice with Membrane Wash Solution (flow-through discarded after each spin) and the membrane dried by centrifugation at 16,000 RCF for 1 min. The DNA bound to the membrane was eluted in 50µL of nuclease-free water after one min of incubation before centrifugation at 16,000 RCF for 1 min. The DNA concentration was measured using NanoDrop. 1µg of purified DNA was used for sequencing using the $1D^2$ sequencing kit (Oxford Nanopore, #SQK-LSK308). The DNA was incubated with Ultra II End-prep reaction buffer, nuclease-free water and enzyme mix for 5 mins at 20°C and 5 mins at 65°C. AMPure XP beads (Beckman, #A63880) where then added to the mixture and incubated for 5 mins at room temperature under continuous tube flicking. The sample was pelleted on a magnet and washed with 70% (v/v) ethanol, before being resuspended in nuclease free water. The sample was incubated for two mins and then pelleted on a magnet. The eluate was removed and incubated with 1D2 Adapter and Blunt/TA Ligase Master Mix (NEB, #M0367S) for 10 mins at room temperature. AMPure XP beads were added to the sample and incubated for 10 mins with continuous tube flicking. The magnet is used to pellet the sample and 70% (v/v) ethanol is used for washing prior sample resuspension in nuclease-free water.

The eluate was removed and incubated in a fresh tube with Barcode Adapter Mix and Blunt/TA Ligase Master Mix for 10 mins at room temperature before another AMPure XP beads incubation for 10 mins under constant tube flicking. The sample was pelleted on a magnet and washed twice with ABB buffer before being resuspended in Elution buffer. The sample was incubated for 10 mins before the beads were pelleted on a magnet and the eluate was transferred into a clean 1.5mL tube. The next step was the preparation of the flow cell. The flow cell was inserted into the MinION. A small amount of buffer was drawn back from the priming port of the flow cell to remove any bubbles. 800µL priming mix (576µL Running buffer with Fuel Mix 624µL of nuclease-free water) was loaded into the flow cell via the priming port and incubated for 5 mins. After the incubation, the remaining 200µL of priming mix was added to the flow cell via the priming port. The prepared DNA sample was mixed with Running buffer with Fuel Mix and Library Loading Beads and loaded onto the flow cell via the sample port.

The MinION was then connected to a computer with the MinKNOW programme. The sequencing run was then started via this programme after selecting the flow cell type. The sequencing was run until around 400,000 reads were acquired.

2.8.2. Sequencing Analysis

The reads were base called using Albacore to generate FASTQ files and sorted according to their barcodes. The read sequences were then aligned to the reference genome for TSC1 Exon 17. A script, written by Dr. Ian Tully, was used to identify if deletions were present in the barcoded samples (Tully 2020). To confirm the presence of deletions, the barcoded reads were checked on Integrative Genomics Viewer.

2.9. Differentiation Protocols

2.9.1. Differentiation of glutamatergic neurons from iPS cells

The neuronal differentiation protocol used in this project is the basic protocol used within the research group to produce forebrain glutamatergic projection neurons. This is a well characterised protocol based upon the dual-SMAD inhibition methods described in publications (Chambers *et al.* 2009; Shi *et al.* 2012). Two days before the start of neural induction (D0), confluent wells of iPS cells were passaged with Gentle Cell (as described previously) and plated onto 12 well plates pre-coated with reduced growth factor Matrigel (Corning, #354230) or Cultrex (Biotechne, #3434-010-02); the standard passage ratio was 1:6. Cells were maintained with E8 until 80-90% confluency after which cells were washed once with DPBS. N2B27-RA (for 150mL: 100mL DMEM/F12 (Thermo Fisher, #12634-010), 50 mL Neurobasal (Thermo Fisher, #21103049), 1mL N2 (Thermo Fisher, #17502001), 1mL B27- (Thermo Fisher, #12587010), 1.5mL PSG (Thermo Fisher, #10378016), 150µl beta-mercaptoethanol (Sigma Aldrich, #M3148)) was used as a media containing LDN193189 (LDN; Sigma-Aldrich, #SML0559, concentration 1:10000) and SB431542 (SB; Sigma-Aldrich #S4317, concentration 1:1000).

iPS cells were maintained in this neural induction medium, with half medium changes every 2 days, for around 8-12 days after which point multi-layered colonies of cells could be seen. After 10 days, the media is switched to N2B27- without LDN and SB. For the first passage, cells were initially pre-treated for 2 hours with 10 µM Y27, after which the medium was removed from cells and DPBS was used for washing the cells. After the DPBS removal, 500 µL of Versene (Thermo Fisher, #15040066) was added to each well and cells were incubated for 3 mins at 37 °C. After Versene aspiration, 500 µL of fresh N2B27-RA with 10 µM Y27 was added to each well and cells were detached from the plate by scratching using a 1 mL pipette tip. The collected cells were then split into a passage ratio of 2:3 and plated onto a pre-coated plate with fibronectin (Millipore; #FC010) with 1.5mL of fresh N2B27 media with 10 µM Y27. Cells were maintained with half medium changes every two days for around 9-10 days, after which multilayer colonies comprising neural rosettes were visible. At this point (D18-22), cells were deemed to be neural precursor cells (NPCs) and differentiations were either continued to produce neurons or NPCs were frozen for storage and later use. If the differentiation is continued, the cells will be passaged around day 18-20, the required coating is PDL (Sigma Aldrich, #P6407-5MG) for 2h, following a DPBS wash and a 2h incubation with Laminin (Sigma Aldrich, #L2020-1MG). Cells are then passaged at a 1:3 ratio (1:2 for TSC1 -/- cell line) with Y27.

After day 26, N2B27 +RA media was continuously used for the cells exchanging B27- with B27 with Vitamin A (Thermo Fisher, #17504001)). Cells required an additional passage around Day 30 due to the continuous proliferation of the remaining NPCs, the ratio was 1:3 (1:2 for TSC1 -/- cell line).

2.9.2. Astrocyte Differentiation protocol

The astrocyte differentiation protocol utilizes the neuronal differentiation protocol for the first 21 days. The cells are deemed to be neural precursors (NPCs) around Day 18-22, and around that time point the cells will have been passaged onto a PDL/Laminin coated plate. Starting on Day 22, the media was changed completely to Astrocyte Media (CalTag Medsystems, #SC-1801) with 2% FBS and then exchanged every 2-3 days based on cell confluency. The cells were kept on the plate for 10 days prior passage using Accutase for 10 min onto a Geltrex coated plate (1h coating incubation required; Thermo Fisher, #15180617). The cells were collected with the accutase in a 15mL flacon with 5mL of media to deactivate the Accutase, prior a 5min spin at 200rcf. The media is then aspirated, the cells are diluted in fresh media and split 1:6 onto the new plate; parts of the old media was kept and then added to the new plate as the expressed factors from the cells in it are required for the cell development. The cells will be passaged according to need with Accutase, as the cell should stay single cells and not develop colonies. When high confluency is reached the cell morphology will resemble neurons. The 2% FBS media is used for 2 weeks, after that a 1% (v/v) FBS astrocyte media will be needed for the cells for another week. During that time, the Geltrex coating will not be necessary anymore as the cell should start resembling early astrocytes which are able to attach to non-coated plates. After the 3 weeks, the Serio media is required for the astrocytes, it includes: 50mL advanced DMEM/F12 (Thermo Fisher, #11540446), 0.5mL Glutamax (Thermo Fisher, #35050038), 0.5mL NEAA (Thermo Fisher, #11140050), 0.5mL N2 (Thermo Fisher, # 17502001) and 0.5mL FBS (Thermo Fisher 16000036). Additionally, 20ng/mL of both BMP4 (Peprotech, #120-05ET) and CNTF (Peprotech, #450-13) will be added to the media for 5 weeks. With the introduction of BMP4 the proliferation rate will drastically decline until it will stop completely, therefore a smaller passage split is recommended to avoid cell loss (2:3 or 1:2).

2.10. Bacterial cloning for Cas13a system

2.10.1. Guides Design for cloning

Cas13 guides (see Table 2) were designed using the RNAxs siRNA design algorithm from the RNAxs Webserver designed by the University of Vienna (Tafer 2018) as this had previously been successfully used in the Harwood group previously to design guides for Cas13. They were lengthened to 28 nucleotides, which is required for Cas13 gRNA efficacy. Guides were ordered as DNA oligonucleotides from IDT with the addition of 4nt overhangs on the 5' end of the guide and reverse complement sequence for cloning into the gRNA plasmid. Each guide and reverse complement were combined and left for 1h at room temperature to anneal together before being cloned into the gRNA plasmid. Guides for TSC1 were designed to target early constitutive exons of *TSC1* (Exons 1, 12 and 17).

Table 2: Cas13a Guide Sequences

Cas13a Guide	Sequence
TSC1 Exon 1 Guide	AAA AGA ATG GCC CAA CAA GCAAAT GTC GGG GA
TSC1 Exon 1 Guide	AAA CTC CCC GAC ATT TGC TTG TTGGGC CAT TC
TSC1 Exon 12 Guide	AAA ACA CTC CCA GTC CTT GTA AAATTC CAC CT
TSC1 Exon 12 Guide	AAA CAG GTG GAA TTT TAC AAGGAC TGG GAG TG
TSC1 Exon 17 Guide	AAA ACG CAC CCT CCG AGA CCAGTT GCT TTT AC
TSC1 Exon 17 Guide	AAA CGT AAA AGC AAC TGG TCTCGG AGG GTG CG

2.10.2. Cloning and Bacteria transformation

TSC1 guides were inserted into the plasmid Ca13pgRNA-CKB (Addgene #73501) (see Figure 2-1) via enzyme digest. For that, 6 µL of PGRNA (Cas13-msfGFP), 1µL of the Restriction Enzyme Esp3I (New England Biolabs, #R0734S) as well as 3,3µL of the Cutsmart Buffer are mixed into a 1.5ml tube (final concentration of vector is 30ng/µL) and incubated for 1h at 37 °C. The following step is the ligation of the linearized and purified vector with small DNA inserts; 30ng of the vector is mixed with the designed guides (1:100 dilution of guides; 1.5 µL of guide), 0.5 µL of Ligase, 1 µL of 10x Buffer and 6 µL of nuclease-free Water and incubated for 1h at room temperature. For a clean ligation product, a 10min incubation of the Ligase product with 0,5µL of Esp3I at 37 °C is recommended.

The first step is to prepare agar plates for the bacteria. Agar is melted by microwaving at 30% power for approx. 30-40 minutes and it is allowed to cool down to approximately 55°C before adding Ampicillin (final concentration of 100mg/ml). Stripettes are then used to add the agar into Petri dishes under a hood, the lids should rest lids half-covering the agar plates until the agar solidifies and cools down so there will be no more condensation on the lids. Plates are the either stored at 4 °C for later use or placed lid down in 37°C oven to warm for immediate use.

The next step is to transform the plasmid into bacteria by using the Heat shock protocol. Single tubes of 5-alpha E. coli (NEB; #C2987I) is thawed on ice for 10 minutes. 25ml per transformation is used and 3ml of plasmid DNA is added to the cell mixture and carefully flicked 4-5 times to mix cells and DNA. The mixture is then placed on ice for 30 minutes before being heat shocked at 42°C for 30 seconds. The cells are them placed on ice for 5 minutes before 950ml of SOC medium is added into mixture (at RT). The cells then rest at 37°C in a shaker (220rpm) for 1 hour while the agar plates are warmed to 37°C. After removing the cells from the shaker, the cells are thoroughly mixed by flicking tube and inverting, before being diluted (about 1:4) in SOC. 100m of each dilution (one for each guide) is then spread onto an agar plate and incubate overnight at 37°C. Since the plasmid includes an Ampicillin resistance gene, only cultures which have the plasmid inside can grow on the agar plate. The next day, colonies are picked and added into liquid culture tubes with 4-5 ml LB broth and 100mg/ml Ampicillin before being incubated in a rotary shaker overnight at 37°C 180-220rpm.

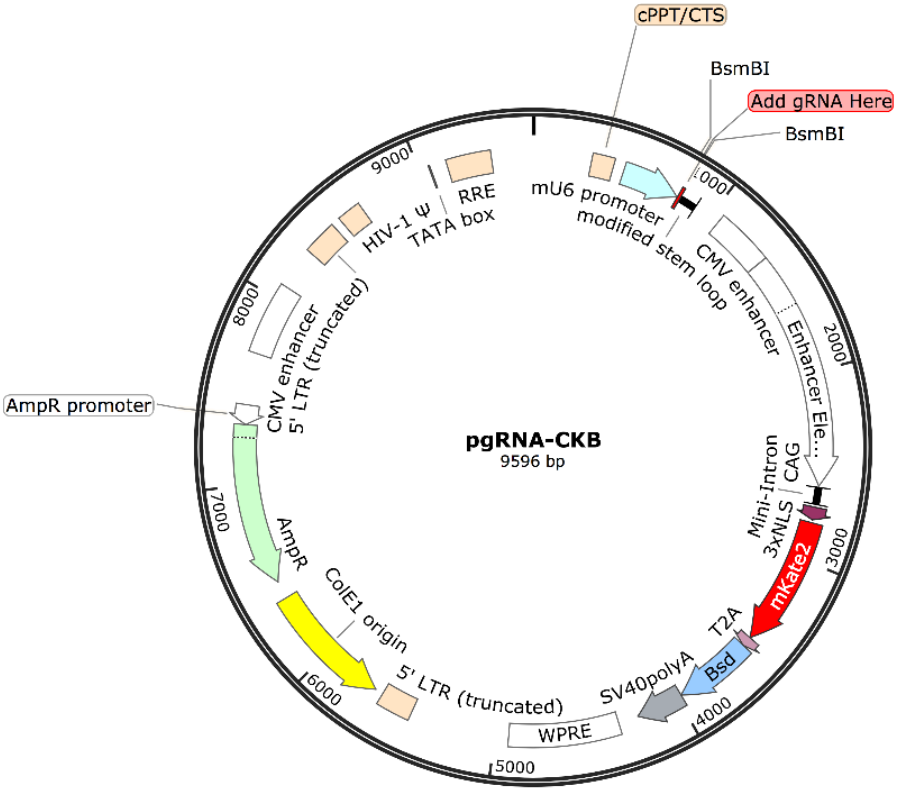

Figure 2-1:Scheme of the Cas13 plasmid (Addgene), TSC1 gRNA was inserted at the BsmBI cut site

2.11. MINI-Prep of plasmid DNA

Aliquots of 1ml are taken from the liquid bacteria into 1.5ml Eppendorf's, the tubes then spin in a centrifuge at 16 000 rpm for 1 min and the supernatant is removed from the cell pellet. Bacterial pellets are resuspended in 100ml P1 resuspension buffer (25mM Tris-HCl, pH 8.0, 10mM EDTA); 2.5ml RNAse A is added per 1ml P1. Then, 100ml of P2 lysis buffer (200nM NaOh, 1% SDS) is added and the Suspension is gently mixed prior a 4 min incubation.

120ml of P3 neutralisation buffer (5M potassium acetate, pH 5.5) is added and gently mixed before incubating it for 3 min. After the incubation spin in the centrifuge at 16 000 rpm for 2 min before the supernatant is taken and transferred into a new tube. For precipitation of the plasmid DNA from the supernatant, 200ml of isopropanol is added and mixed by inverting; mixture incubates for 1 min before a Centrifuge spin 14,000 rpm for 1 min. Supernatant is poured off, and 200ml of 70% ethanol (v/v) is added to the Eppendorf which is then centrifuged at 14,000 rpm for 1 min.

After the spin, the ethanol is poured off immediately and the tubes spin down again at 14,000 rpm for 1 min to get rid of the leftover ethanol. Remaining ethanol is removed with a pipette and the tubes are allowed to air dry for 10 mins with caps open on bench. The DNA is the dissolved in 30ml nuclease-free water and its concentration is measured by using the NanoDrop. To test which bacterial cultures may have the guide inserted, a Digest of the Mini-Prep samples (see Digestion Protocol in 2.10.2) as well as a positive control (plasmid without guide) was performed. Gel electrophoresis with a 1% Agarose Gel with TAE buffer was performed.

2.12. MAXI-Prep of plasmid DNA

For the Maxi-Prep, the PureYield™ Plasmid Maxiprep System kit is used, and the attached protocol was followed. 100–250 ml of transformed E. coli cells are grown overnight. The bacteria culture is poured into 50 ml falcons and the cells were pellet at 5,000 × g for 10 minutes. The supernatant is discarded while the cell pellets are resuspended thoroughly in 12ml of Cell Resuspension Solution by vortexing or pipetting. 12 ml of Cell Lysis Solution is added, mixed, and incubated for 3 minutes at room temperature. Then 12 ml of Neutralization Solution is added, and the falcons are gently inverted 10–15 times to mix. The lysate is centrifuged at 14,000 × g for 20 minutes at room temperature using a fixed angle rotor. For plasmid DNA purification the columns of the kit are assembled and placed on a vacuum manifold.

The lysate is poured into the column and vacuum is applied until the lysate has passed through both the clearing and binding columns. The blue PureYield™ Clearing Column is discarded and the PureYield™ Maxi Binding Column is left on the vacuum manifold. 5 ml of Endotoxin Removal Wash is added to the PureYield™ Maxi Binding Column, and a vacuum is applied to allow the solution to be pulled through the column. 20 ml of Column Wash is added, and the vacuum is applied to pull the solution through the column. The membrane is allowed to dry for 5 min by applying a vacuum. The Pure Yield™ Maxi Binding Column is removed from the vacuum manifold and placed into a new 50 ml centrifuge tube. A 1.5 ml microcentrifuge tube is placed into the base of the Eluator™ Vacuum Elution Device (Promega, #A1071), securing the tube cap in the open position. The Eluator™ Vacuum Elution Device is assembled and the DNA binding column is inserted into the device. The elution device assembly is placed onto a vacuum manifold and 1ml of Nuclease-Free Water is added to the DNA binding membrane in the binding column and incubated for 1 minute. Vacuum is applied until all liquid has passed through the column and the DNA quantified. To verify that the product has the guide inserted, test which bacterial cultures may have the guide in them, the Maxi-Prep sample is digested and gel electrophoresis with a 1% Agarose Gel with TAE buffer is performed.

2.13. Nucleofection of Plasmid

The plasmid was inserted via electroporation into the cells. For that, the Cas13 iPSCs were grown in a 6-well plate until they reached high confluency. Additional plates coated with Cultrex or Matrigel were prepared as each electroporated well will be split 1:4 after the treatment. Prior the nucleofection, the cells were treated with Y27 for at least an hour while the new plates were prepared with E8 media and Y27 (10 µl/ml). P3 solution consisting of 18µl of supplement + 82µl of P3 + plasmid (2.5µg) or GFP (1 µl as control) was prepared, resulting in little of 100ul for each treated well (Amaxa P3 Primary Cell 4D-Nucleofector X Kit L, Lonza, #V4XP-3024). Cells are washed with PBS prior 9 min accutase incubation at 37° C. During the incubation, the Lonza nucleofector machine is set up using the custom programme iP1 with the pulse code CA-137 for iPSCs. After the accutase incubation, the cells are transferred into a 15 ml Eppendorf tube and centrifuged at 150 g for 3 minutes before accutase aspiration and PBS cell wash through gentle pipetting. Cells are then centrifuged again for 3 min at 150 g before being resuspended in the P3-plasmid solution. The cell solution is added to appropriately labelled cuvettes and electroporated in the nucleofector machine. Using a Pasteur pipette, the cells are collected from the cuvettes and split 1:4 into the freshly prepared plates with E8 and Y27. Media is then changed for E8 the following day, 48 h post transfection Blasticidin is a 1:1000 dilution of 5 mg/ml to a final concentration of 5 µg/ml. As the plasmid contains Blasticidin resistance, cells with a successful transfection will survive the treatment while non-transfected cells will die throughout the antibiotic treatment. The treatment continues for 5-7 days or until all GFP control cells have died. As the plasmid contains the fluorescence marker mKATE2 and GFP (the latter is doxycycline induced), the cells can be checked underneath a fluorescence microscope.

2.14. RNA Isolation

For isolating RNA from cell samples, the Qiagen RNeasy Plus Mini Kit (Qiagen, #74136) was used and its protocol followed. The RLT Buffer of the kit was prepared with β-mercaptoethanol according to the protocol, as well as the RPE Buffer. 600 µl of the RLT Buffer was added to the samples prior adding vortexing and adding them to the gDNA tubes for a 30s spin down in the centrifuge at 8000 x g or more. The flowthrough is collected and mixed well with 600 µl of freshly made 70% Ethanol. Then, 700 µl of the sample mix is transferred to a RNeasy Mini spin column placed in a collection tube, the lids are closed and centrifuged for 15 s at 8000 x g or more. The flow-through is discarded and the precious step is repeated with the rest of the sample. After the flowthrough is discarded again, 700 µl of the RW1 Buffer is added to the column prior another centrifugation (15 s). Flowthrough is then discarded and 500µl of RPE Buffer is added and the column is centrifuged (for 15 s) and the flowthrough discarded, before repeating the RPE Buffer step once more (2 min for the second spin). The RNeasy column is then added to a new collection tube and spin empty in order to remove any residual wash buffers for 1 min before putting the RNeasy Mini column into a fresh 1.5 ml tubes and 40 µl of nuclease free water is added directly to the spin column membrane, incubates for 1 min at RT and the column is then centrifuged for 1 min at 8000 x g.

2.15. cDNA-Synthesis

For transforming RNA into cDNA, a final RNA concentration of 0.75 µg/µl is needed, so the samples are diluted accordingly. The High-Capacity cDNA Reverse Transcription Kit (Thermo Fisher, # 4368814) is used for this protocol. For each sample, a Master Mix consisting of 2 µl of 10xRT Buffer, 0,8 µl of 25xdnTP, 1 µl of Transcriptase, 4.2 ul of nuclease free water and 2µl of Random Primers (part of the Kit) are mixed and added to 10 µl of RNA with a 0.75 µg/µl concentration. The samples then undergo a heating protocol in a PCR machine with 10 min at 25° C, 2h at 37° C and 5 min at 85° C. The cDNA is then diluted 1:10 with nuclease free Water prior Nanodrop for concentration measurements. For qPCRs, the cDNA will be diluted to a 75 ng per 2 µl concentration prior the experiment.

2.16. qPCR Protocol

For the qPCR reaction, 2 µl of sample (concentration 75 ng) is used. The sample is topped up by 18 µl of a Mastermix consisting of 6.4 µl nuclease free Water, 0.8µl for both forward and return primer and 10µl of qPCRBIO Blue SyGreen (PCR Biosystems PB20.16). Each sample is tested in a Triplicate. The qPCR plates are run on the StepOne qPCR machines from Thermo Fisher, the qPCR run consists of the Holding stage which is 2 min at 95° C, and the Cycling Stage consisting of 40 cycles (each cycle has 5 seconds at 95° C and 20 seconds at 60° C). Data was exported to Microsoft Excel and analysed using the ΔCt method for relative quantification of the mRNA abundance (Heckmann et al. 2011). Beta-Actin was chosen as the house keeping gene. The primer sequences for the qPCRs utilised in this project can be found in Table 3.

Table 3: qPCR Primer Sequences

Name	Primer Forward 5'-->3'	Primer Reverse 5'-->3'
Beta-Actin	TCACCACCACGGCCGAGCG	TCTCCTTCTGCATCCTGTCG
S100B1	ACAAGGAAGAGGATGTCTGAGCTG	TGTCCACCTCCTGCTCTT
Nestin	AGCAGGAGAAACAGGGCCTAC	CTCTGGGGTCCTAGGGAATTG
Pax6	GTGTCCAACGGATGTGTGAG	CTAGCCAGGTTGCGAAGAAC
FOXG1	AGGAGGGCGAGAAGAAGAAC	TCACGAAGCACTTGTTGAGG
ßIII-Tub	ATGAGGGAGATCGTGCACAT	GCCCCTGAGCGGACACTGT
OTX2	CATGCAGTCCTATCCCAT	AAGCTGGGGACTGATTGAGAT
uPA	GCCTTGCTGAAGATCCGTTC	GGATCGTTATACATCGAGGGGCA
uPAR	TGTAAGACCAACGGGGATTGC	AGCCAGTCCGATAGCTCAGG
SERPINE1	GCACCACAGACGCGATCTT	ACCTCTGAAAAGTCCACTTGC
SERPING1	GCACTGGAGCTGCCTGGTGA	TGTTGCGACCTTCCCTTCGC
tPA	AGCGAGCCAAGGTGTTTCAA	CTTCCCAGCAAATCCTTCGGG
Vimentin	TGGACCAGCTAACCAACGAC	GCCAGAGACGCATTGTCAAC
CD44	AGCATCGGATTTGAGACCTG	GTTGTTTGCTGCACAGATGG
ULK1	AGCACGATTTGGAGGTCGC	GCCACGATGTTTTCATGTTTCA
TFEB	GGAGAATCCCACATCCTA	CAGCAAACTTGTTCCCATA
GSK3	CCCGTCCTCACAAGCTTTAAC	GCAGGAGCTTGATGGGCTAT
TNFa	GAGGCCAAGCCCTGGTATG	CGGGCCGATTGATCTCAGC
IL6	GGTACATCCTCGACGGCATCT	GTGCCTCCTTGCTGCTTTCAC
IL10	AAGGCAGTGGAGCAGGTGAA	CCAGCATCAATACACAC
TSC1	GGTACAACTGCAGGTGGAAAA	TGTGCACGTAGTCATCCGAA

2.17. Calcium Imaging protocol

Astrocytes with the conditional Cas13 TSC1 knockout were generated and plated in µ-Slide 8 well imaging dishes (Sigma). Two days prior Imaging, the cells were treated under three conditions with doxycycline for 48 h: No doxycycline (Control), 2 µl Doxycycline pro 1 ml Media (leads to ~50% loss of TSC1) and 4 µl Doxycycline per 1 ml Media (leads to ~ 80% loss of TSC1). On the day of the Imaging, the cells were treated with 5 µM Fura2-AM (Teflabs) in DMEM with 1% BSA and 0.025% Pluronic acid F127 for 1 h at RT, before being washed in imaging buffer (HBSS, 1 mM HEPES and 1 mM MgCl2) and left at RT for 10 min. The Imaging of the intracellular Ca^{2+} concentrations and responses were recorded with a Colibri LED microscope system, using an Axiocam Mrm CCD camera and Axiovision software with an additional physiology module for live cell Ca^{2+} imaging (Zeiss). Recordings of the Ca^{2+} probe baselines were taken prior to agonist addition in order to provide basal Ca^{2+} measurements of the cell, and all agonist-induced responses were compared at peak height. Release of endoplasmic reticulum (ER) Ca^{2+} was measured after addition of 10 µM of Glutamate.

2.18. Apoptosis Staining of astrocytes with ANXA5.

At day 40, the neurons were passaged to low density on a 24 well plate with coverslips with PDL-Laminin coating. At Day 53, the media of the neurons was aspirated and new media with 10uM Glutamate/Glycine was added for 30 min at 37°C in the tissue culture incubator. After the 30 min, the neurons were washed once with HBSS (1x), then 250 µl staining media consisting of 250 µl HBSS (1x; #14175095, Thermo Fisher), Annexin5 protein (2 µl per 1 ml), propidium iodide (0.5 µl per 1 ml), Hoechst (1 µl per 1 ml), as well as 1 µM of MgCl2, 1.8 µM CaCl2 and nonessential amino acids (1x; #11140050, Thermo Fisher). The cells were then kept at <16°C for another 30min as higher temperatures would cause the metabolization of the AXA5 protein by the neurons, prior double wash with HBSS (1x) and fixed with 3.7% PFA for 5min. PFA is then removed, and the cells are washed once with neuronal media in order to reduce potential background staining, and then washed twice with PBS. The coverslips carrying the neurons are then fixed onto glass slides and let to dry for 24 h prior imaging.

2.19. Study Design and Statistics

For the analysis of the gene expression qPCR data for both Cas13 TSC1 and TSC1 homozygous cell lines, different statistical tests were utilized based on needs. For the differentiations, three wells were used per condition and time point (N=3) and a single mutant line was used for both the Cas13 TSC1 cells and the TSC1 -/-. IBJ4 Cas9 cells were used as a control against the IBJ4 Cas9 TSC1 -/- cells while Cas13 TSC1 without any doxycycline was used as a control against the doxycycline treated Cas13 TSC1 cells (2 µl Doxycycline pro 1 ml). As it is impossible to select the location of the plasmid insertion when using electroporation, the Cas13 TSC1 cells without any doxycycline were used as control in order to eliminate any potential of an inserted mutation by the plasmid leading to gene expression alteration and thus impacting the data.

GraphPad Prism was utilized for both figure generation and statistical analysis of the data. A p-value of ≤0.05 was chosen as the significance threshold. For the analysis of gene expression between CN and TSC1 -/-, an unpaired t-test was chosen while for the gene expression analysis between CN and Cas13 TSC1 treated with doxycycline (24h or 48h) a One-Way ANOVA was performed. For the comparisons of gene expression levels over the differentiation duration, a mixed-effect analysis with Sidak's-test for tighter significance levels were performed. For analysing the calcium base lines and peaks in the Cas 13 TSC1, Mann-Withey U tests were performed due to the nonparametric nature of the data distribution. For the labelling of the statistics in the figure, the following standards were chosen: * = p-value of ≤ 0.05, ** = p-value of ≤ 0.01, *** = p-value: ≤ 0.001, **** = p-value ≤ 0.0001.

Concerning the database analysis, the acquired data file already underwent analysis from the MacKeigan group. For the TSC1/TSC2 expression analysis, the group used pair-wise Welch's t-tests in GraphPad Prism, followed by false discovery rate (FDR) correction (in R) to generate corrected p-values as the samples had failed Bartlett's test for homogeneity of variances, thus ruling out ANOVA as an option. The data was preorganized into the Top 300-fold changes of mRNA expressions between tumours and matched healthy tissue of the TSC patients for the respective sample categories: SEN/SEGAs, TUB, and renal angiomyolipoma (RA). While the MacKeigan group had already organized the identified genes based on specific cell processes or involvement in certain diseases, the data files were again organized with focus to the Top 100 up- and downregulated genes which were then personally categorized into two groups: involved with AD or involved with inflammation (pro- or anti-inflammatory genes alike).

3. Chapter 3: Generation of a TSC1 -/- cell line and the effect total TSC1 loss has on neuronal development.

3.1. Introduction

As homozygous loss of TSC is lethal in embryos, there is still some uncertainty about the effect complete loss of TSC1 has on brain development. Therefore, this thesis aimed to gain an understanding how TSC1 loss in iPSCs affects their neuronal development. Using iPS cells as a model for TSC allows the generation and investigation of human neurons and astrocytes, cell types which are otherwise non-accessible. Animal models allow an insight into the disease structure but are, due to significant genetic and developmental differences to humans, quite limited in their translatability (Zhu and Huangfu 2013). TSC patients are born with a heterozygous loss of *TSC1* or *TSC2* (Franz *et al.* 2010) as a homozygous loss is lethal in-utero (Ehninger *et al.* 2009), though second hit mutations can occur at later stages in life (Lam *et al.* 2017; Goswami and Hsieh 2019), as found in tumour growths. This project aimed to generate a CRISPR Cas9 knockout model, as the utilization of CRISPR on iPSCs has been well established in recent years, involving iPSC lines containing the Cas9 gene under a doxycycline inducible promoter. Kabadi *et al.* showed high success rates of using a cell line with doxycycline inducible Cas9 promoter instead of Cas9 protein, which also reduced the number of off-target hits (Kabadi *et al.* 2014). The CRISPR method therefore only requires transfection with gRNA after induction of Cas9 via doxycycline. Therefore, this method will be used to generate TSC1 knockout mutant lines. As mentioned previously, TSC demonstrates a variability of neuronal and cognitive deficits in patients. The loss of either TSC1 or TSC2 leads to overactivation of mTORC1, whose signalling is required for normal neuronal development and function, and dysregulation of this pathway impairs the development of neural circuits at multiple levels. Animal models of TSC demonstrated that upregulated mTOR*C1* signalling leads to changes in the neuronal phenotype including increased neuronal size, altered dendritic arborizations and spine formation, enhanced glutamatergic neurotransmission (Goto *et al.* 2011), altered axonal pathfinding and growth (Choi *et al.* 2008), as well as impaired synaptic plasticity (Bateup *et al.* 2011; Ruppe *et al.* 2014). The degree of mTORC1 pathway hyperactivation seems to correlate with the severity of neurologic dysfunction especially regarding the epilepsy and the behavioural abnormalities. Mice with conditional Rictor deletion demonstrated disorganized axonal projections and an overall increase in axonal connectivity in the TSC brain, especially within cortical tubers, while presenting an excitatory phenotype and the capability to form abundant synaptic contacts (Carson et al. 2013).

Additionally, iPSC studies of TSC patients demonstrated increased astrocyte proliferation in iPSC derived neuronal cultures (Li *et al.* 2017) as well as delayed neuronal differentiation (Zucco *et al.* 2018), thus making the analysis of developmental markers during the neuronal differentiation an interesting target. As discussed previously, TSC models display significant autophagy disruption due to mTORC1 overactivity. Autophagy itself is an essential function in cells and impaired activity was found to trigger inflammation responses as shown with impaired TAU clearance (Bellucci *et al.* 2004; Yoshiyama *et al.* 2007; Laurent *et al.* 2017). Autophagy related genes such as ULK1 (Di Nardo *et al.* 2014; Abd-Elrahman *et al.* 2018; Wang *et al.* 2019a) and GSK3a (Cohen and Goedert 2004; Avrahami *et al.* 2013) were found to be disrupted in both TSC and AD, while studies established a significant role of TFEB in TAU clearance (Martini-Stoica *et al.* 2018). Thus, these genes were deemed as suitable targets for gene expression analysis.

3.2. Chapter 3: Aims and Objectives

There is still some uncertainty about the effect complete loss of TSC1 has on brain development. The aim of this thesis was to gain an understanding how TSC1 loss in iPS cells affect their neuronal development. The influence of TSC1 loss on a range of developmental and autophagy markers during neuronal development was investigated to ascertain if the genetic mutation would inhibit or alter the neuronal development as homozygous mutations do not occur in patients except in cases of double hit mutation during life.

i. Design of a TSC1 iPSC line utilising CRISPR-Cas9 systems for genome editing
ii. Neuronal development of the TSC1 iPSC line and sample collection throughout development
iii. RT-PCRs for gene expression analysis of developmental and autophagy markers

3.3. Chapter 3: Results

3.3.1. Cas 9 CRISPR for *TSC1* knockout

The TSC1 knockout line was generated from a Cas9 cell line. This cell line is a IBJ4 iPS cell line which has been genetically modified to contain the Cas9 gene under a doxycycline inducible promoter. The Cas9 cells were treated with doxycycline for 24h to induce Cas9 nuclease expression and transfected with the TSC1 guide RNA (see Figure 3-1 A). Both guides, which sequence was generously gifted by Prof Bateup from the university of Berkely, were used at the time to increase the chance of a successful nucleofection. The Bateup group had chosen Exon 17 of TSC1 for the targeted deletion based on the small size and an expected introduction of a frameshift and premature stop codon (Blair *et al.* 2018). After the nucleofection, the cells were subcloned by single- celling into 1:500 and 1:1000 dilutions and DNA was collected from the grown colonies. The DNA was then subsequently amplified using PCR and the amplified product prepared for MinION sequencing to check for the presence of deletions. Using Integrative Genomics Viewer to check for deletions, three colonies demonstrated a successful knockout for *TSC1* with a homozygous loss in Exon 17 (see Figure 3-1 B). Heterozygous knockout was not identified in this CRISPR attempt. The homozygous knockout colonies were expanded, and a stock was frozen down in liquid nitrogen for future use. From the 92 subcloned colonies, around 60-70 survived until the Sequencing, from the tested colonies four were 100% pure homozygous colonies, around 10-15 colonies showed homozygous knockout with some WT DNA contamination. Three colonies showed a nearly 50/50 ratio of WT and knockdown DNA, but further testing showed that these colonies were not heterozygous but mixed homozygous and WT cells. The other cells showed no knockout of *TSC1* and were therefore seen as WT cells.

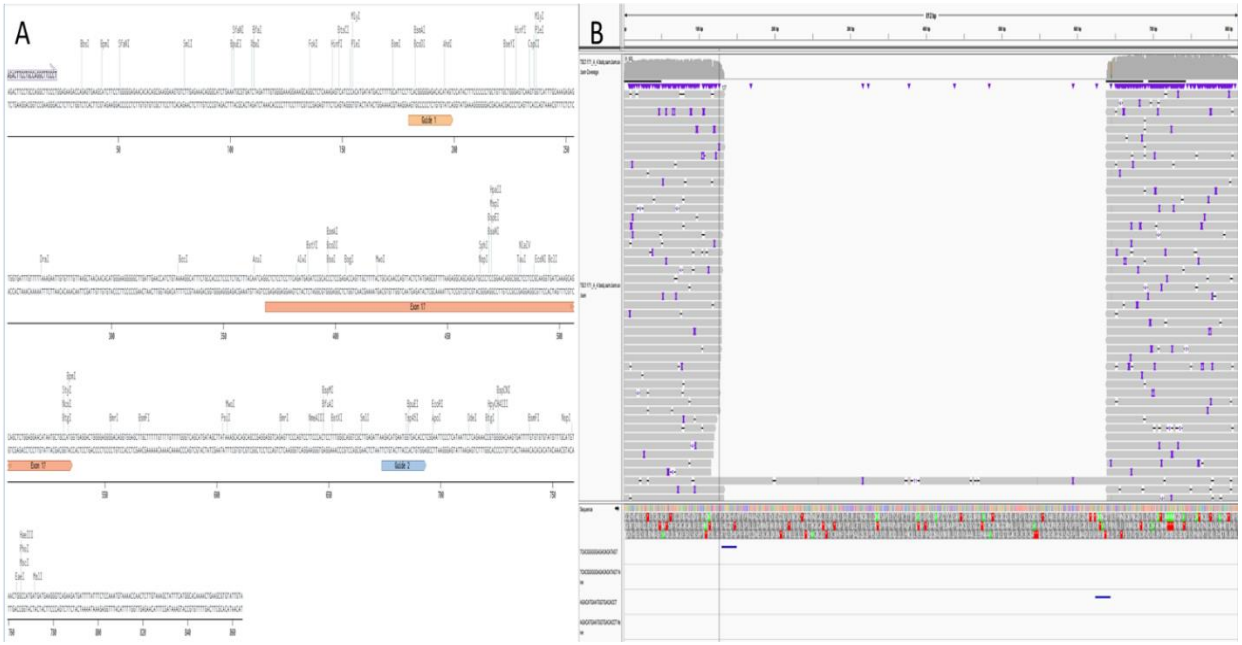

Figure 3-1: A: Scheme of Exon 17 sequence targeted by the guide sequences (visible in bright orange and blue). B: MinION Sequencing Analysis from TSC1 Lipofection, Integrative Genomics Viewer was used. Analysis of the clone A6 shows a clean cut of around 511bp (shown by the white area in the sequencing reads). Guide sequences are marked in blue at the bottom below the sequence.

Analysing the protein expression of TSC1 in the TSC1 -/- cell line via Western Blot (performed by Darius McPhail), demonstrated a clear loss of TSC1 protein in the cell line in comparison to the IBJ4 control.

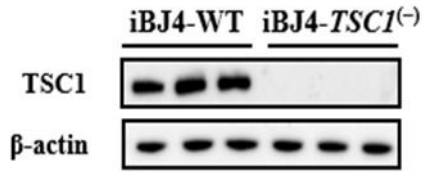

Figure 3-2: Western Blot for TSC1 protein expression in the TSC1 -/- cell line (performed by Darius McPhail). A clear reduction of TSC1 protein levels in comparison to the IBJ4 control can be observed. Beta-Actin was utilised as the control gene for the Western Blot.

One of the TSC1 -/- iPS cell line and the IBJ4 Cas9 line underwent neuronal differentiation and samples were taken at Day 10, Day 20, and Day 50 to capture the developmental timepoints of neuronal stem cells, neural progenitor cells and mature neurons. RNA was isolated from these samples and qPCRs were performed after cDNA synthesis from the RNA. The qPCRs focused on markers of astrocytes, NPCs, neurons, and autophagy.

3.3.2. Expression of astrocytic markers in TSC1 homozygous neurons during neuronal development

Gene expression analysis of TSC1 neuronal stem cells (NSCs) showed significant changes in the expression of several astrocytic markers. S100B1 was increased in TSC1 -/- cells (statistically non-significant) (p-value: 0.2792) (see Figure 3-3).

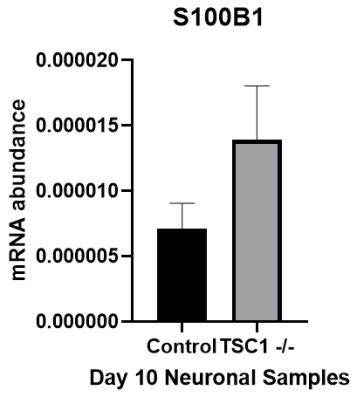

*Figure 3-3: Gene expression of astrocytic markers of TSC1 -/- neuronal stem cells during neuronal differentiation. S100B1 is elevated in the TSC1 homozygous cells (statistically non-significant) (N=3). Values are expressed as mean ± SD. Unpaired t-test were used for the data analysis of the homozygous cells. * = p-value of ≤ 0.05, ** = p-value of ≤ 0.01, *** = p-value: ≤ 0.001, **** = p-value ≤ 0.0001.*

Gene expression analysis of TSC1 neural progenitor cells (NPCs) showed significant changes in the expression of several astrocytic markers. S100B1 was non-significantly increased in TSC1 -/- cells (p-value: 0.4364), while CD44 and Vimentin were significantly increased in the TSC1 -/- cells (p-values: 0.0072 and 0.177) (see Figure 3-4).

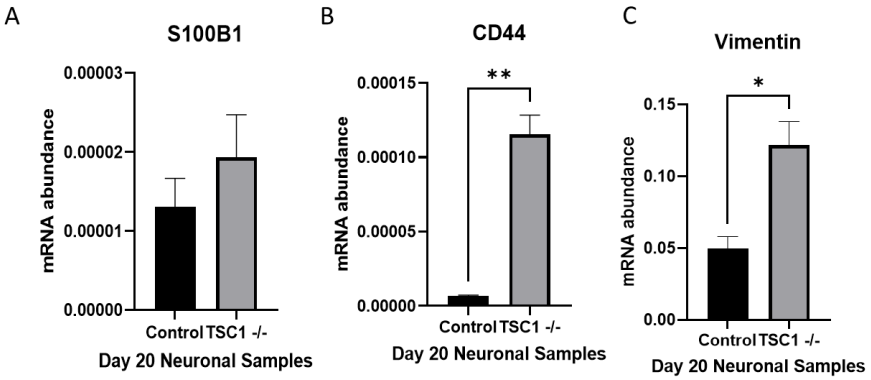

*Figure 3-4: Gene expression of astrocytic markers of TSC1 -/- NPCs during neuronal differentiation. A: S100B1 is elevated in the TSC1 homozygous cells (statistically non-significant). B +C: CD44 and Vimentin are significantly increased in the TSC1 -/- cells (N=3). Values are expressed as mean ± SD. Unpaired t-test were used for the data analysis of the homozygous cells. * = p-value of ≤ 0.05, ** = p-value of ≤ 0.01, *** = p-value: ≤ 0.001, **** = p-value ≤ 0.0001.*

Gene expression analysis of TSC1 neurons against IBJ4 Cas9 control neurons showed significant changes in the expression of several astrocytic markers. S100B1 was significantly increased in TSC1 -/- cells (p-value: 0.012), as was CD44 while Vimentin was non-significantly increased (p-values: 0.0178 and 0.0513 respectively) (see Figure 3-5).

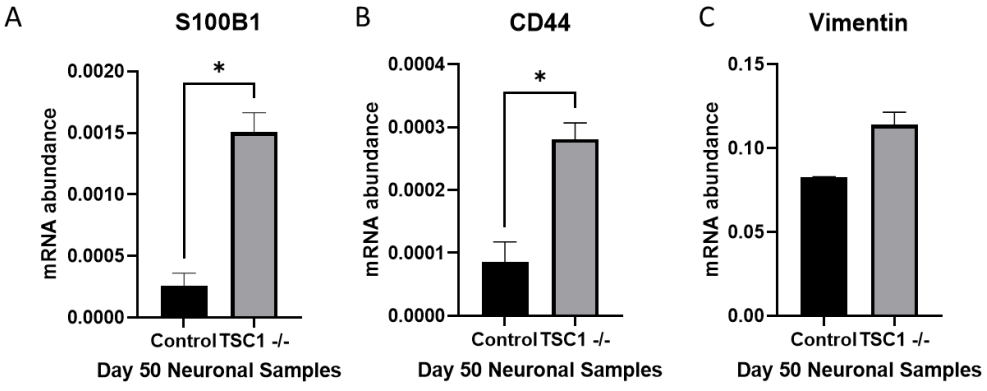

*Figure 3-5: Gene expression of astrocytic markers in homozygous TSC1 neurons during neuronal differentiation. A:CD44 was significantly elevated in the TSC1 NPCs in comparison to Control. B: CD44 expression was significantly increased in TSC1 -/- neurons. C: Vimentin expression in TSC1 NPCs was non-significantly increased (N=3). Values are expressed as mean ± SD. Unpaired t-test were used for the data analysis. * = p-value of ≤ 0.05, ** = p-value of ≤ 0.01, *** = p-value: ≤ 0.001, **** = p-value ≤ 0.0001.*

Analysing the expression changes over the neuronal development shows the increase of astrocytic markers over time. S100B1 expression increased during the development for both control and TSC1 -/- cells and while the expression aligned between both cell lines at the earlier parts of development, the level of S100B1 at Day 50 was significantly higher than in the control (p-values for each time points: 0.9920, >0,9999, 0.0206). CD44 expression increased in both control and TSC1 -/- cells over time but the CD44 expression in the TSC1 -/- cells was continuously significantly higher than in control (D20 p-value: 0.0002, D50: p-value: <0.0001). Vimentin expression was significantly increased at the NPC stage for the TSC1 -/- cells (p- value: 0.0086) and the discrepancy between both cell lines decreased for the neurons and was non-significantly increased in the TSC1 -/- cells (p-value: 0.1536) (see Figure 3-6).

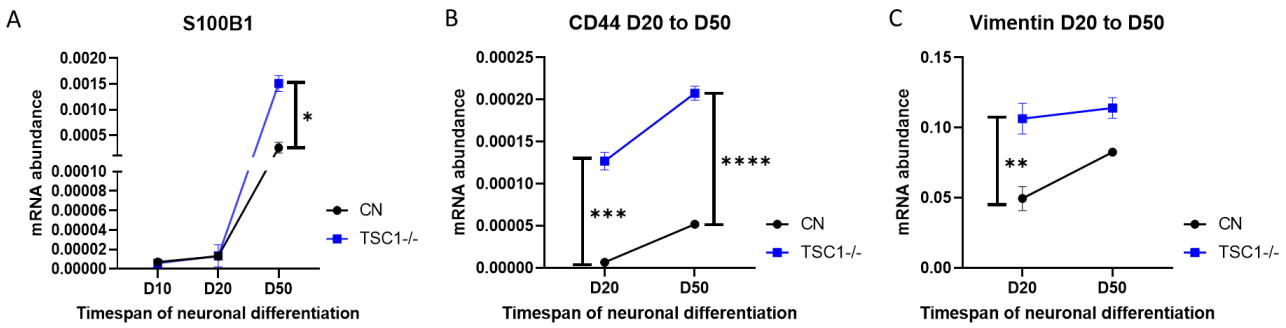

*Figure 3-6: Expression of astrocytic markers during development of TSC1 -/- cells. A: S100B1 shows a significant increase in the TSC1-/- cells at Day 50 and no expression changes during the earlier time points. B: CD44 shows a continuous significant increase in the TSC1-/- cells in comparison to control. B: Vimentin expression in the TSC1-/- cells is significantly increased at Day20 and non-significantly increased at Day 50 in comparison to control. Values are expressed as mean ± SD. Mixed-effect analysis with Sidak's-Test was performed for data analysis. * = p-value of ≤ 0.05, ** = p-value of ≤ 0.01, *** = p-value: ≤ 0.001, **** = p-value ≤ 0.0001.*

3.3.4. Expression of NPC markers in TSC1 homozygous neurons during neuronal development

Gene expression analysis of TSC1 NSCs showed significant changes in the expression of several NPC markers. The NPC markers Nestin and Pax6 were both significantly reduced in TSC1 -/-cells in comparison to control (p-value: 0.0316 and 0.0495 respectively) (see Figure 3-7).

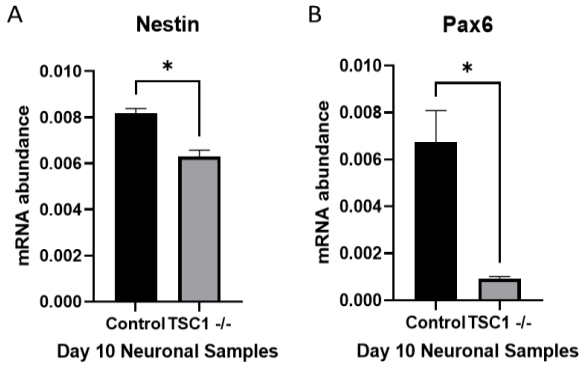

*Figure 3-7: Gene expression of NPC markers of TSC1 -/- neuronal stem cells during neuronal differentiation. A+B: Nestin and Pax6 are significantly downregulated in TSC1 -/- cells (N=3). Values are expressed as mean ± SD. Unpaired t-test were used for the data analysis of the homozygous cells. * = p-value of ≤ 0.05, ** = p-value of ≤ 0.01, *** = p-value: ≤ 0.001, **** = p-value ≤ 0.0001.*

The NPC markers Nestin and Pax6 were either non-significantly reduced or increased in TSC1-/- NPCs in comparison to control (p-value: 0.1336 and 0.2295 respectively) (see Figure 3-8).

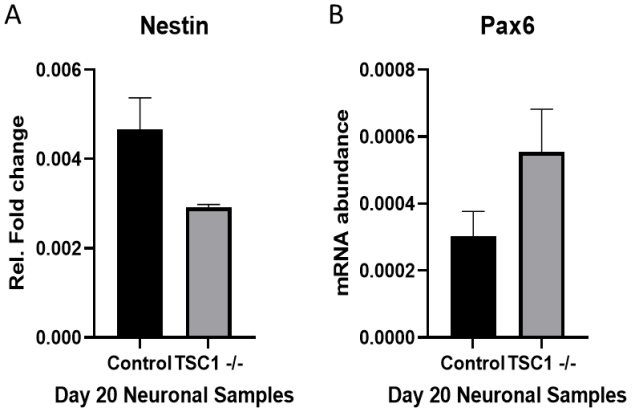

*Figure 3-8: Gene expression of NPC markers of TSC1-/- NPCs during neuronal differentiation. A+B: Nestin is non-significantly reduced in the TSC1 -/- cells while Pax6 was non-significantly increased (N=3). Unpaired t-test were used for the data analysis of the homozygous cells. Values are expressed as mean ± SD. * = p-value of ≤ 0.05, ** = p-value of ≤ 0.01, *** = p-value: ≤ 0.001, **** = p-value ≤ 0.0001.*

Expression analysis of the TSC1-/- neurons shows significant alterations for NPC markers. Nestin was non-significantly reduced (p-value: 0.0942), while Pax6 expression was significantly increased (p-value: 0.0019) (see Figure 3-9).

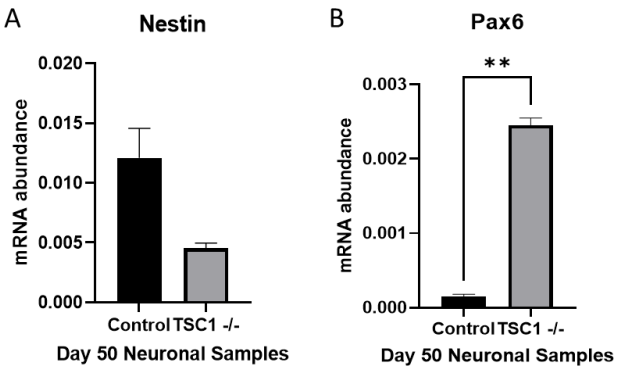

*Figure 3-9: Gene expression of NPC markers in homozygous TSC1 neurons during neuronal differentiation. A +B: Nestin expression in TSC1 NPCs was non-significantly reduced while PAX6 expression was increased significantly (N=3). Values are expressed as mean ± SD. Unpaired t-tests were performed for the statistical analysis. * = p-value of ≤ 0.05, ** = p-value of ≤ 0.01, *** = p-value: ≤ 0.001, **** = p-value ≤ 0.0001.*

Analysing the expression changes over the neuronal development shows the increase of NPC markers over time. Expression of Nestin in the TSC1-/- cells was continuously lower than in control with the biggest discrepancy at Day 50, though no statistical significance was established (p-values for each time points: 0.1075, 0.5657, 0.4720). Pax6 levels were lower during the early developmental points (no significance) and significantly higher at Day 50 (p- values for each time points: 0.3719, 0.9530, 0.0474) (see Figure 3-10).

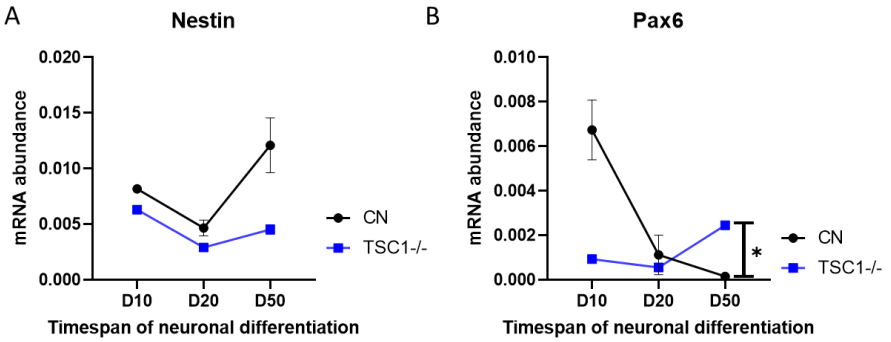

*Figure 3-10: Expression of NPC markers during development of TSC1 -/- cells. A: Nestin expression in the TSC1-/- cells is continuously and non-significantly lower in the TSC1-/- cells in comparison to control. B: Pax6 expression during early development is lower in the TSC1 -/- cell line (statistically non-significant) and significantly increased at Day 50. Values are expressed as mean ± SD. Mixed effect analysis was used for the data analysis. * = p-value of ≤ 0.05, ** = p-value of ≤ 0.01, *** = p-value: ≤ 0.001, **** = p-value ≤ 0.0001.*

3.3.5. Expression of neuronal markers in TSC1 homozygous neurons during neuronal development

Gene expression analysis of TSC1 NSCs showed significant changes in the expression of several neuronal markers. In TSC1 homozygous cells, the neuronal midbrain marker OTX2 and the neuronal marker ßIII-Tub showed significant expression reduction (p-values: 0.0018 and 0.0305) while the neuronal forebrain marker FOXG1 showed a significant increase in expression in the TSC1 -/- (p-value: 0.0395) (see Figure 3-11).

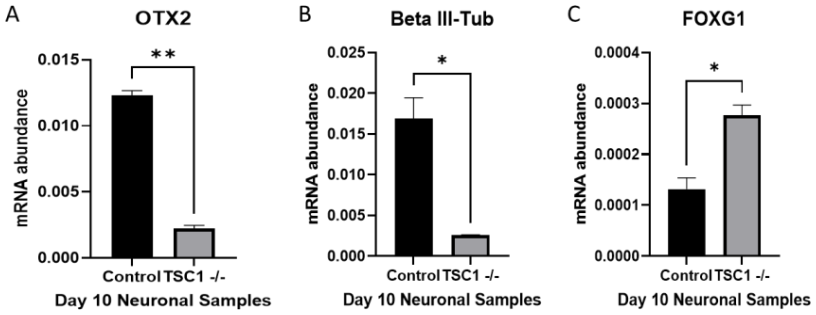

*Figure 3-11: Gene expression of neuronal markers of TSC1 -/- neuronal stem cells during neuronal differentiation. A+B: ßIII-Tub and OTX2 are significantly reduced in the TSC1 -/- cells. C: FOXG1 shows a significant increase in expression in the TSC1 -/- cell line. Values are expressed as mean ± SD. Unpaired t-test were used for the data analysis of the homozygous cells. * = p-value of ≤ 0.05, ** = p-value of ≤ 0.01, *** = p-value: ≤ 0.001, **** = p-value ≤ 0.0001.*

In TSC1 NPCs, neuronal markers displayed significant dysregulation. In TSC1 -/- cells, OTX2 showed no significant expression change (p-values: 0.4141) while ßIII-Tub and FOXG1 showed statistically non-significant increases (p-values: 0.6075 and 0.2395 respectively) (see Figure 3-12).

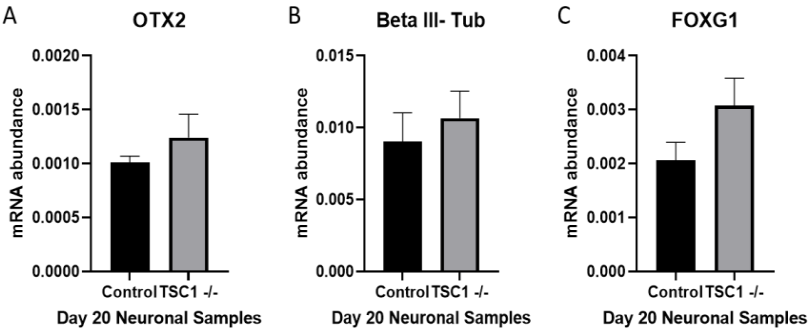

*Figure 3-12: Gene expression of neuronal markers in TSC1-/- NPCs during neuronal differentiation. A-C: The neuronal markers ßIII-Tub and FOXG1 showed no significant increases in expression while OTX2 showed no change in expression in TSC1 -/- cells (N=3). Values are expressed as mean ± SD. Unpaired t-test were used for the data analysis. * = p-value of ≤ 0.05, ** = p-value of ≤ 0.01, *** = p-value: ≤ 0.001, **** = p-value ≤ 0.0001.*

In TSC1 neurons, neuronal markers displayed significant dysregulation. In TSC1 -/- cells, OTX2 was significantly decreased (p-value: <0.0001), while ßIII-Tub and FOXG1 were non- significantly reduced (p-values: 0.3301 and 0.1388, respectively) (see Figure 3-13).

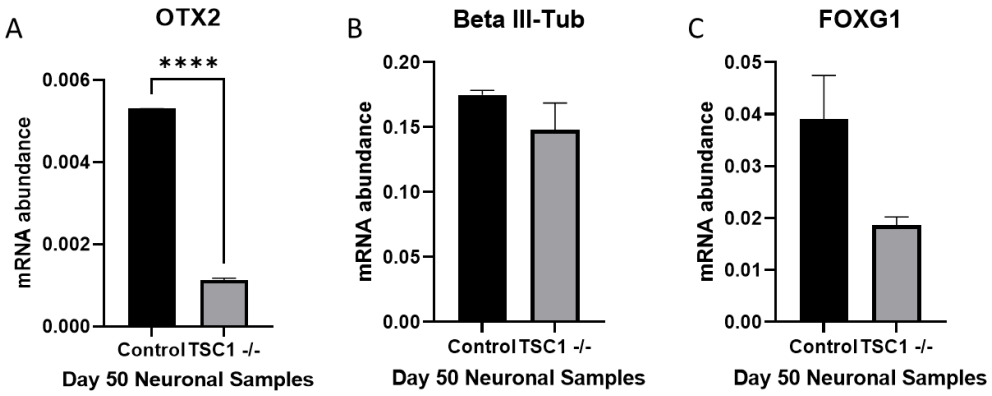

*Figure 3-13: Gene expression of neuronal markers in homozygous TSC1 neurons during neuronal differentiation. A-C: The glutamatergic neuronal markers ßIII-Tub and FOXG1 showed non-significant reductions, while OTX2 showed significant expression reduction (N=3). Values are expressed as mean ± SD. Unpaired t-tests were performed for the statistical analysis. * = p-value of ≤ 0.05, ** = p-value of ≤ 0.01, *** = p-value: ≤ 0.001, **** = p-value ≤ 0.0001.*

Analysing the expression changes over the neuronal development shows dysregulation of several neuronal markers over time. In TSC1 -/- cells, OTX2 expression was significantly lower at Day 10 and Day 50 while Day20 showed no expression changes (p-values for each time points: 0.0089, 0.9996, 0.0003). βIII-Tub expression was slightly lower in the TSC1-/- cells during development but showed no significance (p-values for each time points: 0.3013, 0.6719, 0.7987). FOXG1 expression in the TSC1-/- cells aligned with the control cells during the early development and was lower at Day 50, but no statistical significance in the reduction was found (p-values for each time points: 0.1158, 0.7883, 0.5585) (see Figure 3-14).

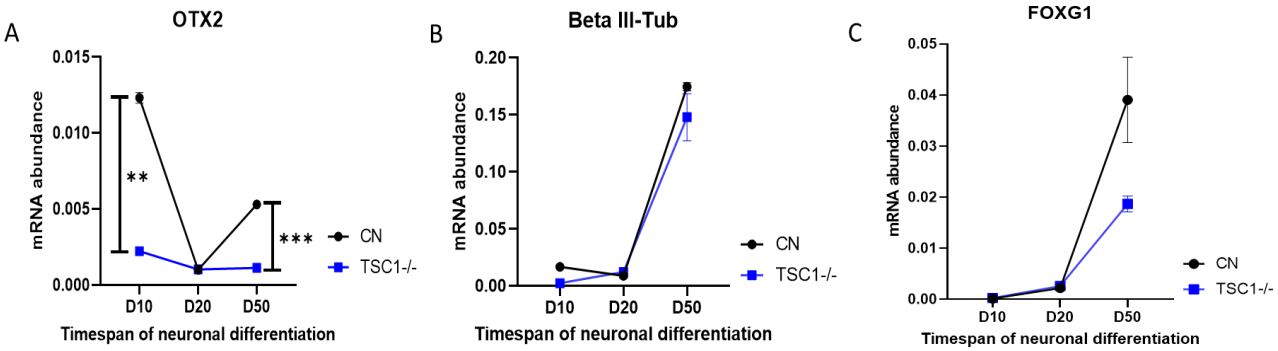

*Figure 3-14: Expression of neuronal markers during development of TSC1 -/- cells. A: OTX2 expression is significantly decreased at Day10 and Day50, no change at Day 20. B: βIII-Tub expression was slightly but non- significantly reduced in the TSC1-/- cells. C: Expression of FOXG1 aligns between both cell lines during early development, levels at Day 50 were lower in TSC1-/- in comparison to control (no significance). Values are expressed as mean ± SD. Mixed-effect analysis with Sidak's-Test was performed for data analysis. * = p-value of ≤ 0.05, ** = p-value of ≤ 0.01, *** = p-value: ≤ 0.001, **** = p-value ≤ 0.0001.*

3.3.6. Expression of autophagy markers in TSC1 homozygous neurons during neuronal development

Gene expression analysis of the TSC1 neuronal stem cells shows significant alterations for autophagy related genes. ULK1 and TFEB were significantly reduced/increased in the TSC1 -/- cells (p-values: 0.0006 and 0.0077 respectively), while GSK3a expression was not changed (p-value: 0.9856) (see Figure 3-15).

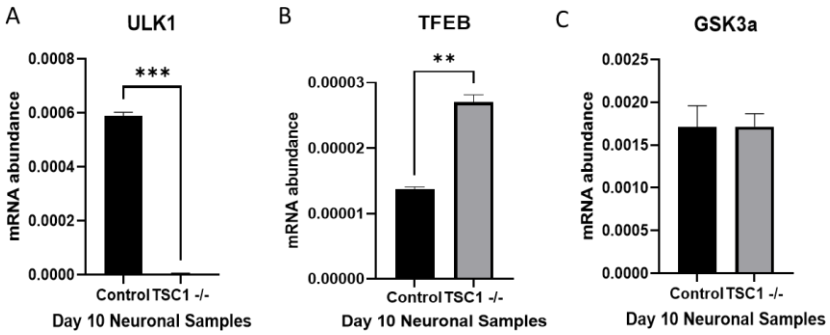

*Figure 3-15: Gene expression of autophagy markers in TSC1-/- neuronal stem cells during neuronal development. A: The expression of ULK1 was significantly reduced in the TSC1-/- cells. B: TFEB expression in TSC1 -/- cells was significantly increased. C: GSK3a expression showed no changes in the TSC1 -/- cells (N=3). Values are expressed as mean ± SD. Unpaired t-test were used for the data analysis of the homozygous cells. * = p-value of ≤ 0.05, ** = p-value of ≤ 0.01, *** = p-value: ≤ 0.001, **** = p-value ≤ 0.0001.*

Gene expression analysis of the TSC1 NPCs shows significant alterations for autophagy related genes. The TSC1 -/- cells display a significant ULK1 reduction (p-value: 0.0027). TFEB expression was non-significantly increased in the TSC1 homozygous cells (p-value: 0.1571), while GSK3a expression was non-significantly increased (p-value: 0.1376) (statistically non- significant) (see Figure 3-16).

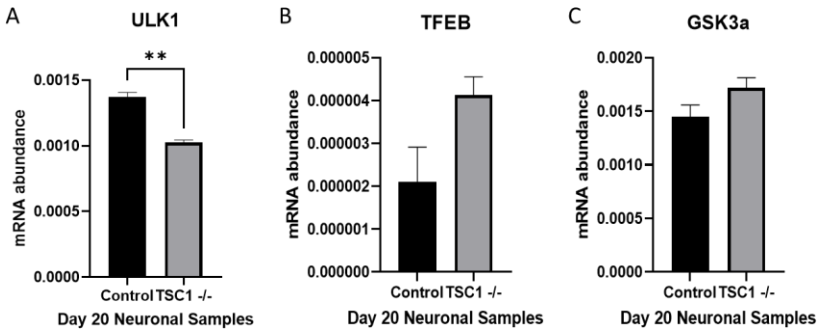

*Figure 3-16: Gene expression of autophagy markers in TSC1 -/- NPCs during neuronal development. A: The expression of ULK1 was significantly reduced in the TSC1-/- cells. B+C: TFEB expression in TSC1 -/- cells was non-significantly increased while GSK3a expression showed no significant changes (N=3). Values are expressed as mean ± SD. Unpaired t- test were used for the data analysis of the homozygous cells. * = p-value of ≤ 0.05, ** = p-value of ≤ 0.01, *** = p-value: ≤ 0.001, **** = p-value ≤ 0.0001.*

Gene expression analysis of the TSC1 neurons shows significant alterations for autophagy related genes. While ULK1 didn´t show significant expression changes to control (p-value: 0.6088), TFEB displayed a non-significant increase (p-value: 0.0593). GSK3a expression were significantly reduced in the TSC1 homozygous neurons (p-value: 0.0091) (see Figure 3-17).

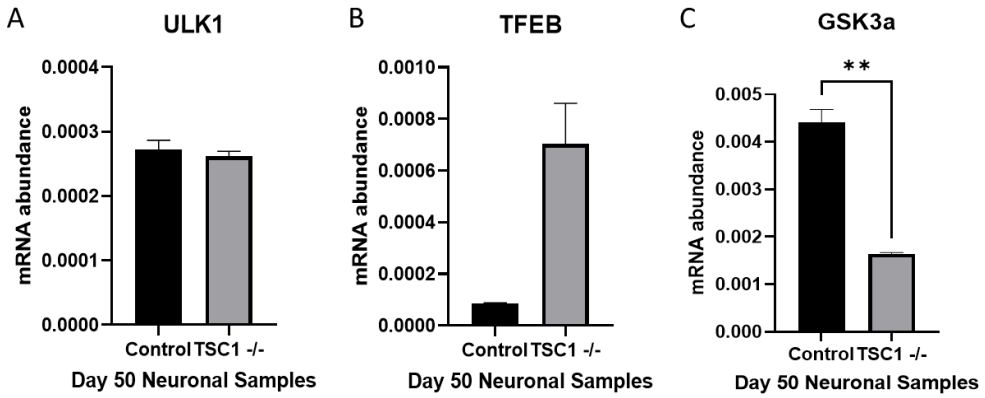

*Figure 3-17: Gene expression of autophagy markers in TSC1 -/- neurons. A: The expression of ULK1 displayed no change in the TSC1-/- cells. B+C: TFEB expression in TSC1 -/- cells was non-significantly increased while GSK3a expression showed a significant decrease (N=3). Values are expressed as mean ± SD. Unpaired t- test were used for the data analysis of the homozygous cells. * = p-value of ≤ 0.05, ** = p-value of ≤ 0.01, *** = p-value: ≤ 0.001, **** = p-value ≤ 0.0001.*

Analysing the expression changes over the neuronal development shows expression changes of the autophagy markers in TSC1 -/- cells over time. ULK1 expression increased towards the NPC stage and decreased when the cells entered the neuronal stage. Expression at Day 10 displayed a significant reduction of D10 in the TSC1 -/- cells and a non-significant reduction at Day 20 in comparison to control (p-values: 0.0093, 0.0828, 0.9604). TFEB expression decreased towards the NPC stage and then increased for neurons, the TSC1 -/- cells displayed a non-significant expression reduction at the neuronal level (p-values: 0.1377, 0.9766, 0.4048). GSK3a expression in TSC1 -/- cells was continuous during development while in control it increases in neurons. While GSK3a expression between both cell lines was close during the early developmental time points, the TSC1 -/- neurons displayed a non-significant decrease (p- values: 0.9815, 0.3613, 0.1392) (see Figure 3-18).

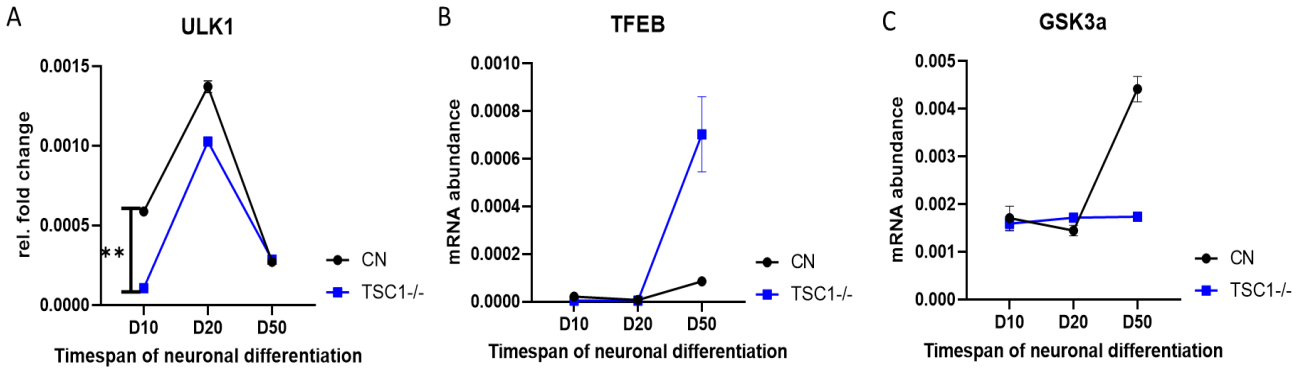

*Figure 3-18: Expression of autophagy markers during development of TSC1 -/- cells. A-C: Only significance was found in ULK1 at D10 of development, while the other genes displayed no significance between TSC1 -/- and control throughout development (N=3). Values are expressed as mean ± SD. Mixed-effect analysis with Sidak's-Test was performed for data analysis. * = p-value of ≤ 0.05, ** = p-value of ≤ 0.01, *** = p-value: ≤ 0.001, **** = p-value ≤ 0.0001.*

3.3.7. Summary of major outcomes in this chapter:

- Generation of *TSC1* -/- IBJ4 cells after CRISPR Cas9 attempt
- Significant dysregulation of developmental and autophagy markers
- Increased expression of astrocyte markers
- Decreased expression of neuronal markers

3.4. Chapter 3: Discussion

3.4.1. Cell Line design:

The Cas9 IBJ4 cell line is a useful model for CRISPR attempts as it allows an easier nucleofection. Once the iCas9 system is induced by doxycycline treatment, only the gRNA and tracrRNA are needed for the transfection, thereby circumventing the need to add Cas9 protein. Kabadi *et al.* had found that doxycycline induced lentiviral Cas9 plasmid transduction had higher success rates for cells than normal transfection, additionally this allows a controlled Cas9 exposure , thereby reducing the chance of off-targets (Kabadi *et al.* 2014). For increasing the target specificity, cleavage efficiency and for decreasing the off targets, several steps can be undertaken. The gRNA is important for the first two characteristics, its specificity is determined by the 20bp sequence and its PAM (Protospacer Adjacent Motif) sequence which is recognized by Cas9. Cho *et al.* demonstrated that it is possible to increase targeting efficiency and reduce off-targets by using dual RNA, consisting of tracrRNA and gRNA (Cho *et al.* 2014). Studies have shown that inactive Cas9 binds to more sites with matching sequences to the gRNA while active Cas9 rarely cuts the DNA at off target binding sites, suggesting that for decoupled binding and cleaving, complimentary sequences between gRNA and target site are necessary for efficient DNA cleavage (Doudna and Charpentier 2014). Overall, CRISPR Cas9 shows similar success rates than TALENs (transcription activator like effector nucleases) or Zinc fingers, while allowing a cheap system as only the guide RNA sequence needs to be altered for targeting several DNA sites instead of the intense protein engineering required for both TALENs and Zinc fingers (Doudna and Charpentier 2014). Still, guide efficiency can show high variability which is why it is usually recommended to test multiple guides for a successful model generation (Hiranniramol *et al.* 2020) but as the iCas9 system used in this project only requires the purchase of different gRNAs, it is a cheap and fast system.

For generating the homozygous *TSC1* cell lines, gRNA sequences given by the Bateup group from UC Berkely were used as previous CRISPR attempts with self-designed gRNA sequences had failed. Oxford Nanopore sequencing shows clear deletions in the target sites of around 511bp, cutting out Exon 17 of TSC1, for the homozygous cells.

3.4.2. Gene Expression:

3.4.2.1. Astrocyte markers:

S100B1 is part of a calcium- binding protein family which is localised in the cytoplasm and the nucleus. S100B1 is involved in the regulation of multiple cellular processes including cell cycle progression and differentiation. It is glia- specific and secreted by astrocytes; and there are suggestions that is involved in neurite extension, stimulation of Ca^{2+} fluxes, inhibition of protein kinase C (PKC)-mediated phosphorylation, axonal proliferation, and inhibition of microtubule assembly. Furthermore, S100B1 acts as a neurotrophic factor and neuronal survival protein in the developing CNS (District 2019). Low concentrations of S100B1 are known to promote cell proliferation and differentiation, whereas higher concentrations induce cell death. Elevated levels of S100B1 have been linked to brain damage and various psychiatric disorders like schizophrenia. For example, elevated levels of S100B1 have been linked to brain dysfunction (Gerlai *et al.* 1995) and mortality in patients with sepsis, or to AD and epilepsy where the gene levels correlated with brain regions of high neuropathology (Petrova *et al.* 2000). S100B1 was shown to suppress oxidative cell damage; whereas oxidative stress impairs the ability of S100 proteins to bind and activate protein phosphatase 5 (PP5), a serine/threonine phosphatase involved in oxidative stress responses (Yamaguchi *et al.* 2016). Unsurprisingly, research has demonstrated that increase of oxidants leads to increased levels to S100B1, seemingly via *NFκB* activation (District 2019). It is well established that ROS can cause severe damage to cells which may lead to apoptosis and cell death (Halliwell 2006; Maes *et al.* 2011). Liu *et al.* also identified the associations of oxidants with S100B1 protein levels (District 2019). On the other hand, higher levels of S100B1 might stimulate cell death via production of oxidative stress by stimulating the generation of NO by activation of NF-κB pathway (Petrova *et al.* 2000). It has been demonstrated that in Down-syndrome NPCs, long-term overexpression of S100B1 leads to an increase in ROS generation and activation of stress responses (Esposito *et al.* 2008). Astrocytes are the most important source of the free radicals in the CNS (Lohr 1991) and S100B1 is primarily expressed in astrocytes. High glucose environments have been shown to be neuroprotective by reducing ROS production (Takahashi 2011). Glucose levels themselves are regulated by GSK3, which will be further discussed later in this chapter (Lee and Kim 2007). The TSC1 -/- cells showed increased levels of S100B1 throughout the neuronal differentiation.

Increased levels at the neuronal stage were originally expected as TSC deficient cells, especially homozygous ones, are known to prefer the astrocytic fate over the neuronal one (Blair *et al.* 2018). The neuronal differentiation of the tested cells was successful as the expression of neuronal markers shows. As it is known that TSC commonly overexpresses HIF1a, a hypoxia related marker (Zhang *et al.* 2016) and as hypoxia is known to promote oxidative stress in cells, it could be hypothesized that TSC cells endure constant low levels of oxidative stress which would then in turn cause an increase of S100B1 expression. As epilepsy (Chong *et al.* 2010) as well as various psychiatric disorders such as anxiety, mood and behavioural disorders are known comorbidities of TSC (Chung *et al.* 2011) and overlap with the disorders known for elevated S100B1 expression, it can be presumed that overly expressed S100B1 is part of TSC pathology.

Vimentin, an intermediate filament protein found in NPCs and astrocytes (Yamada *et al.* 1992), is essential in neuronal development thanks to its role in neurite extension in NPCs (Levin *et al.* 2009). Pattabiraman *et al.* demonstrated that Vimentin seems to play a protective role for differentiating cells against cell stress (Pattabiraman *et al.* 2020) while Matveeva *et al.* demonstrated that Vimentin protects mitochondria from oxidative stress (Matveeva *et al.* 2010). Vimentin expression has been found to be increased in both TSC and AD. Yamada *et al.* demonstrated Vimentin immunoreactivity in neurons affected by amyloid plaques (Yamada *et al.* 1992), while Levin at al. validated these results, suggesting that vimentin expression might be a cell response to cellular or tissue damage (Levin *et al.* 2009). Liang *et al.* showed that loss of *TSC2* led to increased Vimentin levels in kidney tumours (Liang *et al.* 2014) while Hengstschläger *et al.* demonstrated that overexpression of TSC genes also led to an overexpression of Vimentin, suggesting that a balanced level of TSC genes is required for a stable vimentin expression (Hengstschläger *et al.* 2004). Wong *et al.* and Crino *et al.* found Vimentin positive astrocytes in TSC tubers (Crino 2004; Wong and Crino 2012), and the MacKeigan Database also identified a significant upregulation of Vimentin in SEN/SEGAs (database will be discussed in Chapter 5). The TSC1 -/- cells displayed a significant increase of Vimentin expression in comparison to control for both NPCs and neurons. The increased levels of Vimentin in the TSC1 -/- cells at the NPC stage might be a consequence of the potentially increased proliferation rate, a consequence of mTOR overactivity and found in TSC cells. While observation of the cells did show an increased proliferation and metabolism due to increased media usage and quicker confluency, no investigation on the proliferation rate was undertaken in this project.

Since Vimentin expression also responds to cellular stresses like oxidative stress, it could also be a response to cell stress, which is a known consequence of TSC loss (Yang *et al.* 2018; Arena *et al.* 2019). Additionally, the dysregulation of several of the markers tested in this chapter are known to cause cell stress, especially oxidative stress, it could be predicted that part of the expression increase in the NPCs might be a cellular response in order to improve cell survival. The increased expression rate in the neurons might be both a consequence for a higher rate of astrocytes and NPCs in the culture, which is why several astrocytic markers were tested in order to differentiate this. As mentioned before, TSC deficient cells are known to prefer the astrocytic fate over the neuronal one, especially homozygous TSC cells (Blair *et al.* 2018). Therefore, an increased number of astrocytes in TSC cultures would be expected.

CD44 is a transmembrane glycoprotein known to be involved in intracellular signal transduction (Dzwonek and Wilczynski 2015). Originally, it was assumed that only astrocytes were expressing CD44 (Girgrah *et al.* 1991; Vogel *et al.* 1992), research has identified its expression in neural stem cells and oligodendrocyte progenitors (Naruse *et al.* 2013). Additionally, expression of CD44 splice variants in neurons have been identified (Kaaijk *et al.* 1997), going against the previous consensus that CD44 is purely expressed in glia cells. CD44 is a receptor for hyaluronan (HA), an essential player in neuronal development, synaptic plasticity or epileptogenesis (Kochlamazashvili *et al.* 2010; Wlodarczyk *et al.* 2011). Despite that, the exact role of CD44 in neuronal development is uncertain though it has been assumed that it might be involved in axon guidance (Sretavan *et al.* 1994; Lin and Chan 2003). Skupien at al. demonstrated that CD44 is involved in dendritic polarity and the Golgi apparatus morphology in neurons (Skupien *et al.* 2014). Matzke *et al.* demonstrated that CD44 knockout mice displayed a reduced glutamatergic synaptic excitation while GABAergic synaptic inhibition showed no changes (Matzke *et al.* 2007). CD44 expression is known to be strongly induced in AD patient brains (Akiyama *et al.* 1993) and lymphocytes (Uberti *et al.* 2010). Furthermore, AD patients' samples have shown increased levels of several CD44 splice variants, both neuronal and astrocytic variants, therefore suggesting an involvement of CD44 in the pathogenesis of AD (Pinner *et al.* 2017).

CD44 overexpression has been found in TSC patients as well (Arai *et al.* 2000; Maldonado *et al.* 2003; Crino 2004; Boer *et al.* 2010) and it was also included in the Top 300 upregulated Genes of the SEN/SEGA samples from the MacKeigan TSC Database (discussed in Chapter 5). Gene expression analysis showed increased levels of CD44 in the TSC1 -/- cells with significantly increased expression at both NPC and neuronal stage. Combined with the significant expression increases of other astrocytic markers at the neuronal stage, the number of astrocytes in the TSC1 cells is expected to be increased in comparison to the control cells. The increased expression at the NPC stage would be unlikely due to astrocytes as the developmental time point would be too early for any astrocyte generation. Since CD44 is also involved in cell migration, differentiation, and survival (Ponta *et al.* 2003), it might be a cell response in order to increase cell survival and to enable the neuronal differentiation since other differentiation markers tested in this chapter were dysregulated as well. It must be remarked, that while CD44 itself was tested, there was no specific analysis on its splice variants.

In Conclusion, all astrocytic markers were significantly increased in the TSC1 cells at the mature cell stage of the differentiation, thereby suggesting an increased number of astrocytes in the culture, which would align with previous research (Blair *et al.* 2018).

3.4.2.2. NPC markers:

The protein Nestin is involved in several cell processes including organization of the cytoskeleton, cell signalling, and cell metabolism (Fuchs and Weber 1994). Nestin levels are highly expressed at the early developmental stages and nearly absent in mature neurons (Lendahl *et al.* 1990) which is why there are proposals that Nestin might be a candidate of cell differentiation regulation. Despite that, Park *et al.* showed that the loss of Nestin had no impact on neuronal differentiation during development of mice (Park *et al.* 2010). Contrary, Nestin downregulation during myogenesis seems to enhance differentiation with no impact on proliferation (Pallari *et al.* 2011). Upregulation of Nestin in tumours is known to correlate with invasion of melanomas (Strojnik *et al.* 2007). Nestin is presumed to have a role in regulation of assembly and disassembly of other intermediate filaments such as vimentin, during mitosis (Chou *et al.* 2003). However, Nestin knockout mice showed no defects in microfilaments or microtubules, nor changes in proliferation despite the massive reduction in NSC survival and self-renewal (Park *et al.* 2010). There are also some suggestions that Nestin may protect from apoptosis by binding to cyclin-dependent kinase 5 (CDK5); thereby inhibiting its proapoptotic function (Park *et al.* 2010).

Additionally, there have been reports that Nestin seems to be essential for proliferation of embryonic rat cortical neural progenitor cells as Nestin downregulation resulted in G1 cell cycle arrest and reduced numbers of new neurons. The downregulation also inhibited the forming capacity of cultured cortical neural progenitor cells and a suppression in the PI3K pathway under stimulation with growth factors; all of these effects are rescuable with PI3K stimulation (Xue and Yuan 2010). mTORC1 impacts Nestin expression and activity via upregulation of c-Myc which promotes SOX2 and thereby regulates Nestin (Orlova *et al.* 2010). The investigated TSC1 -/- cells showed a stable Nestin expression with few significant down regulations. Nestin expression was significantly reduced at the NSCs stage, and the later stages (NPCs and neurons) showed a trend of non-significant reduction in the TSC1 -/- cells. Therefore, it is overall difficult to conclude that TSC1 loss had an impact on Nestin and its function in neuronal development. The significant loss of Nestin in the homozygous cells early in the development could have a negative effect on the development. As proliferation rates in *TSC1* cells are usually increased due to the mTOR overactivity, the reduced Nestin levels might be an attempt to counteract the proliferation rate so that the differentiation is followed.

Nevertheless, a significant reduction of Nestin expression at a time point where the cells are preparing to enter the NPC stage, will negatively impact the neuronal development of the *TSC1* cells. An increased sample number might be able to discern if there is indeed a trend of Nestin downregulation.

Pax6, a highly conserved transcription factor, is crucial for normal CNS development (Hill *et al.* 1991; Glaser *et al.* 1994; St-Onge *et al.* 1997); studies with Pax6 mutant mice demonstrated significant deficiencies for the neuronal development including abnormalities in NSC and NPC proliferation, as well as defects in neurogenesis and in the generation of more specialized neurons (Sansom *et al.* 2009). Loss of Pax6 in the neocortex leads to microcephaly as well as abnormal development of secondary progenitor cells in the subventricular zone (SVZ) (Sansom *et al.* 2009). The dosage of Pax6 seems to be essential as heterozygous loss of Pax6 leads to aniridia and forebrain abnormalities (Sisodiya *et al.* 2001; Ellison-Wright *et al.* 2004) while homozygous loss leads to a lack of eyes, microcephaly and absent olfactory bulbs (Hill *et al.* 1991; Glaser *et al.* 1994). Increased Pax6 levels on the other hand led to microphthalmia and forebrain abnormalities (Schedl *et al.* 1996; Manuel *et al.* 2007). Estivill-Torrus *et al.* demonstrated that the absence of Pax6 results in an increase of asymmetrical neurogenetic divisions during differentiation (Estivill-Torrus *et al.* 2002). Sansom *et al.* demonstrated that Pax6 controls the balance between NSC self-renewal and differentiation. Gain of Pax6 pushes the cells towards neurogenesis while reduced levels of Pax6 reduces the self-renewal (Sansom *et al.* 2009). The reduction in the pool size of the Pax6 mutant progenitors might explain the reduced production of cortical neurons and the decrease in the cortical thickness of the Pax6 mutant cortex (Georgala *et al.* 2011).

Three processes are essential for the control of generating specific neurons at the correct place and time during development: neural stem cell self-renewal, neurogenesis, and cell fate determination. Gene expression analysis for Pax6 showed significantly altered levels in the TSC1 -/- cells. For the TSC1 -/- cells, *Pax6* expression is mostly dysregulated throughout neuronal differentiation. The NSCs showed significant decrease in Pax6 while the neurons displayed overexpression. In the NPCs, it is statistically non-significantly upregulated. As Pax6 as a transcription factor has an important role in neurogenesis and cell fate determination, it can be predicted that the significant dysregulation in the TSC1 -/- cells should lead to an abnormal neuronal development and impaired cell fate determination.

Day 50 as a time point of sample collection is a time where mature neurons should be expected, but it is not uncommon to find a few NPCs still at this stage. For example, neurons display neuronal activity after 70 days of development whereas the differentiation protocol ends at Day 50. Therefore, it could be suggested that the TSC1 -/- cells show a delayed development and that a higher rate of NPCs existed in the cell colony. Additionally, Pax6 was shown to influence the axon growth (Sebastián-Serrano *et al.* 2012), therefore, the increased level might cause increased axon length or might be caused by double axons which have been identified in TSC cells (Choi *et al.* 2008).

Overall, the NPC markers were significantly dysregulated in the TSC1 -/- cells with Pax6 being significantly upregulated at most developmental time points and Nestin mostly showing no statistical significance but trends of downregulation. Dysregulation of NPC markers during neuronal differentiation which play important roles in the process will cause an abnormal or delayed neuronal development in TSC cells, results which align with previous findings from other groups (Zucco *et al.* 2018; Martin *et al.* 2020).

3.4.2.3. Neuronal markers:

OTX2 is a transcription factor essential for brain and sensory organ development (Acampora *et al.* 1995; Morsli *et al.* 1999; Martinez 2003). Research has shown that OTX2 overexpression leads to: reduced cell proliferation and a senescent phenotype, p53 pathway activation (at least in MED8A cells) (Bunt *et al.* 2010) as well as induction of differentiation, blockage of G1-S cell cycle transition (Bunt *et al.* 2012). Loss of OTX2 in a mouse model was shown to be lethal while decreased OTX2 levels resulted in malformations of the brain (Acampora *et al.* 1995; Fossat *et al.* 2006). Vernay *et al.* investigated OTX2 mutant mice and discovered that OTX2 function does not only involve early brain patterning (Hoch *et al.* 2015) but also regulation of neuronal identity and neurogenesis (Vernay *et al.* 2005). Target genes of OTX2 were also identified to be associated with diseases such as schizophrenia, epilepsy and AD (Sakai *et al.* 2017). OTX2 also plays a role in the promotion of cortical GABAergic interneuron maturation (Hensch *et al.* 1998). The study of Sakai *et al.* also demonstrated the involvement of OTX2 targets in axon guidance, and dopaminergic and glutamatergic synapses (Sakai *et al.* 2017). In addition, OTX2 was found to regulate the expression of OXR1, an important protein in protection against oxidative stress, especially stress induced neurodegeneration (Oliver *et al.* 2011).

OXR1 was found to be involved/dysregulated in both TSC and AD (Stemmer *et al.* 2007; Brownridge III 2020). Sundberg *et al.* demonstrated low levels of OTX2 in her TSC patient derived purkinje cells (Sundberg *et al.* 2018). Expression analysis of OTX2 in the analysed TSC1 -/- cells demonstrated significantly altered levels in comparison to control. The TSC1 -/- cells displayed a mostly significantly reduced expression (except for the NPC stage at Day 20). The mRNA abundance level show that the expression level of OTX2 has its highest point in the NSCs, before falling at the NPC stage and then rising again in the neurons. As the expression was quite significantly reduced in the early developmental stage as well as in the mature neurons, abnormal development as well as abnormal neuronal function can be considered. TSC mutations have been shown to lead to oxidative stress due to increased mTOR activity (Yang *et al.* 2018; Arena *et al.* 2019) and as OTX2 is indirectly involved in the protection against oxidative stress, impaired protection, and consequently increased cell stress might follow the significant reduction. Additionally, as OTX2 is influencing neurogenesis, neuronal identity and axon guidance, abnormal neuronal development and axons can be expected. Impaired neuronal polarity (Choi *et al.* 2008) as well as delayed neuronal development (Zucco *et al.* 2018; Martin *et al.* 2020) and impaired neurogenesis in favour of astrogliogenesis (Blair *et al.* 2018) have been found in various TSC studies, thus the identified expression change in the analysed cell line is not surprising, especially as the low expression levels in the TSC1 -/- are in line with the TSC database from Prof. MacKeigan (discussed in chapter 5) as well as with the findings of Sundberg *et al.* (Sundberg *et al.* 2018). While the utilised neuronal differentiation protocol generates glutamatergic neurons, a small percentage of GABAergic neurons are developed as well and as OTX2 influences neuronal identity, promotes cortical GABAergic interneuron maturation (Hensch *et al.* 1998) and the low expression in measured in TSC might be one of the causes of the imbalance of developed neurons in TSC brains (Alsaqati *et al.* 2020). As OTX2 overexpression leads to differentiation induction and reduced cell proliferation, it can be presumed that the reduction of OTX2 expression would lead to abnormal/ delayed development and increased cell proliferation, both found in TSC due to the mTOR overactivity.

βIII-Tub, also known as βIII--Tubulin, is part of the tubulin/microtubule network. Under non-pathological conditions βIII-Tub expression is primarily restricted to neurons, and at low levels in other tissues (Verdier-Pinard *et al.* 2009; Guo *et al.* 2011). High levels of βIII-Tub expression had been demonstrated in clinical studies of several cancers including lung, breast, prostate, gastric and melanoma cancer (Bernard-Marty *et al.* 2002; Mozzetti *et al.* 2005; Moiseyenko *et al.* 2013). βIII-Tub upregulation in cancer cells has been correlated to decreased survival and resistance to chemotherapeutic agents (Karki *et al.* 2013). Functional studies have confirmed the importance of βIII-Tub in regulating sensitivity to chemotherapeutic agents in non-small cell lung cancer (NSCLC), ovarian cancer and prostate cancer cells (Gan *et al.* 2007; McCarroll *et al.* 2010). Guo *et al.* demonstrated that βIII-Tub doesn't seem to have a role in cell viability of neurons unlike βI-tubulin, an isoform much more widespread in cells and tissues.

Despite that, βIII-Tub is known to be involved in mitotic spindles and interphase microtubule networks, which might imply the potential of having a role in cell viability (Guo *et al.* 2011). Furthermore, research shows that loss of βIII-Tub diminishes neurite outgrowth and negatively regulates further neurite elongation (Ferreira and Caceres 1992). An important discovery that Guo *et al.* made during their study was the protective function of βIII-Tub towards NMDA receptor, as βIII-Tub loss reduces cell viability when treated with glutamate/glycine (Guo *et al.* 2011). Zucco *et al.* demonstrated not only reduced levels of βIII--Tub in the TSC derived neural progenitors but developmental delay as well (Zucco *et al.* 2018). βIII-Tub expression in the *TSC1* -/- cells was reduced in the NSCs while the NPCs and neurons showed no significant dysregulation. As βIII-Tub is part of the microtubule network, it can be expected that it influences neurogenesis especially as it regularly used as a marker for the latter. Therefore, the significant reduction at the NSC stage, which is vulnerable state during the development might impact the further development. As the expression dysregulation vanished during the further development, it is unlikely that any changes in TSC neurite length, as seen in Martin *et al.* (Martin *et al.* 2020), can be a consequence of βIII-Tub dysregulation.

FOXG1, a DNA-binding transcription factor, whose role is the repression of target genes during brain development. FOXG1 mutations are known to cause microcephaly, impaired motor development, and brain malformations. Additionally, FOXG1 is a transcriptional repressor targeting cell cycle inhibitors, transforming growth factors (like TGF) (Guen *et al.* 2011). FOXG1 plays a crucial role in early brain development, and loss of FOXG1 leads to microcephaly, developmental delay, and cerebral atrophy (Hettige and Ernst 2019). FOXG1 itself is regulated by AKT. Loss of TSC which is downstream of AKT, indirectly downregulates the latter via a negative homeostatic feedback loop through mTORC1-S6K1/2, thereby increasing GSK3β activity (Nguyen and Bordey 2021) as AKT plays a role in regulating cell growth via TSC1/2-Rheb-mTORC1 signalling, phosphorylating and inhibiting of GSK3β (Bellacosa *et al.* 2004). During early development, its expression is selective in highly proliferating cell populations in the telencephalon, where it is regulating the neurogenesis rate by keeping cells in a proliferative state and inhibiting their differentiation into neurons (Dastidar *et al.* 2011). FOXG1 is also expressed in neurogenic areas of the postnatal brain such as the subventricular zone and the hippocampal dentate gyrus where it also regulates neurogenesis (Shen *et al.* 2006). Furthermore, FOXG1 was found to influence the balance of GABAergic/glutamatergic neurons with FOXG1 heterozygous iPSC and mice showing an increased expression of GABAergic synaptic markers (Patriarchi *et al.* 2016). In addition to its previously mentioned functions, FOXG1 is involved in the promotion of axonal growth in the developing retina (Dastidar *et al.* 2011), as well as in the regulation of patterning of the developing forebrain (Danesin *et al.* 2009).

Furthermore, FOXG1 mutations have been reported to be associated with neurodevelopmental disorders in humans, like epilepsy and microcephaly (Bahi-Buisson *et al.* 2010). Dastidar *et al.* demonstrated that FOXG1 is also involved in protection from neuronal death in mature cells as FOXG1 suppression promoted apoptosis in otherwise healthy neuronal cultures. Their study also showed that the neuronal survival promotion is AKT dependent and FOXG1 is a downstream effector of IGF-1 (Dastidar *et al.* 2011). FOXG1 overexpression is known to result in increased cell viability, G2/M cell cycle arrest, as well as inhibit cell differentiation (Wang *et al.* 2018). Mariani *et al.* demonstrated in her study that FOXG1 overexpression causes dysregulated expression in ASD organoids and the overproduction of GABAergic neurons (Mariani *et al.* 2015). Gene analysis of FOXG1 expression during the neuronal development of TSC1 -/- cells showed significant dysregulation.

While the TSC1 -/- cells showed an increase of FOXG1 during the earlier developmental stages, the mature neurons displayed a reduction in FOXG1. As FOXG1 is a crucial transcription factor in brain and neuronal development, any changes in expression would have severe consequences, especially as loss or mutations of FOXG1 are known to be associated with neurodevelopmental disorders in humans (Bahi-Buisson *et al.* 2010). The overexpression at the early developmental stages and the trend of reduced expression at the neuronal level might destabilise the balance of glutamatergic and GABAergic neurons, as previous studies demonstrated (Mariani *et al.* 2015; Patriarchi *et al.* 2016) . Overall, the increase in expression for the TSC1 -/- aligns with TSC pathology which also displays abnormal/delayed cell differentiation (Zucco *et al.* 2018; Martin *et al.* 2020), increased number of GABAergic neurons (Alsaqati *et al.* 2020) and has ASD as a known comorbidity (Gipson *et al.* 2013).

Overall, all the neuronal markers displayed significant dysregulation during the neuronal development in TSC1 -/- cells and as several of these marker function as transcriptional factors with essential functions in neuron and brain development, it can be concluded that any dysregulation during any time point of the development could cause abnormalities in the cells and their function.

3.4.2.4. Autophagy markers:

As mentioned previously, GSK3 proteins have an important function as mediators of various signalling pathways, including growth factors and Wnt pathways. Therefore, continuous research suggests the role of GSK3s as a key regulator in multiple neuronal processes such as neurogenesis, neuronal polarization and axon growth and guidance (Hur and Zhou 2010). Among the GSK3 substrates, transcription factors like CREB are known to play important roles in neuronal development. GSK3s regulate these transcription factors by either controlling their protein levels, DNA binding activities and/or nuclear localization. Additionally, GSK3s regulate the activity of several microtubule-associated proteins (MAPs) (Zhou and Snider 2005) and may have influence on essential processes during cell division as well as influencing neuronal migration, axon growth and guidance, as all of which require coordinated control of microtubule dynamics (Kim and Snider 2011).

GSK3β inhibition in hippocampal neurons was shown to induce formation of multiple axons (Yoshimura *et al.* 2005; Yoshimura *et al.* 2006), though the specific role of GSK3s in neurodevelopment is still questioned due to contradictory data; as some studies demonstrated that GSK3 inhibition induces axonal spreading, reduces axonal elongation, and increases growth cone size, and causes no induction of the formation of multiple axons (Challacombe *et al.* 1997; Chen *et al.* 2006; Asada *et al.* 2007). There are suggestions that GSK3 signalling is essential for coordinating the proliferation and differentiation of progenitor cells during brain development (Hur and Zhou 2010). The importance of GSK3s in the developing nervous system has been shown in a study through the selective deletion of both Gsk3a and Gsk3b in neural progenitors of mice (Kim *et al.* 2009). The animal model demonstrated a substantially increased cortical surface area due to an over-expansion of the neural progenitor cells. Gene expression analysis demonstrated that deletion of GSK3 genes markedly enhanced the proliferation of progenitor cells while suppressing neuronal differentiation, resulting in a reduced number of neurons and therefore a thinner cortex of the mice. This suggests that *GSK3* activity is required for normal neuronal development.

Several signalling pathways had already been identified as regulators of neural progenitor proliferation, including Wnt, sonic hedgehog (shh), and the Notch signalling pathway and *GSK3* is implicated in the regulation of each of these pathways (Hur and Zhou 2010). Furthermore, GSK-3s regulate via the *PI3k* pathway the stability of Myc family proteins (Kim and Snider 2011) which are key elements in neural progenitors maintenance differentiation inhibition (Knoepfler *et al.* 2002; Wey *et al.* 2010). It is hypothesized that the GSK3s mediated phosphorylation of c-Myc is essential to its stability. c-Myc plays an important role in inducing cell differentiation; the inhibition of its phosphorylation maintains embryonic stem cell pluripotency (Cartwright *et al.* 2005). As c-Myc is quickly metabolized (Eilers and Eisenman 2008), control of c-Myc stability via phosphorylation might be critical. c-Myc is an important promoter of many genes including cyclins, regulating their transcription. This role as a transcription factor has been primarily considered in maintaining self- renewal and in inhibiting differentiation of stem cells (Kim and Snider 2011). Analysing the GSK3 gene expression during neuronal development in TSC1 -/- knockout showed significant changes in the expression of GSK3 in comparison to the controls. The TSC1 -/- cells displayed at significant reduction in GSK3a expression at the mature neuronal stage while the earlier timepoints demonstrated no significant expression changes.

As GSK3a is suggested to be involved in neurodevelopment, especially influencing axons (Challacombe *et al.* 1997; Chen *et al.* 2006; Asada *et al.* 2007), the strong reduction in the TSC1 -/- cells would imply that the cells might have impaired axonal function/growth. Consequences on Nestin expression due to a potentially impaired c-Myc stability thanks to the loss of GSK3a in the neurons can´t be concluded as no significant changes in Nestin expression have been identified at that time point.

ULK1, which is another major player in autophagy, is controlled via mTOR or AMPK pathway (Di Nardo *et al.* 2014). The loss of TSC1/2 in neurons is known to cause cell stress as the neurons show higher susceptibility to endoplasmic reticulum and oxidative stress; the TSC dependent inhibition of mTOR is required for autophagy regulation in response to ROS and TSC mice model show increased stress responses (Di Nardo *et al.* 2009; Anderl *et al.* 2011). Di Nardo *et al.* also opened the discussion if TSC could also be counted as a neurodegenerative disease as it shows defective autophagy, a hallmark of several neurodegenerative diseases (Di Nardo *et al.* 2014). Next to its role in autophagy, ULK1 also seems to be involved in additional functions in neurons. Li *et al.* demonstrated in their study that loss of ULK1 expression in mice led to neuronal loss in the CNS (Li *et al.* 2018). Furthermore, it is known that ULK1 mutations in *Caenorhabditis elegans,* lead to axonal defects, including premature termination, abnormal trajectories, extra axon branches, and abnormal accumulation of intracellular membranous structures (Ogura *et al.* 1994).

Additionally, ULK1 directly interacts with Unc-14, which through its interactions with further proteins, controls axonal elongation and guidance (Li *et al.* 2018). Demeter *et al.* demonstrated in their mice model that ULK1/2 deficiency in the CNS results in abnormal axon guidance as well as impaired organization of the somatosensory cortex, strengthening the claim of the role of ULK1 in neuronal functions (Demeter *et al.* 2020). mTORC1 activity can be targeted via AMPK and ULK1, despite the latter being directly negatively controlled by mTORC1 activity. Alsaqati *et al.* demonstrated that the TSC phenotype of higher neuronal excitability and decreased synchronicity in mature iPSC derived neurons as well as an imbalance of excitatory/ inhibitory synaptic markers, could be rescued with pharmacological ULK1 activation (Alsaqati *et al.* 2020). Furthermore, research suggests that ULK1 inhibition promotes oxidative stress by promoting a metabolic shift from glycolysis to oxidative mitochondrial metabolism (Ianniciello *et al.* 2021). It is further known that TSC commonly overexpresses HIF1a, a hypoxia related marker (Zhang *et al.* 2016).

As hypoxia is also known to promote oxidative stress in cells, it can be hypothesized that TSC cells endure constant oxidative stress as the ULK1 expression loss was found during different time points of neuronal development in the TSC1 cells investigated in this project. Mahakizadeh *et al.* supported the hypothesis that chronic hypoxia might be a suitable model for AD when they exposed juvenile rats to chronic hypoxia and demonstrated signs of AD in their mice as well as reduced βIII-Tub expression which would suggest a change/delay in the neuronal development (Mahakizadeh *et al.* 2020). As this current project had identified reduced levels of *βIII*-Tub levels in TSC1 cells at different timepoints of neuronal development as well (discussed earlier), it could be hypothesized that the oxidative stress might be one of the sources of the developmental delay found in TSC neurons. Plotting the ULK1 expression over time in the TSC1 -/- cells showcased that the peak of its expression is at the NPC stage (D20). Analysis of D20 samples demonstrated significant reduction of ULK1 levels in comparison to control for the TSC1 cells. As it is a major player in autophagy and its inhibition has been demonstrated to promote oxidative stress (Ianniciello *et al.* 2021), it could be expected that the neuronal differentiation might be negatively impacted as the NPC stage is a fragile state where cell fate is decided and additional cell stress might cause increased cell death (observed in the TSC1 -/- cells during D18 passage).

As previously mentioned, TFEB is a transcription factor whose activation leads to stimulation of lysosomal biogenesis and autophagy, resulting in the breakdown of proteins and lipids for nutrients (Settembre *et al.* 2011; Martini-Stoica *et al.* 2018). Furthermore, TFEB promotes clearance of aberrant storage material in lysosomal storage disorders (Medina *et al.* 2011; Palmieri *et al.* 2017). TFEB and TFE3 also bind to the promoters of genes associated with autophagy and lysosomal exocytosis and thereby regulate these processes. The activity of mouse TFEB is regulated by mTORC1-dependent phosphorylation, which inactivates TFEB as a nuclear transcription factor (Yuizumi *et al.* 2021). Yuizumi *et al.* demonstrated that lysosomes are more abundant in NPCs than in differentiating neurons (in their mice model) and that knockdown of TFEB and TFE3 promotes premature neurogenesis while the expression of an active form of TFEB suppresses neuronal differentiation in the developing brain (Yuizumi *et al.* 2021). mTORC1 controls the localization of TFEB and TFE3 in cells (Raben and Puertollano 2016). With an abundance of nutrients, TFEB and TFE3 remain excluded from the nucleus and accumulate in the cytosol.

Following starvation, both genes translocate to the nucleus and up-regulate multiple genes, thus promoting autophagy and lysosomal biogenesis as a way to help cells adapt and survive nutrient deprivation (Martina *et al.* 2014). There is also some evidence that TFEB and TFE3 are activated in response to mitochondrial and ER stress (Martina *et al.* 2016), which would suggest a more general role in cellular adaptation to stress (Raben and Puertollano 2016). Furthermore, TFEB seems to be involved in inflammatory processes as well as LPS stimulation results in extrusion of mitochondrial contents via a process requires TFEB activation, and this process was shown to be sufficient to induce an inflammatory response (Unuma *et al.* 2015). As mentioned previously, TFEB is an important player in the TAU clearance in AD. Xu *et al.* identified that the process depends on the calcium channel TRPML1 (Xu *et al.* 2021). This calcium channel was identified to be regulated by mTOR and thereby by TSC (Onyenwoke *et al.* 2015). Li *et al.* further demonstrated that TRMPL1 is required for mTORC1 activation, therefore suggesting a feedback loop (Li *et al.* 2016).

Expression analysis of TFEB in the TSC1 cells investigated in this project demonstrated significant changes in comparison to healthy control cells. TSC1 -/- cells displayed a trend of increased TFEB expression with a significant increase in neuronal stem cells. Torra *et al.* investigated the consequences of TFEB overexpression in mouse neurons of a Parkinson´s model and identified several protective roles of TFEB (Torra *et al.* 2018). Firstly, TFEB overexpression was found to drive a neurotrophic effect that increased cell growth. Second, protein synthesis inducers eukaryotic initiation factor 4E (EIF4E) and S6K1 were both activated and decline of protein synthesis of the model was prevented. Third, MAPK and AKT pro-neuronal survival pathways were activated. Lastly, atrophy was counteracted and neuronal integrity and function was preserved (Torra *et al.* 2018). TSC cells are known to display an increased soma size (Hisatsune *et al.* 2021) and while this hasn´t been investigated in this project, it could be considered that the TSC1 -/- cells might demonstrate it as well and that it could be influenced by the increased TFEB expression. The overexpression of TFEB in TSC might be both protective and harmful. As TFEB overexpression was found to counteract atrophy and preserve neuronal integrity and function, it might prevent neuronal death. On the other hand, its ability to prevent of the decline of protein synthesis would be a harmful consequence as increased protein synthesis due to mTOR overactivity is a consequence of TSC1 loss (Franz *et al.* 2010). The prevention of the decline would most likely cause cellular stress though its neuroprotective function might outweigh the resulting cell stress.

As TFEB can suppress neuronal differentiation and impact neuronal survival, it can be predicted that any expression dysregulation would be harmful for neuronal development, despite TFEB levels reaching their peak at the neuronal stage.

Several genes which are either directly or indirectly regulating autophagy demonstrated significant dysregulation of their expression levels. As TSC is known for its impaired autophagy, these results were expected. Their disturbance likely causes cellular stress and impair cell survival and differentiation.

4. Chapter 4: Generation of a conditional TSC1 cell line and consequences of acute TSC1 loss on neuronal development

4.1. Chapter 4: Introduction

There is uncertainty of the effect of acute TSC1 loss on neuronal development. This thesis aimed to gain an understanding how acute TSC1 loss in iPS cells affects neuronal development and which time points of the development are the most sensitive to acute TSC1 loss. As with many other diseases, there is a variability on the impact on life caused by TSC for the patients (Skalicky *et al.* 2015). While it has been established that patients with a TSC2 mutations suffer under a bigger impact of the disease than patients with a TSC1 mutation (Dabora *et al.* 2001), there is still a variability among the patients with the same gene mutation. One explanation for the difference could be their genetic background, while another possibility would be the developmental timepoint at which the mutation occurred. The generation of a conditional knockdown model would allow brief induction of TSC1 loss during the development of neurons or astrocytes at any time point, giving the unique possibility to see the precise consequences of the knock downed gene as well as identifying sensitive time points for TSC loss. By utilizing an iPS cell model for this experiment, the generation and investigation of human neurons and astrocytes is possible, cell types which are otherwise non-accessible (Zhu and Huangfu 2013). This project aimed to generate a conditional knockdown Cas13 model as Abudayyeh *et al.* demonstrated that the knockdown specificity of the Cas13a system is higher than for alternative methods despite comparable levels of gene knockdown (Abudayyeh *et al.* 2017). Further studies demonstrated a high efficiency and specificity for the Cas13a system for mammalian cells (Kleinstiver *et al.* 2015) while others claimed collateral effects by off-target RNA slicing (Wang *et al.* 2019b). As the Cas13 model has demonstrated high efficiency, low off-targeting as well as easy design under a doxycycline inducible promoter than comparable methods, it will be used for generating the conditional knockdown TSC1 cell line. Similar to the previous chapter, developmental and autophagy marker expression were analysed during neuronal differentiation as it is currently unknown if a brief and acute loss of TSC1 would have a prolonged impact on neuronal development. Furthermore, the conditional cell line underwent astrocytic differentiation.

As discussed previously, calcium is a an essential player in neurotransmission and essential for neuronal excitability, synaptic plasticity, dendritic development and programmed cell death amongst other functions (Marambaud *et al.* 2009; Nikoletopoulou and Tavernarakis 2012). Therefore, calcium homeostasis is tightly regulated for normal function of the previously mentioned cell processes. Aging neurons show increased calcium influx into the cell due to increased VOCCs activity as well as reduced calcium export via PMCA and increased calcium release from the ER. These changes overall lead to an increased calcium load in neurons, disturbing neuronal excitability. Disruptions in the calcium homeostasis have been found in TSC: neurons showed an increase of spontaneous calcium transients (Nadadhur *et al.* 2019), while iPSC derived TSC2 -/- neurons demonstrated elevated neuronal activity with highly synchronized calcium spikes, enhanced calcium influx via L-type calcium channels resulting in abnormal neurite extension and sustained CREB activation. Studies have shown that disturbed ER calcium homeostasis significantly contributes to dysfunction and degeneration in AD. AD models for example showed impaired calcium uptake in mitochondria (Nikoletopoulou and Tavernarakis 2012), especially after oxidative stress (Kumar *et al.* 1994).

Glutamate is essential for synaptic transmission as a major excitatory neurotransmitter in the mammalian CNS; however the balance of the signal is crucial (Lauderback *et al.* 2001). Overactive neuronal stimulation by glutamate (known as excitotoxicity) can induce neuronal damage and death (Maragakis and Rothstein 2001). Clearance of glutamate from the synapse is critical for neuronal health and it is recycled by astrocytes (Lauderback *et al.* 2001). Excessive glutamate receptor activation leads to excessive calcium influx, thereby impairing synaptic activation, neuronal plasticity and synthesis of NO, all of which will cause cell death as identified in AD (Sattler and Tymianski 2000; Marambaud *et al.* 2009). Neurons are processing glutamine as it functions as both neurotransmitter and energy substrate and metabolize it into glutamate which is then released by the neurons and transported into astrocytes via glutamate transporters, in order to recycle it back into glutamine. In TSC, glutamate excitotoxicity seems to occur. Knock-out mouse model of TSC (TSC1GFAPCKO mice) demonstrated decreased expression and function of the glutamate transporters GLT-*1* and GLAST, leading to an increase in extracellular glutamate levels and excitotoxic neuronal death (Wong *et al.* 2003; Zeng *et al.* 2007). Abnormal glutamate homeostasis and neuronal death could lead to neurological deficits and promote neuronal hyper excitability and seizures as consequence (Zeng *et al.* 2010).

There is the evidence that abnormal glutamate homeostasis due to impaired astrocyte glutamate transport could be a contributing factor to epilepsy and other neurological deficits in TSC (Wu *et al.* 2005; Zeng *et al.* 2007). These glutamate transporters are also affected in AD as amyloid species like Aβ 1-42 decrease the expression of GLT-*1* and GLAST, two major GLTs in astroglia (De Vivo *et al.* 2010; Matos *et al.* 2012). Therefore, it is presumed that the disruption in the clearance of excitatory neurotransmitters and increased levels of Aβ and TAU from astrocytes are involved in the neuronal excitotoxicity seen in AD (González-Reyes *et al.* 2017).

4.2. Chapter 4: Aims and Objectives

There is uncertainty of the effect of acute TSC1 loss on neuronal development. This thesis aimed to gain an understanding how acute TSC1 loss in iPS cells affects neuronal development and which time points of the development are the most sensitive to acute TSC1 loss. The influence of TSC1 loss on a range of developmental and autophagy markers during neuronal development was investigated to ascertain if the acute loss would alter the neuronal development and if it would mimic the TSC1 knockout cell line. Additionally, the effect of acute TSC1 loss was also tested in astrocytes with focus on their calcium signalling and their reaction to glutamate as previous studies suggested an increased rate of glutamate toxicity in TSC models.

a. Design of a TSC1 iPSC line utilising CRISPR-Cas13a systems for genome editing
b. Neuronal development of the TSC1 iPSC line and sample collection throughout development
c. RT-PCRs for gene expression analysis of developmental and autophagy markers
d. Astrocytic differentiation of the TSC1 iPSC line and acute induction of TSC1 loss for 48 h
e. Calcium imaging of the TSC1 astrocytes with glutamate induced calcium waves.
f. Staining for apoptosis after brief glutamate treatment of the astrocytes

4.3. Chapter 4: Results

4.3.1. Cell line design

A Cas13 cell line was generated for TSC1 as it would allow a real-time loss of the gene following the activation of the guide and a more flexible knockout system without off-target DNA changes due to Cas9. The *TSC1* guides were inserted into the vector, the latter was then used for the bacteria transformation with E. coli. After incubation, several bacterial colonies for each Exon were picked and Mini-Preps performed. To verify that the colonies have the vector with the guides, digests were performed, and the product was tested with gel electrophoresis with a positive control. Several colonies from the Exon 12 bacteria show an undigested product (Figure 4-1), demonstrating that the vector is included as the guide inclusion damages the digestion side, thus preventing the digest by the enzyme.

Figure 4-1: Mini-Prep for TSC1 Exon 12 and 17 guides for Cas13a system. Digest of the Mini-Prep product shows that several bacterial colonies (A, B, C, G) with Exon 12 guide demonstrated a guide insertion as the plasmid was not digested as shown in comparison to the positive control which was digested.

For further verification of the inclusion of the vector in the bacteria, Maxi-Prep were performed for the bacteria colonies which showed an undigested product in the Mini-Prep. The Maxi-Prep demonstrated that the colonies had indeed the vector with the guide inserted (Figure 4-2) by performing gel electrophoresis on the products.

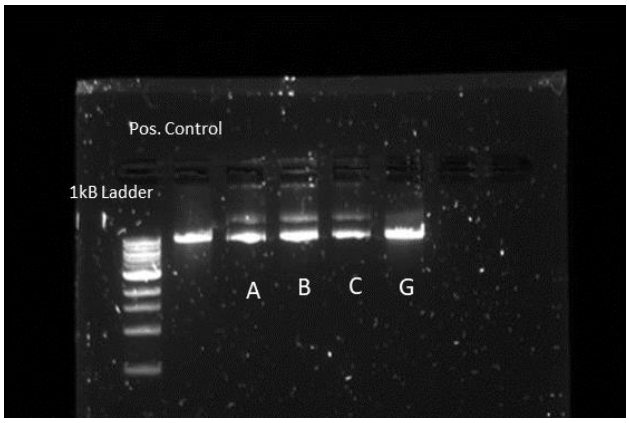

Figure 4-2: Maxi-Prep for TSC1 Exon 12 bacterial cultures. Digest of the Maxi-Prep product shows that the positive control is digested while the bacterial colony samples are not, therefore demonstrating the guide insertion.

The TSC1 plasmid of Exon 12 was transfected into Cas13a iPS cells using electroporation, a transfection with GFP was performed as a positive control. Following this, cells containing the integrated plasmid were selected with antibiotic (Blasticidin) for 7 days. The colonies left after antibiotic selection were checked for GFP expression. Regarding testing the functionality of Cas 13, a 3-day Doxycycline treatment with the following conditions (Control: no doxycycline but DMSO added; 4ul of doxycycline; 8ul doxycycline) was performed with each guide. After the third day, samples were taken for RNA extraction (2 samples for each condition). RNA was isolated using the RNA isolation kit, their concentration was measured prior cDNA transformation. cDNA concentration was measured again before preparing the appropriate dilutions of the samples for qPCR. DMSO was added as the doxycycline was dissolved in DMSO at the time of the cell line generation, and it was aimed to identify any effect of DMSO exposure to the cells. By the time of the cell differentiation discussed in the following pages, doxycycline was dissolved in water thus making the DMSO treatment of the control unnecessary.

The TSC1 Cas13 guide functionality was tested by a qPCR using Beta-Actin as a housekeeping gene and TSC1 primers. Analyses of the data showed that the guide 12c is functioning as the TSC1 expression was significantly reduced after treating the nucleofected cells with doxycycline in comparison to no treatment (see Figure 4-3).

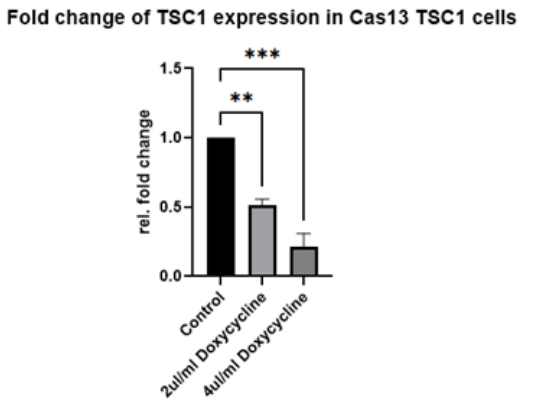

*Figure 4-3: qPCR for TSC1 expression after 48h doxycycline treatment. Both doxycycline treatments showed a significant reduction in the expression (displayed by fold change). Increasing the concentration of doxycycline led to a further reduction of TSC1 expression (N=3). Values are expressed as mean ± SD. The data was analysed via One-Way ANOVA. * = p-value of ≤ 0.05, ** = p-value of ≤ 0.01, *** = p-value: ≤ 0.001, **** = p-value ≤ 0.0001.*

4.3.2. Expression of astrocytic marker in *TSC1* neurons during neuronal development

A neuronal differentiation with the Cas13 TSC1 cells was initiated and the Cas13a system was activated via doxycycline treatment of the cells to induce a heterozygous like loss of TSC1 on the RNA level. The treatment with doxycycline occurred at three different time points of the neuronal development (Day 8, Day 15, and Day 30) where the cells are neuronal stem cells, neuronal progenitor cells or early neurons respectively. The doxycycline treatment itself occurred for either 24 or 48 h before washing the cells with PBS and adding fresh media without any doxycycline (see Figure 4-4). The astrocyte differentiation protocol was followed in order to generate the cells and the Cas13 TSC1 astrocytes were treated 48 h prior the calcium analysis with doxycycline in order to induce a 50% or 80% gene expression reduction of TSC1. As it is impossible to select the location of the plasmid insertion when using electroporation, the Cas13 TSC1 cells without any doxycycline were used as control in order to eliminate any potential of an inserted mutation by the plasmid leading to gene expression alteration and thus impacting the data.

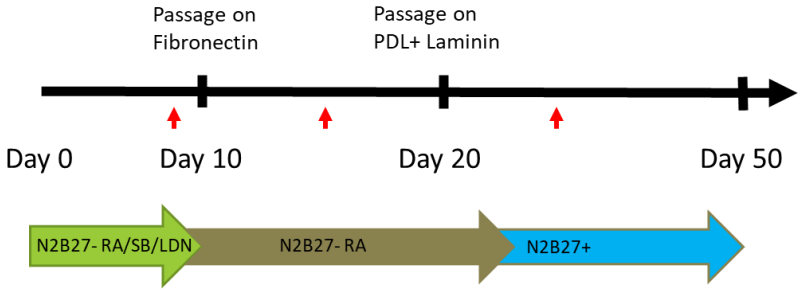

Figure 4-4: Scheme of neuronal differentiation of Cas13 TSC1 cells, time points of doxycycline treatment indicated with red arrows, treatment were for either 24 or 48h.

The analysis of the TSC1 expression in the Cas13 TSC1 cells several days after the doxycycline treatment demonstrates that the TSC1 expression recovers after the acute induction of TSC1 loss (p-value: 0.5539) (see Figure 4-5).

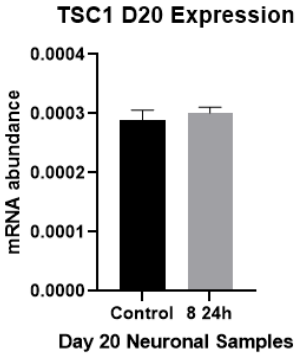

*Figure 4-5: Gene expression of TSc1 in Cas13 TSC1 NPCs. Cells were treated on D8 for 24h with doxycycline and samples were taken on D20. No significant expression changes between the CN and the treated cells were observed (N=3). Values are expressed as mean ± SD. Unpaired t-test was used for the data analysis. * = p-value of ≤ 0.05, ** = p-value of ≤ 0.01, *** = p-value: ≤ 0.001, **** = p-value ≤ 0.0001.*

Gene expression analysis of TSC1 neuronal stem cells (NSCs) showed significant changes in the expression of several astrocytic markers. S100B1 showed a significant increase in the Cas13 TSC1 cells treated for 48 h (p-value: 0.049) while the 24h treatment caused a non-significant increase in expression (p-value: 0.134) (see Figure 4-6).

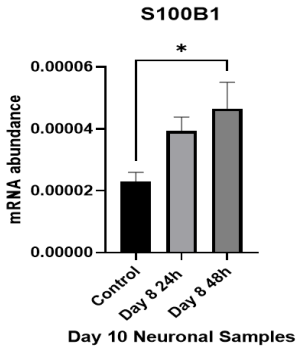

*Figure 4-5: Gene expression of astrocytic markers of Cas13 TSC1 neuronal stem cells during neuronal differentiation. S100B1 is significantly increased for the 48h treatment, while the 24h treatment resulted in a non-significant increase (N=3). Values are expressed as mean ± SD. One-Way ANOVA was used for the data analysis. * = p-value of ≤ 0.05, ** = p-value of ≤ 0.01, *** = p-value: ≤ 0.001, **** = p-value ≤ 0.0001.*

Gene expression analysis of TSC1 neural progenitor cells (NPCs) showed significant changes in the expression of several astrocytic markers. S100B1 showed a significant decrease in the Cas13 TSC1 cells treated for 24 h (p-value: 0.0082). The 48h treatment caused a non-significant decrease in expression (p-value: 0.1798). CD44 and Vimentin were significantly decreased in for either treatment lengths (p-values: 0.0037, 0.0010 for CD44, 0.0008, 0.0013 for Vimentin) (see Figure 4-7).

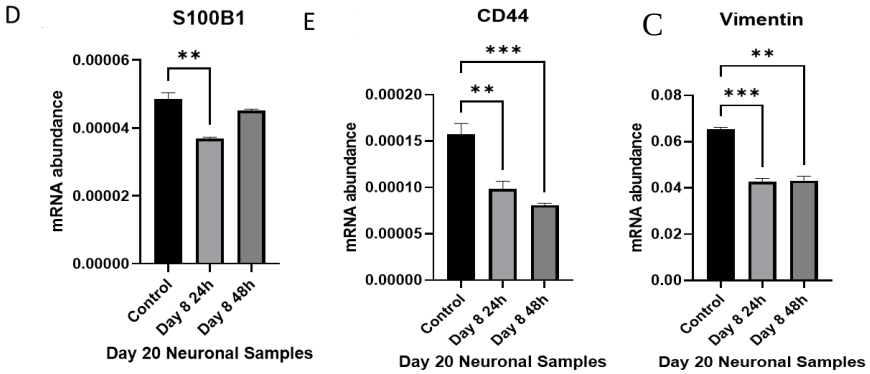

*Figure 4-6: Gene expression of astrocytic markers of Cas13 TSC1 NPCs during neuronal differentiation. A-C: The astrocytic markers S100B1, CD44 and Vimentin were significantly reduced in the cells treated at Day 8 for 24h, cells treated for 48h only showed significant expression reduction for CD44 and Vimentin (N=3). One-Way ANOVA was used for the data analysis, Shapiro-Wilk normality test was passed. * = p-value of ≤ 0.05, ** = p-value of ≤ 0.01, *** = p-value: ≤ 0.001, **** = p-value ≤ 0.0001.*

Gene expression analysis of Cas13 TSC1 neurons showed significant changes in the expression of several astrocytic markers. S100B1 was significantly increased in all conditions of the Cas13 TSC1 cells (p-values: 0.003, 0.0291, 0.0352) treated for 24 h and significant increases in most condition for the 48 h treated cells (p-values: 0.0081, 0.3564, 0.0004). CD44 was significantly increased for cells treated at Day8, while the other treatment time points caused non-significant increases (p-values: 0.0159, 0.439, 0.0504 for 24 h treatment; 0.0007, 0.9597, 0.8579 for 48 h treatment). Vimentin was significantly increased for cells treated at Day 8, while the other treatment time points caused non-significant increases (except for 24 h treatment at Day30) increases (p-values: 0.0369, >0.999, 0.0065for 24 h treatment; 0.0014, 0.1765, 0.1215 for 48 h treatment) (see Figure 4-8).

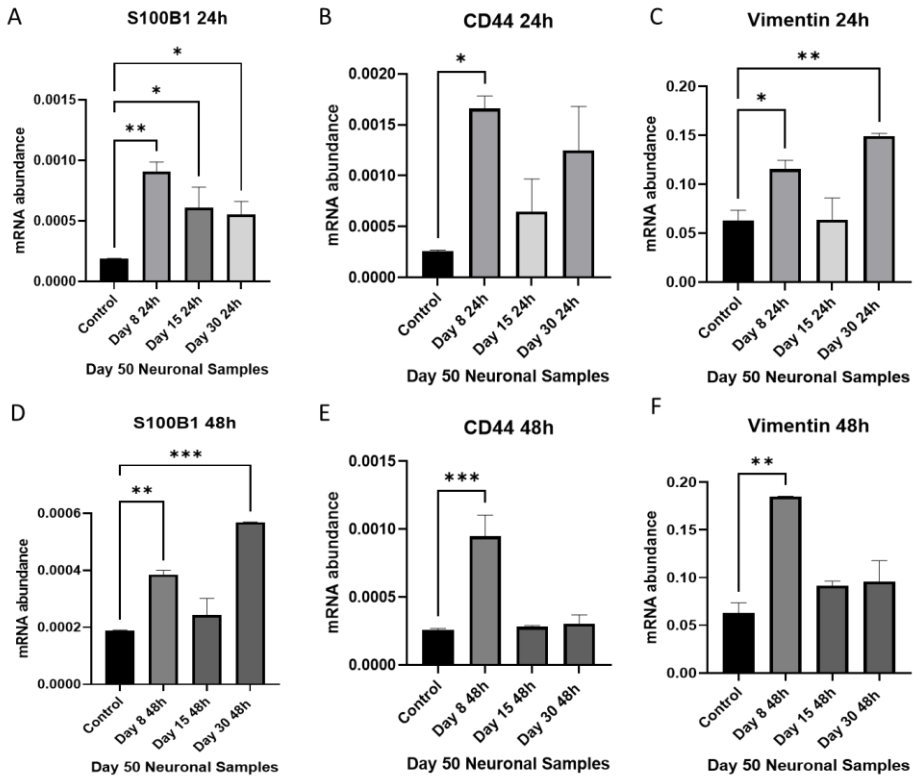

*Figure 4-7: qPCRs of astrocytic markers in Cas13a TSC1 neurons. Loss of TSC1 via doxycycline induced Cas13a system occurred for 24h or 48h. Samples were collected at Day 50 of the 50 Day neuronal protocol; cells were at a mature neuronal state upon collection. A: S100B1 expression was significantly increased for all conditions in comparison to control. B+C: CD44 and Vimentin expression showed significant expression increases for cells treated at Day8. D: Significant expression increases of S100B1 for cells treated at Day8 and Day30 for 48h. E+F: CD44 and Vimentin expression was increased in all conditions with significance for Day8. Values are expressed as mean ± SD (N=3). Data was analysed via One-Way ANOVA. * = p-value of ≤ 0.05, ** = p-value of ≤ 0.01, *** = p-value: ≤ 0.001, **** = p-value ≤ 0.0001.*

In 24 h treated Cas13 TSC1 cells, S100B1 expression increased during the development of both control and Cas 13 TSC1 cells and while the expression aligned between both cell lines at the earlier parts of development, the level of S100B1 at Day 50 was non-significantly higher in the Cas13 TSC1 cells in comparison to the control (p-values for each time points: 0.2601, 0.9879, 0.0963). CD44 expression increased in both control and 24 h treated Cas13 TSC1 cells over time but the CD44 expression in the Cas13 TSC1 cells was significantly higher than in control for the neuronal stage (D20 p-value: 0.9943, D50: p-value: <0.0001). Vimentin expression was significantly decreased at the NPC stage for the Cas13 TSC1 cells (p-value: 0.0167) and was significantly increased in the neurons (p-value: 0.0007). In 48 h treated Cas13 TSC1 cells, S100B1 expression increased during the development for both control and Cas13 TSC1 cells and while the expression aligned between both cell lines at the earlier parts of development, the level of S100B1 at Day50 was significantly higher in the Cas13 TSC1 cells in comparison to the control (p-values for each time points: 0.5942, 0.8588, 0.0322). CD44 expression increased in both control and Cas13 TSC1 cells over time but the CD44 expression in the Cas13 TSC1 cells was significantly higher than in control for the neuronal stage (D20 p-value: 0.3618, D50: p-value: <0.0001). Vimentin expression was significantly decreased at the NPC stage for the Cas13 TSC1 cells (p-value: 0.0325) and was significantly increased in the neurons (p-value: <0.0001) (see Figure 4-9).

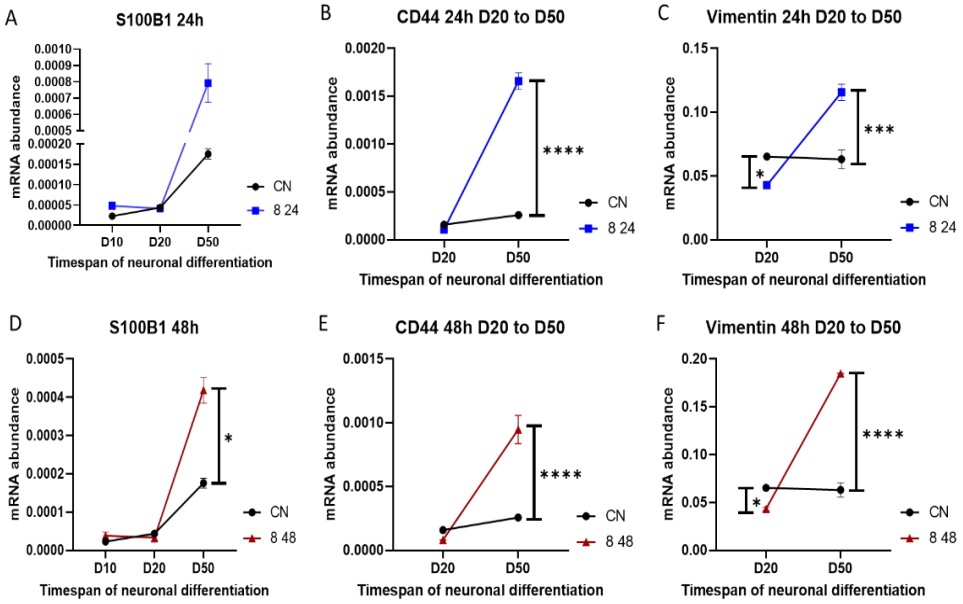

*Figure 4-8: Expression of astrocytic markers during development of Cas13 TSC1 cells. A+D: S100B1 shows a non-significant increase in the Cas13 TSC1 cells at Day 50 and no expression changes during the earlier time points. B+E: CD44 shows a significant increase in the Cas13 TSC1 cells in comparison to control. C+F: Vimentin expression in the Cas13 TSC1 cells is significantly decreased at Day20 and significantly increased at Day 50 in comparison to control. Values are expressed as mean ± SD (N=3). Mixed-effect analysis with Sidaks-Test was performed for data analysis. * = p-value of ≤ 0.05, ** = p-value of ≤ 0.01, *** = p-value: ≤ 0.001, **** = p-value ≤ 0.0001.*

4.3.3. Expression of NPC markers in *TSC1* neurons during neuronal development

In the Cas13 TSC1 cells, Nestin displayed no expression change after the 24 h treatment (p-value: 0.9684), while the 48 h treatment caused a non-significant reduction (p-value: 0.0726). Pax6 showed a statistically non-significant increase after 24 h treatment (p-value: 0.272) and a significant decrease after 48 h (p-value: 0.0158) (see Figure 4-10).

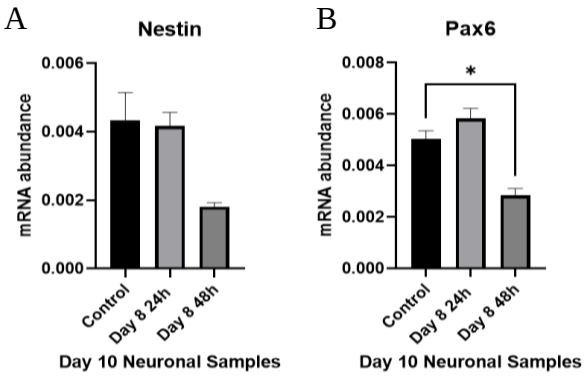

*Figure 4-9: Gene expression of NPC markers of Cas13 TSC1 neuronal stem cells during neuronal differentiation. Cas13 TSC1 display mostly non-significant expression reductions (Pax6 is significantly reduced after 48h treatment) in Cas13 TSC1 cells (N=3). Values are expressed as mean ± SD. Data was analysed via One-Way ANOVA. * = p-value of ≤ 0.05, ** = p-value of ≤ 0.01, *** = p-value: ≤ 0.001, **** = p-value ≤ 0.0001.*

In the Cas13 TSC1 NPCs, Nestin displayed a slight, non-significant increase after the 48 h treatment (p-value: 0.266), while the 24 h treatment caused a significant reduction (p-value: 0.0008). Pax6 showed a statistically non-significant decrease after 24 h treatment (p-value: 0.3155) and a significant increase after 48 h (p-value: 0.006) (see Figure 4-11).

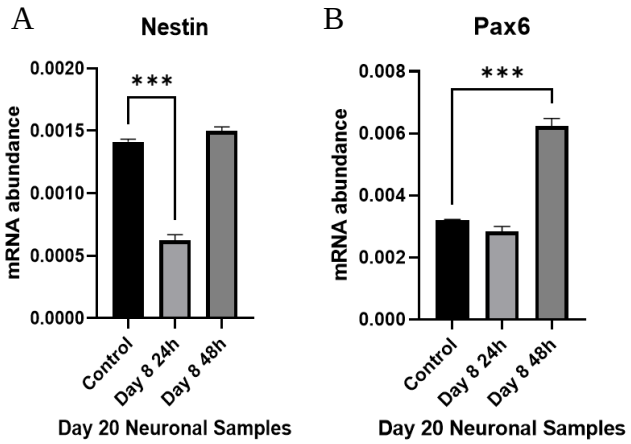

*Figure 4-10: Gene expression of NPC markers of Cas13 TSC1 NPCs during neuronal differentiation. A+B: Cas13 TSC1 display mostly non-significant expression reductions (Pax6 is significantly increased after 48h treatment while the 24h treatment led to a significant decrease in Nestin expression) in Cas13 TSC1 cells (N=3). Values are expressed as mean ± SD. Data was analysed via One-Way ANOVA. * = p-value of ≤ 0.05, ** = p-value of ≤ 0.01, *** = p-value: ≤ 0.001, **** = p-value ≤ 0.0001.*

The 24 h treatment in Cas13 TSC1 neurons led to no obvious expression changes of Nestin expression for Day8 and Day30 cells while the Day15 demonstrate a non-significant drop (p-values: 0.9813, 0.2408, 0.7856). Meanwhile, Pax6 expression was significantly reduced in all 24 h treatment conditions in comparison to control (p-values: 0.0001 and <0.0001 for the Day15 and Day30). The 48 h treatment in Cas13 TSC1 cells led to non-significant expression increases of Nestin for all conditions (p-values: 0.1178, 0.5641, 0.0777), while Pax6 expression was non-significantly reduced for cells treated at Day8 and Day15 while the cells treated at Day30 displayed a significant expression increase (p-value: 0.2580, 0.9990, 0.0173) (see Figure 4-12).

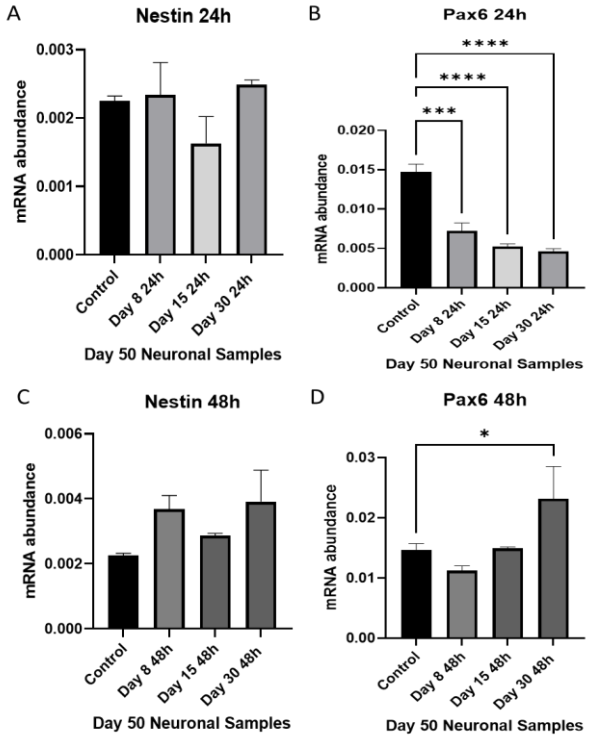

*Figure 4-11: qPCRs of NPC markers in Cas13a TSC1 neurons. Loss of TSC1 via doxycycline induced Cas13a system occurred for 24 or 48h. Samples were collected at Day 50 of the 50 Day neuronal protocol; cells were at a mature neuronal state upon collection. A: 24h treated Cas 13 TSC1 cells displayed non-significant Nestin expression changes, though the treatment at Day15 caused a slight drop in expression. B: 24h treated Cas 13 TSC1 cells displayed significant decreases in Pax6 expression for all conditions. C: 48h treated Cas 13 TSC1 cells displayed non-significant increases in Nestin expression for all conditions. D: 48h treated Cas 13 TSC1 cells displayed no significant changes in Pax6 expression in most conditions while Day30 treatment led to a significant expression increase. Values are expressed as mean ± SD (N=3). Data was analysed via One-Way ANOVA. * = p-value of ≤ 0.05, ** = p-value of ≤ 0.01, *** = p-value: ≤ 0.001, **** = p-value ≤ 0.0001.*

In the 24 h treated Cas13 TSC1 cells, Nestin expression was continuously lower than in control with the biggest discrepancy at Day 10, though no statistical significance was established (p-values for each time points: 0.7908, 0.4393, >0.9999). Pax6 levels were significantly lower at Day 50 for the Cas13 TSC1 cells and aligning to control at the earlier time points (p-values for each time points: 0.5668, 0.9989, 0.0024). Expression of Nestin in the 48 h treated Cas13 TSC1 cells was reduced at Day 10 and increased at Day 50, though no statistical significance was established (p-values for each time points: 0.646, 0.6758, 0.1119). Pax6 levels were significantly reduced at Day 10 and Day 50 for the Cas13 TSC1 cells and significantly increased at Day 20 (p-values for each time points: 0.0433, 0.0113, 0.0327) (see Figure 4-13).

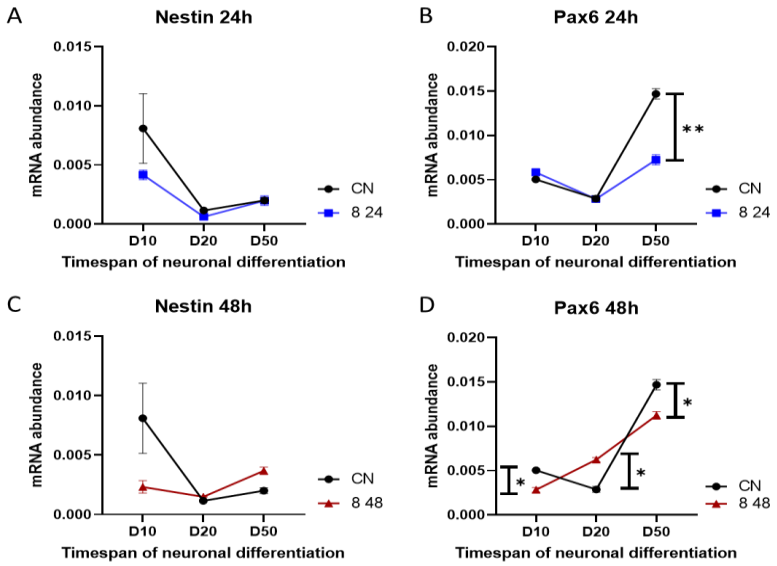

*Figure 4-12: Expression of NPC markers during development in Cas13 TSC1 cells. A: Nestin expression in the Cas13 TSC1 cells independent of treatment length is continuously and non-significantly lower in the TSC1-/- cells in comparison to control. B: Pax6 expression is significantly increased in the 24h treated Cas13 TSC1 cell line at Day50, while no significant changes were observed in the earlier developmental time points. In the 48h treated cells, Pax6 expression is significantly increased in the Cas13 TSC1 cell line at Day 20 and Day 50, while significantly decreased at Day 10. Values are expressed as mean ± SD (N=3). Mixed-effect analysis with Sidaks-Test was performed for data analysis. * = p-value of ≤ 0.05, ** = p-value of ≤ 0.01, *** = p-value: ≤ 0.001, **** = p-value ≤ 0.0001.*

4.3.4. Expression of neuronal markers in *TSC1* during neuronal development

Gene expression analysis of TSC1 NSCs showed significant changes in the expression of several neuronal markers. In the Cas13 TSC1 cells, OTX2 was decreased in both conditions with a significance for the 48 h treatment (p-values: 0.0605 and 0.0383), while ßIII-Tub showed a reduction in both conditions with significance for the 48 h treatment (p-values: 0.2786 and 0.0391 respectively), like FOXG1 where the expression was significantly reduced for both conditions (p-values: 0.0005 and 0.0008) (see Figure 4-14).

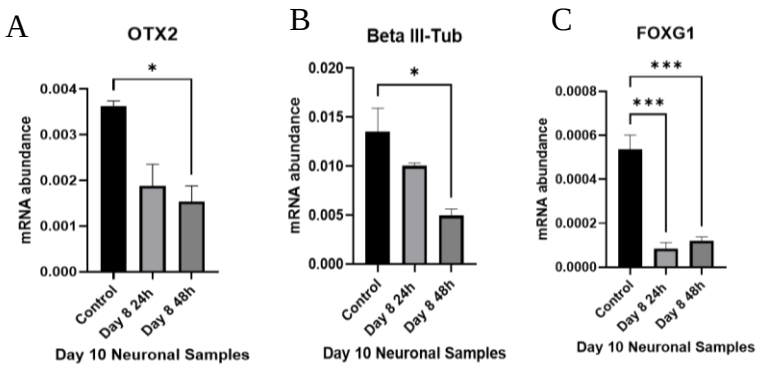

*Figure 4-13: Gene expression of neuronal markers of Cas13 TSC1 neuronal stem cells during neuronal differentiation. A-C: OTX2 and ßIII-Tub expression in Cas13 TSC1 cells is reduced for both 24 and 48h treatment (the latter change is statistically significant). F: In the Ca13 TSC1 cells, FOXG1 expression was significantly reduced for both conditions (N=3). Values are expressed as mean ± SD. Data was analysed via One-Way ANOVA. * = p-value of ≤ 0.05, ** = p-value of ≤ 0.01, *** = p-value: ≤ 0.001, **** = p-value ≤ 0.0001.*

In Cas13 TSC1 NPCs, OTX2 was non-significantly decreased in after 24 h induction (p-value: 0.1808) and significantly increased after the 48 h induction (p-value: 0.0289). ßIII-Tub in the 24h treated cells showed no statistically significant expression changes (p-value: 0.5332) with the 48 h treated cells demonstrated a slight increase in expression (p-value: 0.5026). FOXG1 expression was decreased after 24 h induction (statistically non-significant; p-value: 0.0999) while the 48 h treatment caused no change in FOXG1 levels in comparison to control (p-value: 0.9961) (see Figure 4-15).

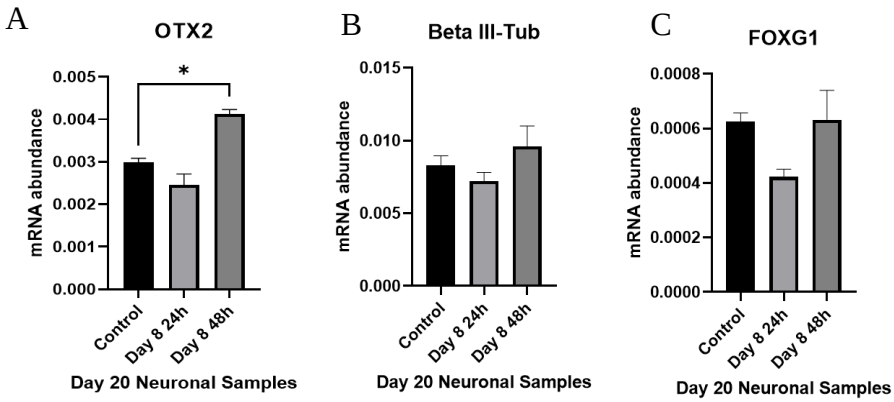

*Figure 4-14: Gene expression of neuronal markers in Cas13 TSC1 NPCs during neuronal differentiation. A-C: In Cas13 TSC1 cells, OTX2 and ßIII-Tub are non-significantly reduced after 24h treatment and significantly increased after 48h treatment in comparison to control. F: FOXG1 expression displayed a slight non-significant increase after 48h treatment while the 24h treatment caused a non-significant decrease in expression (N=3). Values are expressed as mean ± SD. Data was analysed via One-Way ANOVA. * = p-value of ≤ 0.05, ** = p-value of ≤ 0.01, *** = p-value: ≤ 0.001, **** = p-value ≤ 0.0001.*

In 24 h treated Cas13 TSC1 neurons, OTX2 was increased in all conditions in comparison to control with significant expression increases for the Day8 and Day15 cells (p-value: 0.0004, 0.0021, 0.1312). βIII-Tub showed reduced expression in all conditions (p-values: 0.0029, 0.0164, 0.0014), like FOXG1, which expression was significantly decreased for all conditions in comparison to control (p-value: <0.0001 for all conditions). In 48 h treated Cas13 TSC1 cells, OTX2 was increased in all conditions in comparison to control with significant expression increases for cells treated at Day30 (p-values: 0.1704, 0.3201, 0.0058). βIII-Tub showed reduced expression in cells treated at Day8 and Day15 for 48 h while the cells treated at Day30 had non-significantly increased βIII-Tub levels (p-values: 0.9053, 0.0843, 0.8830). FOXG1 expression was decreased in all conditions of cells treated for 48 h with significance for cells treated at Day8 and Day30 (p-values: 0.0025, 0.3894, 0.0001) (see Figure 4-16).

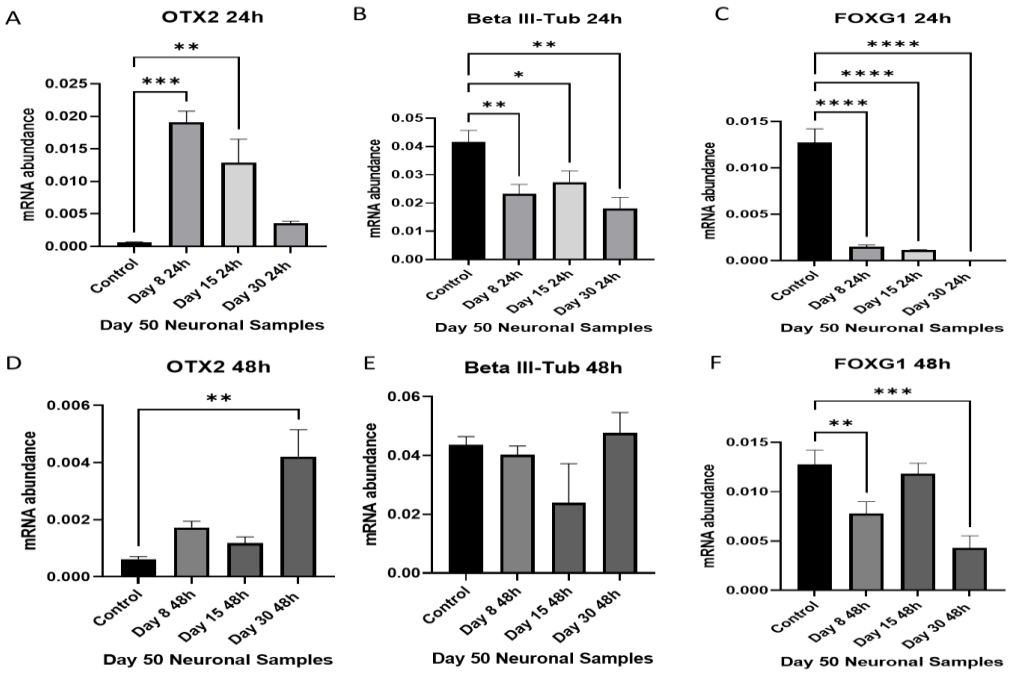

*Figure 4-15: qPCRs of neuronal markers in Cas13a TSC1 neurons. Loss of TSC1 via doxycycline induced Cas13a system occurred for 24 or 48h. Samples were collected at Day 50 of the 50 Day neuronal protocol; cells were at a mature neuronal state upon collection. A+D: In 24h treated Cas13 TSC1 cells, OTX2 expression was increased in all conditions with significance for Day8 and Day15, while the 48h treated cells display expression increases in all conditions with significance for Day30. B+E: βIII-Tub expression was significantly decreased in all conditions in 24h treated cells while the 48h treated cells display no significant expression changes. F: Both treatment lengths display a reduction of FOXG1 expression for all treatment time points with significant expression changes for the majority. Values are expressed as mean ± SD (N=3). Data was analysed via One-Way ANOVA. * = p-value of ≤ 0.05, ** = p-value of ≤ 0.01, *** = p-value: ≤ 0.001, **** = p-value ≤ 0.0001.*

In the 24 h treated Cas13 TSC1 cells, OTX2 expression was non-significantly lower at Day 10 and non-significantly increased at Day 50 in the Cas13 TSC1 cells while Day 20 showed no obvious expression changes (p-values for each time points: 0.3928, 0.5947, 0.1176). βIII-Tub expression was slightly lower in the Cas13 TSC1 cells during development and showed significant reduction in the neurons (p-values for each time points: 0.753, 0.6277, 0.0143). FOXG1 expression in the Cas13 TSC1 cells nearly aligned with the control cells during the early development and was significantly lower at Day 50 (p-values for each time points: 0.0666, 0.07, 0.015). Meanwhile the 48 h treated cells display changes of OTX2 expression with a non-significant reduction at Day10 and a non-significant increase at Day 50 in the Cas13 TSC1 cells while Day 20 showed a significant increase (p-values for each time points: 0.2245, 0.0442, 0.1564). βIII-Tub expression was slightly lower in the 48 h Cas13 TSC1 cells at Day 10 and then aligned to the control at the later stages (p-values for each time points: 0.3866, 0.8856, 0.9714). FOXG1 expression in the Cas13 TSC1 cells nearly aligned with the control cells during the early development and was non-significantly reduced at Day 50 (p-values for each time points: 0.0595, >0.9999, 0.1009) (see Figure 4-17).

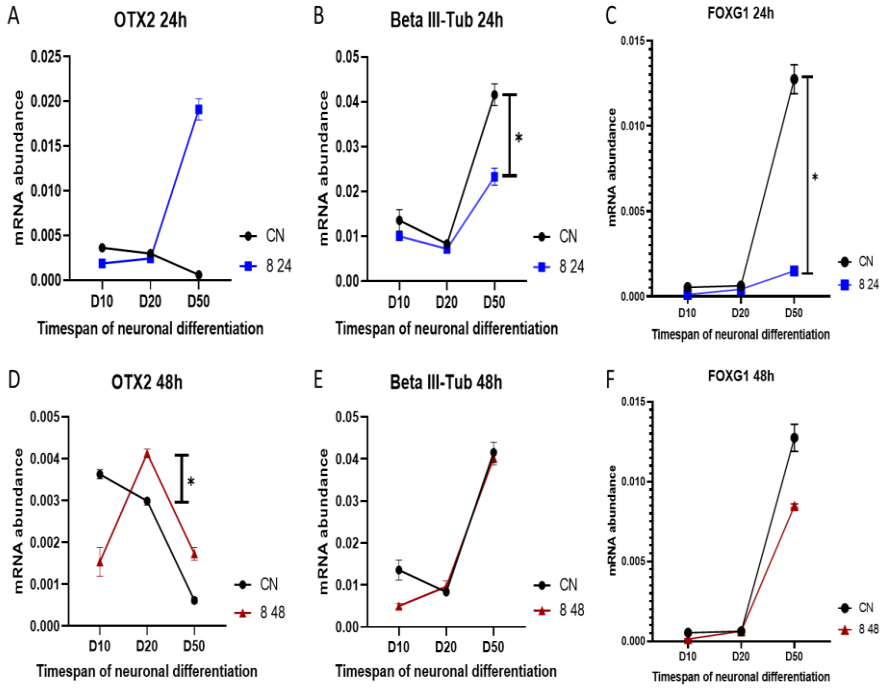

*Figure 4-16: Expression of neuronal markers during development of Cas13 TSC1 cells. A: In the 24h treated Cas13 TSC1 cells, OTX2 expression is non-significantly decreased at Day10 and non-significantly increased at Day50, no change at Day20 while the 48h treated cells display a OTX2 expression with a non-significantly decrease at Day 10 and a non-significantly increase at Day50, while being significantly increased at Day 20. B+E: βIII-Tub expression was slightly but non-significantly reduced in the 24h Cas13 TSC1 cells at the early time points and significantly reduced in the neurons. βIII-Tub expression in the 48h treated cells was non-significantly reduced in the Cas13 TSC1 cells at Day 10 and aligning to control at later time points. C+F: Expression of FOXG1 is non-significantly reduced in the 24h treated Cas13 TSC1 cells during early development, levels at Day50 were significantly lower in Cas13 TSC1 in comparison to control with the 48h treated cells displaying a similar expression except a non-significant reduction at Day 50. Values are expressed as mean ± SD (N=3). Mixed-effect analysis with Sidaks-Test was performed for data analysis. * = p-value of ≤ 0.05, ** = p-value of ≤ 0.01, *** = p-value: ≤ 0.001, **** = p-value ≤ 0.0001.*

4.3.5. Expression of autophagy markers in *TSC1* during neuronal development

Gene expression analysis of the TSC1 neuronal stem cells shows significant alterations for autophagy related genes. The Cas13 TSC1 cells display a ULK1 increase for all conditions after TSC1 heterozygous loss though the only significance was after the 48 h treatment (p-values: 0.097 and 0.0308). TFEB was statistically non-significantly increased for the 24 h condition (p-value: 0.8952) and non-significantly decreased for the 48 h treatment (p-value: 0.7258). GSK3a expression was significantly increased after 24 h TSC1 loss (p-value: 0.0029) and significantly decreased after 48 h TSC1 loss (p-value: 0.0036) (see Figure 4-18).

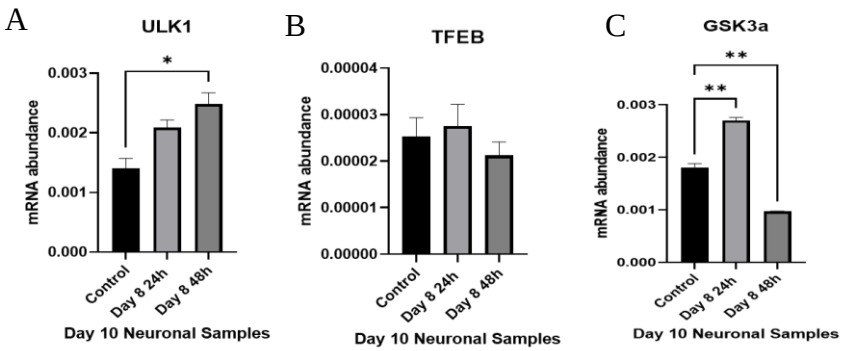

*Figure 4-17: Gene expression of autophagy markers in Cas13 TSC1 neuronal stem cells during neuronal development. A: The expression of ULK1 was increased in the Cas13 TSC1 cells (significance for 48h treatment). B: TFEB expression in Cas13 TSC1 cells showed no significant changes. C: GSK3a expression showed a significant increase after 24h treatment and a significant reduction after 48h loss of TSC1 (N=3). Values are expressed as mean ± SD. Data was analysed via One-Way ANOVA. * = p-value of ≤ 0.05, ** = p-value of ≤ 0.01, *** = p-value: ≤ 0.001, **** = p-value ≤ 0.0001.*

In the Cas13 TSC1 cells, ULK1 was decreased for both conditions with a significant reduction after the 48 h treatment (p-values: 0.3134 and 0.0337). TFEB was significantly increased after 24 h TSC1 loss (p-value: <0.0001) and showed no expression change after 48 h TSC1 loss (p-value: 0.6338). GSK3a expression was increased in both conditions with a significant increase after 24 h loss of TSC1 (p-values: 0.0381 and 0.6275) (see Figure 4-19).

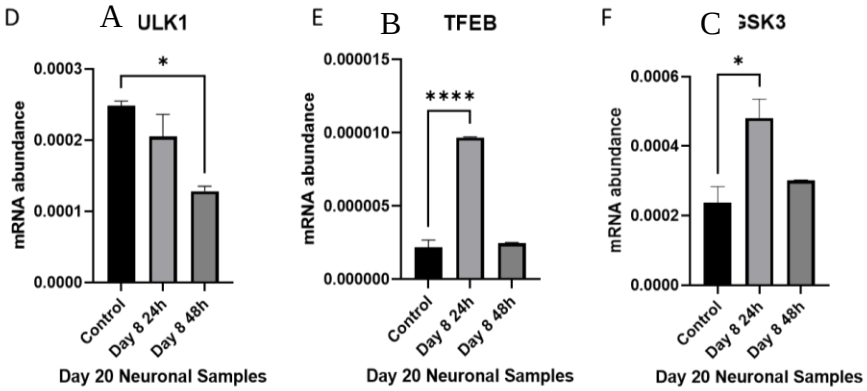

*Figure 4-18: Gene expression of autophagy markers in Cas13 TSC1 NPCs during neuronal development. A: The expression of ULK1 was decreased in the Cas13 TSC1 cells (significance for 48h treatment). B: TFEB expression in the Cas13 TSC1 cells displays a significant increase for the 24h treated cells. C: Cas13 TSC1 cells display a significant increase after 24h treatment and a non-significant increase after 48h loss of TSC1 (N=3). Values are expressed as mean ± SD. Data was analysed via One-Way ANOVA. * = p-value of ≤ 0.05, ** = p-value of ≤ 0.01, *** = p-value: ≤ 0.001, **** = p-value ≤ 0.0001.*

Gene expression analysis of the Cas13a TSC1 neurons shows significant alterations for autophagy related genes. In the 24 h treated Cas13 TSC1 cells, ULK1 was decreased in all conditions with a significant reduction for the Day30 cells (p-values: 0.7613, 0.2524, 0.0209) while the 48 h treated cells displayed a non-significant decrease in the cells treated at Day15 or Day30 with a significant increase at Day8 (p-values: 0.0174, 0.5238, 0.0605). TFEB expression was significantly decreased in all conditions of the 24 h treated cells (p-values: 0.0006 and 0.0004 for Day15 and Day30) while the 48 h treatment caused a significant increase in the cells treated at Day8 and non-significant decreases for the later time points (p-values: 0.0448, 0.9521, 0.0691). GSK3a expression significantly decreased in all conditions of the 24 h treated cells (p-values: 0.0105, 0.0012 and 0.0011). Meanwhile, the 48 h treatment led to significant decreases for the cells treated at Day15 and Day30, and no expression changes for cells treated at Day8 in comparison to control (p-values: 0.9983, 0.0264 and 0.0043) (see Figure 4-20).

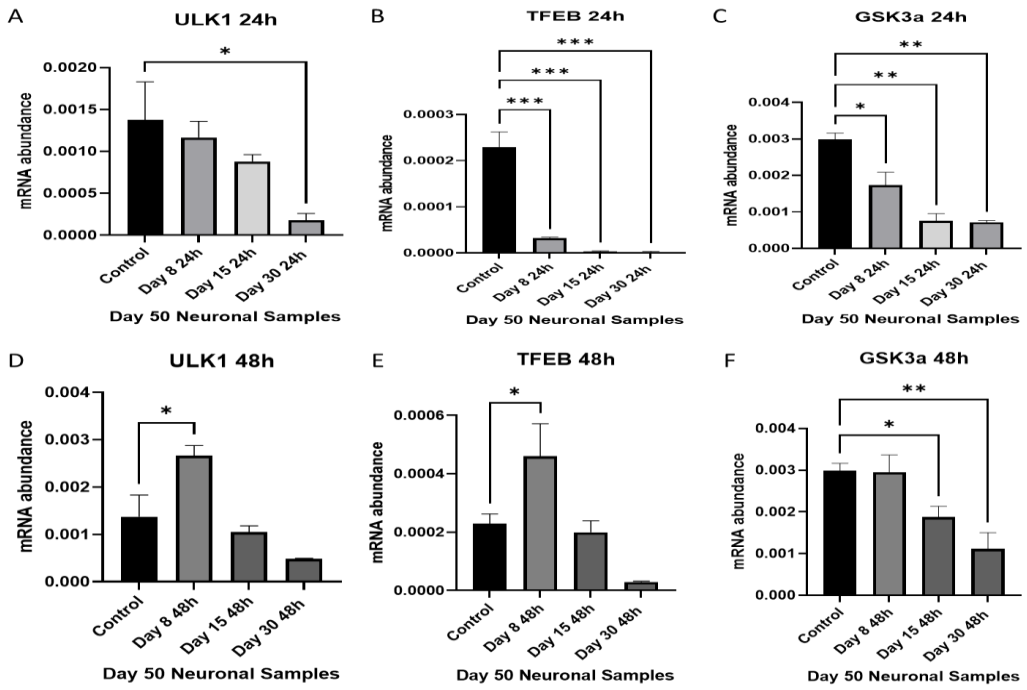

*Figure 4-19: Gene expression of autophagy markers in Cas13a TSC1 neurons. TSC1 heterozygous loss was induced via doxycycline at day 8, 15 or 30 for 24h or 48h. A+D: A non-significant decrease in expression was found for the Day8 and Day15 cells, while TSC1 loss at Day 30 led to significant reduction in ULK1 expression in the 24h treated cells while the 48h cells show a significant increase in expression was found for the Day8 cells, while TSC1 loss at Day 30 led to significant reduction in ULK1 expression. B+E: All conditions led to a significantly reduced expression of TFEB in comparison to control in the 24h treated cells while the 48h treatment led to a significant increase in expression at Day8, with Day15 displayed no expression change while Day30 demonstrated a non-significant reduction. C+F: GSK3a expression in Cas13 TSC1 cells was significantly decreased in all conditions for the 24h treated cells while the 48h treatment showed a significant decrease in cells treated at Day15 or Day30 while treatment at Day8 had no consequences on expression levels. Values are expressed as mean ± SD (N=3). Data was analysed via One-Way ANOVA. * = p-value of ≤ 0.05, ** = p-value of ≤ 0.01, *** = p-value: ≤ 0.001, **** = p-value ≤ 0.0001.*

Analysis of expression changes over the neuronal development in Cas13 TSC1 cells shows expression changes of the autophagy markers over time. In the 24 h treated cells, ULK1 expression decreased towards the NPC stage and increased again when the cells entered the neuronal stage. No significance was found between the Cas13 TSC1 cells and the control (p-values: 0.2408, 0.8174, 0.9516). Similarly, the 48 h treated cells display no significant expression changes with non-significant increases of ULK1 expression at Day 10 and Day 50 (p-values: 0.1525, 0.0709, 0.2971). TFEB expression decreased towards the NPC stage and then increased for neurons. Significance was found between the 24 h treated Cas13 TSC1 cells and the control at the neuronal stage where the expression was significantly reduced in the Cas13 TSC1 cells (p-values: 0.2938, 0.1110, 0.0414). Meanwhile, the 48 h treated cells displayed no significance to control throughout the development (p-values: 0.8865, 0.9656, 0.4954). GSK3a decreased towards the NPC stage and increased again when the cells entered the neuronal stage. GSK3 expression was non significantly increased at Day 10 and non-significantly decreased at Day 50 in the 24 h treated Cas13 TSC1 cells (p-values: 0.4351, 0.6112, 0.2144) while the 48 h treated cells displayed a non-significant GSK3a decrease in the NSC stage and aligned to control at the latter stages of development (p-values: 0.1715, 0.9524, 0.9994) (see Figure 4-21).

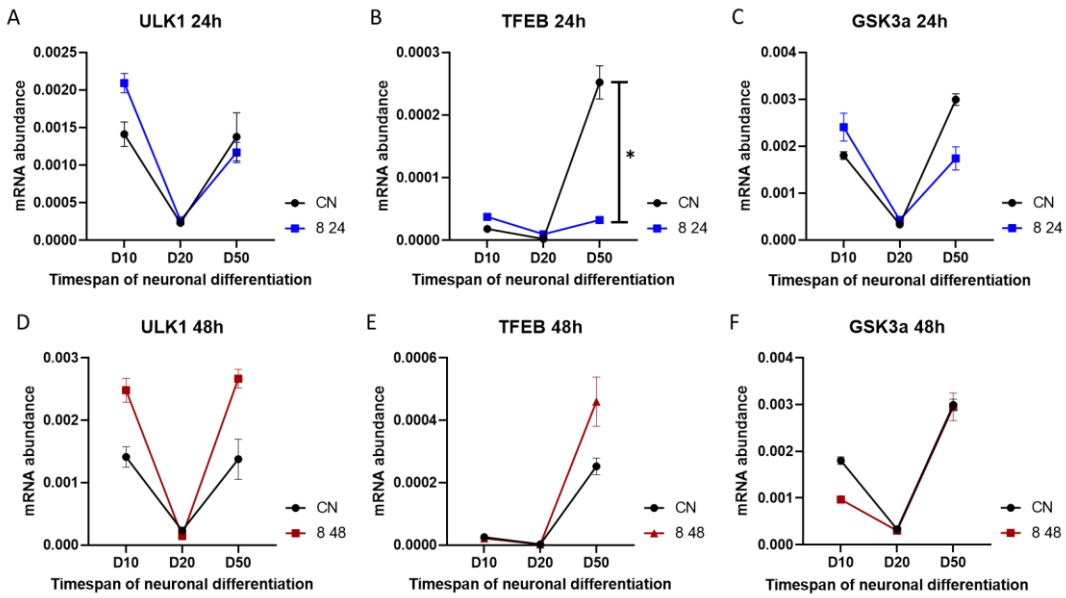

*Figure 4-20: Expression of autophagy markers during development of Cas13 TSC1 cells. A-C: No significance was found for ULK1 and GSK3a between 254h treated Cas13 TSC1 and control throughout development while TFEB expression was significantly reduced in the 24h treated Cas13 TSC1 cells at Day50. D-F: No significance was found for either of the autophagy markers between the 48h treated Cas13 TSC1 and control throughout development. Values are expressed as mean ± SD (N=3). Mixed-effect analysis with Sidaks-Test was performed for data analysis. * = p-value of ≤ 0.05, ** = p-value of ≤ 0.01, *** = p-value: ≤ 0.001, **** = p-value ≤ 0.0001.*

4.3.6. Calcium signalling in Cas13 *TSC1* astrocytes.

The Cas13 TSC1 cells were differentiated into astrocytes in the absence of doxycycline until reaching maturity (Age: D90). 48 h prior the calcium signalling experiment, the 3 cell conditions were set up: no doxycycline (CN), 2µl/ml of doxycycline to induce ~50% reduction of TSC1 and 4µl/ml of doxycycline to induce an ~80% reduction of TSC1. The living cells are stained with Fura2-AM to stain the intracellular calcium 1h prior recording. The cells were recorded for several minutes, to establish the base calcium level of the cells. After this level was established, glutamate (10nM) was added into the media to induce a calcium wave. The recording was stopped several minutes after the calcium wave induction when the cells enter a post-wave homeostasis. Calcium imaging of the Cas13 TSC1 astrocytes showed significant differences between the control and the TSC1 50% cells. The cells with the induced TSC1 loss showed a significantly increased base level of calcium in the cells (p-value: <0.0001) (see Figure 4-21 B) as well as significantly higher peaks (p-value: <0.0001) (see Figure 4-22 C) than the control as well as higher variation between the cells (see increased standard deviation in 4-22 B and C). The example calcium wave (Figure 4-22 A) demonstrates the higher base calcium level of the TSC1 50% astrocytes prior the wave as well as the longer and bigger release of calcium during the monitoring. While the control cells stopped their calcium release into the extracellular and levelled the calcium level, the TSC1 50% cells continued to release calcium.

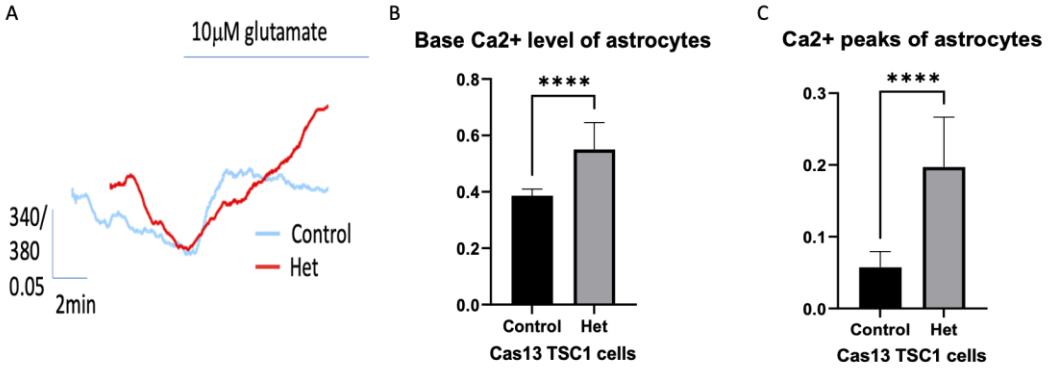

*Figure 4-21: Analysis of calcium base level and signalling in Cas13 TSC1 astrocytes after 48 h of induced TSC1 loss. 340/380 mark the different channels of the Leica microscope for the calcium detection. A: Example of calcium wave in control and TSC1 50% cells. A continuous increase in calcium release is seen in the TSC150% cells, unlike the control cells where the level remains lower and levelled. B: Base level of intracellular calcium in astrocytes prior calcium waves. Cells with induced TSC1 50% loss showed a significantly elevated base level of intracellular calcium. Mann-Whitney Test (N=40). C: Calcium peaks stand for the size of the calcium wave e.g., the amount of calcium which is released during the wave. Calcium peaks of TSC1 50% cells is significantly higher than in control and shows a higher standard deviation. Values are expressed as mean ± SD. For the analysis, Mann-Whitney-U Test was used (N=40). * = p-value of ≤ 0.05, ** = p-value of ≤ 0.01, *** = p-value: ≤ 0.001, **** = p-value ≤ 0.0001.*

Combining the calcium waves of a cluster of astrocytes shows a clear difference between the control and the TSC1 50% cells. While the control cells are synchronous and show close levels of calcium base levels as well as peaks, the TSC1 50% cells not only show less synchronicity as well as increased variability between them. Also, an increased calcium export in the TSC1 50% in comparison to the control is seen (see Figure 4-23).

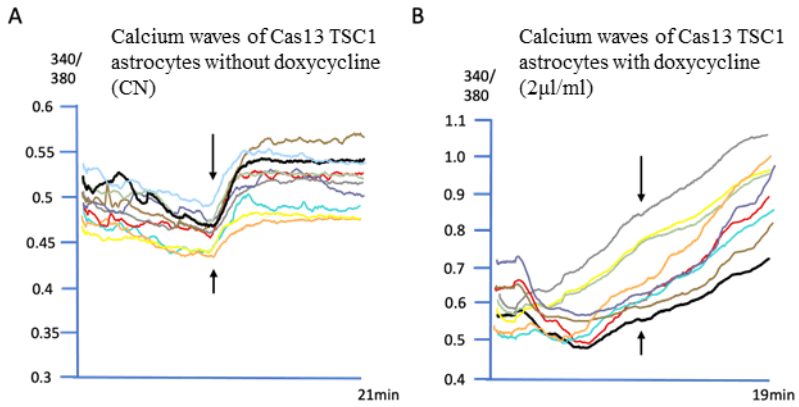

Figure 4-22: Calcium waves of a cluster of ten astrocytes. 340/380 mark the different channels of the Leica microscope for the calcium detection. A: Calcium wave of Cas13 control cells. Recording was performed over 21 min. Black arrows mark the time point of adding glutamate (10nM) to the cell media to induce a calcium wave. B: Calcium wave of Cas13 TSC1 50% cells. Recording was performed over 21 min. Black arrows mark the time point of adding glutamate (10nM) to the cell media to induce a calcium wave.

The Cas13 TSC1 astrocytes were recorded during the calcium imaging. The recording started prior the glutamate treatment, so that any morphology changes would be documented. The control Cas13 TSC1 astrocytes displayed minimal shrinkage and no obvious morphology changes (see Figure 4-24).

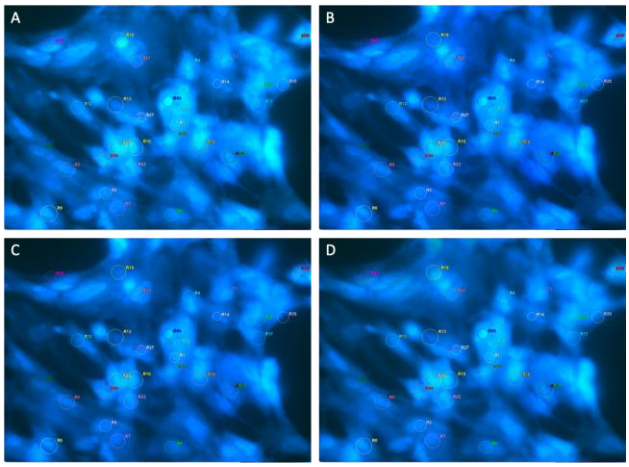

Figure 4-23: Fura2am (Calcium stain) stained control Cas13 TSC1 astrocytes with no doxycycline induced TSC1 loss (CN). Each circle us the labelling on an astrocyte marked for calcium measurements. A: Astrocytes at the beginning of the recording. B: Astrocytes briefly after the glutamate treatment, astrocytes start losing their connections and shrink. C: Astrocytes at the end of the recording, cell shrinkage is clearly visible. D: Overlay of A and C to showcase cell movement during recording

The Cas13 TSC1 astrocytes with a 50% induced TSC1 loss displayed a loss of cell-cell connections after the glutamate treatment and the subsequent induction of a calcium wave. Most cell-cell connection were lost in the centre of the astrocyte colony (see Figure 4-25).

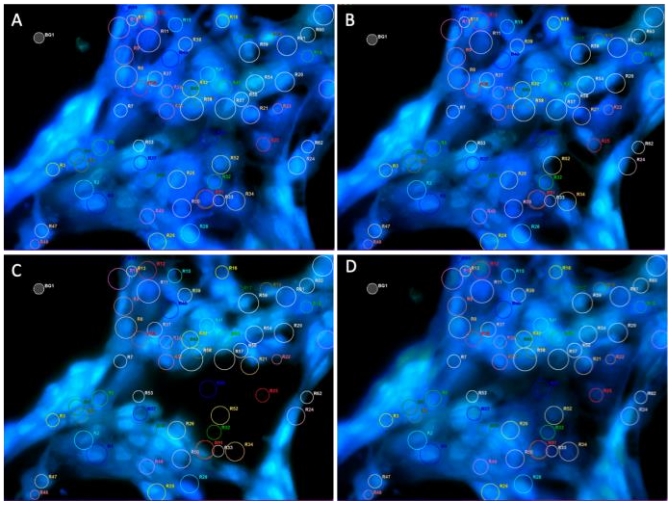

Figure 4-24: Fura2am (Calcium stain) stained Cas13 TSC1 astrocytes with 50% TSC1 loss induced for 48 h. Each circle us the labelling on an astrocyte marked for calcium measurements. A: Astrocytes at the beginning of the recording. B: Astrocytes briefly after the glutamate treatment, astrocytes start losing their connections and shrink. C: Astrocytes at the end of the recording, cell shrinkage is clearly visible. D: Overlay of A and C to showcase cell movement during recording

As the Cas13 astrocytes with a ~80% suppressed TSC1 expression died within a few minutes during the recording, no measurements were possible. Despite this the recording demonstrates an exaggerated phenotype in comparison to the heterozygous cells. Pictures taken from the recording display the shrinkage of the astrocytes after glutamate treatment (see Figure 4-26).

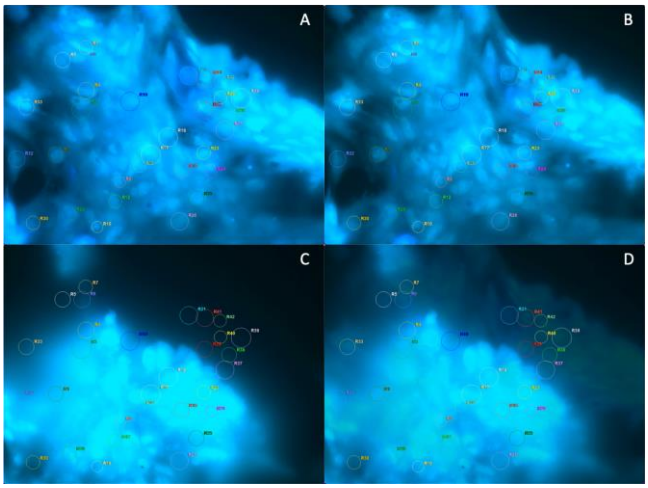

Figure 4-25: Fura2am (Calcium stain) stained Cas13 TSC1 astrocytes with ~80% TSC1 loss induced for 48 h. Each circle us the labelling on an astrocyte marked for calcium measurements. A: Astrocytes at the beginning of the recording. B: Astrocytes briefly after the glutamate treatment, astrocytes start losing their connections and shrink. C: Astrocytes at the end of the recording, cell shrinkage is clearly visible. D: Overlay of A and C to showcase cell movement during recording

4.3.7. Glutamate treatment in Cas13 *TSC1* astrocytes

Staining of the control astrocytes after a 30 min glutamate treatment shows few single cells staining positive for ANXA5, thereby suggesting the occurrence of cell death (see Figure 4-27). In comparison, TSC1 50% cells showed an increased number of cells positive for ANXA5 (see Figure 4-28), suggesting a vulnerability of the cells towards glutamate.

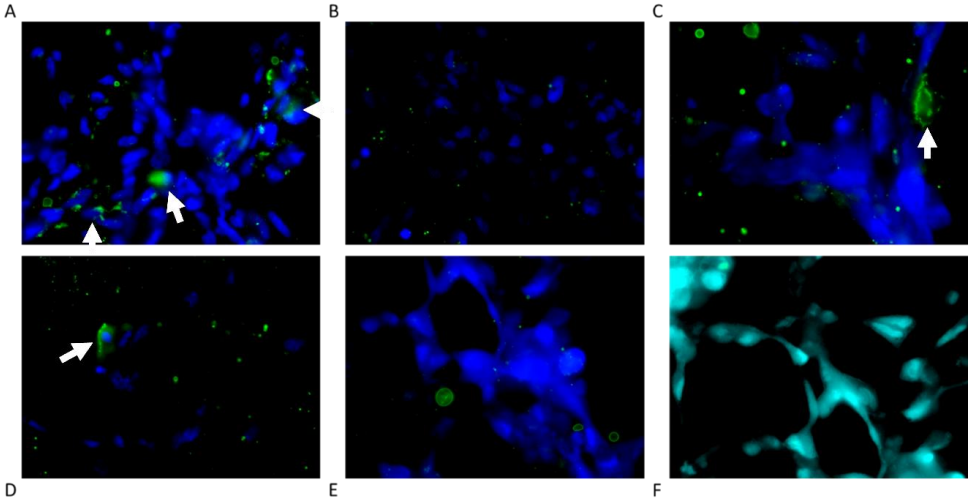

Figure 4-26: Calcium Staining of Cas13 control cells with Hoechst (blue), Fura2am (cyan) and ANXA5 (green). ANXA5 staining marks cell death via apoptosis (and marked with white arrows), while Fura2am stains intracellular calcium. Few cells in A, C and D show ANXA5 stained cell membrane indicating dying or dead cells.

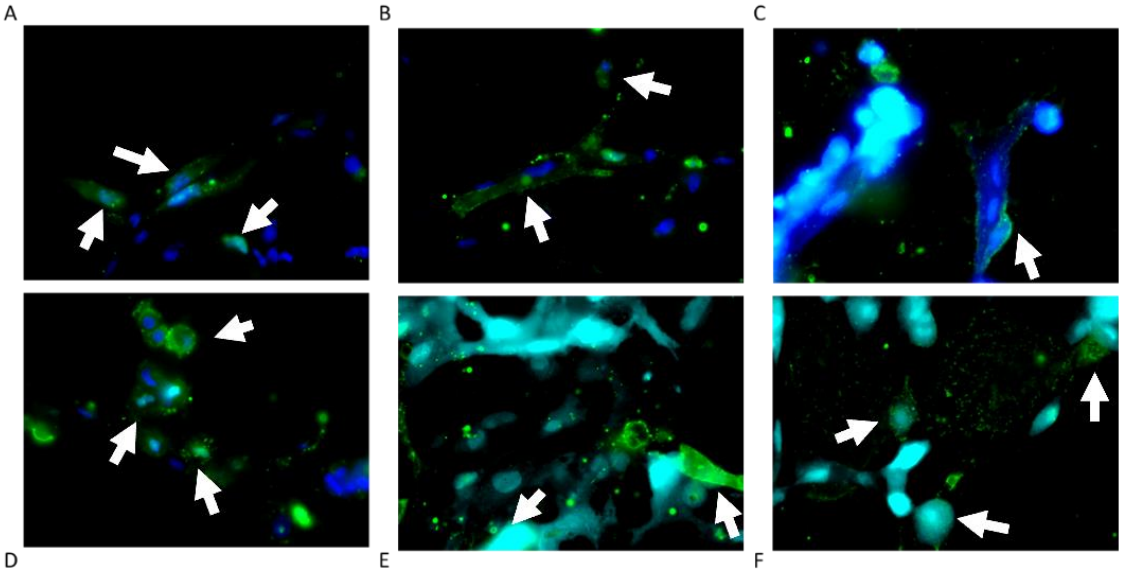

Figure 4-27: Calcium Staining of Cas13 TSC1 50% cells with Hoechst (blue), Fura2am (cyan) and ANXA5 (green). ANXA5 staining marks cell death via apoptosis (and marked with white arrows), while Fura2am stains intracellular calcium. Several cells in show ANXA5 stained cell membrane indicating dying or dead cells.

4.4. Chapter 4: Summary of Major outcomes in this chapter:

- Developmental and autophagy markers were significantly dysregulated in Cas13 TSC1 loss, the effect was prolonged despite acute loss.
- Neuronal markers such as FOXG1 and OTX2 were significantly downregulated in neurons after TSC loss induction, independent of treatment point.
- The base calcium level and calcium peaks of Cas13 induced TSC1 50% loss cells was significantly higher than in control.
- Calcium levels of Cas13 induced TSC1 50% loss cells continued rising and failed to return to a base level, unlike the control astrocytes.
- Calcium imaging suggests that the glutamate treatment in cells with induced TSC1 loss leads to cell shrinkage/cell death as the cells clumped together during the recording.
- Staining suggests that the cells with TSC1 loss display higher level of apoptosis after glutamate treatment than control.

4.5. Chapter 4: Discussion

4.5.1. Cell Line design:

Utilising the Cas13a system in stem cells allows the induction of dose-dependent gene loss at any timepoint and state of cell development, thus making it a prefect model to identify sensitive timepoints during cell development. There are controversial studies of whether the Cas13a system has off-targets like the Cas9 system. Abudayyeh *et al.* demonstrated that the knockdown specificity of the Cas13a system is higher than for shRNA construct despite comparable levels of gene knockdown and that Cas13a knockdown is sensitive to mismatches in the central seed region of the guide-target duplex (Abudayyeh *et al.* 2017). Other papers also demonstrated a high efficiency and specificity for the Cas13a system for mammalian cells (Kleinstiver *et al.* 2015) while others claimed collateral effects by off-target RNA slicing (Wang *et al.* 2019b).

Conditional knockdown cell lines may show a different phenotype than knockout cell lines due to genetic compensation/genetic robustness. The loss of a gene due to a mutation might cause the activation of redundant genes with similar functions and expression patterns in order to compensate for the loss of the gene. Otherwise, genetic compensation upstream of the protein function was suggested. El-Brolosy stated that compensation due to gene knockout is a widespread phenomenon and that knockdown models will have more severe phenotypes due to the lack of compensation in comparison to knockouts (El-Brolosy and Stainier 2017). Therefore, the Cas13a cells are a great tool in order to identify some of the consequences of TSC1 loss, especially as they would differentiate more easily into other cell types as the TSC1 loss would not be active for prolonged time, thereby circumventing the impaired cell differentiation characteristics of TSC cell models. On the other hand, the phenotype would be more severe as El-Brolosy suggested and probably not align perfectly to TSC patients.

4.5.2. Gene Expression:

4.5.2.1. Astrocyte markers:

As discussed in the previous chapter, the tested astrocytic markers S100B1, CD44 and Vimentin play important roles in cell differentiation and cell progression (Kochlamazashvili *et al.* 2010; District 2019; Pattabiraman *et al.* 2020). Thus, their significant dysregulation throughout the neuronal development after acute TSC1 loss, presumably negatively impacted the cell development. The increased levels at the neuronal stage were surprising as it was not expected that a brief loss of TSC1 would have such prolonged effects on gene expression throughout the development. TSC deficient cells are known to prefer the astrocytic fate over the neuronal one (Blair *et al.* 2018), especially homozygous cell lines. The neuronal differentiation of the tested cells was successful as the expression of neuronal markers shows. As epilepsy (Chong *et al.* 2010) as well as various psychiatric disorders such as anxiety, mood and behavioural disorders are known comorbidities of TSC (Chung *et al.* 2011) and overlap with the disorders known for elevated S100B1 expression, it can be presumed that overly expressed S100B1 is part of TSC pathology. As discussed before, both S100B1 and Vimentin are involved in the protection against oxidative stress (Matveeva *et al.* 2010; Yamaguchi *et al.* 2016). HIF1a, a hypoxia related marker is known to be significantly upregulated in TSC models (Zhang *et al.* 2016) and while its expression was not analysed in this thesis, it might be an interesting future endeavour to test if the acute TSC1 loss leads to induced cell/oxidative stress as hypoxia is known to promote oxidative stress in cells, which would then in turn cause an increase of *S100B1* and Vimentin expression and thus explain the significant expression increase of S100B1 at the NSC stage. The exact role of CD44 in neuronal development is uncertain, though it has been considered that it might be involved in axon guidance (Sretavan *et al.* 1994; Lin and Chan 2003) as it was demonstrated that CD44 is involved in dendritic polarity and the Golgi apparatus morphology in neurons (Skupien *et al.* 2014). CD44 expression is known to be strongly induced in AD patient brains (Akiyama *et al.* 1993) and lymphocytes (Uberti *et al.* 2010). Furthermore, AD patients' samples have shown increased levels of several CD44 splice variants, both neuronal and astrocytic variants, therefore suggesting an involvement of CD44 in the pathogenesis of AD (Pinner *et al.* 2017). Vimentin immunoreactivity was found in neurons affected by amyloid plaques (Yamada *et al.* 1992), with further validation and the suggestion that *Vimentin* expression might be a cell response to cellular or tissue damage (Levin *et al.* 2009).

Elevated levels of S100B1 have also been linked to brain dysfunction (Gerlai *et al.* 1995) and mortality in patients with sepsis, or to AD and epilepsy where the gene levels correlated with brain regions of high neuropathology (Petrova *et al.* 2000).

In Conclusion, all astrocytic markers were significantly increased in the Cas13 TSC1 cells at the neuronal stage, thereby suggesting an increased number of astrocytes in the culture, which would align with previous research (Blair *et al.* 2018).

4.5.2.2. NPC markers:

The NPC markers Pax6 and Nestin were also dysregulated in the Cas13 TSC1 cells. Nestin is involved in several cell processes including organisation of the cytoskeleton, cell signalling, and cell metabolism (Fuchs and Weber 1994). Nestin levels are highly expressed at the early developmental stages and nearly absent in mature neurons (Lendahl *et al.* 1990). Pax6, a highly conserved transcription factor, is crucial for normal CNS development and changes of expression lead to severe developmental changes due to significant impact on neuronal development including abnormalities in NSC and NPC proliferation, as well as defects in neurogenesis and in the generation of more specialized neurons (Schedl *et al.* 1996; Manuel *et al.* 2007; Sansom *et al.* 2009).

The Cas13 cells showed a mostly stable Nestin expression throughout the differentiation, except for the NPCs treated at Day8 for 24 h. Therefore, it is overall difficult to conclude that acute TSC1 loss had a severe impact Nestin and therefore its function in neuronal development. As proliferation rate in TSC1 cells is usually increased due to the mTOR overactivity, the reduced Nestin levels at the NPC stage might be an attempt to counteract the proliferation rate so that the differentiation is followed. Nevertheless, a significant reduction of Nestin expression at a time point where the cells are preparing to enter the neuronal stage, will negatively impact the neuronal development of the Cas13 TSC1 cells. The Cas13 TSC1 cells also showed a continuous dysregulation of Pax6, with significant downregulation at the NSC and neuronal stage (for cells treated for 24 h) and significant upregulation for the NPC and the neurons treated at Day 30 for 48 h. The dysregulation at the neuronal level for Cas13 TSC1 cells might impair axonal growth (Sebastián-Serrano *et al.* 2012).

Overall, the NPC markers were significantly dysregulated in the TSC1 model with Pax6 being significantly dysregulated at most developmental time points and Nestin mostly showing no statistical significance but trends of downregulation. Dysregulation of NPC markers during neuronal differentiation which play important roles in the process will cause an impaired neuronal development in TSC cells, results which align with previous findings from other groups (Zucco *et al.* 2018; Martin *et al.* 2020).

4.5.2.3. Neuronal markers:

The analysed neuronal markers OTX2, βIII-Tub and FOXG1, are essential for normal neuronal development (Ferreira and Caceres 1992; Acampora *et al.* 1995; Vernay *et al.* 2005; Guen *et al.* 2011; Sakai *et al.* 2017; Hettige and Ernst 2019). The Cas13a TSC1 cells displayed significant upregulation of OTX2 at the neuronal stage, mostly for the cells which were treated for 24 h, focusing on the cells which were treated at the NSC or NPC stage. The acute loss of TSC1 had significant consequences of the OTX2 expression, weeks after the treatment. As OTX2 changes are known to influence dopaminergic and glutamatergic synapses as well as axon guidance (Sakai *et al.* 2017), the overexpression might have caused a disturbance in the neuronal identity. While the utilised neuronal differentiation protocol generates glutamatergic neurons, a small percentage of GABAergic neurons are developed as well. Since OTX2 influences neuronal identity, promotes cortical GABAergic interneuron maturation (Hensch *et al.* 1998) as well as the synapse influence, it could be expected that the ratio of GABA/glutamatergic neurons might be altered, which had been identified in TSC cells previously (Alsaqati *et al.* 2020). The significant decrease at the NSC stage might have led to altered increased cell proliferation and abnormal/delayed development. The Cas13 TSC1 cells displayed a significant reduction in βIII-Tub and FOXG1 through many timepoints of the neuronal development. The dysregulation of βIII-Tub might therefore impact the neurite outgrowth and the microtubule network, though neither had been tested during this project. The expression reduction of FOXG1 throughout the development might suggest an impaired/abnormal neuronal development as its low expression would impair its function as a transcription factor.

As the cells were used in a 2D model instead of an organoid, it is impossible to tell if microcephaly would occur after the brief treatment, but it might be an interesting objective in the future. Interestingly, these neuronal markers are also affected in AD. Target genes of OTX2 were identified to be associated with AD (Sakai *et al.* 2017) while downregulated FOXG1 had been found in AD (Wang *et al.* 2022), thus leading to the suggestion to target it for upregulation as FOXG1 expression protects healthy neurons from neuronal death (Dastidar *et al.* 2011). Additionally, a chronic hypoxia model in rats for AD demonstrated that chronic hypoxic conditions lead to diminished βIII-Tub expression and AD pathogenesis (Mahakizadeh *et al.* 2020).

Overall, all the neuronal markers displayed significant dysregulation during the neuronal development in both TSC1 models and as several of these marker function as transcriptional factors with essential functions in neuron and brain development, it can be concluded that any dysregulation during any time point of the development could cause abnormalities in the cells and their function.

4.5.2.4. Autophagy markers:

Similarly, to the knockout TSC1 cell line, the Cas13 TSC1 cell line demonstrated dysregulated autophagy markers which would negatively impact neuronal development. GSK3 signalling is essential for coordinating the proliferation and differentiation of progenitor cells during brain development (Hur and Zhou 2010). The importance of GSK3s in the developing nervous system has been shown in a study through the selective deletion of both Gsk3a and Gsk3b in neural progenitors of mice (Kim *et al.* 2009). The TSC1 Cas13 cells demonstrated a significant reduction of GSK3a expression in the neurons and some conditions also caused a significant expression increase during earlier developmental time points.

As normal GSK3 expression is essential for neuronal development, the significant dysregulation of GSK3 found throughout the differentiation suggest that the development may be impaired/abnormal due to the brief loss of TSC1. The significant expression drop in the neuronal cells would suggest impaired axonal function/growth and further tests on axonal function would be an interesting future project.

ULK1, a major player in autophagy controlled via mTOR or AMPK pathway (Di Nardo *et al.* 2014). Loss of TSC1/2 in neurons is known to cause cell stress due to impaired autophagy as mTOR inhibition is required for the regulation of the latter, this was showcased in TSC mice model demonstrating increased stress responses (Di Nardo *et al.* 2009; Anderl *et al.* 2011). The Cas13 TSC1 cells displayed a significant downregulation of ULK1 expression at the NPC and neuronal stage (for the latter 24 h treatment at Day30), while the 48 h treatment at Day 8 led to a significant expression increase. ULK1 inhibition is known to promote oxidative stress by promoting a metabolic shift from glycolysis to oxidative mitochondrial metabolism (Ianniciello *et al.* 2021). As discussed previously, TSC models are known to display oxidative stress/expression of hypoxia related markers (Zhang *et al.* 2016) while chronic hypoxia is seen as a potential model for AD (Mahakizadeh *et al.* 2020). The measured ULK1 dysregulation strengthens the suggestion to test for cell/oxidative stress in the Cas13 TSC1 cells.

TFEB whose activation leads to stimulation of lysosomal biogenesis and autophagy, resulting in the breakdown of proteins and lipids for nutrients (Settembre *et al.* 2011; Martini-Stoica *et al.* 2018), is also involved in inflammatory processes via in extrusion of mitochondrial contents (Unuma *et al.* 2015). The Cas13 TSC1 cells displayed mostly a TFEB overexpression while the NPCs showed a significant upregulation, although the 24 h treatments led to significant expression reduction at Day 50. Torra *et al.* investigated the consequences of TFEB overexpression in mouse neurons of a Parkinson´s model and identified several protective roles of TFEB (Torra *et al.* 2018), involving cell growth and cell survival. As TFEB can suppress neuronal differentiation and impact neuronal survival, it can be concluded that any expression dysregulation would be harmful for neuronal development, despite TFEB levels reaching their peak at the neuronal stage.

These autophagy markers are also associated with AD. GSK3 is now targeted as a potential future common therapeutic target for AD drugs (Beaulieu 2007; Beaulieu *et al.* 2009) as Aβ oligomers in AD brains behave as an antagonist to insulin, thus preventing the activation of the PI3 kinase resulting in an activity increase of GSK3 (Townsend *et al.* 2007). GSK3 phosphorylates TAU in the regions of the microtubule binding domain, resulting in a disturbance of the TAU-microtubule interaction, TAU detachment and self-aggregation (Hernández *et al.* 2010). Thus, GSK3 can be a link between Aβ and TAU.

Additionally, studies demonstrated that GSK3 might be a player in Aβ pathology as its inhibition restored lysosomal acidification leading to clearance of Aβ burden (Cohen and Goedert 2004; Avrahami *et al.* 2013). Though these results are based on GSK3a overexpression, unlike the downregulation measured here (at the neuronal stage). TFEB is an important player in the TAU clearance in AD as Xu *et al.* identified that the process depends on the calcium channel TRPML1 (Xu *et al.* 2021). This calcium channel was identified to be regulated by mTOR and thereby by TSC (Onyenwoke *et al.* 2015). Li *et al.* further demonstrated that TRMPL1 is required for mTORC1 activation, therefore suggesting a feedback loop (Li *et al.* 2016). Several genes which are either directly or indirectly regulating autophagy demonstrated significant dysregulation of their expression levels. As TSC is known for its impaired autophagy, these results were expected. Their disturbance likely causes cellular stress and impair cell survival and differentiation.

4.5.3. Calcium signalling and glutamate in TSC1 astrocytes.

Originally, it was assumed that the only signalling in the brain was performed by neurons, but recent research identified calcium waves as an extra-neuronal signalling in the CNS (Bazargani and Attwell 2016). Calcium functions as a major trigger for neurotransmitter release in the brain. It is essential for neuronal excitability, synaptic plasticity, dendritic development and programmed cell death amongst other functions (Marambaud *et al.* 2009; Nikoletopoulou and Tavernarakis 2012). Therefore, calcium homeostasis is tightly regulated for normal function of the previously mentioned cell processes. Aging neurons show increased calcium influx into the cell due to increased VOCCs activity, as well as reduced calcium export via PMCA and increased calcium release from the ER. Additionally, calcium buffering and mitochondrial sink ability of calcium also decrease with age, leading to an increased calcium load in neurons, disturbing neuronal excitability and thus memory formation. TSC models display disruptions in the calcium homeostasis with neurons showing an increase of spontaneous calcium transients (Nadadhur *et al.* 2019), while iPSC derived *TSC1* -/- neurons demonstrated elevated neuronal activity with highly synchronized calcium spikes, enhanced calcium influx via L-type calcium channels resulting in abnormal neurite extension and sustained CREB activation. Furthermore, increased expression of the calcium channel Cav1.3 LTCC was found to be increased in TSC, with Cav1.3 LTCC being suggested as a downstream target of the mTOR pathway (Hisatsune *et al.* 2021).

Additionally, increased expression of the calcium channels Kv1.1, CaV2.2 was identified in TSC models, with reduction of branch specific potentiation (Raab-Graham 2021). Similar calcium disturbances are found in AD, where disturbed ER calcium homeostasis significantly contributes to dysfunction and degeneration in AD. AD models display impaired calcium uptake in mitochondria (Nikoletopoulou and Tavernarakis 2012), especially after oxidative stress (Kumar *et al.* 1994). Reduced expression of calcium buffers such as calmodulin or calbindin in AD brains has been demonstrated, disturbing calcium homeostasis (Marambaud *et al.* 2009). Glutamate is a major excitatory neurotransmitter in the mammalian CNS, requiring a tight signal balance as increased levels lead to excitotoxicity, inducing neuronal damage and death (Maragakis and Rothstein 2001). Therefore, clearance of glutamate from the synapse is critical for neuronal health. Cellular uptake by glutamate transport is the primary mechanism in maintaining synaptic glutamate concentrations (Anderson and Swanson 2000), mediated by astrocytes (Lauderback *et al.* 2001). TSC is known to display glutamate excitotoxicity with knock-out mouse model demonstrating decreased expression and function of the glutamate transporters GLT-1 and GLAST, leading to an increase in extracellular glutamate levels and excitotoxic neuronal death (Wong *et al.* 2003; Zeng *et al.* 2007). Miller and al. demonstrated reduced glutamate uptake in TSC patient -derived astrocytes in comparison to control (Miller *et al.* 2021), which would align with the reported decrease in glutamate transporters in TSC. Glutamate expression leads to calcium rise in astrocytes (Bazargani and Attwell 2016); excessive glutamate receptor activation leads to excessive calcium influx, thereby impairing synaptic activation, neuronal plasticity and synthesis of NO which will cause cell death which was found in AD (Sattler and Tymianski 2000; Marambaud *et al.* 2009).

In AD, Aβ increases NMDAR receptor vulnerability towards excitotoxicity (Mattson *et al.* 1992; Mattson 2004) and it seems that its oligomers may induce mitochondrial calcium overload resulting in massive calcium influx in toxicity in neurons (Caspersen *et al.* 2005). GLT-1 and GLAST dysregulation is also found in AD (Pajarillo *et al.* 2019). The Cas13 astrocytes displayed a significant difference at the calcium base line between the TSC1 50% cells and control prior any calcium wave. The calcium base line/the calcium release prior wave was significantly higher in the TSC1 cells than in control. Furthermore, the control cells were much closer to each other calcium levels than the TSC1 cells, suggesting a higher rate of synchronization.

Research presented contradicting results concerning signal synchronization in TSC. Alsaqati *et al.* found reduced signalling synchronization in neurons of a TSC patient iPSC line (Alsaqati *et al.* 2020). Hisatsune *et al.* on the other hand, demonstrated highly synchronous calcium signalling in iPSC-derived TSC2 -/- neurons (Hisatsune *et al.* 2021). It must be remarked that both these findings are in neurons and not astrocytes, so differences can be expected. The Cas13 TSC1 control astrocytes displayed an expected calcium wave after adding glutamate to the cell media, after which the calcium level return to a stable base after the induced wave. The astrocytes with induced 50% TSC1 also showed a glutamate induced calcium wave but contrary to the control, the calcium release continued and no return to a base line was found. When comparing the recordings taken during the calcium signalling, a pattern of cell shrinking/dying in the astrocytes with TSC1 loss can be observed, with a more severe pathology in the homozygous cells.

These results combined suggest that the TSC1 astrocytes continue releasing calcium to the detriment of the cell health. This is further strengthened by the staining of the TSC1 astrocytes where the cells were stained for the apoptosis marker ANXA5 after a glutamate treatment. Many of the TSC1 astrocytes were positive for ANXA5, while the control cells barely showed any ANXA5 positivity, thus suggesting that the glutamate treatment induced cell death in the TSC1 astrocytes. As non-transported and recycled glutamate is toxic to cells (Maragakis and Rothstein 2001), these results align with the literature describing excitotoxicity in TSC. While the expression of the glutamate transporters GLT-1 and GLAST has not been tested in this project, the consistent reports of their downregulation in TSC (Wong *et al.* 2003; Zeng *et al.* 2007) can lead to the assumption that they are downregulated in this model as well and thus their function is disturbed. As the lifetime of the glutamate transporters is measured in seconds (Michaluk *et al.* 2021), the induced TSC1 loss of 48 h should impact the transporter expression.

5. Chapter 5: Identifying common targets and pathways between TSC and AD, utilizing a TSC database with focus in inflammation.

5.1. Chapter 5: Introduction

mTORC1 is a regulator of various cell processes and its overactivity due to TSC loss has severe consequences on the cells (Franz *et al.* 2010). This part of the thesis aims to identify additional pathways affected by TSC loss as well as investigate the expression of inflammation markers in both knockout and knockdown TSC1 iPS models, as increased inflammation patterns were found in TSC models (Weichhart *et al.* 2008; Byles *et al.* 2013). RNA Sequencing is a widely used method in order to investigate the transcriptome (total cellular content of RNAs) of samples. This technique shows which genes are active in the samples and the level of their transcription, thereby allowing an overview which genes and pathways might be dysregulated in diseases. As previously mentioned, a hallmark of TSC is the mTORC1 overactivation. The regulation of mTOR, a protein kinase involved in the regulation of processes such as protein synthesis, cellular metabolism, and cell differentiation, was demonstrated to be highly important in the brain. Studies have shown that mTORC1 is important for late-phase long-term potentiation (LTP) (Swiech *et al.* 2008) and that controlled mTOR activity is necessary for normal memory development as overactivity is disrupting memory formation (B Jahrling and Laberge 2015). AD has shown a similar mTOR activity with its downstream targets upregulated as well. The overactivity of a key regulator in cell processes in both diseases might be also a cause for the increased inflammation found in patients and models for both TSC and AD. Microglia in both AD and TSC show an increased expression in proinflammatory cytokines (Weichhart *et al.* 2008; Byles *et al.* 2013; Wang *et al.* 2015; Mammana *et al.* 2018) and Van Skike and Galvan *et al.* have shown that mTOR inhibition seems to prevent BBB breakdown by cytokines in age-associated neurological disorders (Van Skike and Galvan 2018). As AD and TSC share several similarly dysregulated pathways as well as a similar proinflammatory phenotype, the focus on the following database analysis was to further investigate the dysregulation of inflammation related genes as well as AD related genes. For identifying differences of gene expressions and potential markers for future tests when comparing TSC to AD in developed brain cells, a TSC database was analysed. The transcriptome analysis of TSC patient tissue was provided by the lab of Prof. Jeffrey MacKeigan in Michigan, USA (Martin *et al.* 2017).

Among the upregulated pro-inflammatory markers was SERPING1, a member of the urokinase pathway. The urokinase (uPA) pathway has an important role in cells as in involved in the activation of cell signalling pathways regulating differentiation, cellular adhesion, migration, and proliferation through non-plasminogenic mechanisms (Peteri *et al.* 2021). Additionally, it also seems to influence axonal growth in neurons as high levels of uPA expression as well as its proteolytic regulation of axonal growth in rat neuronal tissue (Sumi *et al.* 1992); while it induces ezrin expression in dendritic spines for recovery (Merino and Yepes 2018). Regulators of the proteolytic activity of uPA are the plasminogen activator inhibitors PAI-1 and PAI-2. Research has shown upregulated uPA in TSC patients with Lymphangioleiomyomatosis (LAM), where mTORC1 inhibitor rapamycin further increased uPA expression instead to regulating it (Stepanova *et al.* 2017). Additionally, uPA involvement in several epileptic disorders has been established (Bruneau and Szepetowski 2011). uPA-uPAR interactions result in increased production of plasmin, which aids in the process of inflammatory and neoplastic cell invasion through its ability to degrade extracellular matrix proteins (Walker *et al.* 2002). The plasminogen activation system seems play a significant role in phagocytic cell migration to sites of inflammation. AD pathology shows the accumulation of microglia around aggregated Aβ plaques and NFTs in brain tissue. uPAR is a central coordinator in these processes through its interactions with uPA and CD11b, the latter is expressed by human brain microglia, and is upregulated in AD brains. Studies have furthermore observed that uPA is localized to a subset of plaques in AD brains. Furthermore, uPAR has been shown to be involved in physiological events such as inflammation (Bruneau and Szepetowski 2011). It has been established that uPAR is involved in the interneuron development via HGF which is a downstream target of HG, promoting migration of interneurons during cortical development (Powell *et al.* 2001). A study has demonstrated increased expression of the different components of the urokinase pathway in cortical tubers of TSC patients (Iyer *et al.* 2010). Recent studies suggest that HGF and other growth factors influence mTOR activity (Parker *et al.* 2011). Additionally, increased HGF expression has been found in AD (Yamada *et al.* 1994; Fenton *et al.* 1998; Zhu *et al.* 2018); HGF has been found to be involved in axon outgrowth, neuronal survival, synaptic function and plasticity (Ebens *et al.* 1996; Nakamura and Mizuno 2010; Wright and Harding 2015). As there is a well-documented involvement of the urokinase pathway in both AD and TSC pathology, several members of it were investigated in both TSC1 knockdown and knockout iPS cells during neuronal development.

5.2. Chapter 5: Aims and Objectives

To gain a better understanding about the effect of TSC1 loss has on cells, this project aimed to find additional potentially altered pathways in TSC to test their expression in the previously designed TSC1 cell lines. As studies have shown a strong involvement of inflammation in TSC, the expression of inflammation markers during the neuronal development was also investigated.

a) Performing a database analysis of TSC patients with focus on inflammation and AD
b) RT-PCRs for gene expression of inflammation and urokinase markers

5.3. Chapter 5: Results

5.3.1. Database Analysis:

The transcriptome data of TSC patient tissue was provided by the lab of Prof. Jeffrey MacKeigan in Michigan after its publication (Martin *et al.* 2017). The dataset includes 81 patients and their subependymal nodules and subependymal giant cell astrocytoma **(**SEN/SEGAs), cortical tubers (TUB), and renal angiomyolipoma (RA). The majority of the patients carried a TSC2 mutation (88.88% of patients) with a nearly even distribution of female/male patient ratio (43.2% Women vs 56.7% Men) and an age range from 0.7 years up to 65 years. Concerning the database analysis, the acquired data file already underwent analysis from the MacKeigan group. For the TSC1/TSC2 expression analysis, the group used pair-wise Welch's t-tests in GraphPad Prism, followed by false discovery rate (FDR) correction (in R) to generate corrected p-values as the samples had failed Bartlett's test for homogeneity of variances, thus ruling out ANOVA as an option. The data was preorganized into the Top 300-fold changes of mRNA expressions between tumours and matched healthy (non-tumerous) tissue of the TSC patients for the respective sample categories: SEN/SEGAs, TUB, and renal angiomyolipoma (RA). While the MacKeigan group had already organized the identified genes based on specific cell processes like autophagy or immune response or their involvement in certain diseases by utilising Gene Analytics, the data file was again organized with focus to the Top 100 up- and downregulated genes which were then personally categorized into two groups: involved with AD or involved with inflammation (pro- or anti-inflammatory genes alike).

These genes were then further be analysed using Gene Analytics from LifeMap Sciences, which allowed a comprehensive identification of the gene involvement in AD and inflammation. The data visualization was possible thanks to a code generously given by Darius McPhail. For this analysis, the focus was on inflammation and AD related genes.

Focusing on the Top 300 upregulated genes in the tumour samples, several genes were found to be involved in inflammation. Plotting the gene expression for inflammation related genes in the different tumour groups demonstrated a clear pattern of significant upregulation of these markers in the TSC tumour samples (see Figure 5-1, 5-2 and 5-3).

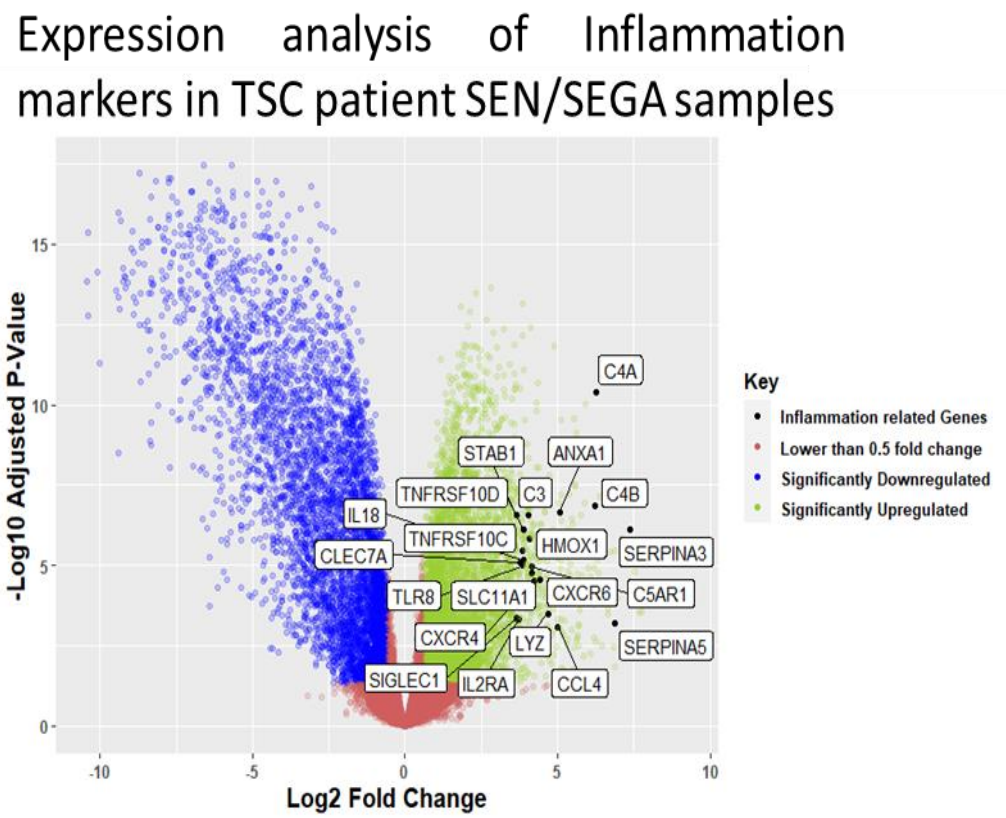

Figure 5-1: Volcano plot representation of differential expression gene (DEG) analysis for Inflammation correlating genes in the Prof. MacKeigan TSC Database. Analysed tissues were from TSC patient's vs healthy controls. Green and blue points mark the genes with significantly increased or decreased expression respectively, while black marks the inflammation correlating genes in TSC patient's vs healthy control. The x-axis shows log2fold-changes in expression and the y-axis the log odds of a gene being differentially expressed. The SEN/SEGA samples were compared to healthy brain tissue and showed a significant upregulation of inflammation correlating genes.

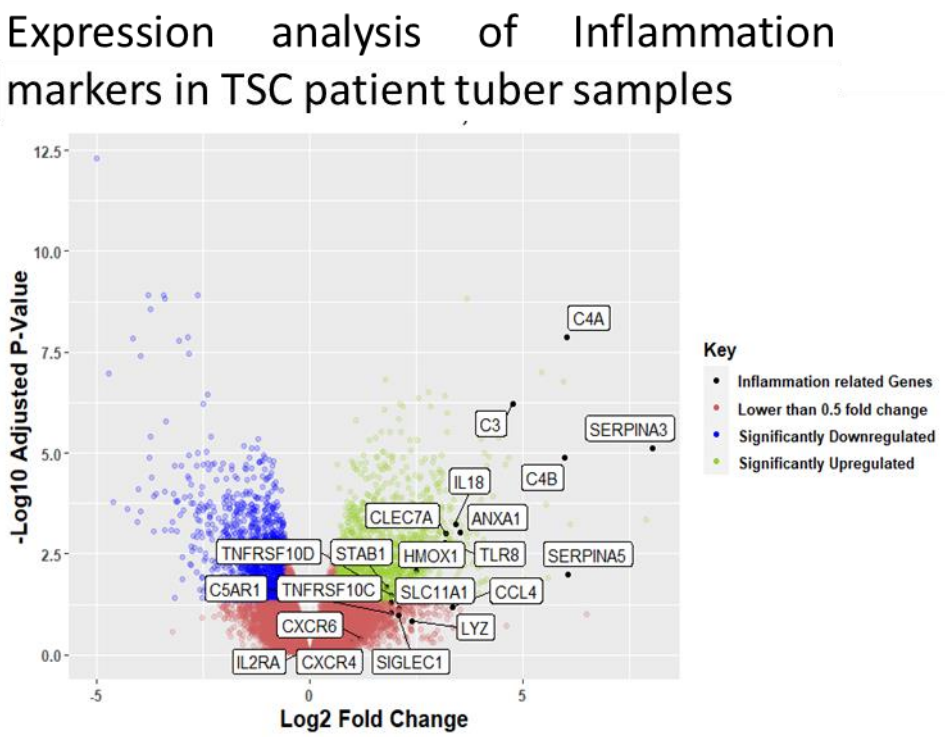

Figure 5-2: Volcano plot representation of differential expression gene (DEG) analysis for Inflammation correlating genes in the Prof. MacKeigan TSC Database. Analysed tissues were from TSC patient's vs healthy controls. Green and blue points mark the genes with significantly increased or decreased expression respectively, while black marks the inflammation correlating genes in TSC patient's vs healthy control. The x-axis shows log2fold-changes in expression and the y-axis the log odds of a gene being differentially expressed. The Tuber samples were compared to healthy brain tissue and showed a significant upregulation of inflammation correlating genes.

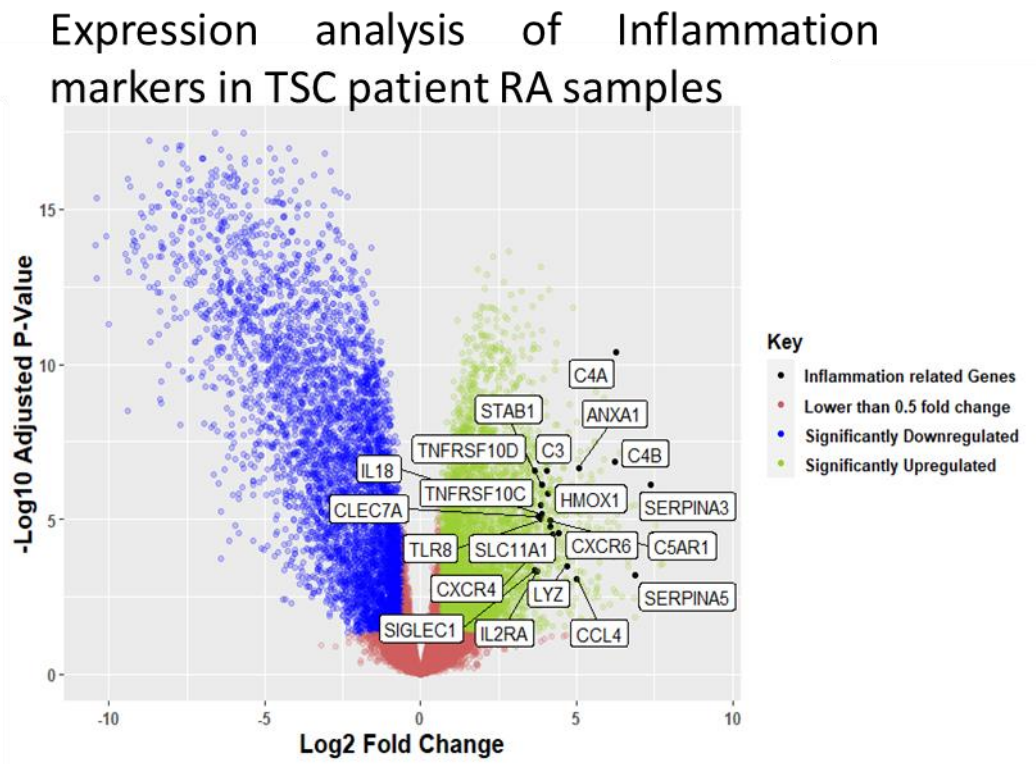

Figure 5-1: Volcano plot representation of differential expression gene (DEG) analysis for Inflammation correlating genes in the Prof. MacKeigan TSC Database. Analysed tissues were from TSC patient's vs healthy controls. Green and blue points mark the genes with significantly increased or decreased expression respectively, while black marks the inflammation correlating genes in TSC patient's vs healthy control. The x-axis shows log2fold-changes in expression and the y-axis the log odds of a gene being differentially expressed. The TSC tumour renal angiomyolipoma (RA) samples were compared to healthy brain tissue and showed a significant upregulation of inflammation correlating genes.

Plotting the AD associated genes in the three tumour groups demonstrated a clear pattern of upregulation of these genes in the SEN/SEGA samples, with many genes being significantly upregulated (see Figure 5-4). In the TUB samples, most genes displayed an upregulation beneath the 0.5-fold change threshold with few exceptions like SERPINA3 or HMOX1 being significantly upregulated (see Figure 5-5). The RA samples demonstrated a significant upregulation of HMOX1 and SERPINA3 as well, but most genes expression increases were found to be below 0.5-fold, similar to the TUB samples (see Figure 5-6).

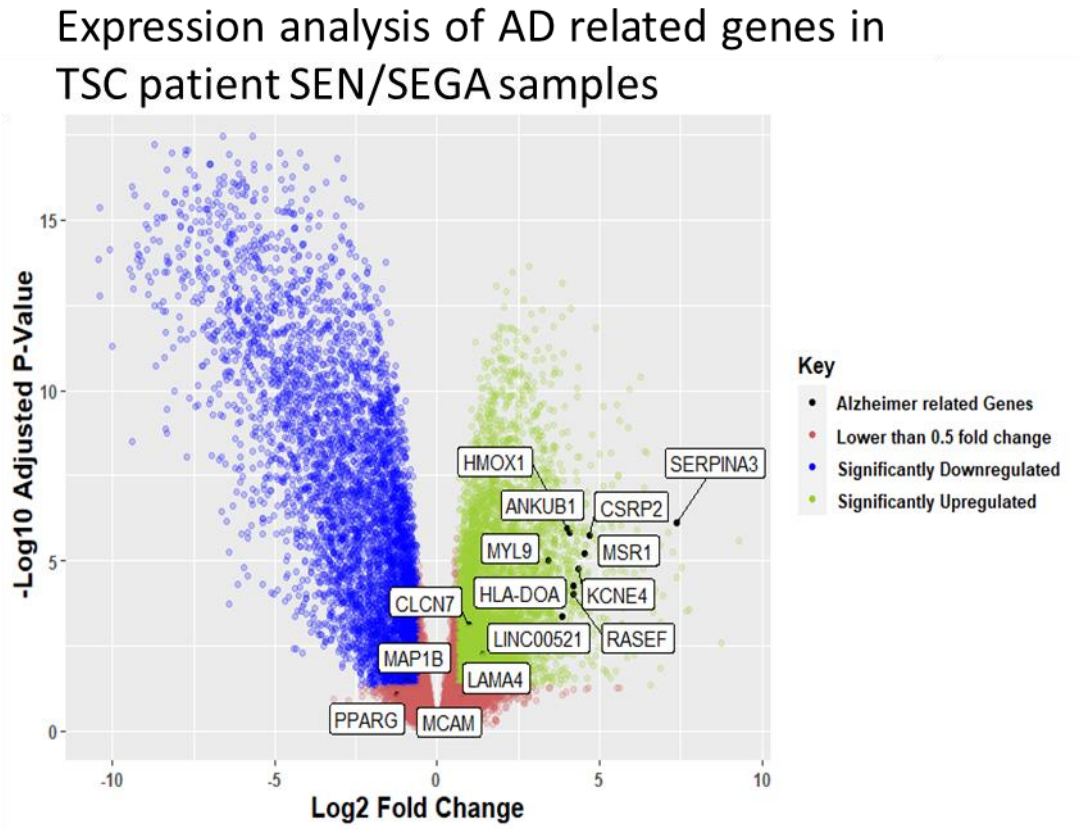

Figure 5-2: Volcano plot representation of differential expression gene (DEG) analysis for Alzheimer's Disease (AD) correlating genes in the Prof. MacKeigan TSC Database. Analysed tissues were from TSC patient's vs healthy controls. Green and blue points mark the genes with significantly increased or decreased expression respectively, while black marks the AD related genes in TSC patient's vs healthy control. The x-axis shows log2fold-changes in expression and the y-axis the log odds of a gene being differentially expressed. The SEN/SEGA samples were compared to healthy brain tissue and showed a significant upregulation of the AD genes.

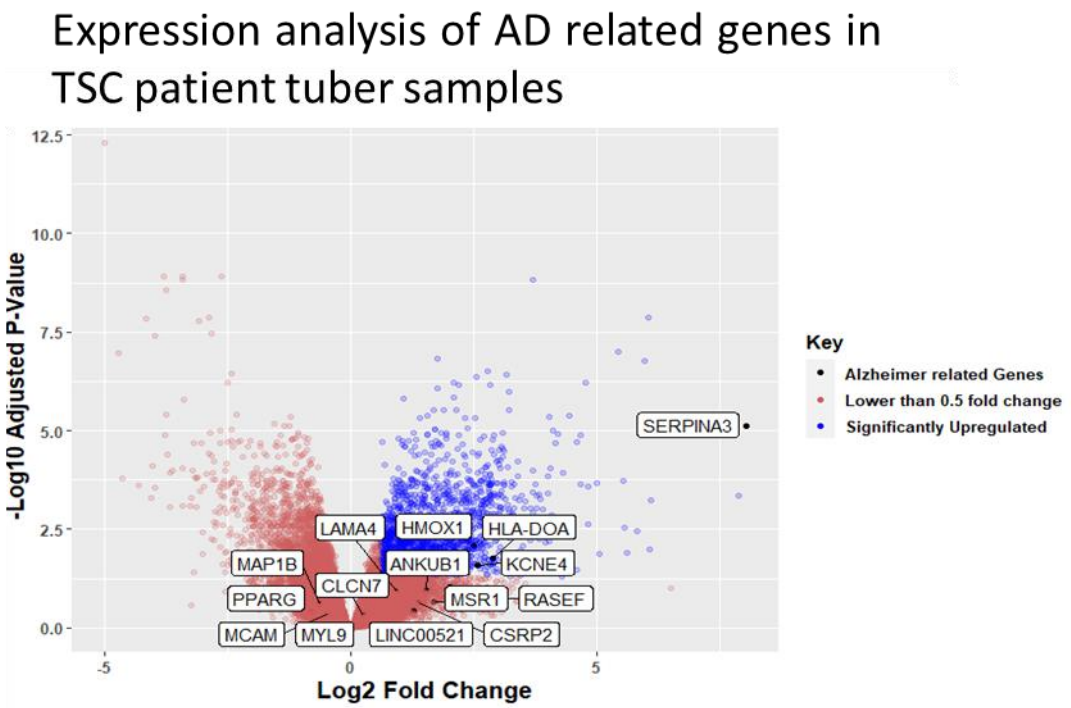

Figure 5-3: Volcano plot representation of differential expression gene (DEG) analysis for Alzheimer's Disease (AD) correlating genes in the Prof. MacKeigan TSC Database. Analysed tissues were from TSC patient's vs healthy controls. Green and blue points mark the genes with significantly increased or decreased expression respectively, while black marks the AD related genes in TSC patient's vs healthy control. The x-axis shows log2fold-changes in expression and the y-axis the log odds of a gene being differentially expressed. The Tuber samples were compared to healthy brain tissue and showed a significant upregulation of the AD genes.

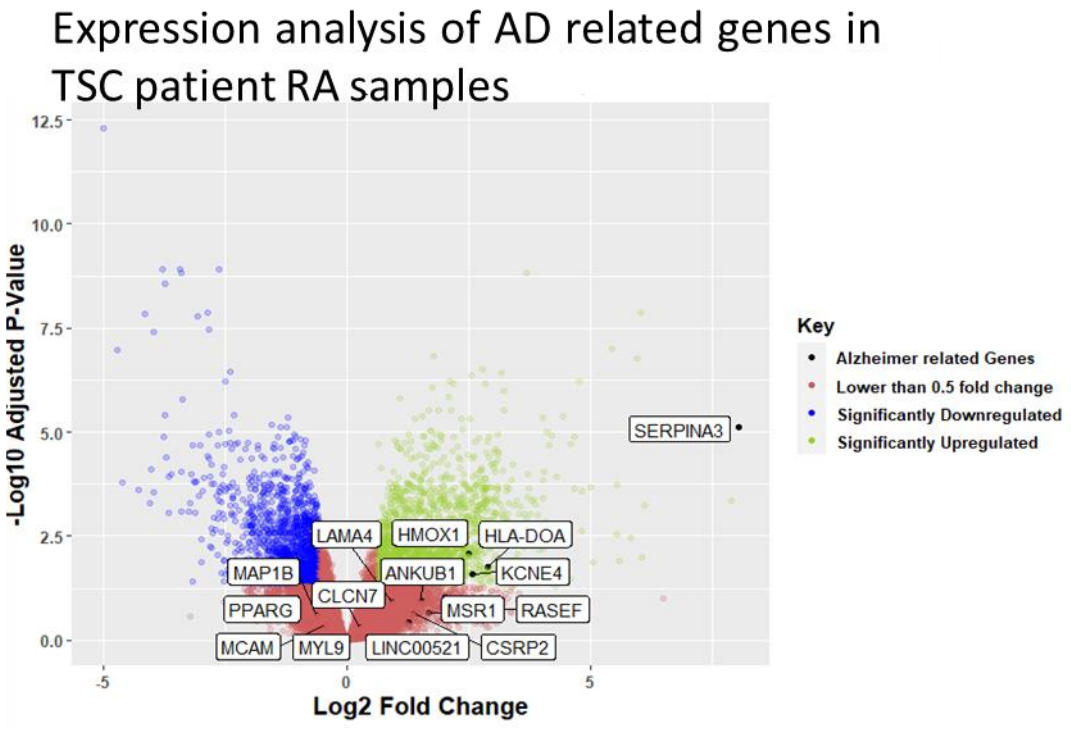

Figure 5-4: Volcano plot representation of differential expression gene (DEG) analysis for Alzheimer's Disease (AD) correlating genes in the Prof. MacKeigan TSC Database. Analysed tissues were from TSC patient's vs healthy controls. Green and blue points mark the genes with significantly increased or decreased expression respectively, while black marks the AD related genes in TSC patient's vs healthy control. The x-axis shows log2fold-changes in expression and the y-axis the log odds of a gene being differentially expressed. The TSC tumour renal angiomyolipoma (RA) samples were compared to healthy brain tissue and showed a significant upregulation of the AD genes.

5.3.2. Inflammation markers in TSC1 cells during neuronal development

A neuronal differentiation with the Cas13 *TSC1* cells was initiated and the Cas13a system was activated via doxycycline treatment of the cells to induce a heterozygous like loss of TSC1 on the RNA level. The treatment with doxycycline occurred at three different time points of the neuronal development (Day 8, Day 15, and Day 30) where the cells are neuronal stem cells, neuronal progenitor cells or early neurons respectively. The doxycycline treatment itself occurred for either 24 or 48 h before washing the cells with PBS and adding fresh media without any doxycycline (see Figure 5-7). As it is impossible to select the location of the plasmid insertion when using electroporation, the Cas13 TSC1 cells without any doxycycline were used as control in order to eliminate any potential that insertion mutation would lead to gene expression alteration and thus impact the data.

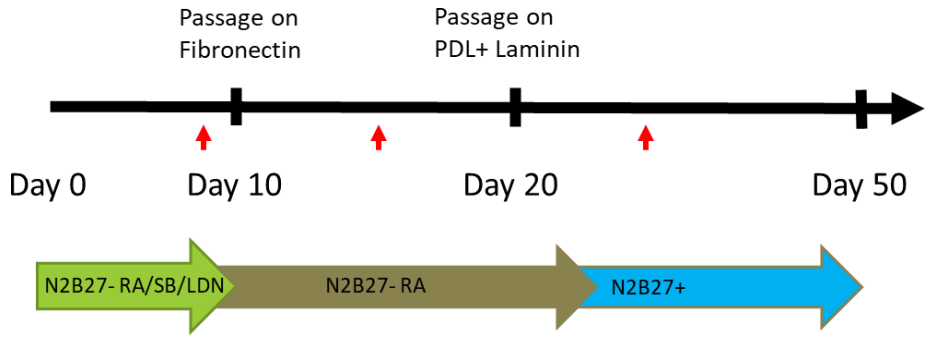

Figure 5-7: Scheme of neuronal differentiation of Cas13 TSC1 cells, time points of doxycycline treatment indicated with red arrows, treatment were for either 24 or 48h.

IL6 expression was significantly decreased in the TSC1 -/- NPCs in comparison to the control (p-value: 0.0424), IL10 was non-significantly reduced in TSC1 -/- cells (p-values: 0.6008) and TNFa expression was slightly, non-significantly increased (p-values: 0.7205) (see Figure 5-8).

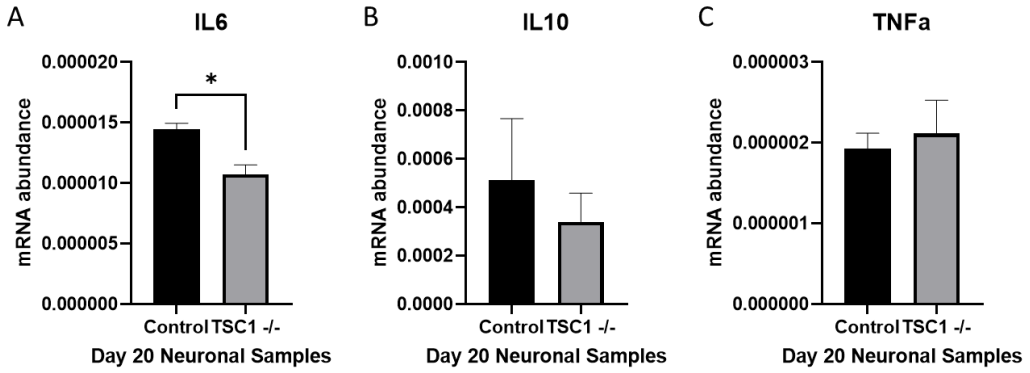

*Figure 5-8: Gene expression of inflammatory cytokines in TSC1 homozygous NPCs. A-C: Expression of the inflammatory cytokines IL6 and IL10 were decreased in TSC1 neurons (with significance for IL6) (N=3), while TNFa expression was statistically non-significantly increased. Values are expressed as mean ± SD. Unpaired t-tests were performed for the statistical analysis. * = p-value of ≤ 0.05, ** = p-value of ≤ 0.01, *** = p-value: ≤ 0.001, **** = p-value ≤ 0.0001.*

Expression analysis of the TSC1 neurons shows significant alterations for inflammatory cytokines. All three cytokines showed elevated expression in TSC1 homozygous neurons, with IL6 showing a non-significant increase (p-value: 0.0577) while IL10 and TNFa demonstrate significant increases in the TSC1 -/- cells in comparison to control (p-values: 0.0123 and 0.0186 respectively) (see Figure 5-9).

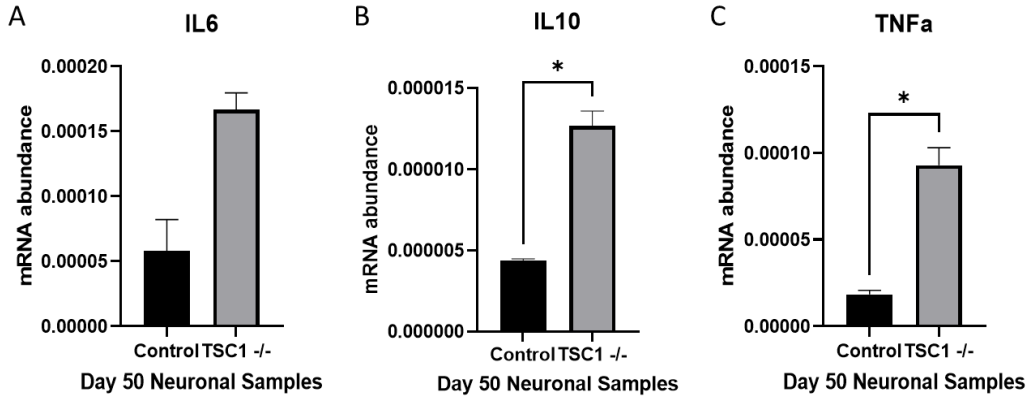

*Figure 5-9: Gene expression of inflammatory cytokines in TSC1 homozygous neurons. A-C: Expression of the cytokines IL6, IL10 and TNFa were increased in TSC1 neurons (with significance for IL10 and TNFa) (N=3). Values are expressed as mean ± SD. Unpaired t-tests were performed for the statistical analysis. * = p-value of ≤ 0.05, ** = p-value of ≤ 0.01, *** = p-value: ≤ 0.001, **** = p-value ≤ 0.0001.*

Analysing the expression changes over the neuronal development shows the increase of expression of pro-inflammation markers over time. IL6 expression increased from the NPC stage towards the neuronal stage for both control and TSC1 -/- but the level of IL6 in TSC1-/- was significantly higher than in control at the neuronal stage (p-values: 0.9691, 0.0030). IL10 expression decreased from the NPC stage towards the neuronal stage with no significance between TSC1 -/- and control (p-values: 0.6785, 0.9990). TNFa expression increased from the NPC stage towards the neuronal stage with a significant increase in the TSC1 -/- cell line in comparison to control at Day 50 (p-values: 0.9993, 0.0010) (see Figure 5-10).

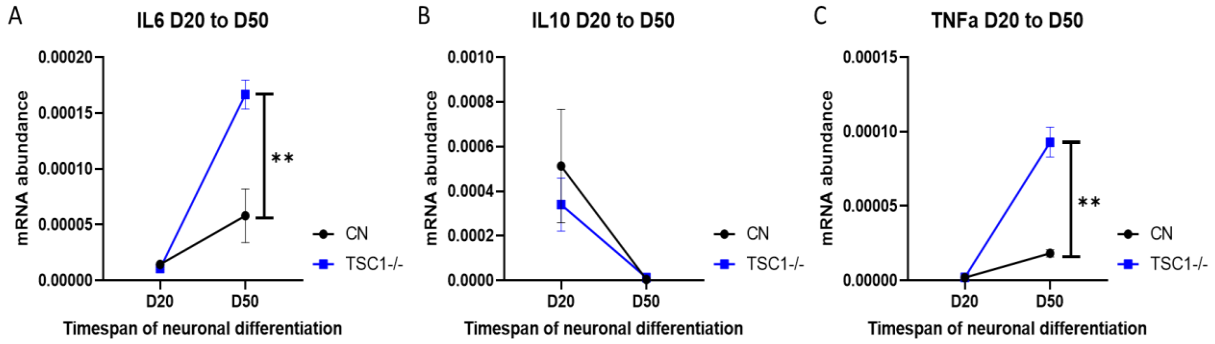

*Figure 5-10: Expression of inflammation markers during development. A-C: Significant expression increases in the TSC1 -/- cells in comparison to control were found for both IL6 and TNFa at the neuronal stage. IL10 levels decreased from the NPC to neuronal stage and no significance between both cell lines was found. Values are expressed as mean ± SD. Mixed-effect analysis with Sidaks-Test was performed for data analysis. * = p-value of ≤ 0.05, ** = p-value of ≤ 0.01, *** = p-value: ≤ 0.001, **** = p-value ≤ 0.0001.*

Gene expression analysis of the Cas13a TSC1 NPCs shows significant alterations for inflammation related markers. IL6 expression showed significant decreases for both conditions in comparison to control (p-values: 0.0050 and 0.0099). IL10 expression was increased in both conditions with significance for the 24h treatment (p-values: 0.0043 and 0.2554). TNFa expression was decreased for both conditions with a significant reduction after 24h TSC1 loss (p-values: 0.019 and 0.1483) (see Figure 5-11).

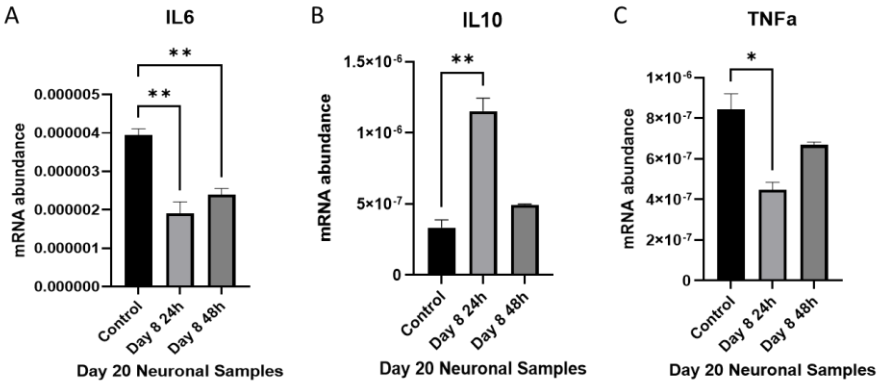

*Figure 5-11: Gene expression of autophagy markers in Cas13a TSC1 NPCs. TSC1 heterozygous loss was induced via doxycycline at Day 8 for either 24h or 48h. A: IL6 expression significantly decreased after both 24h and 48h treatment. B: 24h loss of TSC1 leads to a significant increase in IL10 expression while the 48h treatment leads to a non-significant increase in expression. C: TNFa expression is significantly decreased after 24h treatment and statistically non-significantly reduced after 48h loss of TSC1. Values are expressed as mean ± SD. Data was analysed via One-Way ANOVA. * = p-value of ≤ 0.05, ** = p-value of ≤ 0.01, *** = p-value: ≤ 0.001, **** = p-value ≤ 0.0001.*

Gene expression analysis of the Cas13a TSC1 neurons shows significant alterations for inflammation related markers. IL6 expression showed statistically significant decrease in all conditions in comparison to control (p-values: 0.0061, 0.003, 0.0028). IL10 expression was statistically significantly increased for the condition Day15 24h. The other conditions demonstrated statistically non-significant decreases in expression (p-values: 0.5306, 0.0017, 0.6596). TNFa expression was significantly decreased for all conditions (p-values: 0.0001 for the first two conditions, <0.0001 for Day 30 24h) (see Figure 5-12).

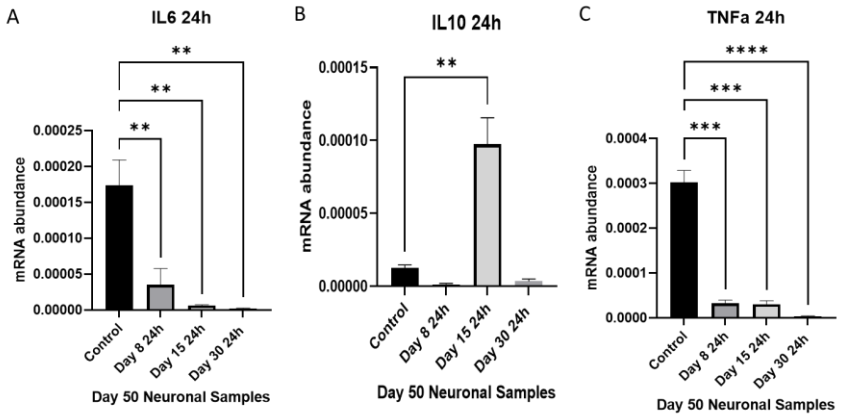

*Figure 5-12: Figure 5: Gene expression of autophagy markers in Cas13a TSC1 neurons. TSC1 heterozygous loss was induced via doxycycline at D8, 15 or 30 for 24h. A: IL6 expression significantly decreased in all conditions. B: Cells treated at Day8 and Day30 displayed a non-significant reduction of IL10 while cells treated at Day15 displayed a significant increase in expression. C: TNFa expression is significantly decreased for all timepoints treated for 24h. Values are expressed as mean ± SD (N=3). Data was analysed via One-Way ANOVA. * = p-value of ≤ 0.05, ** = p-value of ≤ 0.01, *** = p-value: ≤ 0.001, **** = p-value ≤ 0.0001.*

Gene expression analysis of the Cas13a TSC1 neurons shows significant alterations for inflammation related markers. IL6 expression showed significant decrease in all conditions in comparison to control with significance in cells treated at Day30 (p-values: 0.1453, 0.6972, 0.0108). IL10 expression was statistically significantly increased for cells treated at Day8 while the other conditions showed a faint non-significant increase in comparison to control (p-values: <0.0001, 0.2409, 0.2092). TNFa expression was decreased for all conditions with a significant reduction in the cells treated at Day 30 (p-values: 0.1091, 0.4686, 0.0109) (see Figure 5-13).

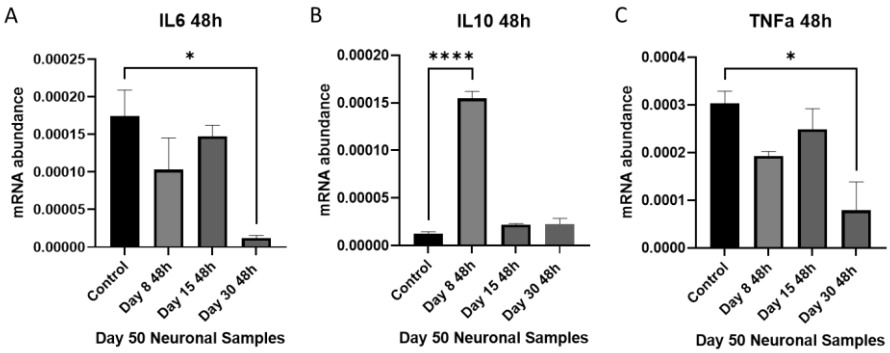

*Figure 5-13: Gene expression of autophagy markers in Cas13a TSC1 neurons. TSC1 heterozygous loss was induced via doxycycline at Day 8, 15 or 30 for 48h. A: IL6 expression decreased in all conditions with a significant decrease for cells treated at Day30. B: The loss of TSC1 at Day8 led to a significant increase of IL10 while cells treated at later time points led a non-significant increase. C: TNFa expression is decreased for all conditions with a significant decrease for cells treated at Day30. Values are expressed as mean ± SD (N=3). Data was analysed via One-Way ANOVA. * = p-value of ≤ 0.05, ** = p-value of ≤ 0.01, *** = p-value: ≤ 0.001, **** = p-value ≤ 0.0001.*

Analysing the expression changes over the neuronal development shows the increase of expression of inflammation markers over time. IL6 expression increased from the NPC stage towards the neuronal stage for both control and Cas13 TSC1 but the level of IL6 in Cas13 TSC1 cells was significantly lower than in control (p-values: 0.9988, 0.0020). IL10 expression increased from the NPC stage towards the neuronal stage for the control, while the Cas13 TSC1 cells showed no expression increase, leading to a significant expression reduction at the neuronal stage for the Cas13 TSC1 cells (p-values: 0.7431, 0.0010). TNFa expression increased from the NPC stage towards the neuronal stage with a significant decrease between the Cas13 TSC1 cell line in comparison to control (p-values: 0.9995, <0.0001) (see Figure 5-14).

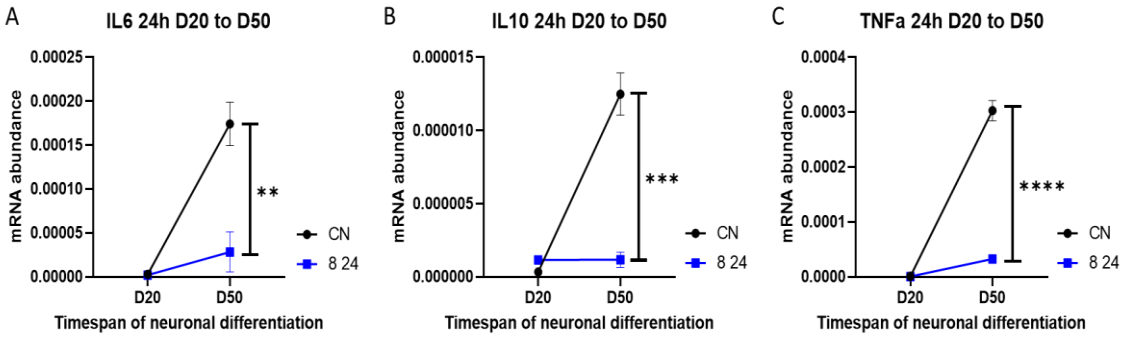

*Figure 5-14: Expression of inflammation markers during development. A-C: Significant expression decreases in the Cas13 TSC1 cells in comparison to control were found for all markers at the neuronal stage. Values are expressed as mean ± SD (N=3). Mixed-effect analysis with Sidaks-Test was performed for data analysis. * = p-value of ≤ 0.05, ** = p-value of ≤ 0.01, *** = p-value: ≤ 0.001, **** = p-value ≤ 0.0001.*

Analysing the expression changes over the neuronal development shows the increase of expression of inflammation markers over time. IL6 expression increased from the NPC stage towards the neuronal stage for both control and Cas13 TSC, the Cas13 TSC1 cells show a non-significant decrease at the neuronal stage (p-values: 0.9979, 0.0675). IL10 expression increased from the NPC stage towards the neuronal stage. The Cas13 TSC1 cells showed a significantly increased expression in comparison to control at Day 50 (p-values: 0.9990, <0.0001). TNFa expression increased from the NPC stage towards the neuronal stage with no significant difference between both cell lines at Day 50 (p-values: >0.9999, 0.7306) (see Figure 8).

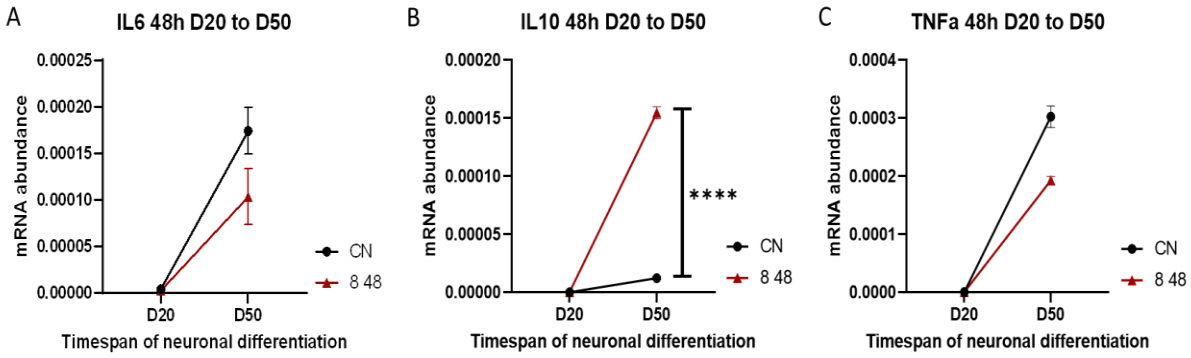

*Figure 8: Expression of inflammation markers during development. A-C: Non-significant expression decreases in the Cas13 TSC1 cells in comparison to control were found for IL6 and TNFa at the neuronal stage. Cas13 TSC1 neurons displayed a significant increase in IL10 expression. Values are expressed as mean ± SD (N=3). Mixed-effect analysis with Sidaks-Test was performed for data analysis. * = p-value of ≤ 0.05, ** = p-value of ≤ 0.01, *** = p-value: ≤ 0.001, **** = p-value ≤ 0.0001.*

5.3.3. Urokinase expression in TSC1 cells

A neuronal differentiation with the Cas13 *TSC1* cells was initiated and the Cas13a system was activated via doxycycline treatment of the cells to induce a heterozygous like loss of TSC1 on the RNA level. The treatment with doxycycline occurred at three different time points of the neuronal development (Day 8, Day 15, and Day 30) where the cells are neuronal stem cells, neuronal progenitor cells or early neurons respectively. The doxycycline treatment itself occurred for either 24 or 48 h before washing the cells with PBS and adding fresh media without any doxycycline (see Figure 5-7). As it is impossible to select the location of the plasmid insertion when using electroporation, the Cas13 TSC1 cells without any doxycycline were used as control in order to eliminate any potential that insertion mutation would lead to gene expression alteration and thus impact the data.

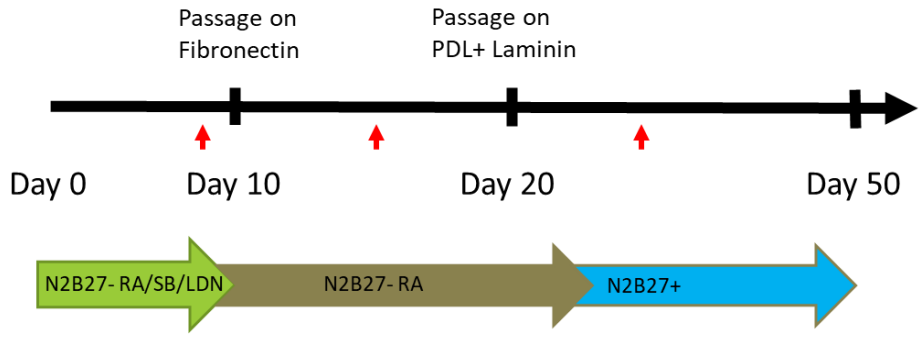

Figure 5-5: Scheme of neuronal differentiation of Cas13 TSC1 cells, time points of doxycycline treatment indicated with red arrows, treatment were for either 24 or 48h.

Gene expression analysis of the TSC1 NSCs shows significant alterations for the urokinase markers. While uPA itself was non-significantly increased in TSC1 -/- cells (p-value: 0.2733), the Cas13 TSC1 cells displayed non-significant reductions in both conditions in comparison to control, with a bigger reduction for the 24 h treatment (p-values: 0.0668 and 0.1259). uPAR was significantly reduced in comparison to control (p-value: 0.0422) for the TSC1 -/- cells, similarly to the Cas13 TSC1 cells displaying reduction for both conditions with significance for the 24 h treated cells (p-values: 0.0205 and 0.0876). tPA expression on the other hand was non-significantly increased in the TSC1 -/- cells (p-value: 0.2325) similarly to the Cas13 TSC1 cells with a non-significant reduction for the 24 h treated cells while the 48-h treatment led to a significant expression reduction (p-values: 0.4778 and 0.0055) (see Figure 5-8).

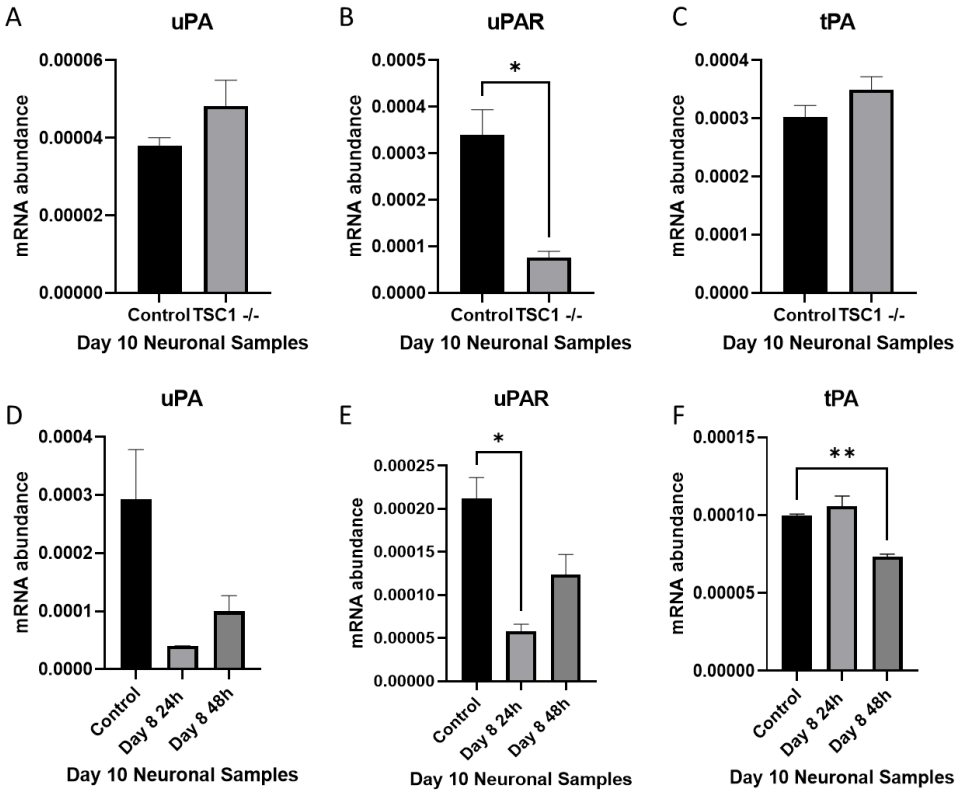

*Figure 5-6: Gene expression of urokinase markers in TSC1 neuronal stem cells during neuronal differentiation. A+D: uPA expression is non-significantly reduced in TSC1 -/- cells while the Cas13 TSC1 display a significant reduction of uPA expression after TSC1 induction for both conditions with the reduction was more severe in the 24h treatment. B+E: uPAR expression was significantly reduced in the TSC1 -/- cells while the Cas13 TSC1 cells show a reduction of uPAR expression in both conditions with significance for the 24h treatment. C+F: tPA was non-significantly increased in the TSC1 -/- cells in comparison to control while the 24h treatment led to a non-significant increase of tPA expression while the 48h treatment caused a significant decrease in the Cas13 TSC1 cells (N=3). Values are expressed as mean ± SD. Unpaired t-test were used for the data analysis of the homozygous cells, Shapiro-Wilk normality test was passed, while the Cas13 samples were analysed with a One-Way ANOVA. * = p-value of ≤ 0.05, ** = p-value of ≤ 0.01, *** = p-value: ≤ 0.001, **** = p-value ≤ 0.0001.*

Gene expression analysis of the TSC1 NPCs shows significant alterations for the urokinase pathway. uPA expression in the TSC1 -/- cells was non-significantly increased (p-value: 0.0619), while the Cas13 TSC1 cells display a reduced uPA expression in both conditions in comparison to control, with a significant reduction for the 48-h treatment (p-values: 0.0728 and 0.0003). uPAR expression was significantly increased in the TSC1 -/- NPCs (p-values: 0.0300) and statistically non-significantly reduced for both conditions of the Cas13 TSC1 cells with a bigger reduction for the 24 h treatment (p-values: 0.1225 and 0.9711). tPA expression was significantly increased in the TSC1 -/- cells in comparison to control (p-value: 0.0007), similarly to the Cas13 TSC1 cells with an increased tPA expression for both conditions in comparison to control with a significant increase for the 48 h treated cells (p-values: 0.3999 and 0.0203) (see Figure 5-9).

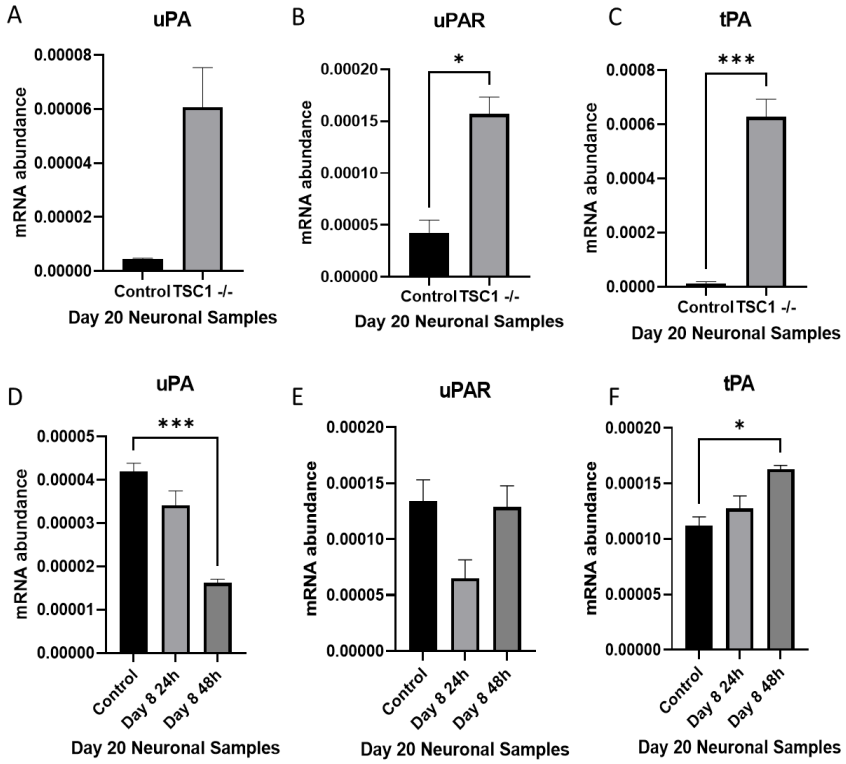

*Figure 5-7: Gene expression of urokinase markers in TSC1 NPCs during neuronal differentiation. A+D: uPA expression is non-significantly increased in the TSC1 -/- cells, while the Cas13 TSC1 cells show a reduction of uPA expression for both conditions with significance for the 48-h treatment. B+E: The TSC1 -/- cells displays a significant expression increase of uPAR while the Cas13 TSC1 cells show a statistically non-significant reduction for both conditions (N=3). Values are expressed as mean ± SD. Unpaired t-test were used for the data analysis of the homozygous cells, Shapiro-Wilk normality test was passed, while the Cas13 samples were analysed with a One-Way ANOVA. * = p-value of ≤ 0.05, ** = p-value of ≤ 0.01, *** = p-value: ≤ 0.001, **** = p-value ≤ 0.0001.*

Gene expression analysis of the TSC1 neurons shows significant alterations for the urokinase pathway. Both uPA and uPAR were increased in TSC1 cells with significance for the uPAR expression (p-values: 0.1348 and 0.0157). tPA expression was significantly increased in the TSC1 cells (p-value: 0.0009) (see Figure 5-10).

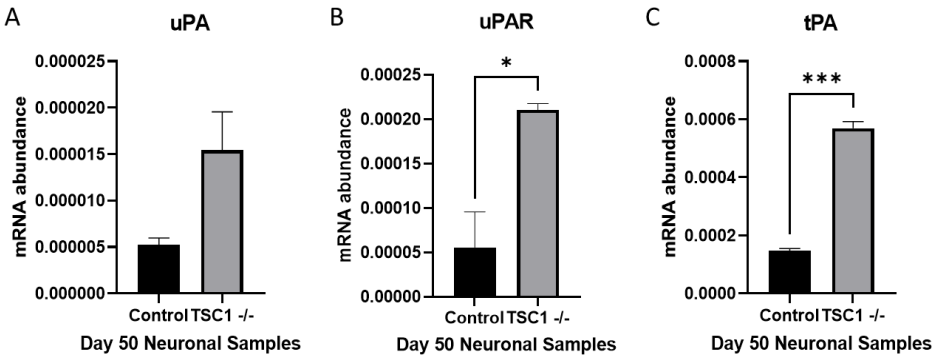

*Figure 5-8: Gene expression of urokinase markers in TSC1 homozygous neurons. A+B: uPA and uPAR expression is increased in TSC1 -/- cells, with a significant increase for uPAR. E: tPA expression was significantly increased in the TSC1 cells (N=3). Values are expressed as mean ± SD. Unpaired t-tests were performed for the statistical analysis. * = p-value of ≤ 0.05, ** = p-value of ≤ 0.01, *** = p-value: ≤ 0.001, **** = p-value ≤ 0.0001.*

Gene expression analysis of the Cas13a TSC1 neurons shows significant alterations for the urokinase pathway after 24 h and 48 h TSC1 loss at different time points of development. uPA expression was significantly reduced in all conditions in comparison to control for the 24 h treatment (p-values: 0.0084 for all three conditions) while the 48 h treated cells displayed a decrease in all conditions in comparison to control with a significant decrease for cells treated at Day30 (p-values: 0.1840, 0.0854,0.0065). uPAR expression was reduced for all conditions with significant reductions for cells treated at Day8 and Day15 (p-values: 0.0196, 0.0058 and 0.1060) for the 24 h treated cells and 48 h treatment led to reduced uPAR expression was reduced for all conditions with significant reductions for cells treated at Day8 and Day30 (p-values: 0.0324, 0.0610 and 0.0320). tPA expression in the 24 h treated cells were significantly reduced with bigger reductions for the cells treated at Day15 and Day30 (p-values: 0.0010, 0.0002 for both Day15 and Day30) while the 48-h treatment led to significant reduction in all conditions (p-values: 0.0002, 0.0001, 0.0002) (see Figure 5-11).

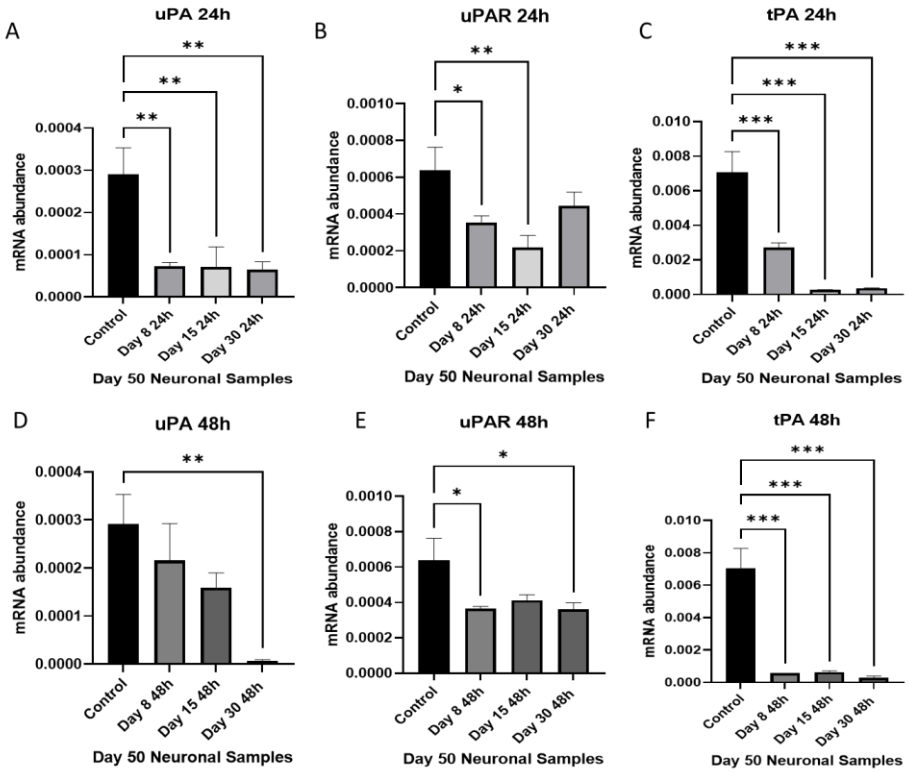

*Figure 5-9: Gene expression of urokinase markers in Cas13a TSC1 neurons. Heterozygous loss of TSC1 was induced at Day 8, 15 and 30 for either 24 or 48h. A+D: All conditions show a significant reduction of uPA expression for cells treated for 24h, the 48h treatment led to reductions in all conditions with significance at Day30. B+E: All conditions show a reduction of uPAR expression after TSC1 induction for both time lengths with significance for the cells treated at Day8 and Day15 (24h) or Day8 and Day30 (48h). C+F: All conditions show a significant decrease of SERPINE1 expression after TSC1 induction independent of treatment length. Values are expressed as mean ± SD. Data was analysed via One-Way ANOVA. * = p-value of ≤ 0.05, ** = p-value of ≤ 0.01, *** = p-value: ≤ 0.001, **** = p-value ≤ 0.0001.*

Analysing the expression changes over the neuronal development shows the decrease of several plasmin related markers over time. uPA expression dropped from the NSC to the NPC stage and stayed low towards the neuronal stage. While the expression of uPA in the TSC1 -/- cells was higher, no statistical significance was found throughout development (p-values for each time points: 0.7171, 0.6515, 0.5526). Expression of uPAR also dropped towards the NPC stage and then slightly increased in the neurons for the control. The expression level of uPAR was higher throughout than uPA. The TSC1 -/- cells displayed an increase of uPAR expression from the NSC to the neuronal stage. No statistical significance was found between both cell lines throughout the development (p-values for each time points: 0.2999, 0.1044, 0.3908). tPA expression dropped towards the NPC stage and then increased in the neurons for the control while the TSC1 -/- cells displayed a higher expression level from the start which increased towards the NPC stage and slightly lowered in the neurons, significance between both lines was found at Day 20 and Day 50 (p-values for each time points: 0.5137, 0.0326, 0.0040) (see Figure 5-12).

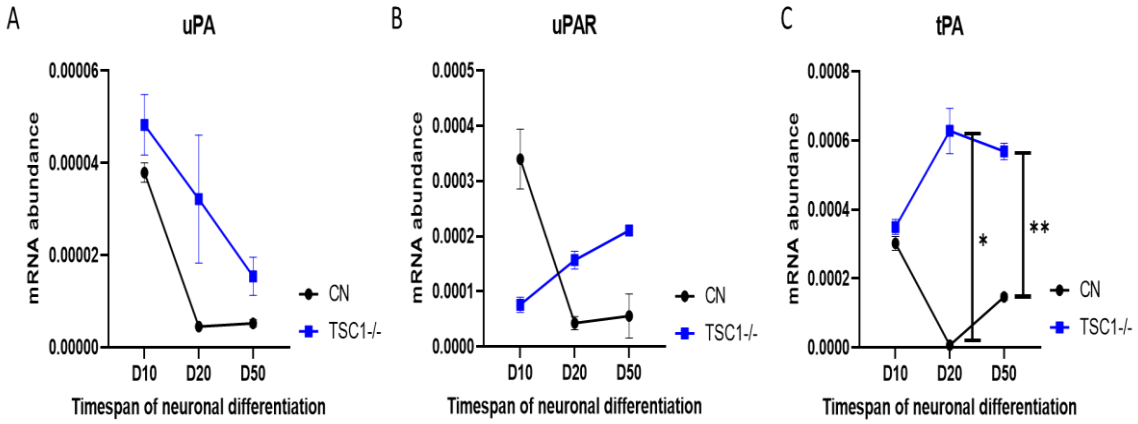

*Figure 5-10: Expression of urokinase markers during development of TSC1 -/- cells. A: uPA expression in TSC1 cells is non-significantly increased throughout the development. B: uPAR expression in the TSC1-/- cells is lower at Day 10 than in control and then increases while uPAR in control decreases during development. No significant difference between both cell lines. C: tPA expression at Day 10 aligned between both cell line. While tPA levels decreased in control towards Day 20 and then increased again to Day 50, TSC1 cells show an increase of tPA towards Day 20 and then a slight decrease towards Day 20. Therefore, tPA levels were significantly increased in the TSC1 cells at Day 20 and Day 50 in comparison to control. Values are expressed as mean ± SD (N=3). Mixed-effect analysis with Sidaks-Test was performed for data analysis. * = p-value of ≤ 0.05, ** = p-value of ≤ 0.01, *** = p-value: ≤ 0.001, **** = p-value ≤ 0.0001.*

Analysing the expression changes over the neuronal development shows the decrease of several plasmin related markers over time. uPA expression dropped from the NSC to the NPC stage and increased towards the neuronal stage while the Cas13 TSC1 cells displayed a continuous low expression of uPA. While the expression of uPA in the TSC1 cells was lower, no statistical significance was found throughout development for the 24 h treated cells (p-values for each time points: 0.4804, 0.4917, 0.1001). The 48-h treated Cas13 TSC1 cells displayed a continuous low expression of uPA with a significant reduction at Day 20 between both conditions (p-values for each time points: 0.5389, 0.0056, 0.9275). Expression of uPAR also dropped towards the NPC stage and then increased in the neurons for the control while Cas13 TSC1 cells displayed a continuous expression increase while starting at a lower level then the control. No statistical significance was found between both conditions throughout the development for the 24 h treated cells (p-values for each time points: 0.2227, 0.8612, 0.4320), similarly to the 48 h treated cells (p-values for each time points: 0.2026, 0.9976, 0.4722). *tPA* expression in the 24 h treated cells continued towards the NPC stage before increasing in the neurons in both lines with the Cas13 TSC1 cells displaying a non-significant reduction of *tPA* in the neurons in comparison to control (p-values for each time points: 0.8300, >0.9999, 0.5702). Meanwhile, the 48 h treated cells display significantly reduced tPA levels at Day 10 in the *TSC1* cells (p-values for each time points: 0.0015, 0.2111, 0.2127) (see Figure 5-13).

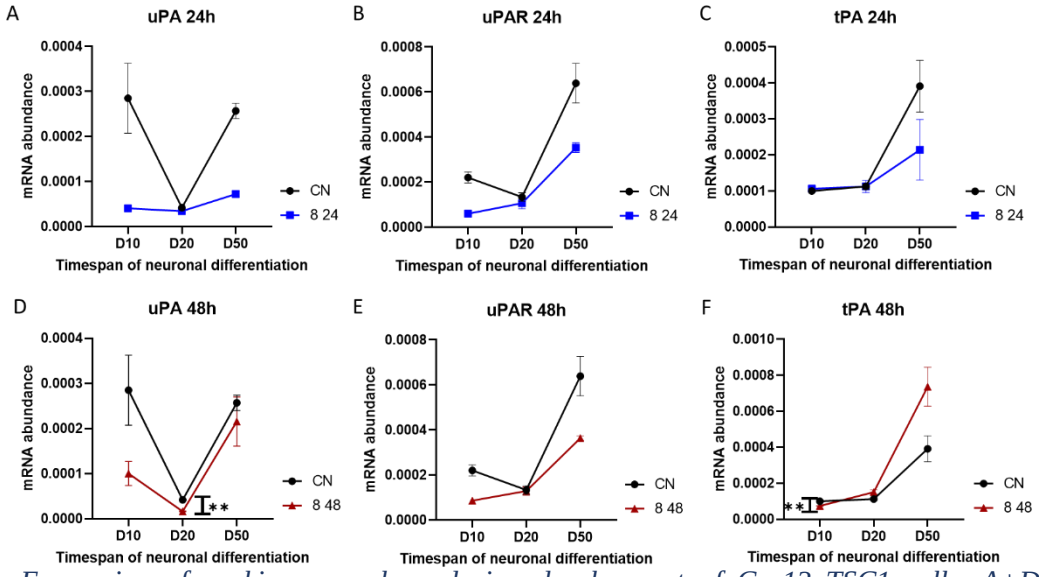

*Figure 5-11: Expression of urokinase markers during development of Cas13 TSC1 cells. A+D: uPA expression in Cas13 TSC1 cells is non-significantly decreased throughout the development for the 24h treated cells while the 48h treatment led to a significant reduction at Day 20. B+E: uPAR expression in the Cas13 TSC1 cells is continuously non-significantly lower than in control for both treatment lengths. C+F: tPA expression displayed no significant changes in the Cas13 TSC1 cells with exception of D10 for the 48h treatment. Values are expressed as mean ± SD. Mixed-effect analysis with Sidaks-Test was performed for data analysis. * = p-value of ≤ 0.05, ** = p-value of ≤ 0.01, *** = p-value: ≤ 0.001, **** = p-value ≤ 0.0001.*

5.3.4. Urokinase regulators in TSC1

SERPINE1 was non-significantly reduced in the TSC1 -/- cells (p-value: 0.1523) while the Cas13 TSC1 cells demonstrated significant reductions for both conditions with a bigger reduction for the 48-h treatment (p-values: 0.0186 and 0.0086). SERPING1 was significantly reduced (p-value: 0.0014) in the TSC1 -/- cells, and the Cas13 TSC1 cells displayed a non-significant reduction for both treatment conditions with a bigger reduction for the 24h treatment (p-values: 0.1293 and 0.2043) (see Figure 5-14).

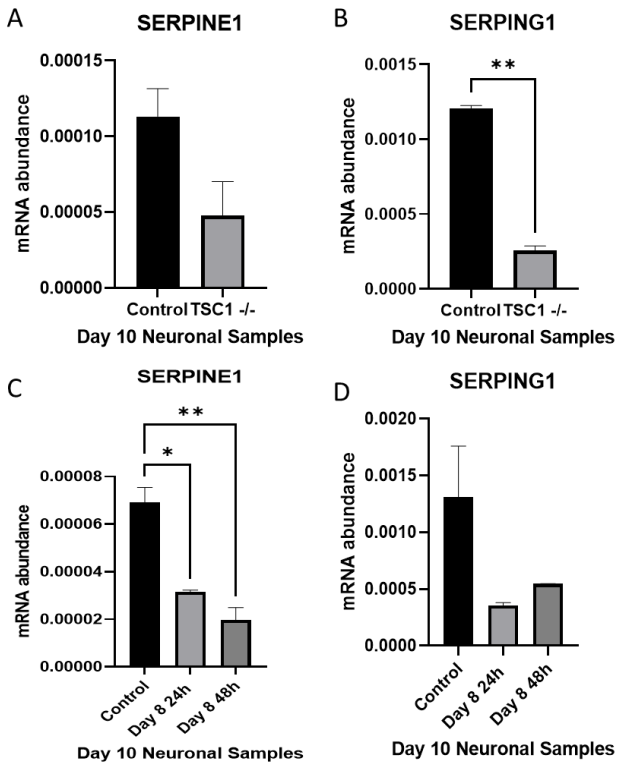

*Figure 5-12: Gene expression of urokinase regulators in TSC1 neuronal stem cells. A+C: Expression of SERPINE1 is non-significantly reduced in TSC1 -/- cells, while the Cas13 TSC1 cells display a significant reduction of SERPINE1 levels in both conditions. B+D: SERPING1 is significantly reduced in TSC1 -/- cells while the Cas13 TSc1 cells display a non-significant reduction (N=3). Values are expressed as mean ± SD. Unpaired t-test were used for the data analysis of the homozygous cells, while the Cas13 samples were analysed with a One-Way ANOVA. * = p-value of ≤ 0.05, ** = p-value of ≤ 0.01, *** = p-value: ≤ 0.001, **** = p-value ≤ 0.0001.*

SERPINE1 was non-significantly decreased in the TSC1 -/- NPCs while the Cas13 TSC1 cells displayed a reduction for both conditions with a significant reduction for the 48-h treatment (p-values: 0.0609 and 0.0067). SERPING1 expression was non-significantly increased in the TSC1 -/- cells (p-values: 0.4130 and 0.0713 respectively) while the Cas13 TSC1 cells showed no expression change foe the 24h treated cells while the 48-h treatment led to a non-significant increase (p-values: 0.9981 and 0.1137) (see Figure 5-15).

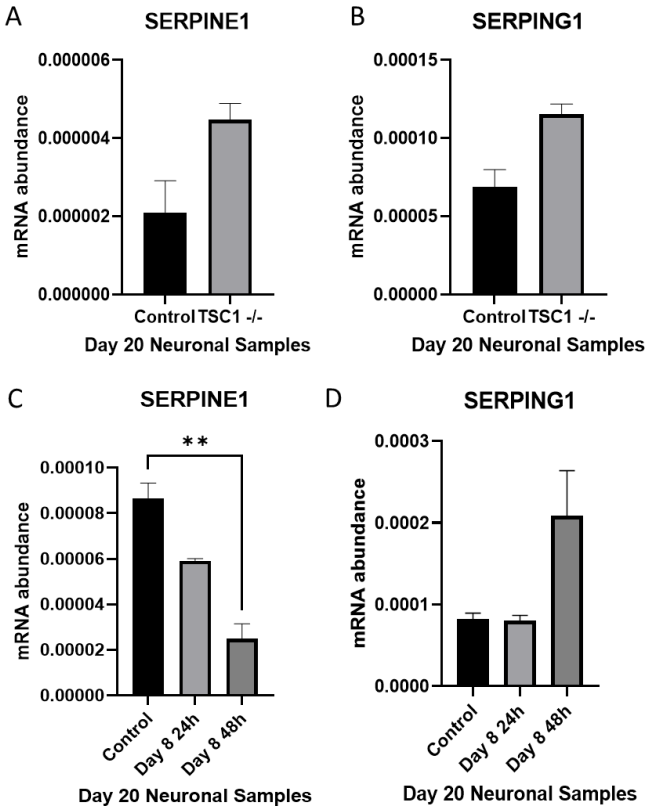

*Figure 5-13: Gene expression of urokinase regulators in TSC1 NPCs. A+C: The TSC1 -/- cells displayed a non-significant increase of SERPINE1 levels, while the Cas13 cells showed a reduction of SERPINE1 expression in both conditions with significance for the 48h treatment. B+D: SERPING1 in the TSC1 -/- cells was non-significantly increased while the Cas13 TSC1 cells showed no expression change for the 24h treatment and a non-significant increase in expression for the 48h treatment. Values are expressed as mean ± SD. Unpaired t-test were used for the data analysis of the homozygous cells, while the Cas13 samples were analysed with a One-Way ANOVA. * = p-value of ≤ 0.05, ** = p-value of ≤ 0.01, *** = p-value: ≤ 0.001, **** = p-value ≤ 0.0001.*

SERPINE1 was non-significantly decreased while SERPING1 was non-significantly increased (p-values: 0.4130 and 0.0713 respectively). tPA expression was significantly increased in the TSC1 cells (p-value: 0.0009) (see Figure 5-16).

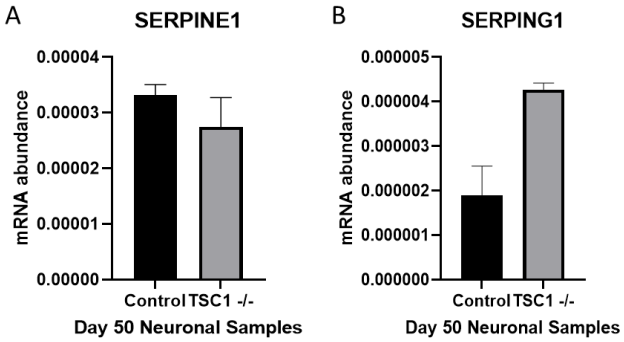

*Figure 5-14: Gene expression of urokinase regulators in TSC1 neurons. A: The TSC1 -/- cells displayed a non-significant decrease of SERPINE1 levels. B: SERPING1 in the TSC1 -/- cells was non-significantly increased. Values are expressed as mean ± SD. Data was analysed via t-test. * = p-value of ≤ 0.05, ** = p-value of ≤ 0.01, *** = p-value: ≤ 0.001, **** = p-value ≤ 0.0001.*

SERPINE1 expression was reduced for all conditions independent of the treatment length with significance for the 24 h treatments (p-values 24 h: 0.0051, 0.0021 for both Day15 and Day30) (p-values 48 h: 0.2433, 0.2433, 0.0555). SERPING1 expression was significantly increased for all conditions of the 24 h treatment (p-values: 0.0020, 0.0186, 0.0005) while being significantly decreased for the 48-h treatment (p-values: <0.0001 for all) (see Figure 5-17).

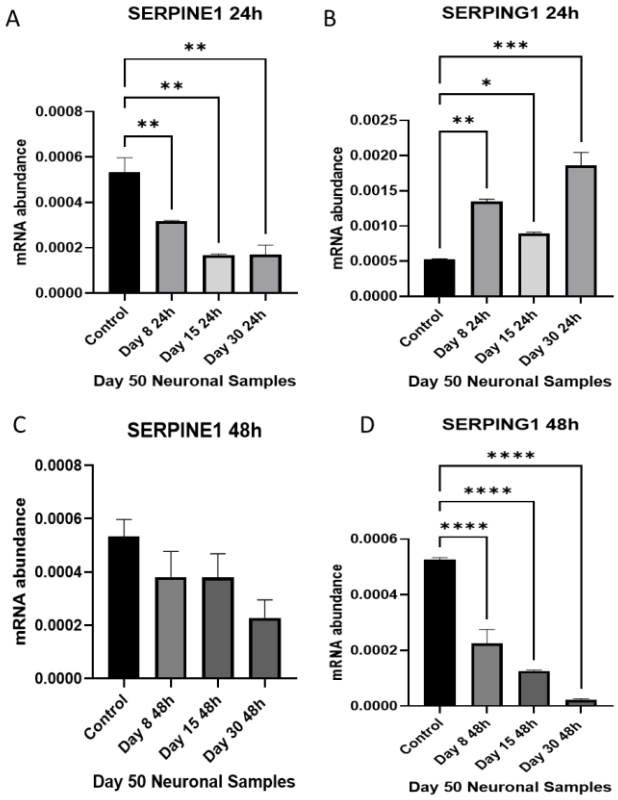

*Figure 5-15: Gene expression of urokinase regulators in the Cas13a TSC1 neurons. Heterozygous loss of TSC1 was induced at Day 8, 15 and 30 for either 24 or 48h. A+C: All conditions show a decrease of SERPINE1 expression after TSC1 induction with significance for the 24h treatments. B+D: All conditions of the 24h treatment led to a significant increase of SERPING1 expression while the 48h treatment led to significant reductions of SERPING1 levels. Values are expressed as mean ± SD. Data was analysed via One-Way ANOVA. * = p-value of ≤ 0.05, ** = p-value of ≤ 0.01, *** = p-value: ≤ 0.001, **** = p-value ≤ 0.0001.*

SERPINE1 expression dropped towards the NPC stage and then slightly increased in the neurons for the control while the TSC1 -/- cells showed a low expression throughout with its lowest point at Day 20 before increasing slightly in the neurons, no significance between both cell lines was established (p-values for each time points: 0.2298, 0.3867, 0.9590). SERPING1 expression dropped continuously throughout the expression for the control while the TSC1 -/- cells showed a low expression throughout with its lowest point at Day 50, at Day 10 the expression was significantly lower in the TSC1 -/- cells (p-values for each time points: 0.0091, 0.9430, 0.1666) (see Figure 5-18).

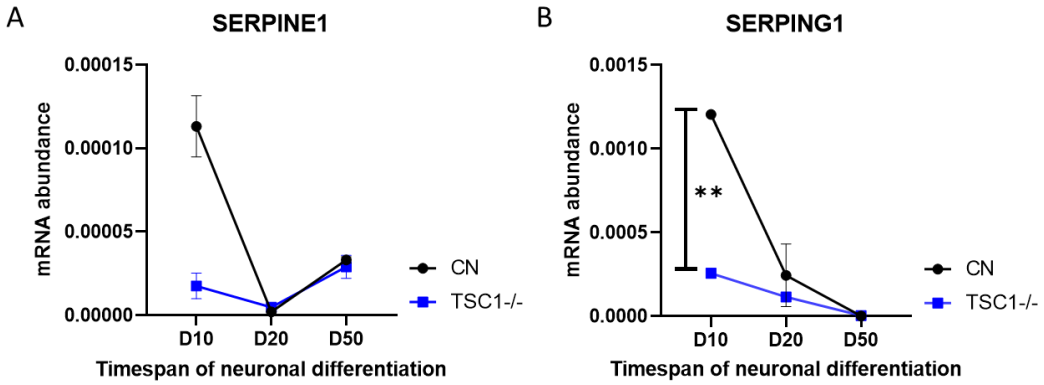

*Figure 5-16: Expression of urokinase regulators during development in TSC1 -/- cells. A: SERPINE1 expression is non-significantly decreased in the TSC1 cell line at Day 10, while its expression at Day 20 and Day 50 aligns to control. B: SERPING1 expression is significantly decreased at Day 10 in the TSC1 cells and then aligns towards the control at later time points. Values are expressed as mean ± SD. Mixed-effect analysis with Sidaks-Test was performed for data analysis. * = p-value of ≤ 0.05, ** = p-value of ≤ 0.01, *** = p-value: ≤ 0.001, **** = p-value ≤ 0.0001.*

Analysing the expression changes over the neuronal development shows the decrease of urokinase regulators over time. SERPINE1 expression slightly dropped towards the NPC stage and then increased in the neurons for both conditions. The expression level in the Cas13 TSC1 cells was continuously non-significantly lower than control for both the 24 h treatment (p-values for each time points: 0.2706, 0.2454, 0.3436) and the 48-h treatment (p-values for each time points: 0.2306, 0.1797, 0.5303). SERPING1 expression dropped towards the NPC stage and increased again in the neurons for the control while the Cas13 TSC1 cells showing a higher increase of the SERPING1 level in the neurons. Statistical significance between both cell lines was found at Day 50 for both conditions with an increase for the 24 h treatment (p-values for each time points: 0.9399, 0.9759, 0.0374) and a decrease for the 48-h treatment (p-values for each time points: >0.9999, 0.7804, 0.0325) (see Figure 5-19).

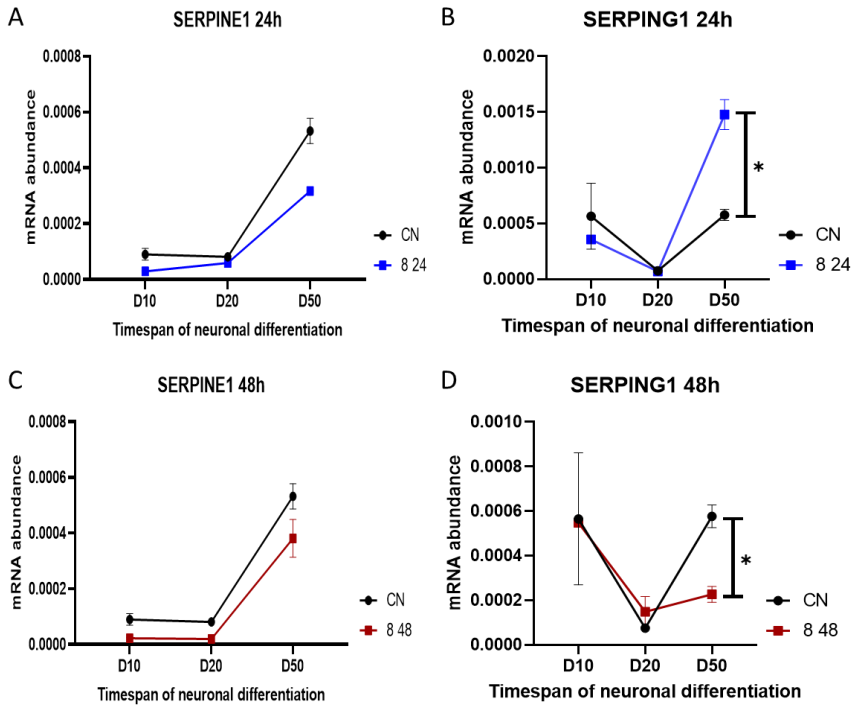

*Figure 5-17: Expression of urokinase regulators during development of Cas13 TSC1 cells. A+C: SERPINE1 expression is non-significantly decreased in the Cas13 TSC1 cell line throughout the differentiation in comparison to control for both conditions. B+D: SERPING1 expression is non-significantly decreased at Day 10 in the 24h TSC1 cells, aligns at the NPC stage to the control and is then significantly increased at Day 50 while the 48h cells display a significant decrease at Day 50 and non-significant increase at Day 20 in the TSC1 cells to the control. Values are expressed as mean ± SD (N=3). Mixed-effect analysis with Sidaks-Test was performed for data analysis. * = p-value of ≤ 0.05, ** = p-value of ≤ 0.01, *** = p-value: ≤ 0.001, **** = p-value ≤ 0.0001.*

5.4. Summary of major outcomes in this chapter:

- Inflammation related genes are significantly upregulated in TSC cells of patients; trend of expression increases of AD related genes in TSC patients.
- *uPA* expression shows few significant changes while *uPAR* expression showed trend of dysregulation; *tPA* expression was significantly altered in both *TSC1* models.
- *SERPINE1* and *SERPING1* expression showed trends of dysregulation in the Cas13 *TSC1* cells.

5.5. Chapter 5: Discussion

5.5.1. Database Analysis:

This analysis showed that TSC and AD have common molecular pathways which are dysregulated. Inflammation related genes, whose dysregulated expression was already suggested in other studies, were found in the database, and cross-referencing with AD research established their involvement in AD. Additionally, AD related genes themselves were found in the Top 150 and Top 300 genes in the several tumour samples of the TSC patients. From these genes, some were chosen for further investigation in the generated TSC1 models.

Inflammation inhibiting genes such as ANXA1, SERPING1, or HMOX1 were found to have significantly upregulated expression in the TSC patients' samples analysed in the database project and they are also implicated in AD, making them therefore interesting targets for future experiments. ANXA1, which was upregulated in the SEN/SEGA samples, is a calcium-dependent phospholipid-binding protein that initially characterizes as phospholipase A2-inhibitory activities and possesses anti-inflammatory activities. Its wide variety of cellular functions includes membrane aggregation, phagocytosis, proliferation, differentiation, and apoptosis. It has been further reported that ANXA1 plays a role in membrane trafficking and vesiculation of multivesicular bodies that might be involved in autophagy (Shi *et al.* 2018). ANXA1 was associated with AD in genome-wide study (Li *et al.* 2008) and was found to be upregulated in AD samples (Watanabe *et al.* 2007), which was concurrent with the activation of microglial cells in AD patients. It is hypothesized, that ANXA1 overexpression may indicate an attempt to limit sustained inflammatory damage due to unknown factors in AD and since Aβ can activate microglia it might also be capable of promoting ANXA1 expression (Watanabe *et al.* 2007). Another study found that ANXA1 treatment increased microglial clustering around Aβ plaques and induces the secretion of anti-inflammatory markers, demonstrating the possibility that ANXA1 seems to play a pivotal role in Aβ clearance, modulating inflammation, and maintaining BBB integrity in AD (Blair *et al.* 2018). HMOX1 on the other hand is a heat shock protein that exists in the endoplasmic reticulum. Its expression is induced by oxidative, nitrosative, or inflammatory stress or Aß and shows high expression in hippocampal and cortical astrocytes and neurons in patients with AD or mild cognitive impairment (MCI), where it co-localizes with senile plaques, neurofibrillary tangles, and corpora amylacea.

In contrast to the protective effects of HMOX1, studies show that the up regulation of HMOX1 increases oxidative stress through the accumulation of Fe^{2+} in mitochondria and other cellular compartments of astroglia and promotes mitochondrial damage and macro-autophagy (Shi *et al.* 2012). Overexpression of HMOX1 was implicated in cognitive deficits in AD as it was demonstrated the long-term overexpression of HMOX1 induces memory decline in transgenic mice through an HMOX1-induced tauopathy mechanism (Han and Sahin 2011). HMOX1 demonstrated upregulated expression in several tumours of TSC patients (Knox *et al.* 2007) and showed increased expression in the samples included in the database. SERPING1, a protease inhibitor, was found to show increased expression in the TSC patient samples, which aligns to the finding of Boer *et al.* (Boer *et al.* 2010). SERPING1 is involved in the complement system and seems to be involved in neuronal stem cell proliferation as well as having a role in cortical development (Gorelik *et al.* 2017). Additionally, its expression has also been demonstrated in AD, which may reflect ongoing inflammation in the brains of the patients (Veerhuis *et al.* 1998; Yasojima *et al.* 1999; Walker *et al.* 2002). It has been identified to have a significant association to AD (Williams *et al.* 2015). Therefore, SERPING1 expression was investigated in the cell models of this project.

Pro-inflammatory genes like SERPINA 3 and 5, ANGPTL2, and GPMNB were also found with altered gene expression and involvement in TSC (see Figure 9-11) and AD. SERPINA3 and other serpins are found within the fibrillar amyloid plaques of AD. SERPINA3 may facilitate fibril formation by serving as a chaperone for Aβ (Kumar *et al.* 2005). Another study indicated that the increased levels of SERPINA3 may affect age-at-onset and disease duration of AD (Jaworski *et al.* 2005). SERPINA3 is also elevated in TSC, as shown in several studies (Tavazoie *et al.* 2005; Meikle *et al.* 2007). Magri *et al.* showed that STAT3 is a central player in inducing premature neuronal and astroglial differentiation in TSC1 mutant endogenous neural stem cells (eNSCs), and its target genes, such as GFAP and SERPINA3, are known to be significantly overexpressed in mutant eNSC and TSC lesions (Meikle *et al.* 2007). As SERPINA3 and SERPINA5 are both inflammation related genes with the first also being associated with AD (Jaworski *et al.* 2005; Kumar *et al.* 2005) and TSC (Tavazoie *et al.* 2005; Meikle *et al.* 2007), attempts for gene expression analysis in the TSC1 cell lines were made but low qPCR primer quality prevented any in depth analysis.

As gene mapping suggested that SERPINA3 and SERPINA5 are involved with plasminogen and thereby indirectly or directly with uPA, both genes are seen as interesting targets for future experiments. Inflammatory related cytokines such as IL6, IL10, TNFa or IL18 were found to be significantly involved with both TSC and AD via literature (Weichhart *et al.* 2008; Byles *et al.* 2013; Wang *et al.* 2015; Mammana *et al.* 2018) and the latter two were also found in the Top 300 dysregulated genes of the TSC database analysis. Therefore, the expression of several of these cytokines were tested in the cell models as well. Additionally, the database analysis also identified increased expression levels for genes which correlate with AD. These genes are CLCN7, encoding for the chloride channel ClC-7; LAMA4, a Laminin subunit involved in processes such as cell adhesion, differentiation, signalling and neurite outgrowth; MAP1B, which encodes for a microtubule-associated protein which is involved in neurogenesis; MCAM, which is involved in cell adhesion, MYL9, encoding for a motor protein, PPARG, which encodes for an adipocyte regulator.

Overall, the database analysis of the RNA sequencing of TSC patients lead to a more targeted approach for further investigations as the common targets of dysregulation for both TSC and AD had been identified. Therefore, this project focused on the inflammation associated cytokines IL6, IL10, TNFα and the urokinase pathway around SERPING1.

5.5.2. Inflammation markers:

The cytokine IL6 was originally considered to be a pure pro-inflammatory cytokine, but recent studies are contradicting that statement. It is expressed by both glia cells and neurons. IL6 antagonizes the actions of IL1β and TNFa via induction of the soluble IL1 receptor antagonist and the soluble TNF-α receptor (Ulich et al. 1991; Trig et al. 1994). Furthermore, IL6 is essential for the control of pro-inflammatory cytokine levels like TNFa in vivo after endotoxic insults (Xing et al. 1998). Induction of IL6 production includes various stimuli like neurotransmitters, depolarization or the presence of other pro-inflammatory cytokines (Spooren et al. 2011). IL6 is crucial in the BBB for its integrity, where it influences astrocyte shape by affecting cell adhesion molecules (Shrikant et al. 1995; Oh et al. 1998). Therefore, it was suggested that IL6 carries an anti-inflammatory function in this instance by helping to maintain blood–brain barrier integrity in neuroinflammatory conditions.

Furthermore, IL6 is also seen as a neurotrophic factor, based on its substantial role in homeostasis and development of the nervous system where it induces neuronal survival, proliferation, differentiation and regeneration, as well as influencing synaptic release of neurotransmitters and neural activity (Spooren et al. 2011). IL6 has been shown to stimulate the differentiation various neurons subtypes (Hirota et al. 1996; Cao et al. 2006; Zhang et al. 2007). Additionally, IL6 also promotes survival of neurons in the presence of oxidative stress (Nakajima et al. 2002; Bissonnette et al. 2004; Fujita et al. 2009). It is produced by astrocytes after hypoxia in order to promote the survival of PC12 cells in culture (Maeda et al. 1994). Loss of IL6 was shown to lead to increased neuronal death after physical damage towards dorsal root ganglia neurons in mice (Murphy et al. 1999). The self-renewal ability of NSCs is tightly controlled by STAT3 signalling cascades (Shi et al. 2008) which activity is controlled by IL6. Therefore, IL6 contributes to stem cell generation and expansion of neural stem cell pools, as well as regulating several neuronal markers as well as neural outgrowth (Niwa et al. 1998; Bowen et al. 2011; Brady et al. 2013). Loss of IL6 has been shown to lead to depletion as well as impairment of forebrain NSC pool expansion (Shimazaki et al. 2001) and activation of IL6 as well as the subsequent downstream activation of STAT3 promotes early neurogenesis (Kummer et al. 2021). IL6 influences cell differentiation by promoting both astrogliogenesis and neurogenesis, as well as by inhibiting the survival and growth of neural stem and progenitor cells (Spooren et al. 2011). Excitotoxicity also induces IL6 production in the brain (Masakazu et al. 1994; de Bock et al. 1996; Ali et al. 2000) as it protects neurons against excitotoxicity (Carlson et al. 1999; Pizzi et al. 2004; Peng et al. 2005). Controversially, some authors also found that IL6 enhances NMDA-induced excitotoxicity in cerebellar granule neurons (Qiu et al. 1998; Conroy et al. 2004). In addition, IL6 is essential for neuronal excitability and function due to its role in regulation of several voltage- gated as well as receptor operated channels (Vezzani and Viviani 2015). For example, IL6 reduces L-type calcium channel currents, counteracting potassium-induced intracellular Ca^{2+} overload and therefore protecting the neurons (Ma et al. 2012b). IL6 treatment of cultured hippocampal neurons as well as IL6 over- expression in vivo reduces L-type Ca^{2+} channel $Ca_V1.2$ protein expression (Vereyken et al. 2007). TSC is known to display increased levels of IL6 production (Wang et al. 2021a), similarly to AD where IL6 influences both tau and Aβ.

Firstly, several studies suggested that IL6 promotes the hyperphosphorylation of tau (Quintanilla et al. 2004; Orellana et al. 2005). However, another study demonstrated no effect of IL-6 on tau phosphorylation in hippocampal neurons (Hüll et al. 1999). Secondly, while IL6 induces expression of APP, in primary rat cortical neurons (Del Bo et al. 1995) and influences its processing (Brugg et al. 1995), Aβ was shown to induce IL6 expression (Jana et al. 2008; Vukic et al. 2009). IL6 expression analysis in the TSC1 -/- and Cas13 TSC1 cells shows significant changes in comparison to control cells during the neuronal development. Both TSC1 models displayed a significant reduction of IL6 expression at the NPC stage and while IL6 expression in neurons is generally low as it is usually expressed by glia cells, the significant reduction of its expression should impact the differentiation. Since IL6 plays a role in neuronal development and offers protection against oxidative stress, the reduced expression level would suggest an impaired development and reduced protection for the cell against stress, though its dysregulation probably plays a less significant role as the previously discussed markers, solely based on the level of expression. The TSC1 -/- cells showed nearly significantly elevated levels of IL6 expression in the neurons in comparison to control. This increase might be the result from not only the TSC1 loss itself but also due to the assumed increase of astrocytic cells in the culture, which would align with the increased level of astrocytic markers in the TSC1 neurons. As IL6 expression is known to cause the expression of other inflammation related cytokines, further markers were tested and will be discussed below. As calcium channels haven't been investigated in this project, it is not possible to say if the TSC1 cells show changes in L-type Ca^{2+} channel $Ca_V1.2$ protein expression (Vereyken et al. 2007). The Cas13 TSC1 cells displayed a significant drop of IL6 expression in the neurons, which was surprising as the astrocytic markers were significantly elevated and a phenotype like the TSC1 -/- model was therefore expected. Therefore, it could be assumed that the IL6 expression is less based on the astrocytes in the Cas13 TSC1 culture and is truly expressed by the neurons themselves. As IL6 is involved in neuronal survival, proliferation, regeneration, as well as influencing synaptic release of neurotransmitters and neural activity (Spooren et al. 2011), it can be assumed that these function are most likely disturbed in the Cas13 TSC1 cells, though further experiments would need to be performed in order to strengthen that assumption.

IL10 is classified as an anti-inflammatory cytokine which is known to promote neuronal survival after injuries (Dietrich et al. 1999; Grilli et al. 2000; Jackson et al. 2005) and inhibiting the synthesis and release of proinflammatory mediators such as TNFa, IL1β, IL6, IL8, and IL12 (Howard et al. 1992; Moore et al. 2001), thereby counteracting potentially harmful consequences. Research suggests that IL10 activates signalling pathways involved in neuronal survival and growth (Zhou et al. 2009) and it is known to prevent apoptosis in several neuronal cells after cellular stress caused by glutamate toxicity or serum deprivation (Brewer et al. 1999; Zhou et al. 2009). Zhou et al. demonstrated that IL10 engages the downstream signalling cascades Jak–STAT3, PI3K–AKT, and GSK3β in order to prevent the apoptosis (Zhou et al. 2009). Perez-Asensio et al. demonstrated that IL10 regulates the expression of neural progenitor markers like Nestin or SOX2, cell cycle activity of progenitors, and the production of new neuroblasts (Perez-Asensio et al. 2013). Pereira et al identified that this regulation of adult neurogenesis works via the STAT3 (Pereira et al. 2015) as shown in rat neurons. Therefore, it can be concluded that IL10 regulates progenitor differentiation and modulates neurogenesis in adult brain. Furthermore, Levin et al. demonstrated that IL10 also counteracts hypoxia and its subsequent hyperexcitability in neurons (Levin and Godukhin 2011). Disruption of IL10 levels during neuronal development have been shown to have long-lasting consequences as IL10, like IL6 or TNFa modulate neuronal differentiation (Ling et al. 1998), survival (Jarskog et al. 1997) and dendrite growth and complexity in vitro (Gilmore et al. 2004). Furthermore, these cytokines are hypothesized to play a crucial role in long-term behaviour and cognition (Shi et al. 2003; Zuckerman et al. 2003; Meyer et al. 2006; Romero et al. 2007). Meyer at al. demonstrated that enhanced levels of IL10 after exposure to pro-inflammatory cytokines during prenatal development prevented the emergence of multiple behavioural and pharmacological abnormalities in the adult offspring. Increased IL10 levels while pro-inflammatory signals were absent, led to behavioural abnormalities in adulthood (Meyer et al. 2008). Therefore, Meyer et al. concluded that the balance between pro- and anti-inflammatory cytokines is crucial for proper prenatal development (Meyer et al. 2008). IL10 also seems to be involved in synapse formation via microglia and inhibition of the former prevents the formation in hippocampal neurons (Lim et al. 2013).

Gene expression analysis of IL10 demonstrated significant alterations in the TSC1 -/- and Cas13 TSC1 cells during neuronal development. While IL10 expression was non-significantly reduced at the NPC stage in the TSC1 -/- model, the expression in the neurons was significantly increased. The Cas13 TSC1 cells demonstrated a significantly increased expression in the NPCs and neurons. Therefore, while no significance in the homozygous model was found, it could be assumed that TSC1 loss does impact IL10 expression during neuronal development and a higher sample size would strengthen that claim. As IL10 has several protective functions including improving cell survival and growth (Zhou et al. 2009), regulation of neural progenitor marker expression (Perez-Asensio et al. 2013), counteracting hypoxia (Levin and Godukhin 2011), it can be assumed that changes in its expression are to the detriment of the cell differentiation as disruption of IL10 levels during neuronal development have been shown to have long-lasting consequences as it is modulating neuronal differentiation (Ling et al. 1998). Again, the significantly increased levels at the neuronal stage might be partly a consequence of an increase of the number in astrocytes in the TSC1 cultures in comparison to control. Since IL10 expression is usually a cell response to the expression of pro-inflammatory markers like IL6 or TNFa, which are both significantly increased in the TSC1 models it was expected. As long-term overexpression of IL10 has negative consequences for cells and since a fine balance between pro- and anti-inflammatory cytokines is crucial for proper prenatal development (Meyer et al. 2008), it could be assumed that the development and functions of the neurons are impaired, though further experiments would be needed. Impaired neuronal function in TSC1 cells would be expected as studies and patients display it.

TNFa is a pro-inflammatory cytokine involved in various functions in the CNS including regulation of synaptic transmission and plasticity as well as induction of inflammation, excitotoxicity, and oxidative tissue damage under disease conditions (Papazian et al. 2021). TNFa functions via its receptor TNFR1 to mediate harmful TNF effects (Brambilla et al. 2011; Taoufik et al. 2011), including an inhibitory effect on remyelination (Karamita et al. 2017), while TNFa via its receptor TNFR2 mediates beneficial effects, such as remyelination (Arnett et al. 2001). Aligning with Papazian et al. results of beneficial effects mediated by TNFa, some research suggests that it might mediate a protective function against metabolic, excitotoxic or oxidative stresses (Merrill 1992; Cheng et al. 1994; Merrill and Benveniste 1996).

Further research suggests that TNFa is also involved in neuronal development as it was demonstrated that lack of TNFa results in faster dentate gyrus growth due to enhanced levels of nerve growth factor (NGF) while TNFa overexpression inhibits NGF expression, thereby suppressing hippocampal development (Fiore et al. 2000). TNFa is known to have potent neurodevelopmental effects by inhibiting neuronal cell survival (Jarskog et al. 1997) and cortical dendrite development (Gilmore et al. 2004) and several cytokines are cooperating in these processes (Jeohn et al. 1998; Gilmore et al. 2004). Elevated TNFa levels in foetus brains have also been implicated in increased neuronal apoptosis in postnatal life (Meyer et al. 2006). Furthermore, increased maternal TNFa levels during pregnancy have been directly associated with a higher incidence of adult psychosis in the offspring (Buka et al. 2001). Hence, there is considerable evidence linking abnormal maternal/ foetal TNFa to a higher incidence of brain and behavioural pathology in the grown offspring (Meyer et al. 2008).Furthermore, TNFa expression is known to influence the expression of other cytokines like IL6 (Lan et al. 2012). Altered TNFa expression is known to be involved in AD (McAlpine et al. 2009). TNFa has been found to be able to increase Aβ and Aβ related apoptosis, as well as to cause memory impairments in animal models (Blasko et al. 1997). Therefore, it is assumed that TNFa plays an important role in processes related to memory degeneration in diseases as both animal models and AD brains showed the altered TNFa levels (Blasko et al. 1997; Lanzrein et al. 1998; Tarkowski et al. 1999). Gene expression analysis for TNFa showed significant dysregulation in both TSC1 -/- and Cas13 TSC1 cells. While the TSC1 -/- cells show significant elevated levels neuronal stage, no significant changes were found in the NPCs. The Cas13 TSC1 cells displayed significant downregulation at both the NPC and neuronal stage.

Therefore, it can be assumed that TSC1 loss is able to influence TNFa expression during neuronal development, though the true scope of its influence during the early development is still unknown. The expression increases at the neuronal stage in the TSC1 -/- cells was expected as TNFa expression tends to align to the expression of markers like IL6 or IL10. Again, it might be explained partly by the number of astrocytes in the TSC1 culture compared to the control cell line and as TNFa is able to negatively affect neuronal cell survival (Jarskog et al. 1997) and cortical dendrite development (Gilmore et al. 2004) as well as increase neuronal apoptosis (Meyer et al. 2006), increased cell stress and death in the TSC1 cells could be expected. Apoptosis or cell stress markers haven't been tested in this project, but as TSC models/cells are known to express increased ox. stress markers (Zhang et al. 2016), this would align with previous studies.

Furthermore, the TSC1 -/- displayed a delayed/abnormal neuronal development, as seen by the dysregulation of NPC and neuronal markers, a phenotype which would align with TNFa overexpression (Fiore et al. 2000). As mentioned before, the Cas13 TSC1 cells showed significantly decreased levels of TNFa at the NPC and neuronal stage. While literature suggest that a downregulation of TNFa leads to enhanced neuronal development (Fiore et al. 2000), it is difficult to claim that this was the case in the Cas13 TSC1 cells. While several developmental markers for neuronal development were significantly dysregulated, their expression change proposes an abnormal and delayed development, not an enhanced one. As TNFa does have several protective functions in the brain, the significant reduction of expression for several conditions at the neuronal stage would suggest an increased vulnerability to certain stress factors like oxidative stress (Merrill 1992; Cheng et al. 1994; Merrill and Benveniste 1996).

Several genes which are either pro- or anti-inflammatory and directly or indirectly influencing neuronal development demonstrated significant dysregulation of their expression levels throughout the neuronal development. As TSC is known for inflammation, these results were expected. Their disturbance likely causes cellular stress and impair cell survival and differentiation.

5.5.3. Urokinase Pathway:

As mentioned previously, *uPA* is a serine protease which catalyses plasminogen activation and plasmin generation as initiation of the proteolysis cascade (Peteri *et al.* 2021). uPA is also involved in the activation of cell signalling pathways regulating differentiation, cellular adhesion, migration, and proliferation through non-plasminogenic mechanisms (Peteri *et al.* 2021). Sumi *et al.* suggested that uPAs proteolytic regulation is controlling axonal growth and that intracellular proteolytic degradation might regulate axoplasmic traffic, suggesting a role for uPA in neuronal plasticity (Sumi *et al.* 1992). uPA interaction with its receptor uPAR can result in increased cleavage of cell-associated plasminogen with the production of the protease processing plasmin, the latter's production aids in the process of inflammatory and neoplastic cell invasion through its ability to degrade extracellular matrix proteins (Walker *et al.* 2002). Using a uPA null mice model, Semina *et al.* investigated the involvement of uPA and uPAR in neuronal development (Semina *et al.* 2016). Both uPA and uPAR are involved in dendritic and axonal growth and branching as well as in neural cell migration. The interaction between both uPA and uPAR was found to be required for the exertion of these functions as uPA inhibition supressed the cell migration and axonal growth. uPAR expression levels themselves were found to be less important for the uPA-dependent axon growth and cell migration stimulation. Blocking the interaction by uPAR blockage led to suppressed neural cell migration and an increased number of neurites and enhanced branching in neurons (Semina *et al.* 2016). uPA-null mice displayed elevated levels of uPAR and a higher rate of neurite outgrowth as uPAR can engage ligands independent of uPA such as vitronectin or integrins (Engelholm *et al.* 2003; Franco *et al.* 2006; Madsen *et al.* 2007; Lino *et al.* 2014). uPAR null mice lack GABA-interneurons neurons (Eagleson *et al.* 2005) and are characterized by brain abnormalities associated with seizures and impaired behaviour (Royer-Zemmour *et al.* 2008; Bruneau and Szepetowski 2011). This phenotype strengthens the claim that uPA-independent uPAR function is essential for normal neuronal development.

In axons, the appropriate interaction of cell adhesion molecules with extracellular matrix is crucial for development of nervous system. Axon growth and polarization during neurogenesis is highly dependent upon integrins which have been implicated in uPA/uPAR-dependent activation of cell adhesion and cell morphology changes in non-neuronal systems (Blasi and Carmeliet 2002; Franco *et al.* 2006; Blasi and Sidenius 2010). It has been shown that uPA is involved in neuritogenesis during which it activates focal adhesion kinase, which is involved in the reorganization of the cytoskeleton and cell locomotion. For this function, interaction of uPA with its receptor uPAR is required with signal transduction via membrane co-receptors including integrins α5 and ß1 (Lino *et al.* 2014). uPA has also been found to be involved with the expression and function regulation of GAP-43, a central player in synaptogenesis and synaptic plasticity. Merino *et al.* demonstrated that uPA-uPAR binding induces GAP-43 mobilization from the axon shaft to presynaptic terminals. They further indicated that this function was independent on plasmin generation but mediated by open NMDA receptors (Merino *et al.* 2020). The expression of uPA and uPAR in the developing CNS is particularly high in neurons (Wu *et al.* 2014; Merino *et al.* 2017) and astrocytes (Liu *et al.* 2010) and progressively decreases during neuronal maturation. Increase in uPA levels have been found after neuronal injury, suggesting a role in neuronal repair (Merino *et al.* 2017).

Gene expression analysis of both TSC1 models displayed significant dysregulation of both uPA and uPAR during neuronal development. While uPA expression in the TSC1 -/- cells was non-significantly upregulated, uPAR expression was significantly downregulated at the NSC stage and continuously significantly upregulated for the following neuronal development. Plotting the expression over the timespan of development did not establish significance for the genes but it did showcase that uPA expression in TSC1 -/- dropped linear while the control cells displayed a sharp drop from the NSC to the NPC stage. Significance might be established with an increased sample size. uPAR expression over time on the other hand increased in the TSC1 -/- cells unlike in the control where it dropped with progressive cell differentiation/maturation. uPA overexpression had been found in TSC models previously and therefore aligned with the expectations. As both uPA and uPAR are involved in several essential processes of neurogenesis, it can be predicted that their dysregulation in the TSC1 -/- cells would have a negative impact on their function and development. TSC mutations are known to negatively impact cell polarity, synapse assembly and axonal growth (Knox *et al.* 2007).

As both uPA and uPAR are involved in these functions, it can be expected that the identified dysregulation of both genes might be partly causative for the impaired function and development of the neurons. As no experiment to test their synaptic or axonal growth/function have been performed in this project, at this point it is not possible to distinguish the precise involvement of uPA and uPAR in these functions in TSC. Since uPA expression is involved in the normal development of GABAergic cells and gene expression analysis in the previous chapter established the dysregulation of transcription factors which are also involved in this development, further experiments investigating the specific impact of uPA/uPAR dysregulation on neuronal development in TSC would further the understanding. Throughout the neuronal development, expression levels of both genes were downregulated with significance at the neuronal stage. As uPA inhibition has been found to negatively impact axonal growth, cell migration and increased number of neurites (Semina *et al.* 2016) it could be considered that these phenotypes might also occur in this cell model after the brief treatment, but no experiments were performed to confirm that due to a tight time schedule.

tPA, an important player in neuronal plasticity, axonal regeneration, neuroinflammation and excitotoxicity (Chevilley *et al.* 2015; Hebert *et al.* 2016), is expressed in neurons, astrocytes, microglia and oligodendrocytes (Hebert *et al.* 2016). Studies demonstrated that mice models lacking either tPA, uPA or plasminogen were found to have impaired function displayed delayed neuronal repair/recovery after injury (Siconolfi and Seeds 2001); furthermore, tPA deficient mice were also more susceptible to neuronal death induced by both NMDAR and non-NMDAR agonists (Tsirka *et al.* 1995). Exogenous tPA was reported to be neurotoxic for cortical neurons by over-activating of NMDAR, thus resulting in excitotoxicity (Nicole *et al.* 2001; Reddrop *et al.* 2005; Park *et al.* 2008). Excessive tPA promotes damages in Purkinje cells (Lu and Tsirka 2002; Li *et al.* 2006; Li *et al.* 2013), by altering neurotrophic mechanisms in control their postnatal development (Li *et al.* 2006; Li *et al.* 2013). Chevilley *et al.* pointed out that the maturation of neurons influences their sensitivity to tPA (Chevilley *et al.* 2015) as mouse primary cultures of cortical neurons become sensitive to NMDA-induced neuronal death after more than a week *in vitro*, an effect exacerbated by exogenous tPA (Launay *et al.* 2008). In the meanwhile, less matured neurons require trophic factors contained in culture media to survive (Hetman *et al.* 2000; Terro *et al.* 2000) and exogenous tPA was shown to have a protective effect against the neuronal apoptosis occurring with media deprivation (Liot *et al.* 2006).

The type of neurons might also be important according to Chevilley *et al.* (Chevilley *et al.* 2015) as the neurotoxic effects of tPA were mainly described in cortical neurons (Nicole *et al.* 2001) or Purkinje neurons (Li *et al.* 2013), while the protective effect were described for hippocampal neurons (Flavin and Zhao 2001; Lemarchand *et al.* 2016) and on cortical neurons (Liot *et al.* 2006; Wu *et al.* 2013). Research has shown that the protective/anti-apoptotic effect of tPA is independent of its proteolytic activity, while requiring the activation of either PI3K/Akt, AMPK- or mTOR-HIF1α-dependent signalling pathways (Correa *et al.* 2011; Wu *et al.* 2012). tPA is also involved in neurodevelopmental disorders; increased tPA levels had been found in the serum of male ASD patients (Şimşek *et al.* 2016; Bozkurt *et al.* 2021). tPA upregulation also occurs during neuroinflammation as it modulates neuroinflammatory processes in the brain, thereby affecting the integrity of the blood brain barrier (Mehra *et al.* 2016). Goeke at al. demonstrated that increased levels of tPA are found in the developing brain (Goeke *et al.* 2022), suggesting a role in axonal and dendritic arborization and synaptogenesis (Farhy-Tselnicker and Allen 2018). Furthermore, they also demonstrated that exposing astrocytes to excessive tPA as well as inhibition of tPA in astrocytes leads to inhibition of neurite outgrowth (Goeke *et al.* 2022). This effect is consistent with tPA role with the extracellular matrix based on the proteolytic activity of plasmin (Guizzetti *et al.* 2008), which supports neurons with adhesion necessary for neurite and axon growth (Goeke *et al.* 2022). Like uPA, tPA is known to be involved in diseases like AD (Tucker *et al.* 2002; Fabbro and Seeds 2009) or Epilepsy (Iyer *et al.* 2010). Furthermore, TSC lesions like cortical tubers or glia-neural tumours are known to display high levels of both uPA and tPA expression which potentially exacerbate the neuronal excitability by increasing NMDA receptor signalling (Iyer *et al.* 2010), while TSC giant cells are also known to display high levels of tPA (Cepeda *et al.* 2003; Cepeda *et al.* 2005).

Gene expression analysis of tPA in both TSC1 models demonstrated significant expression changes throughout the neuronal development. The TSC1 -/- demonstrated a continuous overexpression of tPA in comparison to control, with significance from the NPC stage onwards. The significant overexpression and the involvement of tPA neuronal plasticity, axonal regeneration, neuroinflammation and excitotoxicity (Chevilley *et al.* 2015; Hebert *et al.* 2016) would suggest negative consequences for the neurons and their development. Especially, as excessive tPA was found to promote damages in Purkinje cells (Lu and Tsirka 2002; Li *et al.* 2006; Li *et al.* 2013), by altering neurotrophic mechanisms in control their postnatal development (Li *et al.* 2006; Li *et al.* 2013). Therefore, it could be concluded that cellular stress and a potential increase of neuronal death might occur in the TSC1 -/- cells.

As these cells displayed increased death when passaged during the neuronal development, it might be considered that tPA overexpression might have been one of the causes. It must be acknowledged that most studies focusing on tPA overexpression utilised tPA injections, ergo exogenous tPA. Therefore, it is difficult to identify the exact consequences of a continuous overexpression of tPA during neuronal development due to a lack of literature. As tPA upregulation occurs during neuroinflammation (Mehra *et al.* 2016), it could be expected that the increased inflammation related cytokines might exacerbate the tPA expression, thus it would be interesting to see if inhibiting their expression might reduce the overexpression of tPA in the TSC1 -/- cells. A role of tPA in axonal and dendritic arborization and synaptogenesis (Farhy-Tselnicker and Allen 2018) had been suggested, therefore the overexpression might be partly causative for the altered neuronal physiology of TSC neurons including altered dendrite density and size (Tavazoie *et al.* 2005). The Cas13 TSC1 cells displayed a significant downregulation of tPA expression at the NSC and neuronal stage while the NPCs demonstrated a significant overexpression of tPA. As research demonstrated that lack of tPA or uPA leads to impaired/delayed neuronal repair/recovery after injury in mice (Siconolfi and Seeds 2001) as well as a higher susceptibility to neuronal death induced by both NMDAR and non-NMDAR agonists (Tsirka *et al.* 1995), it could be estimated that the Cas13 TSC1 neurons might display a similar phenotype as both uPA and tPA were downregulated. This would need to be tested in the future as no experiments concerning neuronal death or NMDAR agonists had been performed during this project. Additionally, based on the suspected role of tPA in axonal and dendritic arborization and synaptogenesis (Farhy-Tselnicker and Allen 2018) it would be of interest to analyse the dendrites in Cas13 TSC1 neurons in order to see if any changes occur after brief TSC1 loss, aligning with the measured dysregulated gene expression.

SERPINE1 functions as an inhibitor of tPA and uPA, supporting the maintenance of clot formation, thus playing a significant role in non-neoplastic disorders, such as atherosclerosis or stroke (Furuya *et al.* 2020). While its specific role in neuronal cells is still unclear, it has been shown that SERPINE1 supresses neuronal differentiation and is a key regulator for cell proliferation (Su *et al.* 2017). SERPINE1 expression is regulated by intrinsic factors such as cytokines and growth factors and extrinsic factors like cellular stress. SERPINE1 is partly regulated by TGFβ, an important controller of differentiation (Meng *et al.* 2016) via SMAD (Cengiz *et al.* 2019), and which itself is controlled by TSC1 (Thien *et al.* 2015).

TGFβ signalling is involved in development and tissue homeostasis and signalling dysregulation has been linked to tumorigenesis and metastasis (Meulmeester and Ten Dijke 2011). Furthermore, it is also associated with protective functions against excitotoxicity, hypoxia, and ischemia, as well as with interfering with cell death induced by compounds such as Aβ (Caraci *et al.* 2011). Thien *et al.* independently knocked down either TSC1 or TSC2 in HeLA cells by inducible shRNA. They discovered that TSC1 is not only required for TGFβ induced SMAD 2/3 regulation, but this function is also independent from mTORC1 and Rheb. Furthermore, TSC1 is the link between Insulin-PI3K-Akt Signalling and the TGFβ-SMAD2/3 pathway and it is required for the TGFβ induced growth arrest of cells. Thien at al. proposes that the TSC1 dependent TGFβ-SMAD activation might be a rescue mechanism to control over-proliferation of cells by regulating Akt activity as aberrantly activated Akt may in contrast induce apoptosis and cellular senescence, a state of permanent cell-cycle arrest while normal Akt activity stimulates cell proliferation and survival (Minamino *et al.* 2004; Miyauchi *et al.* 2004; Los *et al.* 2009). Genestine at al. demonstrated that SERPINE1 increases interneuron migration and neuronal differentiation/maturation, thought the molecular basis for this function is still yet unknown (Genestine *et al.* 2021). Wang *et al.* demonstrated increased levels of SERPINE1 in an *in vitro* model of intracerebral haemorrhage (ICH) and that silencing this expression increase attenuates neuronal apoptosis and neuroinflammation; indicated by reduced levels of TNFa, IL6 and IL1ß (Wang et al. 2021b). The SERPINE1 upregulation was found to be dependent on TGFß1 and knocking down SERPINE1 allowed to ease the effect of TGFß1 on neuronal damage (Wang et al. 2021b). Strengthening the role of SERPINE1 in neuroinflammation, research identified its involvement in the direction of neutrophils to injured tissue (Praetner *et al.* 2018) and that the SERPINE1 antagonist TM5484 reduces the expression of cytokines such as TNFa, IL6 and increases levels of IL10 (Pelisch *et al.* 2015).

Downregulated TGFß is found in AD (Das and Golde 2006); thereby probably reducing SERPINE1 expression and consequently increasing uPA levels. The reduction of the TGFß-SMAD pathway had been corroborated by further research in AD patients (Colangelo *et al.* 2002). TGFß1-dependent regulatory mechanisms had been found to be dysregulated in aged models, as aged microglia show a basal activated status, which is known to be linked to neuronal damage, cognitive impairment, and an increased susceptibility to neurodegenerative diseases, such as AD (Block *et al.* 2007).

Gene expression analysis of SERPINE1 levels in TSC1 knockout and knockdown neurons demonstrated significant dysregulation throughout the development. While the TSC1 -/- cells showed a trend of downregulation at Day 10 and Day 50, with upregulation at Day 20, no statistical significance was found in the tested cells. The Cas13 TSC1 cells on the other hand had a consistent significant downregulation of SERPINE1 expression through the neuronal development. Therefore, it might be concluded that loss of TSC1 leads to a reduction of SERPINE1 expression levels, a claim strengthened by RNASeq data generously provided by Prof. Tee. That expression level decline can be explained by the TSC1 dependent (Thien *et al.* 2015) TGF-β-SMAD2/3 pathway which activates SERPINE1 expression (Cengiz *et al.* 2019). As SERPINE1 is a key regulator for cell proliferation (Su *et al.* 2017) and increases interneuron migration and neuronal differentiation/maturation (Genestine *et al.* 2021), disrupted regulation of cell proliferation and neuronal maturation would be a consequence of SERPINE1 downregulation. Since TSC cells commonly show increased cell proliferation, a phenotype directly caused by increased mTORC1 activity, and abnormal neuronal differentiation and maturation (Zucco *et al.* 2018; Martin *et al.* 2020), a phenotype which was further discussed in chapter 3, the decreased SERPINE1 levels of both TSC1 cell models follow the expectations. As neuronal migration was not tested in this project, no comments on it can be made for the TSC1 neurons. Increased levels of pro-inflammatory cytokines had been measured in both cell lines, thus suggesting that the decreased levels of SERPINE1 did not completely attenuate the increased inflammation related cytokine expression, though rescuing the SERPINE1 levels might further exacerbate their expression. As the mRNA level of SERPINE1 was quite low throughout the development, it could be debated how severe the impact of its expression reduction is on the neuronal development, especially as the previously discussed developmental and autophagy markers (see Chapter 3 and 4) demonstrated much higher mRNA expression and significant dysregulation as well.

SERPING1, a protease inhibitor, had been identified as a potential missing factor that regulates SERPINE1/2 overexpression (Furuya *et al.* 2020). It is seen as a A1 astrocyte marker (Qian *et al.* 2019) and SERPING1 overexpression was found in the TSC database analysis. SERPING1 is known to inhibit the initiation of the complement cascade and knockdown or knockout of SERPING1 affects neuronal stem cell proliferation and impaired neuronal migration in mice, thus impairing cortical layering (Gorelik *et al.* 2017). Utilising a Parkinson mouse model, SERPING1 overexpression was linked to increased death of GABAergic neurons (Seo and Yeo 2020).

Gene expression analysis of both TSC1 models throughout neuronal development showcased a significant dysregulation of SERPING1 expression. The TSC1 -/- cells displayed a significant reduction at the NSC stage and non-significant increase in expression from the NPC stage onwards. The Cas13 TSC1 cells showed a non-significant reduction at the NSC stage and a non-significant increase in expression at the NPC stage. Interestingly, both significant down- and up-regulation had been measured at the neuronal stage; the 24 h treatment caused a significant increase of SERPING1 levels, while the 48-h treatment consistently led to a significant downregulation though it is unknown why the treatment duration caused such opposite effects.

While Dominguez at al. demonstrated that cells can inhibit transgene expression after 24 h (Dominguez *et al.* 2022) , their work was performed in human iPSCs and not in differentiating cells, therefore it is uncertain if that ability carries into iPSC-derived differentiated cells. As increased SERPING1 levels had been identified in the utilised TSC1 models, it could be predicted that the dysregulation of SERPING1 expression might further dysregulate the balance between glutamatergic and GABAergic neurons in the culture. As discussed in the previous chapters, a disrupted balance between GABAergic and glutamatergic neurons had been found in TSC (Alsaqati *et al.* 2020), though the consensus was on an increased number of GABAergic neurons. Increased neuronal death due to ox. stress has been established in TSC models (Di Nardo *et al.* 2009); as several of the previously discussed genes are either known to cause ox. stress when dysregulated (such as ULK1) or being dysregulated because of ox. stress (such as ßIII-Tub) (both discussed in Chapter 3 and 5), it could be concluded that the increased SERPING1 levels are supporting cell stress or maybe even neuronal death (Seo and Yeo 2020).

6. General Discussion

TSC is a rare disease (Franz *et al.* 2010) and as TSC2 mutations are the most common form of the disease, the majority of studies focus on it with much less research utilising TSC1 models. For example, the patients of the TSC database analysed in Chapter 5 carried mostly the TSC2 mutation (88% of the patients).

This project aimed to design human iPSC models for TSC1 by utilising CRISPR Cas9 and Cas13a systems. Using iPS cells as a model for TSC allows the generation and investigation of human neurons and astrocytes, cell types which are otherwise non-accessible. While animal models allow an insight into the disease structure but they have limited translatability due to significant genetic and developmental differences to humans (Zhu and Huangfu 2013). Doxycycline inducible Cas9 and Cas13 cell lines were used as it was demonstrated that doxycycline inducible systems lead to a reduced rate of off-targets (Kabadi *et al.* 2014). Despite CRISPR generated iPSC models allowing a more suitable model for investigation than animal models, they do not carry patient mutations and might therefore show slightly different phenotypes. In addition, TSC homozygous mutation do not appear in patients as it is lethal in embryos, though second-hit homozygous cells have been found in TSC tumours. Therefore, differences between gene expression data analysed in this project and TSC patients are expected. The Cas13 TSC1 cells will not resemble TSC patients, as the TSC1 loss is inducible and time limited. Furthermore, conditional knockdown cell lines are expected to display a different phenotype than knockout cell lines due to lack of genetic compensation/genetic robustness, therefore potentially leading to a more severe phenotypes due to the lack of compensation in comparison to knockouts (El-Brolosy and Stainier 2017). The Cas13 cell model allows experiments on mature cell types with inductions of mutations at later developmental stages. It must be remarked that a more prolonged induction of the mutation might display a more patient like phenotype, but this would require future experiments. Therefore, it could be concluded that the Cas13a system is a very suitable model to investigate which pathways are affected by certain mutations (TSC1 in this case) and less suitable to analyse if the pathways are down- or up-regulated.

The gene expression analysis in this project demonstrated contradicting dysregulation of some genes in comparison to studies with patients or TSC knockout model (down- instead of up-regulation for example, like uPA (see Chapter 5)). The second aim of the project was to investigate the effect acute as well as continuous TSC1 loss have on neuronal differentiation. Literature suggests an increased number of astrocytes in TSC neuronal differentiation (Blair *et al.* 2018) as well as an abnormal/delayed neuronal development (Zucco *et al.* 2018; Martin *et al.* 2020). This aim was fulfilled by utilising RT-PCR analysis to investigate various developmental, astrocytic markers as well as genes related to inflammation or autophagy. The gene expression analysis demonstrated a consistent increase of astrocytic markers (CD44, Vimentin and S100B1) in both TSC1 models during most of the neuronal development, thus suggesting an increased number of astrocytes in the culture, which would align with previous research (Blair *et al.* 2018). mTOR is a major player in cell differentiation and as any TSC mutation results in an overactivation of mTOR (Franz *et al.* 2010), dysregulation of normal cell differentiation is unsurprising. The tested NPC markers Pax6 and Nestin displayed significant dysregulation as well, especially Pax6. As Pax6 is a highly conserved transcription factor, crucial for normal CNS development (Hill *et al.* 1991; Glaser *et al.* 1994; St-Onge *et al.* 1997) and whose mutations or dysregulations are known to cause significant deficiencies in neuronal development including abnormalities in NSC and NPC proliferation, as well as defects in neurogenesis (Sansom *et al.* 2009), the observed significant dysregulation would suggest abnormal neuronal differentiation of the TSC1 models, thereby aligning with the literature (Zucco *et al.* 2018; Martin *et al.* 2020).

The expression of three neuronal markers was analysed in this project: OTX2, a marker mostly expressed in the midbrain and an essential transcription factor for brain and sensory organ development (Acampora *et al.* 1995; Morsli *et al.* 1999; Martinez 2003); βIII-Tub, a neuronal tubulin network marker (Verdier-Pinard *et al.* 2009; Guo *et al.* 2011) and FOXG1, a DNA-binding transcription factor, whose role is the repression of target genes during brain development and whose mutations are known to cause microcephaly, impaired motor development, and brain malformations (Guen *et al.* 2011). Both TSC1 models displayed significant dysregulation of these neuronal markers, thus suggesting an abnormal development as these markers influence cell proliferation and differentiation induction as well as neuronal identity (GABAergic or glutamatergic).

Furthermore, several genes involved in autophagy were analysed during the neuronal development of both TSC1 models. GSK3a, a key regulator in multiple neuronal processes such as neurogenesis, neuronal polarization and axon growth and guidance (Hur and Zhou 2010) and a gene whose activity changes are associated with neurodegenerative or psychiatric diseases, such as AD, and ASD (Beaulieu 2007; Beaulieu *et al.* 2009).
ULK1, a major player in autophagy controlled via mTOR or AMPK pathway (Di Nardo *et al.* 2014), where inhibition is known to promote oxidative stress (Ianniciello *et al.* 2021) and ULK1/2 deficiency results in abnormal axon guidance as well as impaired organization of the somatosensory cortex (Demeter *et al.* 2020). TFEB, a transcription factor whose activation leads to stimulation of lysosomal biogenesis and autophagy (Settembre *et al.* 2011; Martini-Stoica *et al.* 2018) and knockdown is known to promote premature neurogenesis (Yuizumi *et al.* 2021) while TFEB overexpression was found to drive increased cell growth (Torra *et al.* 2018). As TSC is known for its impaired autophagy, the results displaying their dysregulation throughout the differentiation were expected. Their disturbance likely causes cellular stress and impair cell survival and differentiation.

In addition, inflammation related cytokines were analysed via RT-PCRs in the TSC1 models: IL6, a pro-inflammatory cytokine with neurotrophic influence, based on its substantial role in homeostasis and development of the nervous system by inducing neuronal survival, proliferation, differentiation as well as influencing synaptic release of neurotransmitters and neural activity (Spooren *et al.* 2011). IL10, an anti-inflammatory cytokine involved in neuronal survival and growth (Zhou *et al.* 2009). It has been demonstrated that IL10 regulates the expression of neural progenitor markers like Nestin or SOX2, cell cycle activity of progenitors, and the production of new neuroblasts (Perez-Asensio *et al.* 2013), thus influencing adult neurogenesis via STAT3 (Pereira *et al.* 2015) as shown in rat neurons. TNFa, a pro-inflammatory cytokine involved in regulation of synaptic transmission, neuronal plasticity as well as induction of inflammation, excitotoxicity, and oxidative tissue damage under disease conditions (Papazian *et al.* 2021). Since a sensitive balance of these cytokines is required for normal neuronal development (Meyer *et al.* 2008), the observed dysregulation would negatively affect the latter. Overall, dysregulation of the analysed autophagy markers and cytokines have been identified to negatively affect neuronal development. As the developmental markers (mentioned prior) showed significant changes, it can be concluded that the neuronal development was altered by both the TSC1 knockout as well as the acute TSC1 loss in the Cas13 TSC1 model.

Abnormal/ impaired neuronal development is a phenotype of TSC models (Zucco *et al.* 2018; Martin *et al.* 2020), therefore the observed impairment of the neuronal differentiation in the cell models is expected and thus demonstrating that both cell lines are suitable models for TSC. This project also aimed to analyse the effect of TSC1 loss on the plasminogen/urokinase pathway. The urokinase pathway analysed in Chapter 5 included several genes which are all known to influence neuronal development and/or function as which displayed significant expression changes in the TSC1 models in comparison to the healthy control. uPA is involved in the activation of cell signalling pathways regulating differentiation, cellular adhesion, migration, and proliferation through non-plasminogenic mechanisms (Peteri *et al.* 2021) and might control axonal growth, thus influencing neuronal plasticity (Sumi *et al.* 1992). Its receptor uPAR was found to influence axon growth and polarization during neurogenesis by activating integrins (Blasi and Carmeliet 2002; Franco *et al.* 2006; Blasi and Sidenius 2010). tPA also plays an important role in neuronal plasticity, axonal regeneration, neuroinflammation and excitotoxicity (Chevilley *et al.* 2015; Hebert *et al.* 2016) and the uPA/tPA inhibitor SERPINE1 is known to supresses neuronal differentiation and regulate cell proliferation (Su *et al.* 2017) as well as affecting neuronal maturation (Genestine *et al.* 2021). SERPINE1 expression indirectly regulated by TSC1 as one of its regulators TGFβ, an important controller of differentiation (Meng *et al.* 2016), requires TSC1 activation (see Figure 6-1) (Thien *et al.* 2015). SERPING1, which was found to influence SERPINE1 activity (Furuya *et al.* 2020), though the interaction and effect are still unclear, is known to inhibit the initiation of the complement cascade. Knockdown or knockout of SERPING1 affects neuronal stem cell proliferation and impaired neuronal migration in mice, thus impairing cortical layering (Gorelik *et al.* 2017) while SERPING1 overexpression was linked to increased death of GABAergic neurons (Seo and Yeo 2020). In summary, each member of the pathway is known to influence neuronal development and as their expression was significantly dysregulated in both TSC1 models, it can be concluded that these genes were causative to the observed abnormal neuronal differentiation. Further literature research linked one of the developmental markers directly to the plasminogen pathway. FOXG1, as a transcriptional repressor controls TGFß activity (Guen *et al.* 2011), allowing the mediation of neuronal and astrocytic differentiation by controlling cell fate due to FOXG1 regulation (Adesina *et al.* 2007) and thus influencing SERPINE1 and therefore uPA activity (see Figure 6-1).

Overall, this project demonstrated the sensitivity of cells towards any expression changes of TSC1, as both acute and prolonged loss had severe consequences on cell development and function.

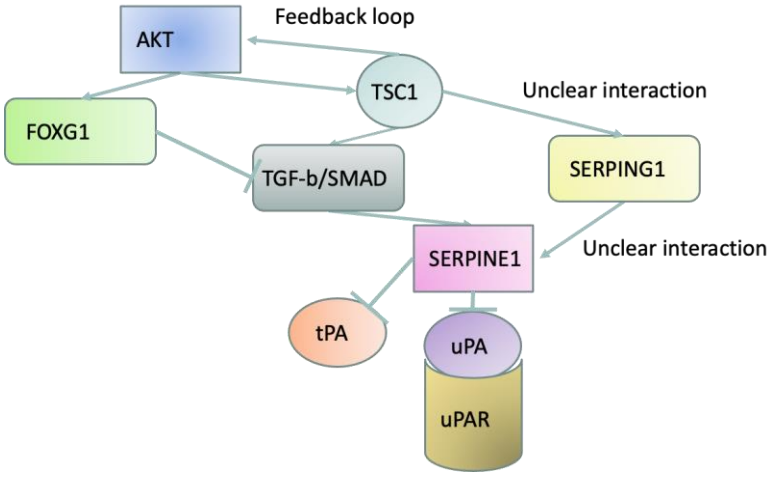

Figure 6-1: Scheme of the FOXG1-Urokinase Pathway-Interaction with TSC1 being one of the essential players.

Furthermore, as described in the discussion of Chapter 3 to Chapter 5, several of the analysed genes display a similar dysregulation in AD than in TSC. TSC had been discussed as a potential treatment target for AD (Ferrando-Miguel *et al.* 2005) and a correlation between mTOR pathway disruption in lymphocytes had been found to correlate with cognitive decline in AD (Paccalin *et al.* 2006; Yates *et al.* 2013). Additionally, up-regulation of various components of the mTOR pathway, downstream of mTORC1, has been demonstrated in AD (An *et al.* 2003; Götz *et al.* 2004). The database analysis from Chapter 5 also displayed the significant upregulation of several markers related to AD in the TSC patient samples. TSC is a neurodevelopmental disorder, though there has been the proposal to also include it in the list of neurodegenerative diseases due to its dysregulated autophagy (Di Nardo *et al.* 2009), while AD is a common neurodegenerative disease.

While neither disease include the other as a known comorbidity, the similar dysregulation of pathways would propose an involvement of TSC-mTOR in AD, a claim strengthened by the mTOR overactivity in AD (Caccamo *et al.* 2011). Both are commonly known for their neuroinflammation and their dysregulated autophagy and while AD occurs in the later stages of life, unlike TSC, it could be predicted that mutations (or epigenetics) targeting the TSC-mTOR pathway later in life could explain the many similarities between both diseases.

Lifestyle, next to genetics, was shown to heavily influence the risk of AD (Pope *et al.* 2003; Ko and Chye 2020), therefore the assumption that pathway dysregulation or mutations might be an explanation for the similarities in pathway dysregulation between both diseases should be further investigated as it would open new targets for patient treatments.

An additional similarity between AD and TSC is the calcium homeostasis and signalling dysregulation in neurons and astrocytes. As discussed in Chapter 4, TSC models are known to display disruptions in the calcium homeostasis with neurons showing an increase of spontaneous calcium transients (Nadadhur *et al.* 2019), with iPSC derived TSC2 -/- neurons demonstrating elevated neuronal activity with highly synchronized calcium spikes, enhanced calcium influx via L-type calcium channels resulting in abnormal neurite extension (Hisatsune *et al.* 2021). Similar calcium disturbances are found in AD, where disturbed ER calcium homeostasis significantly contributes to dysfunction and degeneration in AD. AD models display impaired calcium uptake in mitochondria (Nikoletopoulou and Tavernarakis 2012), especially after oxidative stress (Kumar *et al.* 1994). Increased expression of the calcium channel Cav1.3 LTCC was found in TSC, a suggested target downstream of the mTOR pathway (Hisatsune *et al.* 2021). Increased expression of LTCC like Cav1.3 were found in AD as well (Anekonda and Quinn 2011). Additionally, TSC is known to display glutamate excitotoxicity with knock-out mouse model demonstrating decreased expression and function of the glutamate transporters GLT-1 and GLAST, leading to an increase in extracellular glutamate levels and excitotoxic neuronal death (Wong *et al.* 2003; Zeng *et al.* 2007). Miller and al. demonstrated reduced glutamate uptake in TSC patient -derived astrocytes in comparison to control (Miller *et al.* 2021), which would align with the reported decrease in glutamate transporters in TSC. Glutamate expression leads to calcium rise in astrocytes (Bazargani and Attwell 2016); excessive glutamate receptor activation leads to excessive calcium influx, thereby impairing synaptic activation, neuronal plasticity and synthesis of NO which will cause cell death which was found in AD (Sattler and Tymianski 2000; Marambaud *et al.* 2009).

Therefore, one aim on this project was to investigate the effect of acute TSC1 loss in astrocytes in terms of cell function, especially after glutamate treatment. Increased calcium base levels as well as increased calcium release after a glutamate induced calcium wave were observed in the TSC1 astrocytes.

Furthermore, the calcium recordings suggest shrinking of the cell colonies with induced TSC1 loss, with an increased severity in the homozygous TSC1 cells. Staining for apoptosis after glutamate treatment of the astrocytes (via ANXA5 staining) suggest an increased number of ANXA5 positive cells in the TSC1 astrocytes in comparison to control, thus suggesting glutamate toxicity. These results are aligning with the available literature on TSC and AD. As excitotoxicity in AD had been proposed due to excessive NMDAR activity (Hynd *et al.* 2004) and GLT-1 and GLAST dysregulation was also found in AD (Pajarillo *et al.* 2019), this further strengthens the claim of similarities between TSC and AD, potentially based on a common dysregulated TSC-mTOR pathway.

The main limitation concerning this project is the sample size of the differentiations. The N-number of the samples was N=3 for each condition, time point and differentiations. This sample number allows the identification of any potential gene dysregulation, but the common variability between wells during neuronal differentiation might mask trends of gene expression. Differentiations are long and complex protocols utilising standardized protocols, but it is near unavoidable that slight changes of conditions will induce variability between the cells (Volpato *et al.* 2018). Repeating the experiments with a higher sample number would solidify the results observed in this project but the repeat of these differentiations would invite a new variability between the cells as long-term care of iPSC and the number of passages required during their maintenance will allow the occurrence of mutation gains which might alter the gene expression and differentiation (Volpato and Webber 2020). Unfortunately, time constraints prevented the repeats of the differentiation to acquire a bigger sample size. An additional limitation is the method of qPCRs during this project. qPCRs allow a sensitive analysis of gene expression of samples. The sensitivity of the system is also one of its disadvantages. Any quality issues of the samples such as contaminated RNA or cDNA will impair the data analysis. Additionally, qPCRs require sometimes extensive primer optimization to ensure a single specific amplicon and no primer dimers, especially when SYBR Green is used (Smith and Osborn 2009). The sensitivity of the system will also underline any differences in cell variability during differentiations (Volpato and Webber 2020). As qPCRs solely analyse the mRNA levels of a gene, no complete conclusion can be made about the protein levels. mRNA and protein levels do not always correlate 1:1 as there are several regulators influencing the translation of any mRNA to proteins such as miRNAs (Selbach *et al.* 2008). Additionally, some gene expression might vary throughout the day, also called cyclic gene expression.

While this expression pattern does not occur in all genes, it does affect genes involved in the metabolism (Schibler 2022) and there is evidence that autophagy follows a diurnal pattern (Ma et al. 2012a). While this was kept in mind during sample collection, thus leading to a similar collection time throughout the differentiations, repeats of the experiment combined with a different collection time could lead to different results. Furthermore, the high passage number for both utilised cell lines could lead to acquired genetic mutations (Volpato *et al.* 2018) thus potentially impact the gene expressions and development of the cells. While it was aimed to minimise any genetic variability by utilising cells with either a similar passage number (in case of the CN vs TSC1 -/- cells) or utilising the same cells (Cas13 TSC1 cells with/without doxycycline due to unknown location of plasmid insert), the potential of it affecting the generated data cannot be ignored.

Validation via Western Blot (performed by Darius McPhail) shows a clear loss of TSC1 protein in the TSC1 -/- cells in comparison to IBJ4 WT, underlines the successful CRSPR induced deletion. While no Western Blot was performed on the Cas13 TSC1 cells, the TSC1 gene expression was analysed on D20 of neuronal differentiation on cells which had doxycycline induced loss of TSC1 on D8. TSC1 expression had no significant alteration to the control, thus strengthening the claim that the Cas13 cell model is a well-functioning system for inducible knockdown. Still, further validation of the Cas13 TSC1 cells via Western Blot would be a suitable endeavour for the future. Another limitation of the project in the lack of quantification of the calcium and ANXA5 staining, thus only suggested observations can be made. For clear results, the experiment should be repeated in a manner that would allow appropriate quantification e.g., lower cell density in order to measure the cell death/shrinkage of the astrocytes.

This project opens several potential avenues for future research. First, dysregulation of cellular functions like autophagy or inflammation were observed in the project. As literature suggests a role of these function in neuronal development, targeted treatment in order to restore function, and investigating if it would ease TSC pathology in neurons, would be a suitable next step in TSC developmental research. Second, the AKT-FOXG1-TGFβ-SERPINE1-uPA-pathway would be a promising future target for further investigation. This project observed significant dysregulation in both TSC1 models. Investigating if restoring FOXG1 expression might rescue the expression of the downstream genes and potentially the TSC pathologies like abnormal neuronal development or epilepsy as uPA and uPAR are known to be involved in epilepsy (Liu *et al.* 2010).

As FOXG1 is also a proposed target for AD (Wang *et al.* 2022) and uPA plays a role in AD by its indirect involvement of Aβ clearance via plasminogen (Walker *et al.* 2002), investigating this pathway would also be beneficial for AD research. Third, this project observed glutamate toxicity in Cas13 astrocytes after a 48-h induced 50% or 80% TSC1 loss. A potential explanation of the observed phenotype is a reduction of glutamate transporters, as known in TSC (Wong *et al.* 2003; Zeng *et al.* 2007). Therefore, investigating the expression of these transporters or analysing glutamate uptake in TSC1 astrocytes (from both Cas13 and knockout cell models) would be a suitable future endeavour. Additionally, co-culturing TSC astrocytes with WT neurons (and vice versa) in order to investigate glutamate excitotoxicity would be an interesting approach, especially when combined with drugs targeting the TSC-mTOR pathway in order to restore normal function as it would give a helpful insight for both TSC and AD. Fourth, as several of the investigated genes impact neuronal development, it would be an interesting endeavour to utilize iPSC-derived organoids with TSC mutations. Recently, there have been some developments in TSC research in regards of organoids with Blair *et al.* discussing their potential for the investigation of the neuronal development in TSC for new insights (Blair and Bateup 2020), while Eichmüller *et al.* utilized TSC patient-derived iPSCs in order to generate organoids mimicking both tumours and tubers of the brain by using media with different nutrient concentrations (Eichmüller et al. 2022). They observed morphological phenotypes mimicking human SEN/SEGAs in the nutrient rich media while the organoids in the nutrient poor media displayed enlarged cells and thickened processes, thus resembling tubers. This observation sets a new light on the potential of organoids as a neurodevelopmental model for TSC. Utilising drugs targeting the previously mentioned genes influencing neuronal development such as FOXG1, OTX2 etc. in TSC organoid models would allow a new insight on the role of these genes in the altered development of TSC neurons and would potentially allow the development of new drug treatments. The use of organoid models would be especially significant, if by investigating SEN/SEGA and tuber like organoids non-surgical treatments could be developed to either prevent or reduce these growths as they have severe negative impacts on patients' health. At last, further investigations of Cas13 cell models would be useful for both this area of research and other fields. As of yet, very few papers of Cas13 iPSC models are published apart from the original papers focusing on the suitability of system as an inducible knockdown model itself.

Therefore, this project is novel by its utilization of the Cas13 system in order to induce acute TSC1, especially by comparing two different lengths of induction. As such, further investigation of the effect of various induction time lengths would be extremely useful for future use of Cas13 models as well as learning more about TSC1 loss. As the activation of rescue mechanisms might explain the variety between different induction lengths, identifying these proposed mechanisms would be a major step for both TSC research and the Cas13 models. Recently, a paper utilizing the Cas13 system in both patient iPSC-derived neurons and mice models for Huntington Disease (HD) has been published (Morelli et al. 2023). The group utilised CRISPR Cas13 to reduce the expression of mutant huntingtin (HTT) RNA in both models, for the iPSC cell halfway through the neuronal development, while the mice were injected at 2 months of age and observed for the following 8 months. Morelli *et al.* demonstrated that the administration of their designed HTT-targeting Cas13 system in HD mice resulted in an allele-selective suppression of mutant HTT mRNA and protein while maintaining normal mRNA and protein levels with limited off-target effects on the mouse transcriptome. The effect was shown to be long-term with 8 months postinjection into the mice striatum. This strengthens the claim that the Cas13 system is a suitable model for neuronal research and also underlines the long-term effect observed in this project.

In conclusion, this project gave insight on the effect TSC1 loss has on neuronal development, both acute and absolute, continuous TSC1 loss. The cell models displayed a clear pattern of increased astrocytic markers, dysregulation of both NPC and neuronal markers as well as impaired autophagy, thus suggesting an impaired neuronal development and cell biology. The Cas13 TSC1 model identified the early developmental stage of NSCs as a sensitive time point for TSC1 loss as significant dysregulation of genes could still be found in neurons weeks after the induced TSC1 loss. Additionally, the calcium imaging of the Cas13 TSC1 cells demonstrated that TSC1 loss at a mature developmental time point, still has a significant impact on their function/calcium signalling and sensitivity to glutamate toxicity. Thus, demonstrating that TSC1 loss at mature cell stages can have severe consequences. Thanks to the database analysis, a targeted investigation of inflammation markers as well as the urokinase pathway, a pathway dysregulated in both AD and TSC, was performed. Both iPS models displayed a significant dysregulation of these markers, showing that any dysregulation of TSC1 will impact these targets, whose dysregulation are known to negatively impact neuronal development, thus making them interesting future research targets for both diseases.

7. References

Abbott, N. J., Rönnbäck, L. and Hansson, E. 2006. Astrocyte–endothelial interactions at the blood–brain barrier. *Nature Reviews Neuroscience* 7(1), pp. 41-53.

Abd-Elrahman, K. S., Hamilton, A., Vasefi, M. and Ferguson, S. S. 2018. Autophagy is increased following either pharmacological or genetic silencing of mGluR5 signaling in Alzheimer's disease mouse models. *Molecular Brain* 11(1), pp. 1-8.

Abudayyeh, O. O. et al. 2017. RNA targeting with CRISPR–Cas13. *Nature* 550(7675), p. 280.

Abudayyeh, O. O. et al. 2016. C2c2 is a single-component programmable RNA-guided RNA-targeting CRISPR effector. *Science* 353(6299), p. aaf5573.

Acampora, D., Mazan, S., Lallemand, Y., Avantaggiato, V., Maury, M., Simeone, A. and Brûlet, P. 1995. Forebrain and midbrain regions are deleted in Otx2−/− mutants due to a defective anterior neuroectoderm specification during gastrulation. *Development* 121(10), pp. 3279-3290.

Addgene. *pgRNA Plasmid*. Addgene: Available at: https://www.addgene.org/73501/ [Accessed.

Akiyama, H., Tooyama, I., Kawamata, T., Ikeda, K. and McGeer, P. L. 1993. Morphological diversities of CD44 positive astrocytes in the cerebral cortex of normal subjects and patients with Alzheimer's disease. *Brain research* 632(1-2), pp. 249-259.

Ali, C. et al. 2000. Ischemia-induced interleukin-6 as a potential endogenous neuroprotective cytokine against NMDA receptor-mediated excitoxicity in the brain. *Journal of Cerebral Blood Flow & Metabolism* 20(6), pp. 956-966.

Alsaqati, M., Heine, V. M. and Harwood, A. J. 2020. Pharmacological intervention to restore connectivity deficits of neuronal networks derived from ASD patient iPSC with a TSC2 mutation. *Molecular autism* 11(1), pp. 1-13.

An, W.-L. et al. 2003. Up-regulation of phosphorylated/activated p70 S6 kinase and its relationship to neurofibrillary pathology in Alzheimer's disease. *The American journal of pathology* 163(2), pp. 591-607.

Anderl, S., Freeland, M., Kwiatkowski, D. J. and Goto, J. 2011. Therapeutic value of prenatal rapamycin treatment in a mouse brain model of tuberous sclerosis complex. *Human molecular genetics* 20(23), pp. 4597-4604.

Anderson, C. M. and Swanson, R. A. 2000. Astrocyte glutamate transport: review of properties, regulation, and physiological functions. *Glia* 32(1), pp. 1-14.

Anekonda, T. S. and Quinn, J. F. 2011. Calcium channel blocking as a therapeutic strategy for Alzheimer's disease: the case for isradipine. *Biochimica et Biophysica Acta (BBA)-Molecular Basis of Disease* 1812(12), pp. 1584-1590.

Arai, Y., Takashima, S. and Becker, L. E. 2000. CD44 expression in tuberous sclerosis. *Pathobiology* 68(2), pp. 87-92.

Arena, A. et al. 2019. Oxidative stress and inflammation in a spectrum of epileptogenic cortical malformations: molecular insights into their interdependence. *Brain Pathology* 29(3), pp. 351-365.

Arnett, H. A., Mason, J., Marino, M., Suzuki, K., Matsushima, G. K. and Ting, J. P.-Y. 2001. TNFα promotes proliferation of oligodendrocyte progenitors and remyelination. *Nature neuroscience* 4(11), pp. 1116-1122.

Aronica, E., Gorter, J. A., Ijlst-Keizers, H., Rozemuller, A. J., Yankaya, B., Leenstra, S. and Troost, D. 2003. Expression and functional role of mGluR3 and mGluR5 in human astrocytes and glioma cells: opposite regulation of glutamate transporter proteins. *European Journal of Neuroscience* 17(10), pp. 2106-2118.

Asada, N., Sanada, K. and Fukada, Y. 2007. LKB1 regulates neuronal migration and neuronal differentiation in the developing neocortex through centrosomal positioning. *Journal of Neuroscience* 27(43), pp. 11769-11775.

Avrahami, L., Farfara, D., Shaham-Kol, M., Vassar, R., Frenkel, D. and Eldar-Finkelman, H. 2013. Inhibition of Glycogen Synthase Kinase-3 Ameliorates β-Amyloid Pathology and Restores Lysosomal Acidification and Mammalian Target of Rapamycin Activity in the Alzheimer Disease Mouse Model IN VIVO AND IN VITRO STUDIES. *Journal of Biological Chemistry* 288(2), pp. 1295-1306.

B Jahrling, J. and Laberge, R.-M. 2015. Age-related neurodegeneration prevention through mTOR inhibition: potential mechanisms and remaining questions. *Current topics in medicinal chemistry* 15(21), pp. 2139-2151.

B. Jahrling, J. and Laberge, R.-M. 2015. Age-related neurodegeneration prevention through mTOR inhibition: potential mechanisms and remaining questions. *Current topics in medicinal chemistry* 15(21), pp. 2139-2151.

Bae, T., Hur, J. W., Kim, D. and Hur, J. K. 2019. Recent trends in CRISPR-Cas system: genome, epigenome, and transcriptome editing and CRISPR delivery systems. *Genes & genomics*, pp. 1-7.

Bahi-Buisson, N. et al. 2010. Revisiting the phenotype associated with FOXG1 mutations: two novel cases of congenital Rett variant. *Neurogenetics* 11(2), pp. 241-249.

Ballatore, C., Lee, V. M.-Y. and Trojanowski, J. Q. 2007. Tau-mediated neurodegeneration in Alzheimer's disease and related disorders. *Nature Reviews Neuroscience* 8(9), p. 663.

Barrangou, R. et al. 2007. CRISPR provides acquired resistance against viruses in prokaryotes. *Science* 315(5819), pp. 1709-1712.

Basak, J. M., Verghese, P. B., Yoon, H., Kim, J. and Holtzman, D. M. 2012. Low-density lipoprotein receptor represents an apolipoprotein E-independent pathway of Aβ uptake and degradation by astrocytes. *Journal of Biological Chemistry* 287(17), pp. 13959-13971.

Bassil, R., Shields, K., Granger, K., Zein, I., Ng, S. and Chih, B. 2021. Improved modeling of human AD with an automated culturing platform for iPSC neurons, astrocytes and microglia. *Nature communications* 12(1), pp. 1-21.

Bateup, H. S., Takasaki, K. T., Saulnier, J. L., Denefrio, C. L. and Sabatini, B. L. 2011. Loss of Tsc1 in vivo impairs hippocampal mGluR-LTD and increases excitatory synaptic function. *Journal of Neuroscience* 31(24), pp. 8862-8869.

Bazargani, N. and Attwell, D. 2016. Astrocyte calcium signaling: the third wave. *Nature neuroscience* 19(2), pp. 182-189.

Beaulieu, J.-M. 2007. Not only lithium: regulation of glycogen synthase kinase-3 by antipsychotics and serotonergic drugs. *International Journal of Neuropsychopharmacology* 10(1), pp. 3-6.

Beaulieu, J.-M., Gainetdinov, R. R. and Caron, M. G. 2009. Akt/GSK3 signaling in the action of psychotropic drugs. *Annual review of pharmacology and toxicology* 49, pp. 327-347.

Bellacosa, A., Testa, J. R., Moore, R. and Larue, L. 2004. A portrait of AKT kinases: human cancer and animal models depict a family with strong individualities. *Cancer biology & therapy* 3(3), pp. 268-275.

Bellucci, A., Westwood, A. J., Ingram, E., Casamenti, F., Goedert, M. and Spillantini, M. G. 2004. Induction of inflammatory mediators and microglial activation in mice transgenic for mutant human P301S tau protein. *The American journal of pathology* 165(5), pp. 1643-1652.

Bernard-Marty, C. et al. 2002. Microtubule-associated parameters as predictive markers of docetaxel activity in advanced breast cancer patients: results of a pilot study. *Clinical breast cancer* 3(5), pp. 341-345.

Beumer, K. J. et al. 2013. Comparing zinc finger nucleases and transcription activator-like effector nucleases for gene targeting in Drosophila. *G3: Genes, Genomes, Genetics* 3(10), pp. 1717-1725.

Bibikova, M., Golic, M., Golic, K. G. and Carroll, D. 2002. Targeted chromosomal cleavage and mutagenesis in Drosophila using zinc-finger nucleases. *Genetics* 161(3), pp. 1169-1175.

Bissonnette, C. J., Klegeris, A., McGeer, P. L. and McGeer, E. G. 2004. Interleukin 1α and interleukin 6 protect human neuronal SH-SY5Y cells from oxidative damage. *Neuroscience letters* 361(1-3), pp. 40-43.

Blair, J. D. and Bateup, H. S. 2020. New frontiers in modeling tuberous sclerosis with human stem cell-derived neurons and brain organoids. *Developmental Dynamics* 249(1), pp. 46-55.

Blair, J. D., Hockemeyer, D. and Bateup, H. S. 2018. Genetically engineered human cortical spheroid models of tuberous sclerosis. *Nature medicine* 24(10), pp. 1568-1578.

Blasi, F. and Carmeliet, P. 2002. uPAR: a versatile signalling orchestrator. *Nature reviews Molecular cell biology* 3(12), pp. 932-943.

Blasi, F. and Sidenius, N. 2010. The urokinase receptor: focused cell surface proteolysis, cell adhesion and signaling. *FEBS letters* 584(9), pp. 1923-1930.

Blasko, I., Schmitt, T., Steiner, E., Trieb, K. and Grubeck-Loebenstein, B. 1997. Tumor necrosis factor α augments amyloid β protein (25–35) induced apoptosis in human cells. *Neuroscience letters* 238(1-2), pp. 17-20.

Block, M. L., Zecca, L. and Hong, J.-S. 2007. Microglia-mediated neurotoxicity: uncovering the molecular mechanisms. *Nature Reviews Neuroscience* 8(1), pp. 57-69.

Boer, K. et al. 2010. Gene expression analysis of tuberous sclerosis complex cortical tubers reveals increased expression of adhesion and inflammatory factors. *Brain Pathology* 20(4), pp. 704-719.

Boer, K. et al. 2008a. Inflammatory processes in cortical tubers and subependymal giant cell tumors of tuberous sclerosis complex. *Epilepsy research* 78(1), pp. 7-21.

Boer, K. et al. 2008b. Clinicopathological and immunohistochemical findings in an autopsy case of tuberous sclerosis complex. *Neuropathology* 28(6), pp. 577-590.

Boer, K. et al. 2008c. Cellular localization of metabotropic glutamate receptors in cortical tubers and subependymal giant cell tumors of tuberous sclerosis complex. *Neuroscience* 156(1), pp. 203-215.

Bongaarts, A. et al. 2017. Subependymal giant cell astrocytomas in Tuberous Sclerosis Complex have consistent TSC1/TSC2 biallelic inactivation, and no BRAF mutations. *Oncotarget* 8(56), p. 95516.

Bouskila, M. et al. 2010. Allosteric regulation of glycogen synthase controls glycogen synthesis in muscle. *Cell metabolism* 12(5), pp. 456-466.

Bowen, K. K., Dempsey, R. J. and Vemuganti, R. 2011. Adult interleukin-6 knockout mice show compromisedneurogenesis. *Neuroreport* 22(3), pp. 126-130.

Bozkurt, H., Şimşek, Ş. and Şahin, S. 2021. Elevated levels of cortisol, brain-derived neurotropic factor and tissue plasminogen activator in male children with autism spectrum disorder. *Autism Research* 14(10), pp. 2078-2084.

Braak, H. and Braak, E. 1995. Staging of Alzheimer's disease-related neurofibrillary changes. *Neurobiology of aging* 16(3), pp. 271-278.

Brady, J. J., Li, M., Suthram, S., Jiang, H., Wong, W. H. and Blau, H. M. 2013. Early role for IL-6 signalling during generation of induced pluripotent stem cells revealed by heterokaryon RNA-Seq. *Nature cell biology* 15(10), pp. 1244-1252.

Brambilla, R., Ashbaugh, J. J., Magliozzi, R., Dellarole, A., Karmally, S., Szymkowski, D. E. and Bethea, J. R. 2011. Inhibition of soluble tumour necrosis factor is therapeutic in experimental autoimmune encephalomyelitis and promotes axon preservation and remyelination. *Brain* 134(9), pp. 2736-2754.

Brewer, K. L., Bethea, J. R. and Yezierski, R. P. 1999. Neuroprotective effects of interleukin-10 following excitotoxic spinal cord injury. *Experimental neurology* 159(2), pp. 484-493.

Brownridge III, G. W. 2020. Neuroprotection against Alzheimer’s and lifespan extension induced by dietary restriction are associated with metabolomic changes and depend on oxidative resistance protein 1 (OXR1).

Brugg, B., Dubreuil, Y. L., Huber, G., Wollman, E. E., Delhaye-Bouchaud, N. and Mariani, J. 1995. Inflammatory processes induce beta-amyloid precursor protein changes in mouse brain. *Proceedings of the National Academy of Sciences* 92(7), pp. 3032-3035.

Bruneau, N. and Szepetowski, P. 2011. The role of the urokinase receptor in epilepsy, in disorders of language, cognition, communication and behavior, and in the central nervous system. *Current pharmaceutical design* 17(19), pp. 1914-1923.

Buka, S. L., Tsuang, M. T., Torrey, E. F., Klebanoff, M. A., Wagner, R. L. and Yolken, R. H. 2001. Maternal cytokine levels during pregnancy and adult psychosis. *Brain, behavior, and immunity* 15(4), pp. 411-420.

Bunt, J., de Haas, T. G., Hasselt, N. E., Zwijnenburg, D. A., Koster, J., Versteeg, R. and Kool, M. 2010. Regulation of Cell Cycle Genes and Induction of Senescence by Overexpression of OTX2 in Medulloblastoma Cell LinesOTX2 Regulates Cell Cycle Genes and Induces Senescence. *Molecular Cancer Research* 8(10), pp. 1344-1357.

Bunt, J., Hasselt, N. E., Zwijnenburg, D. A., Hamdi, M., Koster, J., Versteeg, R. and Kool, M. 2012. OTX2 directly activates cell cycle genes and inhibits differentiation in medulloblastoma cells. *International journal of cancer* 131(2), pp. E21-E32.

Byles, V., Covarrubias, A. J., Ben-Sahra, I., Lamming, D. W., Sabatini, D. M., Manning, B. D. and Horng, T. 2013. The TSC-mTOR pathway regulates macrophage polarization. *Nature communications* 4, p. 2834.

Caccamo, A., Magrì, A., Medina, D. X., Wisely, E. V., López-Aranda, M. F., Silva, A. J. and Oddo, S. 2013. mTOR regulates tau phosphorylation and degradation: implications for Alzheimer's disease and other tauopathies. *Aging cell* 12(3), pp. 370-380.

Caccamo, A., Majumder, S., Richardson, A., Strong, R. and Oddo, S. 2010. Molecular interplay between mammalian target of rapamycin (mTOR), amyloid-β, and Tau: effects on cognitive impairments. *Journal of Biological Chemistry* 285(17), pp. 13107-13120.

Caccamo, A., Maldonado, M. A., Majumder, S., Medina, D. X., Holbein, W., Magrí, A. and Oddo, S. 2011. Naturally secreted amyloid-β increases mammalian target of rapamycin (mTOR) activity via a PRAS40-mediated mechanism. *Journal of Biological Chemistry* 286(11), pp. 8924-8932.

Cahoy, J. D. et al. 2008. A transcriptome database for astrocytes, neurons, and oligodendrocytes: a new resource for understanding brain development and function. *Journal of Neuroscience* 28(1), pp. 264-278.

Cao, Z. et al. 2006. The cytokine interleukin-6 is sufficient but not necessary to mimic the peripheral conditioning lesion effect on axonal growth. *Journal of Neuroscience* 26(20), pp. 5565-5573.

Caraci, F. et al. 2011. TGF-β1 pathway as a new target for neuroprotection in Alzheimer's disease. *CNS neuroscience & therapeutics* 17(4), pp. 237-249.

Carlson, N. G., Wieggel, W. A., Chen, J., Bacchi, A., Rogers, S. W. and Gahring, L. C. 1999. Inflammatory cytokines IL-1α, IL-1β, IL-6, and TNF-α impart neuroprotection to an excitotoxin through distinct pathways. *The Journal of Immunology* 163(7), pp. 3963-3968.

Carson, R. P., Fu, C., Winzenburger, P. and Ess, K. C. 2013. Deletion of Rictor in neural progenitor cells reveals contributions of mTORC2 signaling to tuberous sclerosis complex. *Human molecular genetics* 22(1), pp. 140-152.

Cartwright, P., McLean, C., Sheppard, A., Rivett, D., Jones, K. and Dalton, S. 2005. LIF/STAT3 controls ES cell self-renewal and pluripotency by a Myc-dependent mechanism.

Caspersen, C. et al. 2005. Mitochondrial Aβ: a potential focal point for neuronal metabolic dysfunction in Alzheimer's disease. *The FASEB Journal* 19(14), pp. 2040-2041.

Catania, M. V., D'Antoni, S., Bonaccorso, C. M., Aronica, E., Bear, M. F. and Nicoletti, F. 2007. Group I metabotropic glutamate receptors: a role in neurodevelopmental disorders? *Molecular neurobiology* 35(3), pp. 298-307.

Cengiz, P. et al. 2019. Developmental differences in microglia morphology and gene expression during normal brain development and in response to hypoxia-ischemia. *Neurochemistry international* 127, pp. 137-147.

Cepeda, C., André, V. M., Vinters, H. V., Levine, M. S. and Mathern, G. W. 2005. Are cytomegalic neurons and balloon cells generators of epileptic activity in pediatric cortical dysplasia? *Epilepsia* 46, pp. 82-88.

Cepeda, C. et al. 2010. Comparative study of cellular and synaptic abnormalities in brain tissue samples from pediatric tuberous sclerosis complex and cortical dysplasia type II. *Epilepsia* 51, pp. 160-165.

Cepeda, C. et al. 2003. Morphological and electrophysiological characterization of abnormal cell types in pediatric cortical dysplasia. *Journal of neuroscience research* 72(4), pp. 472-486.

Chaboub, L. S. and Deneen, B. eds. 2013. *Astrocyte form and function in the developing central nervous system*. *Seminars in pediatric neurology.* Elsevier.

Challacombe, J. F., Snow, D. M. and Letourneau, P. C. 1997. Dynamic microtubule ends are required for growth cone turning to avoid an inhibitory guidance cue. *Journal of Neuroscience* 17(9), pp. 3085-3095.

Chambers, S. M., Fasano, C. A., Papapetrou, E. P., Tomishima, M., Sadelain, M. and Studer, L. 2009. Highly efficient neural conversion of human ES and iPS cells by dual inhibition of SMAD signaling. *Nature biotechnology* 27(3), p. 275.

Chano, T., Okabe, H. and Hulette, C. M. 2007. RB1CC1 insufficiency causes neuronal atrophy through mTOR signaling alteration and involved in the pathology of Alzheimer's diseases. *Brain research* 1168, pp. 97-105.

Chávez-Gutiérrez, L. et al. 2012. The mechanism of γ-secretase dysfunction in familial Alzheimer disease. *The EMBO journal* 31(10), pp. 2261-2274.

Chen, Y. et al. 2006. Microtubule affinity-regulating kinase 2 functions downstream of the PAR-3/PAR-6/atypical PKC complex in regulating hippocampal neuronal polarity. *Proceedings of the National Academy of Sciences* 103(22), pp. 8534-8539.

Cheng, B., Christakos, S. and Mattson, M. P. 1994. Tumor necrosis factors protect neurons against metabolic-excitotoxic insults and promote maintenance of calcium homeostasis. *Neuron* 12(1), pp. 139-153.

Chevilley, A., Lesept, F., Lenoir, S., Ali, C., Parcq, J. and Vivien, D. 2015. Impacts of tissue-type plasminogen activator (tPA) on neuronal survival. *Frontiers in cellular neuroscience* 9, p. 415.

Chiarini, A., Armato, U., Gardenal, E., Gui, L. and Dal Prà, I. 2017. Amyloid β-exposed human astrocytes overproduce phospho-tau and overrelease it within exosomes, effects suppressed by calcilytic NPS 2143—further implications for Alzheimer's therapy. *Frontiers in neuroscience* 11, p. 217.

Cho, S. W., Kim, S., Kim, Y., Kweon, J., Kim, H. S., Bae, S. and Kim, J.-S. 2014. Analysis of off-target effects of CRISPR/Cas-derived RNA-guided endonucleases and nickases. *Genome research* 24(1), pp. 132-141.

Choi, Y.-J., Di Nardo, A., Kramvis, I., Meikle, L., Kwiatkowski, D. J., Sahin, M. and He, X. 2008. Tuberous sclerosis complex proteins control axon formation. *Genes & development* 22(18), pp. 2485-2495.

Chong, Z. Z., Shang, Y. C., Zhang, L., Wang, S. and Maiese, K. 2010. Mammalian target of rapamycin: hitting the bull's-eye for neurological disorders. *Oxidative medicine and cellular longevity* 3(6), pp. 374-391.

Chou, Y.-H., Khuon, S., Herrmann, H. and Goldman, R. D. 2003. Nestin promotes the phosphorylation-dependent disassembly of vimentin intermediate filaments during mitosis. *Molecular biology of the cell* 14(4), pp. 1468-1478.

Chung, T. K., Lynch, E. R., Fiser, C. J., Nelson, D. A., Tudor, C., Franz, D. N. and Krueger, D. A. 2011. Psychiatric comorbidity and treatment response in patients with tuberous sclerosis complex. *, 23, 4* 23(4), pp. 263-269.

Cohen, P. and Goedert, M. 2004. GSK3 inhibitors: development and therapeutic potential. *Nature reviews Drug discovery* 3(6), p. 479.

Colangelo, V., Schurr, J., Ball, M. J., Pelaez, R. P., Bazan, N. G. and Lukiw, W. J. 2002. Gene expression profiling of 12633 genes in Alzheimer hippocampal CA1: transcription and neurotrophic factor down-regulation and up-regulation of apoptotic and pro-inflammatory signaling. *Journal of neuroscience research* 70(3), pp. 462-473.

Conroy, S. M. et al. 2004. Interleukin-6 produces neuronal loss in developing cerebellar granule neuron cultures. *Journal of neuroimmunology* 155(1-2), pp. 43-54.

Consortium, E. C. T. S. 1993. Identification and characterization of the tuberous sclerosis gene on chromosome 16. *Cell* 75(7), pp. 1305-1315.

Correa, F. et al. 2011. Tissue plasminogen activator prevents white matter damage following stroke. *Journal of Experimental Medicine* 208(6), pp. 1229-1242.

Costa, V. et al. 2016. mTORC1 inhibition corrects neurodevelopmental and synaptic alterations in a human stem cell model of tuberous sclerosis. *Cell reports* 15(1), pp. 86-95.

Cox, D. B., Gootenberg, J. S., Abudayyeh, O. O., Franklin, B., Kellner, M. J., Joung, J. and Zhang, F. 2017. RNA editing with CRISPR-Cas13. *Science* 358(6366), pp. 1019-1027.

Crino, P. B. 2004. Molecular pathogenesis of tuber formation in tuberous sclerosis complex. *Journal of Child Neurology* 19(9), pp. 716-725.

Dabora, S. L. et al. 2001. Mutational analysis in a cohort of 224 tuberous sclerosis patients indicates increased severity of TSC2, compared with TSC1, disease in multiple organs. *The American Journal of Human Genetics* 68(1), pp. 64-80.

Danesin, C., Peres, J. N., Johansson, M., Snowden, V., Cording, A., Papalopulu, N. and Houart, C. 2009. Integration of telencephalic Wnt and hedgehog signaling center activities by Foxg1. *Developmental cell* 16(4), pp. 576-587.

Das, P. and Golde, T. 2006. Dysfunction of TGF-β signaling in Alzheimer's disease. *The Journal of clinical investigation* 116(11), pp. 2855-2857.

Dastidar, S. G., Landrieu, P. M. Z. and D'Mello, S. R. 2011. FoxG1 promotes the survival of postmitotic neurons. *Journal of Neuroscience* 31(2), pp. 402-413.

de Bock, F., Dornand, J. and Rondouin, G. 1996. Release of TNF alpha in the rat hippocampus following epileptic seizures and excitotoxic neuronal damage. *Neuroreport* 7(6), pp. 1125-1129.

De Calignon, A. et al. 2012. Propagation of tau pathology in a model of early Alzheimer's disease. *Neuron* 73(4), pp. 685-697.

De Vivo, L., Melone, M., Rothstein, J. D. and Conti, F. 2010. GLT-1 promoter activity in astrocytes and neurons of mouse hippocampus and somatic sensory cortex. *Frontiers in neuroanatomy* 3, p. 31.

Del Bo, R., Angeretti, N., Lucca, E., De Simoni, M. G. and Forloni, G. 1995. Reciprocal control of inflammatory cytokines, IL-1 and IL-6, and β-amyloid production in cultures. *Neuroscience letters* 188(1), pp. 70-74.

Demeter, A., Romero-Mulero, M. C., Csabai, L., Ölbei, M., Sudhakar, P., Haerty, W. and Korcsmáros, T. 2020. ULK1 and ULK2 are less redundant than previously thought: computational analysis uncovers distinct regulation and functions of these autophagy induction proteins. *Scientific reports* 10(1), pp. 1-17.

Di Nardo, A., Kramvis, I., Cho, N., Sadowski, A., Meikle, L., Kwiatkowski, D. J. and Sahin, M. 2009. Tuberous sclerosis complex activity is required to control neuronal stress responses in an mTOR-dependent manner. *Journal of Neuroscience* 29(18), pp. 5926-5937.

Di Nardo, A. et al. 2014. Neuronal Tsc1/2 complex controls autophagy through AMPK-dependent regulation of ULK1. *Human molecular genetics* 23(14), pp. 3865-3874.

Dietrich, W. D., Busto, R. and Bethea, J. R. 1999. Postischemic hypothermia and IL-10 treatment provide long-lasting neuroprotection of CA1 hippocampus following transient global ischemia in rats. *Experimental neurology* 158(2), pp. 444-450.

District, C. 2019. Serum levels of oxidants and protein S100B were associated in the first-episode drug naïve patients with schizophrenia. *Global Clin. Translational Res*, pp. 84-92.

Dolmetsch, R. and Geschwind, D. H. 2011. The human brain in a dish: the promise of iPSC-derived neurons. *Cell* 145(6), pp. 831-834.

Dominguez, A. A., Chavez, M. G., Urke, A., Gao, Y., Wang, L. and Qi, L. S. 2022. CRISPR-mediated Synergistic Epigenetic and Transcriptional Control. *The CRISPR Journal* 5(2), pp. 264-275.

Doudna, J. A. and Charpentier, E. 2014. The new frontier of genome engineering with CRISPR-Cas9. *Science* 346(6213), p. 1258096.

Dunlop, E. A., Hunt, D. K., Acosta-Jaquez, H. A., Fingar, D. C. and Tee, A. R. 2011. ULK1 inhibits mTORC1 signaling, promotes multisite Raptor phosphorylation and hinders substrate binding. *Autophagy* 7(7), pp. 737-747.

Dzwonek, J. and Wilczynski, G. M. 2015. CD44: molecular interactions, signaling and functions in the nervous system. *Frontiers in cellular neuroscience* 9, p. 175.

Eagleson, K. L., Bonnin, A. and Levitt, P. 2005. Region-and age-specific deficits in γ-aminobutyric acidergic neuron development in the telencephalon of the uPAR–/–mouse. *Journal of Comparative Neurology* 489(4), pp. 449-466.

Ebens, A. et al. 1996. Hepatocyte growth factor/scatter factor is an axonal chemoattractant and a neurotrophic factor for spinal motor neurons. *Neuron* 17(6), pp. 1157-1172.

Ehninger, D., De Vries, P. and Silva, A. 2009. From mTOR to cognition: molecular and cellular mechanisms of cognitive impairments in tuberous sclerosis. *Journal of Intellectual Disability Research* 53(10), pp. 838-851.

Ehninger, D. et al. 2008. Reversal of learning deficits in a Tsc2+/− mouse model of tuberous sclerosis. *Nature medicine* 14(8), p. 843.

Eichmüller, O. L. et al. 2022. Amplification of human interneuron progenitors promotes brain tumors and neurological defects. *Science* 375(6579), p. eabf5546.

Eilers, M. and Eisenman, R. N. 2008. Myc's broad reach. *Genes & development* 22(20), pp. 2755-2766.

El-Brolosy, M. A. and Stainier, D. Y. 2017. Genetic compensation: A phenomenon in search of mechanisms. *PLoS genetics* 13(7), p. e1006780.

Ellison-Wright, Z. et al. 2004. Heterozygous PAX6 mutation, adult brain structure and fronto-striato-thalamic function in a human family. *European Journal of Neuroscience* 19(6), pp. 1505-1512.

Engelholm, L. H. et al. 2003. uPARAP/Endo180 is essential for cellular uptake of collagen and promotes fibroblast collagen adhesion. *The Journal of cell biology* 160(7), pp. 1009-1015.

Esposito, G. et al. 2008. Genomic and functional profiling of human Down syndrome neural progenitors implicates S100B and aquaporin 4 in cell injury. *Human molecular genetics* 17(3), pp. 440-457.

Ess, K. C., Uhlmann, E. J., Li, W., Li, H., Declue, J. E., Crino, P. B. and Gutmann, D. H. 2004. Expression profiling in tuberous sclerosis complex (TSC) knockout mouse astrocytes to characterize human TSC brain pathology. *Glia* 46(1), pp. 28-40.

Estivill-Torrus, G., Pearson, H., van Heyningen, V., Price, D. J. and Rashbass, P. 2002. Pax6 is required to regulate the cell cycle and the rate of progression from symmetrical to asymmetrical division in mammalian cortical progenitors.

Fabbro, S. and Seeds, N. W. 2009. Plasminogen activator activity is inhibited while neuroserpin is up-regulated in the Alzheimer disease brain. *Journal of neurochemistry* 109(2), pp. 303-315.

Farhy-Tselnicker, I. and Allen, N. J. 2018. Astrocytes, neurons, synapses: a tripartite view on cortical circuit development. *Neural development* 13(1), pp. 1-12.

Feliciano, D. M. 2020. The neurodevelopmental pathogenesis of tuberous sclerosis complex (TSC). *Frontiers in neuroanatomy* 14, p. 39.

Fenton, H. et al. 1998. Hepatocyte growth factor (HGF/SF) in Alzheimer's disease. *Brain research* 779(1-2), pp. 262-270.

Ferrando-Miguel, R., Rosner, M., Freilinger, A., Lubec, G. and Hengstschläger, M. 2005. Tuberin–A New Molecular Target in Alzheimer's Disease? *Neurochemical research* 30(11), pp. 1413-1419.

Ferreira, A. and Caceres, A. 1992. Expression of the Class III β-tubulin isotype in developing neurons in culture. *Journal of neuroscience research* 32(4), pp. 516-529.

Fiore, M., Angelucci, F., Alleva, E., Branchi, I., Probert, L. and Aloe, L. 2000. Learning performances, brain NGF distribution and NPY levels in transgenic mice expressing TNF-alpha. *Behavioural brain research* 112(1-2), pp. 165-175.

Flavin, M. P. and Zhao, G. 2001. Tissue plasminogen activator protects hippocampal neurons from oxygen-glucose deprivation injury. *Journal of neuroscience research* 63(5), pp. 388-394.

Fossat, N., Chatelain, G., Brun, G. and Lamonerie, T. 2006. Temporal and spatial delineation of mouse Otx2 functions by conditional self-knockout. *EMBO reports* 7(8), pp. 824-830.

Franco, P. et al. 2006. Activation of urokinase receptor by a novel interaction between the connecting peptide region of urokinase and αvβ5 integrin. *Journal of cell science* 119(16), pp. 3424-3434.

Franz, D., Bissler, J. and McCormack, F. 2010. Tuberous sclerosis complex: neurological, renal and pulmonary manifestations. *Neuropediatrics* 41(5), p. 199.

Frisén, J. 2016. Neurogenesis and gliogenesis in nervous system plasticity and repair. *Annual review of cell and developmental biology* 32, pp. 127-141.

Fuchs, E. and Weber, K. 1994. Intermediate filaments: structure, dynamics, function and disease. *Annual review of biochemistry* 63(1), pp. 345-382.

Fujita, T., Tozaki-Saitoh, H. and Inoue, K. 2009. P2Y1 receptor signaling enhances neuroprotection by astrocytes against oxidative stress via IL-6 release in hippocampal cultures. *Glia* 57(3), pp. 244-257.

Furuya, H. et al. 2020. Plasminogen activator inhibitor-2 (PAI-2) overexpression supports bladder cancer development in PAI-1 knockout mice in N-butyl-N-(4-hydroxybutyl)-nitrosamine-induced bladder cancer mouse model. *Journal of translational medicine* 18(1), pp. 1-12.

Gan, P. P., Pasquier, E. and Kavallaris, M. 2007. Class III β-tubulin mediates sensitivity to chemotherapeutic drugs in non–small cell lung cancer. *Cancer research* 67(19), pp. 9356-9363.

Genestine, M. et al. 2021. Vascular-derived SPARC and SerpinE1 regulate interneuron tangential migration and accelerate functional maturation of human stem cell-derived interneurons. *Elife* 10, p. e56063.

Georgala, P. A., Carr, C. B. and Price, D. J. 2011. The role of Pax6 in forebrain development. *Developmental neurobiology* 71(8), pp. 690-709.

Gerlai, R., Wojtowicz, J. M., Marks, A. and Roder, J. 1995. Overexpression of a calcium-binding protein, S100 beta, in astrocytes alters synaptic plasticity and impairs spatial learning in transgenic mice. *Learning & Memory* 2(1), pp. 26-39.

Gilmore, J. H., Fredrik Jarskog, L., Vadlamudi, S. and Lauder, J. M. 2004. Prenatal infection and risk for schizophrenia: IL-1β, IL-6, and TNFα inhibit cortical neuron dendrite development. *Neuropsychopharmacology* 29(7), pp. 1221-1229.

Gipson, T. T., Gerner, G., Wilson, M. A., Blue, M. E. and Johnston, M. V. 2013. Potential for treatment of severe autism in tuberous sclerosis complex. *World journal of clinical pediatrics* 2(3), p. 16.

Girgrah, N., Letarte, M., Becker, L. E., Cruz, T. F., Theriault, E. and Moscarello, M. A. 1991. Localization of the CD44 glycoprotein to fibrous astrocytes in normal white matter and to reactive astrocytes in active lesions in multiple sclerosis. *Journal of Neuropathology & Experimental Neurology* 50(6), pp. 779-792.

Giulian, D. 1999. Microglia and the immune pathology of Alzheimer disease. *The American Journal of Human Genetics* 65(1), pp. 13-18.

Glaser, T., Jepeal, L., Edwards, J. G., Young, S. R., Favor, J. and Maas, R. L. 1994. PAX6 gene dosage effect in a family with congenital cataracts, aniridia, anophthalmia and central nervous system defects. *Nature genetics* 7(4), pp. 463-471.

Goeke, C. M., Zhang, X., Hashimoto, J. G. and Guizzetti, M. 2022. Astrocyte tissue plasminogen activator expression during brain development and its role in pyramidal neuron neurite outgrowth. *Neuroscience letters* 769, p. 136422.

González-Reyes, R. E., Nava-Mesa, M. O., Vargas-Sánchez, K., Ariza-Salamanca, D. and Mora-Muñoz, L. 2017. Involvement of astrocytes in Alzheimer's disease from a neuroinflammatory and oxidative stress perspective. *Frontiers in Molecular Neuroscience* 10, p. 427.

Gorelik, A., Sapir, T., Woodruff, T. M. and Reiner, O. 2017. Serping1/C1 inhibitor affects cortical development in a cell autonomous and non-cell autonomous manner. *Frontiers in cellular neuroscience* 11, p. 169.

Goswami, S. and Hsieh, J. 2019. One-hit wonders and 2-hit tubers: a second-hit to TSC2 Causes tuber-like cells in spheroids. *Epilepsy Currents* 19(1), pp. 49-50.

Goto, J. et al. 2011. Regulable neural progenitor-specific Tsc1 loss yields giant cells with organellar dysfunction in a model of tuberous sclerosis complex. *Proceedings of the National Academy of Sciences* 108(45), pp. E1070-E1079.

Götz, J. et al. 2004. Transgenic animal models of Alzheimer's disease and related disorders: histopathology, behavior and therapy. *Molecular psychiatry* 9(7), p. 664.

Grilli, M., Barbieri, I., Basudev, H., Brusa, R., Casati, C., Lozza, G. and Ongini, E. 2000. Interleukin-10 modulates neuronal threshold of vulnerability to ischaemic damage. *European Journal of Neuroscience* 12(7), pp. 2265-2272.

Guen, T. L. et al. 2011. A missense mutation within the fork-head domain of the forkhead box G1 Gene (FOXG1) affects its nuclear localization. *Human mutation* 32(2), pp. E2026-E2035.

Guillozet, A. L., Weintraub, S., Mash, D. C. and Mesulam, M. M. 2003. Neurofibrillary tangles, amyloid, and memory in aging and mild cognitive impairment. *Archives of neurology* 60(5), pp. 729-736.

Guizzetti, M., Moore, N. H., Giordano, G. and Costa, L. G. 2008. Modulation of neuritogenesis by astrocyte muscarinic receptors. *Journal of Biological Chemistry* 283(46), pp. 31884-31897.

Gül Mert, G. et al. 2019. Factors affecting epilepsy prognosis in patients with tuberous sclerosis. *Child's Nervous System* 35, pp. 463-468.

Guo, J., Qiang, M. and Ludueña, R. F. 2011. The distribution of β-tubulin isotypes in cultured neurons from embryonic, newborn, and adult mouse brains. *Brain research* 1420, pp. 8-18.

Gutierrez, G. C., Smalley, S. L. and Tanguay, P. E. 1998. Autism in tuberous sclerosis complex. *Journal of autism and developmental disorders* 28(2), pp. 97-103.

Gutmann, D. H., Zhang, Y., Hasbani, M. J., Goldberg, M. P., Plank, T. L. and Henske, E. P. 2000. Expression of the tuberous sclerosis complex gene products, hamartin and tuberin, in central nervous system tissues. *Acta neuropathologica* 99(3), pp. 223-230.

Halliwell, B. 2006. Oxidative stress and neurodegeneration: where are we now? *Journal of neurochemistry* 97(6), pp. 1634-1658.

Han, J. M. and Sahin, M. 2011. TSC1/TSC2 signaling in the CNS. *FEBS letters* 585(7), pp. 973-980.

Hara, T., Takamura, A., Kishi, C., Iemura, S.-i., Natsume, T., Guan, J.-L. and Mizushima, N. 2008. FIP200, a ULK-interacting protein, is required for autophagosome formation in mammalian cells. *The Journal of cell biology* 181(3), pp. 497-510.

Hayashi, Y., Nomura, M., Yamagishi, S. I., Harada, S. I., Yamashita, J. and Yamamoto, H. 1997. Induction of various blood-brain barrier properties in non-neural endothelial cells by close apposition to co-cultured astrocytes. *Glia* 19(1), pp. 13-26.

Hebert, M., Lesept, F., Vivien, D. and Macrez, R. 2016. The story of an exceptional serine protease, tissue-type plasminogen activator (tPA). *Revue neurologique* 172(3), pp. 186-197.

Heckmann, L.-H., Sørensen, P. B., Krogh, P. H. and Sørensen, J. G. 2011. NORMA-Gene: a simple and robust method for qPCR normalization based on target gene data. *BMC bioinformatics* 12, pp. 1-7.

Heneka, M. T. et al. 2015. Neuroinflammation in Alzheimer's disease. *The Lancet Neurology* 14(4), pp. 388-405.

Hengstschläger, M., Rosner, M., Fountoulakis, M., Oh, J.-e. and Lubec, G. 2004. Protein levels of α1-tubulin, protein disulfide isomerase, tropomyosins and vimentin are regulated by the tuberous sclerosis gene products. *Cancer letters* 210(2), pp. 219-226.

Hensch, T. K., Fagiolini, M., Mataga, N., Stryker, M. P., Baekkeskov, S. and Kash, S. F. 1998. Local GABA circuit control of experience-dependent plasticity in developing visual cortex. *Science* 282(5393), pp. 1504-1508.

Heras-Sandoval, D., Pérez-Rojas, J. M., Hernández-Damián, J. and Pedraza-Chaverri, J. 2014. The role of PI3K/AKT/mTOR pathway in the modulation of autophagy and the clearance of protein aggregates in neurodegeneration. *Cellular signalling* 26(12), pp. 2694-2701.

Hernández, F., de Barreda, E. G., Fuster-Matanzo, A., Lucas, J. J. and Avila, J. 2010. GSK3: a possible link between beta amyloid peptide and tau protein. *Experimental neurology* 223(2), pp. 322-325.

Hetman, M., Cavanaugh, J. E., Kimelman, D. and Xia, Z. 2000. Role of glycogen synthase kinase-3β in neuronal apoptosis induced by trophic withdrawal. *Journal of Neuroscience* 20(7), pp. 2567-2574.

Hettige, N. C. and Ernst, C. 2019. FOXG1 dose in brain development. *Frontiers in pediatrics* 7, p. 482.

Hill, R. E. et al. 1991. Mouse small eye results from mutations in a paired-like homeobox-containing gene. *Nature* 354(6354), pp. 522-525.

Hirai, K. et al. 2001. Mitochondrial abnormalities in Alzheimer's disease. *Journal of Neuroscience* 21(9), pp. 3017-3023.

Hiranniramol, K., Chen, Y., Liu, W. and Wang, X. 2020. Generalizable sgRNA design for improved CRISPR/Cas9 editing efficiency. *Bioinformatics* 36(9), pp. 2684-2689.

Hirota, H., Kiyama, H., Kishimoto, T. and Taga, T. 1996. Accelerated Nerve Regeneration in Mice by upregulated expression of interleukin (IL) 6 and IL-6 receptor after trauma. *The Journal of experimental medicine* 183(6), pp. 2627-2634.

Hisatsune, C., Shimada, T., Miyamoto, A., Lee, A. and Yamagata, K. 2021. Tuberous sclerosis complex (TSC) inactivation increases neuronal network activity by enhancing Ca2+ influx via L-type Ca2+ channels. *Journal of Neuroscience* 41(39), pp. 8134-8149.

Hoch, R. V., Lindtner, S., Price, J. D. and Rubenstein, J. L. 2015. OTX2 transcription factor controls regional patterning within the medial ganglionic eminence and regional identity of the septum. *Cell reports* 12(3), pp. 482-494.

Holmes, C. et al. 2009. Systemic inflammation and disease progression in Alzheimer disease. *Neurology* 73(10), pp. 768-774.

Hong, C. H., Tu, H. P., Lin, J. R. and Lee, C. H. 2016. An estimation of the incidence of tuberous sclerosis complex in a nationwide retrospective cohort study (1997–2010). *British Journal of Dermatology* 174(6), pp. 1282-1289.

Hooper, C., Killick, R. and Lovestone, S. 2008. The GSK3 hypothesis of Alzheimer's disease. *Journal of neurochemistry* 104(6), pp. 1433-1439.

Howard, M., O'Garra, A., Ishida, H., de Waal Malefyt, R. and De Vries, J. 1992. Biological properties of interleukin 10. *Journal of clinical immunology* 12(4), pp. 239-247.

Hüll, M., Eistetter, J., Fiebich, B. L. and Bauer, J. 1999. Glutamate but not interleukin-6 influences the phosphorylation of tau in primary rat hippocampal neurons. *Neuroscience letters* 261(1-2), pp. 33-36.

Hulshof, H. M. et al. 2022. Association of early MRI characteristics with subsequent epilepsy and neurodevelopmental outcomes in children with tuberous sclerosis complex. *Neurology* 98(12), pp. e1216-e1225.

Hur, E.-M. and Zhou, F.-Q. 2010. GSK3 signalling in neural development. *Nature Reviews Neuroscience* 11(8), pp. 539-551.

Hynd, M. R., Scott, H. L. and Dodd, P. R. 2004. Glutamate-mediated excitotoxicity and neurodegeneration in Alzheimer's disease. *Neurochemistry international* 45(5), pp. 583-595.

Ianniciello, A. et al. 2021. ULK1 inhibition promotes oxidative stress–induced differentiation and sensitizes leukemic stem cells to targeted therapy. *Science Translational Medicine* 13(613), p. eabd5016.

Iyer, A. et al. 2010. Tissue plasminogen activator and urokinase plasminogen activator in human epileptogenic pathologies. *Neuroscience* 167(3), pp. 929-945.

Jackson, C. A., Messinger, J., Peduzzi, J. D., Ansardi, D. C. and Morrow, C. D. 2005. Enhanced functional recovery from spinal cord injury following intrathecal or intramuscular administration of poliovirus replicons encoding IL-10. *Virology* 336(2), pp. 173-183.

Jana, M., Palencia, C. A. and Pahan, K. 2008. Fibrillar amyloid-β peptides activate microglia via TLR2: implications for Alzheimer's disease. *The Journal of Immunology* 181(10), pp. 7254-7262.

Jarskog, L. F., Xiao, H., Wilkie, M. B., Lauder, J. M. and Gilmore, J. H. 1997. Cytokine regulation of embryonic rat dopamine and serotonin neuronal survival in vitro. *International journal of developmental neuroscience* 15(6), pp. 711-716.

Jaworski, J., Spangler, S., Seeburg, D. P., Hoogenraad, C. C. and Sheng, M. 2005. Control of dendritic arborization by the phosphoinositide-3'-kinase–Akt–mammalian target of rapamycin pathway. *Journal of Neuroscience* 25(49), pp. 11300-11312.

Jeohn, G.-H., Kong, L.-Y., Wilson, B., Hudson, P. and Hong, J.-S. 1998. Synergistic neurotoxic effects of combined treatments with cytokines in murine primary mixed neuron/glia cultures. *Journal of neuroimmunology* 85(1), pp. 1-10.

Johnson, G. V. and Stoothoff, W. H. 2004. Tau phosphorylation in neuronal cell function and dysfunction. *Journal of cell science* 117(24), pp. 5721-5729.

Julia, T. 2019. Human iPSC application in Alzheimer's disease and Tau-related neurodegenerative diseases. *Neuroscience letters* 699, pp. 31-40.

Kaaijk, P., Pals, S. T., Morsink, F., Bosch, D. A. and Troost, D. 1997. Differential expression of CD44 splice variants in the normal human central nervous system. *Journal of neuroimmunology* 73(1-2), pp. 70-76.

Kabadi, A. M., Ousterout, D. G., Hilton, I. B. and Gersbach, C. A. 2014. Multiplex CRISPR/Cas9-based genome engineering from a single lentiviral vector. *Nucleic acids research* 42(19), pp. e147-e147.

Kaczorowska, M. et al. 2011. Cerebral tuber count and its impact on mental outcome of patients with tuberous sclerosis complex. *Epilepsia* 52(1), pp. 22-27.

Karamita, M., Barnum, C., Möbius, W., Tansey, M. G., Szymkowski, D. E., Lassmann, H. and Probert, L. 2017. Therapeutic inhibition of soluble brain TNF promotes remyelination by increasing myelin phagocytosis by microglia. *JCI insight* 2(8),

Karki, R., Mariani, M., Andreoli, M., He, S., Scambia, G., Shahabi, S. and Ferlini, C. 2013. βIII-Tubulin: biomarker of taxane resistance or drug target? *Expert opinion on therapeutic targets* 17(4), pp. 461-472.

Kim, E. S., Leonardo, E. D. and Dranovsky, A. 2018. iPSC-derived neurons as a tool for probing molecular pharmacology of antipsychotic action. *bioRxiv*, p. 308486.

Kim, H.-J. et al. 2003. Selective neuronal degeneration induced by soluble oligomeric amyloid beta protein. *The FASEB Journal* 17(1), pp. 118-120.

Kim, W.-Y. and Snider, W. D. 2011. Functions of GSK-3 signaling in development of the nervous system. *Frontiers in Molecular Neuroscience* 4, p. 44.

Kim, W.-Y., Wang, X., Wu, Y., Doble, B. W., Patel, S., Woodgett, J. R. and Snider, W. D. 2009. GSK-3 is a master regulator of neural progenitor homeostasis. *Nature neuroscience* 12(11), pp. 1390-1397.

Kleinstiver, B. P. et al. 2015. Engineered CRISPR-Cas9 nucleases with altered PAM specificities. *Nature* 523(7561), pp. 481-485.

Knoepfler, P. S., Cheng, P. F. and Eisenman, R. N. 2002. N-myc is essential during neurogenesis for the rapid expansion of progenitor cell populations and the inhibition of neuronal differentiation. *Genes & development* 16(20), pp. 2699-2712.

Knox, S. et al. 2007. Mechanisms of TSC-mediated control of synapse assembly and axon guidance. *PLoS One* 2(4), p. e375.

Ko, Y. and Chye, S. M. 2020. Lifestyle intervention to prevent Alzheimer's disease. *Reviews in the Neurosciences* 31(8), pp. 817-824.

Kochlamazashvili, G. et al. 2010. The extracellular matrix molecule hyaluronic acid regulates hippocampal synaptic plasticity by modulating postsynaptic L-type Ca2+ channels. *Neuron* 67(1), pp. 116-128.

Koenigsknecht, J. and Landreth, G. 2004. Microglial phagocytosis of fibrillar β-amyloid through a β1 integrin-dependent mechanism. *Journal of Neuroscience* 24(44), pp. 9838-9846.

Koistinaho, M. et al. 2004. Apolipoprotein E promotes astrocyte colocalization and degradation of deposited amyloid-β peptides. *Nature medicine* 10(7), pp. 719-726.

Kumar, U., Dunlop, D. M. and Richardson, J. S. 1994. Mitochondria from Alzheimer's fibroblasts show decreased uptake of calcium and increased sensitivity to free radicals. *Life sciences* 54(24), pp. 1855-1860.

Kumar, V., Zhang, M.-X., Swank, M. W., Kunz, J. and Wu, G.-Y. 2005. Regulation of dendritic morphogenesis by Ras–PI3K–Akt–mTOR and Ras–MAPK signaling pathways. *Journal of Neuroscience* 25(49), pp. 11288-11299.

Kummer, K. K., Zeidler, M., Kalpachidou, T. and Kress, M. 2021. Role of IL-6 in the regulation of neuronal development, survival and function. *Cytokine* 144, p. 155582.

LaFerla, F. M. and Green, K. N. 2012. Animal models of Alzheimer disease. *Cold Spring Harbor perspectives in medicine* 2(11), p. a006320.

Lam, H. C., Nijmeh, J. and Henske, E. P. 2017. New developments in the genetics and pathogenesis of tumours in tuberous sclerosis complex. *The Journal of pathology* 241(2), pp. 219-225.

Lambert, M. P. et al. 1998. Diffusible, nonfibrillar ligands derived from Aβ1–42 are potent central nervous system neurotoxins. *Proceedings of the National Academy of Sciences* 95(11), pp. 6448-6453.

Lan, X., Chen, Q., Wang, Y., Jia, B., Sun, L., Zheng, J. and Peng, H. 2012. TNF-α affects human cortical neural progenitor cell differentiation through the autocrine secretion of leukemia inhibitory factor. *PLoS One* 7(12), p. e50783.

Lanzrein, A.-S., Johnston, C. M., Perry, V. H., Jobst, K. A., King, E. M. and Smith, A. D. 1998. Longitudinal study of inflammatory factors in serum, cerebrospinal fluid, and brain tissue in Alzheimer disease: interleukin-1beta, interleukin-6, interleukin-1 receptor antagonist, tumor necrosis factor-alpha, the soluble tumor necrosis factor receptors I and II, and alpha1-antichymotrypsin. *Alzheimer disease and associated disorders* 12(3), pp. 215-227.

Lauderback, C. M., Hackett, J. M., Huang, F. F., Keller, J. N., Szweda, L. I., Markesbery, W. R. and Butterfield, D. A. 2001. The glial glutamate transporter, GLT-1, is oxidatively modified by 4-hydroxy-2-nonenal in the Alzheimer's disease brain: the role of Aβ1–42. *Journal of neurochemistry* 78(2), pp. 413-416.

Launay, S. et al. 2008. HtrA1-dependent proteolysis of TGF-β controls both neuronal maturation and developmental survival. *Cell Death & Differentiation* 15(9), pp. 1408-1416.

Laurent, C. et al. 2017. Hippocampal T cell infiltration promotes neuroinflammation and cognitive decline in a mouse model of tauopathy. *Brain* 140(1), pp. 184-200.

Lee, A. et al. 2010. Rapid loss of glutamine synthetase from astrocytes in response to hypoxia: implications for excitotoxicity. *Journal of Chemical Neuroanatomy* 39(3), pp. 211-220.

Lee, J. and Kim, M.-S. 2007. The role of GSK3 in glucose homeostasis and the development of insulin resistance. *Diabetes research and clinical practice* 77(3), pp. S49-S57.

Lemarchand, E., Maubert, E., Haelewyn, B., Ali, C., Rubio, M. and Vivien, D. 2016. Stressed neurons protect themselves by a tissue-type plasminogen activator-mediated EGFR-dependent mechanism. *Cell Death & Differentiation* 23(1), pp. 123-131.

Lendahl, U., Zimmerman, L. B. and McKay, R. D. 1990. CNS stem cells express a new class of intermediate filament protein. *Cell* 60(4), pp. 585-595.

Levin, E. C., Acharya, N. K., Sedeyn, J. C., Venkataraman, V., D'Andrea, M. R., Wang, H.-Y. and Nagele, R. G. 2009. Neuronal expression of vimentin in the Alzheimer's disease brain may be part of a generalized dendritic damage-response mechanism. *Brain research* 1298, pp. 194-207.

Levin, S. G. and Godukhin, O. V. 2011. Anti-inflammatory cytokines, TGF-β1 and IL-10, exert anti-hypoxic action and abolish posthypoxic hyperexcitability in hippocampal slice neurons: Comparative aspects. *Experimental neurology* 232(2), pp. 329-332.

Li, J., Ma, Y., Teng, Y. D., Zheng, K., Vartanian, T. K., Snyder, E. Y. and Sidman, R. L. 2006. Purkinje neuron degeneration in nervous (nr) mutant mice is mediated by a metabolic pathway involving excess tissue plasminogen activator. *Proceedings of the National Academy of Sciences* 103(20), pp. 7847-7852.

Li, J. et al. 2013. Tissue plasminogen activator regulates Purkinje neuron development and survival. *Proceedings of the National Academy of Sciences* 110(26), pp. E2410-E2419.

Li, R.-J., Xu, J., Fu, C., Zhang, J., Zheng, Y. G., Jia, H. and Liu, J. O. 2016. Regulation of mTORC1 by lysosomal calcium and calmodulin. *Elife* 5, p. e19360.

Li, X., Krawetz, R., Liu, S., Meng, G. and Rancourt, D. E. 2008. ROCK inhibitor improves survival of cryopreserved serum/feeder-free single human embryonic stem cells. *Human reproduction* 24(3), pp. 580-589.

Li, Y. et al. 2017. Abnormal neural progenitor cells differentiated from induced pluripotent stem cells partially mimicked development of TSC2 neurological abnormalities. *Stem cell reports* 8(4), pp. 883-893.

Li, Z. et al. 2018. Ulk1 governs nerve growth factor/TrkA signaling by mediating Rab5 GTPase activation in porcine hemagglutinating encephalomyelitis virus-induced neurodegenerative disorders. *Journal of Virology* 92(16), pp. e00325-00318.

Liang, S., Salas, T., Gencaslan, E., Li, B. and Habib, S. L. 2014. Tuberin-deficiency downregulates N-cadherin and upregulates vimentin in kidney tumor of TSC patients. *Oncotarget* 5(16), p. 6936.

Lim, S.-H., Park, E., You, B., Jung, Y., Park, A.-R., Park, S. G. and Lee, J.-R. 2013. Neuronal synapse formation induced by microglia and interleukin 10. *PLoS One* 8(11), p. e81218.

Lin, L. and Chan, S. O. 2003. Perturbation of CD44 function affects chiasmatic routing of retinal axons in brain slice preparations of the mouse retinofugal pathway. *European Journal of Neuroscience* 17(11), pp. 2299-2312.

Ling, Z. D., Potter, E. D., Lipton, J. W. and Carvey, P. M. 1998. Differentiation of mesencephalic progenitor cells into dopaminergic neurons by cytokines. *Experimental neurology* 149(2), pp. 411-423.

Lino, N., Fiore, L., Rapacioli, M., Teruel, L., Flores, V., Scicolone, G. and Sánchez, V. 2014. uPA-uPAR molecular complex is involved in cell signaling during neuronal migration and neuritogenesis. *Developmental Dynamics* 243(5), pp. 676-689.

Liot, G., Roussel, B. D., Lebeurrier, N., Benchenane, K., López-Atalaya, J. P., Vivien, D. and Ali, C. 2006. Tissue-type plasminogen activator rescues neurones from serum deprivation-induced apoptosis through a mechanism independent of its proteolytic activity. *Journal of neurochemistry* 98(5), pp. 1458-1464.

Liu, A. J. et al. 2020. Association of cognitive and behavioral features between adults with tuberous sclerosis and frontotemporal dementia. *JAMA neurology* 77(3), pp. 358-366.

Liu, B. et al. 2010. Increased expression of urokinase-type plasminogen activator receptor in the frontal cortex of patients with intractable frontal lobe epilepsy. *Journal of neuroscience research* 88(12), pp. 2747-2754.

Liu, L. et al. 2017. The molecular architecture for RNA-guided RNA cleavage by Cas13a. *Cell* 170(4), pp. 714-726. e710.

Liu, Y.-Y. and Bian, J.-S. 2010. Hydrogen sulfide protects amyloid-β induced cell toxicity in microglia. *Journal of Alzheimer's Disease* 22(4), pp. 1189-1200.

Lledo, P.-M., Merkle, F. T. and Alvarez-Buylla, A. 2008. Origin and function of olfactory bulb interneuron diversity. *Trends in neurosciences* 31(8), pp. 392-400.

Lohr, J. B. 1991. Oxygen radicals and neuropsychiatric illness: some speculations. *Archives of general psychiatry* 48(12), pp. 1097-1106.

Los, M., Maddika, S., Erb, B. and Schulze-Osthoff, K. 2009. Switching Akt: from survival signaling to deadly response. *Bioessays* 31(5), pp. 492-495.

Lu, W. and Tsirka, S. E. 2002. Partial rescue of neural apoptosis in the Lurcher mutant mouse through elimination of tissue plasminogen activator.

Ma, D., Li, S., Molusky, M. M. and Lin, J. D. 2012a. Circadian autophagy rhythm: a link between clock and metabolism? *Trends in Endocrinology & Metabolism* 23(7), pp. 319-325.

Ma, S.-H., Li, B., Huang, H.-W., Peng, Y.-P. and Qiu, Y.-H. 2012b. Interleukin-6 inhibits L-type calcium channel activity of cultured cerebellar granule neurons. *The Journal of Physiological Sciences* 62(5), pp. 385-392.

Madsen, C. D., Ferraris, G. M. S., Andolfo, A., Cunningham, O. and Sidenius, N. 2007. uPAR-induced cell adhesion and migration: vitronectin provides the key. *The Journal of cell biology* 177(5), pp. 927-939.

Maeda, Y. et al. 1994. Hypoxia/reoxygenation-mediated induction of astrocyte interleukin 6: a paracrine mechanism potentially enhancing neuron survival. *The Journal of experimental medicine* 180(6), pp. 2297-2308.

Maes, M., Galecki, P., Chang, Y. S. and Berk, M. 2011. A review on the oxidative and nitrosative stress (O&NS) pathways in major depression and their possible contribution to the (neuro) degenerative processes in that illness. *Progress in Neuro-Psychopharmacology and Biological Psychiatry* 35(3), pp. 676-692.

Mahakizadeh, S., Mokhtari, T., Navaee, F., Poorhassan, M., Tajik, A. and Hassanzadeh, G. 2020. Effects of chronic hypoxia on the expression of seladin-1/Tuj1 and the number of dark neurons of hippocampus. *Journal of Chemical Neuroanatomy* 104, p. 101744.

Maldonado, M. et al. 2003. Expression of ICAM-1, TNF-α, NFκB, and MAP kinase in tubers of the tuberous sclerosis complex. *Neurobiology of disease* 14(2), pp. 279-290.

Mammana, S. et al. 2018. The role of macrophages in neuroinflammatory and neurodegenerative pathways of alzheimer's disease, amyotrophic lateral sclerosis, and multiple sclerosis: Pathogenetic cellular effectors and potential therapeutic targets. *International journal of molecular sciences* 19(3), p. 831.

Manning, B. D. 2004. Balancing Akt with S6K: implications for both metabolic diseases and tumorigenesis. *J cell biol* 167(3), pp. 399-403.

Manuel, M. et al. 2007. Controlled overexpression of Pax6 in vivo negatively autoregulates the Pax6 locus, causing cell-autonomous defects of late cortical progenitor proliferation with little effect on cortical arealization.

Maragakis, N. J. and Rothstein, J. D. 2001. Glutamate transporters in neurologic disease. *Archives of neurology* 58(3), pp. 365-370.

Marambaud, P., Dreses-Werringloer, U. and Vingtdeux, V. 2009. Calcium signaling in neurodegeneration. *Molecular neurodegeneration* 4(1), pp. 1-15.

Mariani, J. et al. 2015. FOXG1-dependent dysregulation of GABA/glutamate neuron differentiation in autism spectrum disorders. *Cell* 162(2), pp. 375-390.

Martin, K. R. et al. 2017. The genomic landscape of tuberous sclerosis complex. *Nature communications* 8(1), pp. 1-13.

Martin, P. et al. 2020. TSC patient-derived isogenic neural progenitor cells reveal altered early neurodevelopmental phenotypes and rapamycin-induced MNK-eIF4E signaling. *Molecular autism* 11(1), pp. 1-15.

Martina, J. A., Diab, H. I., Brady, O. A. and Puertollano, R. 2016. TFEB and TFE 3 are novel components of the integrated stress response. *The EMBO journal* 35(5), pp. 479-495.

Martina, J. A., Diab, H. I., Lishu, L., Jeong-A, L., Patange, S., Raben, N. and Puertollano, R. 2014. The nutrient-responsive transcription factor TFE3 promotes autophagy, lysosomal biogenesis, and clearance of cellular debris. *Science signaling* 7(309), pp. ra9-ra9.

Martinez, S. 2003. The isthmic organizer and brain regionalization. *International Journal of Developmental Biology* 45(1), pp. 367-371.

Martini-Stoica, H. et al. 2018. TFEB enhances astroglial uptake of extracellular tau species and reduces tau spreading. *Journal of Experimental Medicine* 215(9), pp. 2355-2377.

Masakazu, H. et al. 1994. Expression of the α2-macroglobulin-encoding gene in rat brain and cultured astrocytes. *Gene* 141(2), pp. 155-162.

Matos, M., Augusto, E., Machado, N. J., dos Santos-Rodrigues, A., Cunha, R. A. and Agostinho, P. 2012. Astrocytic adenosine A 2A receptors control the amyloid-β peptide-induced decrease of glutamate uptake. *Journal of Alzheimer's Disease* 31(3), pp. 555-567.

Mattson, M. P. 2004. Pathways towards and away from Alzheimer's disease. *Nature* 430(7000), pp. 631-639.

Mattson, M. P., Cheng, B., Davis, D., Bryant, K., Lieberburg, I. and Rydel, R. E. 1992. beta-Amyloid peptides destabilize calcium homeostasis and render human cortical neurons vulnerable to excitotoxicity. *Journal of Neuroscience* 12(2), pp. 376-389.

Matveeva, E., Chernoivanenko, I. and Minin, A. 2010. Vimentin intermediate filaments protect mitochondria from oxidative stress. *Biochemistry (Moscow) Supplement Series A: Membrane and Cell Biology* 4(4), pp. 321-331.

Matzke, A. et al. 2007. Haploinsufficiency of c-Met in cd44−/− mice identifies a collaboration of CD44 and c-Met in vivo. *Molecular and cellular biology* 27(24), pp. 8797-8806.

McAlpine, F. E. et al. 2009. Inhibition of soluble TNF signaling in a mouse model of Alzheimer's disease prevents pre-plaque amyloid-associated neuropathology. *Neurobiology of disease* 34(1), pp. 163-177.

McCarroll, J. A., Gan, P. P., Liu, M. and Kavallaris, M. 2010. βIII-Tubulin Is a Multifunctional Protein Involved in Drug Sensitivity and Tumorigenesis in Non–Small Cell Lung Cancer. *Cancer research* 70(12), pp. 4995-5003.

McKhann, G. M. et al. 2011. The diagnosis of dementia due to Alzheimer’s disease: Recommendations from the National Institute on Aging-Alzheimer’s Association workgroups on diagnostic guidelines for Alzheimer's disease. *Alzheimer's & dementia* 7(3), pp. 263-269.

McKinney, C. E. 2017. Using induced pluripotent stem cells derived neurons to model brain diseases. *Neural regeneration research* 12(7), p. 1062.

Medina, D. L. et al. 2011. Transcriptional activation of lysosomal exocytosis promotes cellular clearance. *Developmental cell* 21(3), pp. 421-430.

Mehra, A., Ali, C., Parcq, J., Vivien, D. and Docagne, F. 2016. The plasminogen activation system in neuroinflammation. *Biochimica et Biophysica Acta (BBA)-Molecular Basis of Disease* 1862(3), pp. 395-402.

Meikle, L. et al. 2007. A mouse model of tuberous sclerosis: neuronal loss of Tsc1 causes dysplastic and ectopic neurons, reduced myelination, seizure activity, and limited survival. *Journal of Neuroscience* 27(21), pp. 5546-5558.

Meng, X.-m., Nikolic-Paterson, D. J. and Lan, H. Y. 2016. TGF-β: the master regulator of fibrosis. *Nature Reviews Nephrology* 12(6), pp. 325-338.

Menon, S. et al. 2014. Spatial control of the TSC complex integrates insulin and nutrient regulation of mTORC1 at the lysosome. *Cell* 156(4), pp. 771-785.

Merck, Co, Sharp, M. and Dohme. 1899. *The Merck manual of diagnosis and therapy*. Merck.

Merino, P., Diaz, A., Jeanneret, V., Wu, F., Torre, E., Cheng, L. and Yepes, M. 2017. Urokinase-type plasminogen activator (uPA) binding to the uPA receptor (uPAR) promotes axonal regeneration in the central nervous system. *Journal of Biological Chemistry* 292(7), pp. 2741-2753.

Merino, P., Diaz, A., Torre, E. R. and Yepes, M. 2020. Urokinase-type plasminogen activator (uPA) regulates the expression and function of growth-associated protein 43 (GAP-43) in the synapse. *Journal of Biological Chemistry* 295(2), pp. 619-630.

Merino, P. and Yepes, M. 2018. Urokinase-type plasminogen activator induces neurorepair in the ischemic brain. *Journal of neurology and experimental neuroscience* 4(2), p. 24.

Merrill, J. E. 1992. Tumor necrosis factor alpha, interleukin 1 and related cytokines in brain development: normal and pathological. *Developmental neuroscience* 14(1), pp. 1-10.

Merrill, J. E. and Benveniste, E. N. 1996. Cytokines in inflammatory brain lesions: helpful and harmful. *Trends in neurosciences* 19(8), pp. 331-338.

Meulmeester, E. and Ten Dijke, P. 2011. The dynamic roles of TGF-β in cancer. *The Journal of pathology* 223(2), pp. 206-219.

Meyer, U., Murray, P., Urwyler, A., Yee, B., Schedlowski, M. and Feldon, J. 2008. Adult behavioral and pharmacological dysfunctions following disruption of the fetal brain balance between pro-inflammatory and IL-10-mediated anti-inflammatory signaling. *Molecular psychiatry* 13(2), pp. 208-221.

Meyer, U. et al. 2006. The time of prenatal immune challenge determines the specificity of inflammation-mediated brain and behavioral pathology. *Journal of Neuroscience* 26(18), pp. 4752-4762.

Michaluk, P., Heller, J. P. and Rusakov, D. A. 2021. Rapid recycling of glutamate transporters on the astroglial surface. *Elife* 10,

Miller, D. R. et al. 2021. A bistable, multiport valve enables microformulators creating microclinical analyzers that reveal aberrant glutamate metabolism in astrocytes derived from a tuberous sclerosis patient. *Sensors and Actuators B: Chemical* 341, p. 129972.

Minamino, T., Miyauchi, H., Tateno, K., Kunieda, T. and Komuro, I. 2004. Akt-induced cellular senescence: implication for human disease. *Cell cycle* 3(4), pp. 447-449.

Minter, M. R., Taylor, J. M. and Crack, P. J. 2016. The contribution of neuroinflammation to amyloid toxicity in Alzheimer's disease. *Journal of neurochemistry* 136(3), pp. 457-474.

Miyauchi, H., Minamino, T., Tateno, K., Kunieda, T., Toko, H. and Komuro, I. 2004. Akt negatively regulates the in vitro lifespan of human endothelial cells via a p53/p21-dependent pathway. *The EMBO journal* 23(1), pp. 212-220.

Moiseyenko, V. M. et al. 2013. Evidence for predictive role of BRCA1 and bTUBIII in gastric cancer. *Medical oncology* 30(2), pp. 1-9.

Moore, K. W., de Waal Malefyt, R., Coffman, R. L. and O'Garra, A. 2001. Interleukin-10 and the interleukin-10 receptor. *Annual review of immunology* 19, p. 683.

Morelli, K. H. et al. 2023. An RNA-targeting CRISPR–Cas13d system alleviates disease-related phenotypes in Huntington's disease models. *Nature neuroscience* 26(1), pp. 27-38.

Morsli, H., Tuorto, F., Choo, D., Postiglione, M. P., Simeone, A. and Wu, D. K. 1999. Otx1 and Otx2 activities are required for the normal development of the mouse inner ear. *Development* 126(11), pp. 2335-2343.

Mota, S. I., Ferreira, I. L. and Rego, A. C. 2014. Dysfunctional synapse in Alzheimer's disease–A focus on NMDA receptors. *Neuropharmacology* 76, pp. 16-26.

Mozzetti, S. et al. 2005. Class III β-tubulin overexpression is a prominent mechanism of paclitaxel resistance in ovarian cancer patients. *Clinical Cancer Research* 11(1), pp. 298-305.

Mulder, S. D., Veerhuis, R., Blankenstein, M. A. and Nielsen, H. M. 2012. The effect of amyloid associated proteins on the expression of genes involved in amyloid-β clearance by adult human astrocytes. *Experimental neurology* 233(1), pp. 373-379.

Muller, S., Brun, S., René, F., de Sèze, J., Loeffler, J.-P. and Jeltsch-David, H. 2017. Autophagy in neuroinflammatory diseases. *Autoimmunity reviews* 16(8), pp. 856-874.

Murphy, P. G., Borthwick, L. S., Johnston, R. S., Kuchel, G. and Richardson, P. M. 1999. Nature of the retrograde signal from injured nerves that induces interleukin-6 mRNA in neurons. *Journal of Neuroscience* 19(10), pp. 3791-3800.

Nadadhur, A. G. et al. 2019. Neuron-Glia Interactions Increase Neuronal Phenotypes in Tuberous Sclerosis Complex Patient iPSC-Derived Models. *Stem cell reports* 12(1), pp. 42-56.

Nakajima, A., Yamada, K., Zou, L.-B., Yan, Y., Mizuno, M. and Nabeshima, T. 2002. Interleukin-6 protects PC12 cells from 4-hydroxynonenal-induced cytotoxicity by increasing intracellular glutathione levels. *Free Radical Biology and Medicine* 32(12), pp. 1324-1332.

Nakamura, T. and Mizuno, S. 2010. The discovery of hepatocyte growth factor (HGF) and its significance for cell biology, life sciences and clinical medicine. *Proceedings of the Japan Academy, Series B* 86(6), pp. 588-610.

Narasimhan, S. et al. 2017. Pathological tau strains from human brains recapitulate the diversity of tauopathies in nontransgenic mouse brain. *Journal of Neuroscience* 37(47), pp. 11406-11423.

Naruse, M., Shibasaki, K., Yokoyama, S., Kurachi, M. and Ishizaki, Y. 2013. Dynamic changes of CD44 expression from progenitors to subpopulations of astrocytes and neurons in developing cerebellum. *PLoS One* 8(1), p. e53109.

Net, A. s. 2019. *Alzheimer´s Statistics*. Alzheimers.net: Available at: https://www.alzheimers.net/alzheimers-statistics [Accessed: 16.11.22].

Nguyen, L. H. and Bordey, A. 2021. Convergent and divergent mechanisms of epileptogenesis in mTORopathies. *Frontiers in neuroanatomy* 15, p. 664695.

Nicole, O. et al. 2001. The proteolytic activity of tissue-plasminogen activator enhances NMDA receptor-mediated signaling. *Nature medicine* 7(1), pp. 59-64.

Nikoletopoulou, V. and Tavernarakis, N. 2012. Calcium homeostasis in aging neurons. *Frontiers in genetics* 3, p. 200.

Niwa, H., Burdon, T., Chambers, I. and Smith, A. 1998. Self-renewal of pluripotent embryonic stem cells is mediated via activation of STAT3. *Genes & development* 12(13), pp. 2048-2060.

Nixon, R. A. 2004. Niemann-Pick Type C disease and Alzheimer's disease: the APP-endosome connection fattens up. *The American journal of pathology* 164(3), pp. 757-761.

Numis, A., Major, P., Montenegro, M., Muzykewicz, D., Pulsifer, M. and Thiele, E. 2011. Identification of risk factors for autism spectrum disorders in tuberous sclerosis complex. *Neurology* 76(11), pp. 981-987.

O'Brien, R. J. and Wong, P. C. 2011. Amyloid precursor protein processing and Alzheimer's disease. *Annual review of neuroscience* 34, pp. 185-204.

Oceguera-Yanez, F. et al. 2016. Engineering the AAVS1 locus for consistent and scalable transgene expression in human iPSCs and their differentiated derivatives. *Methods* 101, pp. 43-55.

Ogura, K.-i., Wicky, C., Magnenat, L., Tobler, H., Mori, I., Müller, F. and Ohshima, Y. 1994. Caenorhabditis elegans unc-51 gene required for axonal elongation encodes a novel serine/threonine kinase. *Genes & development* 8(20), pp. 2389-2400.

Oh, J.-W., Van Wagoner, N. J., Rose-John, S. and Benveniste, E. N. 1998. Role of IL-6 and the soluble IL-6 receptor in inhibition of VCAM-1 gene expression. *The Journal of Immunology* 161(9), pp. 4992-4999.

Oliver, P. L. et al. 2011. Oxr1 is essential for protection against oxidative stress-induced neurodegeneration. *PLoS genetics* 7(10), p. e1002338.

Onyenwoke, R. U., Sexton, J. Z., Yan, F., Díaz, M. C. H., Forsberg, L. J., Major, M. B. and Brenman, J. E. 2015. The mucolipidosis IV Ca2+ channel TRPML1 (MCOLN1) is regulated by the TOR kinase. *Biochemical Journal* 470(3), pp. 331-342.

Orellana, D. I., Quintanilla, R. A., Gonzalez-Billault, C. and Maccioni, R. B. 2005. Role of the JAKs/STATs pathway in the intracellular calcium changes induced by interleukin-6 in hippocampal neurons. *Neurotoxicity research* 8(3), pp. 295-304.

Orlova, K. A. et al. 2010. Early progenitor cell marker expression distinguishes type II from type I focal cortical dysplasias. *Journal of Neuropathology & Experimental Neurology* 69(8), pp. 850-863.

Paccalin, M. et al. 2006. Activated mTOR and PKR kinases in lymphocytes correlate with memory and cognitive decline in Alzheimer's disease. *Dementia and geriatric cognitive disorders* 22(4), pp. 320-326.

Pajarillo, E., Rizor, A., Lee, J., Aschner, M. and Lee, E. 2019. The role of astrocytic glutamate transporters GLT-1 and GLAST in neurological disorders: potential targets for neurotherapeutics. *Neuropharmacology* 161, p. 107559.

Pal, R., Xiong, Y. and Sardiello, M. 2019. Abnormal glycogen storage in tuberous sclerosis complex caused by impairment of mTORC1-dependent and-independent signaling pathways. *Proceedings of the National Academy of Sciences* 116(8), pp. 2977-2986.

Pallari, H.-M., Lindqvist, J., Torvaldson, E., Ferraris, S. E., He, T., Sahlgren, C. and Eriksson, J. E. 2011. Nestin as a regulator of Cdk5 in differentiating myoblasts. *Molecular biology of the cell* 22(9), pp. 1539-1549.

Palmieri, M. et al. 2017. mTORC1-independent TFEB activation via Akt inhibition promotes cellular clearance in neurodegenerative storage diseases. *Nature communications* 8(1), pp. 1-19.

Palygin, O., Lalo, U., Verkhratsky, A. and Pankratov, Y. 2010. Ionotropic NMDA and P2X1/5 receptors mediate synaptically induced Ca2+ signalling in cortical astrocytes. *Cell calcium* 48(4), pp. 225-231.

Papazian, I. et al. 2021. Fundamentally different roles of neuronal TNF receptors in CNS pathology: TNFR1 and IKKβ promote microglial responses and tissue injury in demyelination while TNFR2 protects against excitotoxicity in mice. *Journal of neuroinflammation* 18(1), pp. 1-21.

Parameshwaran, K., Dhanasekaran, M. and Suppiramaniam, V. 2008. Amyloid beta peptides and glutamatergic synaptic dysregulation. *Experimental neurology* 210(1), pp. 7-13.

Parfenova, H., Tcheranova, D., Basuroy, S., Fedinec, A. L., Liu, J. and Leffler, C. W. 2012. Functional role of astrocyte glutamate receptors and carbon monoxide in cerebral vasodilation response to glutamate. *American Journal of Physiology-Heart and Circulatory Physiology* 302(11), pp. H2257-H2266.

Park, D. et al. 2010. Nestin is required for the proper self-renewal of neural stem cells. *Stem Cells* 28(12), pp. 2162-2171.

Park, L. et al. 2008. Key role of tissue plasminogen activator in neurovascular coupling. *Proceedings of the National Academy of Sciences* 105(3), pp. 1073-1078.

Parker, W. E. et al. 2011. Enhanced epidermal growth factor, hepatocyte growth factor, and vascular endothelial growth factor expression in tuberous sclerosis complex. *The American journal of pathology* 178(1), pp. 296-305.

Parsons, R. G., Gafford, G. M. and Helmstetter, F. J. 2006. Translational control via the mammalian target of rapamycin pathway is critical for the formation and stability of long-term fear memory in amygdala neurons. *Journal of Neuroscience* 26(50), pp. 12977-12983.

Patriarchi, T. et al. 2016. Imbalance of excitatory/inhibitory synaptic protein expression in iPSC-derived neurons from FOXG1+/− patients and in foxg1+/− mice. *European Journal of Human Genetics* 24(6), pp. 871-880.

Pattabiraman, S. et al. 2020. Vimentin protects differentiating stem cells from stress. *Scientific reports* 10(1), pp. 1-15.

Pei, J.-J., Björkdahl, C., Zhang, H., Zhou, X. and Winblad, B. 2008. p70 S6 kinase and tau in Alzheimer's disease. *Journal of Alzheimer's Disease* 14(4), pp. 385-392.

Pelisch, N., Dan, T., Ichimura, A., Sekiguchi, H., Vaughan, D. E., Van Ypersele de Strihou, C. and Miyata, T. 2015. Plasminogen activator inhibitor-1 antagonist TM5484 attenuates demyelination and axonal degeneration in a mice model of multiple sclerosis. *PLoS One* 10(4), p. e0124510.

Peng, Y.-P., Qiu, Y.-H., Lu, J.-H. and Wang, J.-J. 2005. Interleukin-6 protects cultured cerebellar granule neurons against glutamate-induced neurotoxicity. *Neuroscience letters* 374(3), pp. 192-196.

Pereira, L., Font-Nieves, M., Van den Haute, C., Baekelandt, V., Planas, A. M. and Pozas, E. 2015. IL-10 regulates adult neurogenesis by modulating ERK and STAT3 activity. *Frontiers in cellular neuroscience* 9, p. 57.

Perez-Asensio, F. J., Perpiñá, U., Planas, A. M. and Pozas, E. 2013. Interleukin-10 regulates progenitor differentiation and modulates neurogenesis in adult brain. *Journal of cell science* 126(18), pp. 4208-4219.

Perry, V. H., Cunningham, C. and Holmes, C. 2007. Systemic infections and inflammation affect chronic neurodegeneration. *Nature Reviews Immunology* 7(2), p. 161.

Peteri, U. K. et al. 2021. Urokinase plasminogen activator mediates changes in human astrocytes modeling fragile X syndrome. *Glia* 69(12), pp. 2947-2962.

Petrova, T. V., Hu, J. and Van Eldik, L. J. 2000. Modulation of glial activation by astrocyte-derived protein S100B: differential responses of astrocyte and microglial cultures. *Brain research* 853(1), pp. 74-80.

Pinner, E., Gruper, Y., Ben Zimra, M., Kristt, D., Laudon, M., Naor, D. and Zisapel, N. 2017. CD44 splice variants as potential players in Alzheimer's disease pathology. *Journal of Alzheimer's Disease* 58(4), pp. 1137-1149.

Pizzi, M. et al. 2004. Prevention of neuron and oligodendrocyte degeneration by interleukin-6 (IL-6) and IL-6 receptor/IL-6 fusion protein in organotypic hippocampal slices. *Molecular and Cellular Neuroscience* 25(2), pp. 301-311.

Polito, V. A. et al. 2014. Selective clearance of aberrant tau proteins and rescue of neurotoxicity by transcription factor EB. *EMBO molecular medicine* 6(9), pp. 1142-1160.

Ponta, H., Sherman, L. and Herrlich, P. A. 2003. CD44: from adhesion molecules to signalling regulators. *Nature reviews Molecular cell biology* 4(1), pp. 33-45.

Pope, S. K., Shue, V. M. and Beck, C. 2003. Will a healthy lifestyle help prevent Alzheimer's disease? *Annual review of public health* 24, p. 111.

Powell, E. M., Mars, W. M. and Levitt, P. 2001. Hepatocyte growth factor/scatter factor is a motogen for interneurons migrating from the ventral to dorsal telencephalon. *Neuron* 30(1), pp. 79-89.

Praetner, M. et al. 2018. Plasminogen activator inhibitor-1 promotes neutrophil infiltration and tissue injury on ischemia–reperfusion. *Arteriosclerosis, thrombosis, and vascular biology* 38(4), pp. 829-842.

Qian, D. et al. 2019. Blocking Notch signal pathway suppresses the activation of neurotoxic A1 astrocytes after spinal cord injury. *Cell cycle* 18(21), pp. 3010-3029.

Qiu, Z., Sweeney, D. D., Netzeband, J. G. and Gruol, D. L. 1998. Chronic interleukin-6 alters NMDA receptor-mediated membrane responses and enhances neurotoxicity in developing CNS neurons. *Journal of Neuroscience* 18(24), pp. 10445-10456.

Quintanilla, R. A., Orellana, D. I., González-Billault, C. and Maccioni, R. B. 2004. Interleukin-6 induces Alzheimer-type phosphorylation of tau protein by deregulating the cdk5/p35 pathway. *Experimental cell research* 295(1), pp. 245-257.

Quiroz, E. J. and Ryan, A. L. 2019. CRISPR/Cas9 Editing in Induced Pluripotent Stem Cells: A Way Forward for Treating Cystic Fibrosis?*Stem Cell-Based Therapy for Lung Disease*. Springer, pp. 153-178.

Raab-Graham, K. 2021. *Investigative Studies into mTORC1-Dependent Dendritic Branch Potentiation in TSC*.

Raben, N. and Puertollano, R. 2016. TFEB and TFE3, linking lysosomes to cellular adaptation to stress. *Annual review of cell and developmental biology* 32, p. 255.

Rabinovici, G. D. 2019. Late-onset Alzheimer disease. *Continuum: Lifelong Learning in Neurology* 25(1), p. 14.

Razzaq, A. and Masood, A. 2018. CRISPR/Cas9 system: a breakthrough in genome editing. *Mol Biol* 7(210), p. 2.

Reddrop, C. et al. 2005. Vampire bat salivary plasminogen activator (desmoteplase) inhibits tissue-type plasminogen activator-induced potentiation of excitotoxic injury. *Stroke* 36(6), pp. 1241-1246.

Rodríguez-Arellano, J., Parpura, V., Zorec, R. and Verkhratsky, A. 2016. Astrocytes in physiological aging and Alzheimer's disease. *Neuroscience* 323, pp. 170-182.

Romero, E., Ali, C., Molina-Holgado, E., Castellano, B., Guaza, C. and Borrell, J. 2007. Neurobehavioral and immunological consequences of prenatal immune activation in rats. Influence of antipsychotics. *Neuropsychopharmacology* 32(8), pp. 1791-1804.

Rouet, P., Smih, F. and Jasin, M. 1994. Introduction of double-strand breaks into the genome of mouse cells by expression of a rare-cutting endonuclease. *Molecular and cellular biology* 14(12), pp. 8096-8106.

Royer-Zemmour, B. et al. 2008. Epileptic and developmental disorders of the speech cortex: ligand/receptor interaction of wild-type and mutant SRPX2 with the plasminogen activator receptor uPAR. *Human molecular genetics* 17(23), pp. 3617-3630.

Rudin, N., Sugarman, E. and Haber, J. E. 1989. Genetic and physical analysis of double-strand break repair and recombination in Saccharomyces cerevisiae. *Genetics* 122(3), pp. 519-534.

Ruppe, V. et al. 2014. Developmental brain abnormalities in tuberous sclerosis complex: a comparative tissue analysis of cortical tubers and perituberal cortex. *Epilepsia* 55(4), pp. 539-550.

Sakai, A. et al. 2017. Genome-wide target analyses of Otx2 homeoprotein in postnatal cortex. *Frontiers in neuroscience* 11, p. 307.

Sansom, S. N. et al. 2009. The level of the transcription factor Pax6 is essential for controlling the balance between neural stem cell self-renewal and neurogenesis. *PLoS genetics* 5(6), p. e1000511.

Sardiello, M. et al. 2009. A gene network regulating lysosomal biogenesis and function. *Science* 325(5939), pp. 473-477.

Sarnat, H. B. and Flores-Sarnat, L. 2015. Infantile tauopathies: Hemimegalencephaly; tuberous sclerosis complex; focal cortical dysplasia 2; ganglioglioma. *Brain and Development* 37(6), pp. 553-562.

Sattler, R. and Tymianski, M. 2000. Molecular mechanisms of calcium-dependent excitotoxicity. *Journal of molecular medicine* 78(1), pp. 3-13.

Scearce-Levie, K., Sanchez, P. E. and Lewcock, J. W. 2020. Leveraging preclinical models for the development of Alzheimer disease therapeutics. *Nature reviews Drug discovery* 19(7), pp. 447-462.

Schedl, A., Ross, A., Lee, M., Engelkamp, D., Rashbass, P., van Heyningen, V. and Hastie, N. D. 1996. Influence of PAX6 gene dosage on development: overexpression causes severe eye abnormalities. *Cell* 86(1), pp. 71-82.

Schibler, U. 2022. The daily timing of gene expression and physiology in mammals. *Dialogues in clinical neuroscience*,

Sebastián-Serrano, A., Sandonis, A., Cardozo, M., Rodríguez-Tornos, F. M., Bovolenta, P. and Nieto, M. 2012. Pαx6 expression in postmitotic neurons mediates the growth of axons in response to SFRP1. *PLoS One* 7(2), p. e31590.

Selbach, M., Schwanhäusser, B., Thierfelder, N., Fang, Z., Khanin, R. and Rajewsky, N. 2008. Widespread changes in protein synthesis induced by microRNAs. *Nature* 455(7209), pp. 58-63.

Selkoe, D. J. 2002. Alzheimer's disease is a synaptic failure. *Science* 298(5594), pp. 789-791.

Semina, E., Rubina, K., Sysoeva, V., Rysenkova, K., Klimovich, P., Plekhanova, O. and Tkachuk, V. 2016. Urokinase and urokinase receptor participate in regulation of neuronal migration, axon growth and branching. *European Journal of Cell Biology* 95(9), pp. 295-310.

Seo, M. H. and Yeo, S. 2020. Association of increase in Serping1 level with dopaminergic cell reduction in an MPTP-induced Parkinson's disease mouse model. *Brain Research Bulletin* 162, pp. 67-72.

Settembre, C. et al. 2011. TFEB links autophagy to lysosomal biogenesis. *Science* 332(6036), pp. 1429-1433.

Shankar, G. M., Bloodgood, B. L., Townsend, M., Walsh, D. M., Selkoe, D. J. and Sabatini, B. L. 2007. Natural oligomers of the Alzheimer amyloid-β protein induce reversible synapse loss by modulating an NMDA-type glutamate receptor-dependent signaling pathway. *Journal of Neuroscience* 27(11), pp. 2866-2875.

Shankar, G. M. et al. 2008. Amyloid-β protein dimers isolated directly from Alzheimer's brains impair synaptic plasticity and memory. *Nature medicine* 14(8), p. 837.

Shen, L., Nam, H. S., Song, P., Moore, H. and Anderson, S. A. 2006. FoxG1 haploinsufficiency results in impaired neurogenesis in the postnatal hippocampus and contextual memory deficits. *Hippocampus* 16(10), pp. 875-890.

Shi, L., Fatemi, S. H., Sidwell, R. W. and Patterson, P. H. 2003. Maternal influenza infection causes marked behavioral and pharmacological changes in the offspring. *Journal of Neuroscience* 23(1), pp. 297-302.

Shi, Q., Saifetiarova, J., Taylor, A. M. and Bhat, M. A. 2018. mTORC1 Activation by Loss of Tsc1 in Myelinating Glia Causes Downregulation of Quaking and Neurofascin 155 Leading to Paranodal Domain Disorganization. *Frontiers in cellular neuroscience* 12,

Shi, Y., Kirwan, P. and Livesey, F. J. 2012. Directed differentiation of human pluripotent stem cells to cerebral cortex neurons and neural networks. *Nature protocols* 7(10), p. 1836.

Shi, Y., Sun, G., Zhao, C. and Stewart, R. 2008. Neural stem cell self-renewal. *Critical reviews in oncology/hematology* 65(1), pp. 43-53.

Shi, Z.-M. et al. 2016. Upstream regulators and downstream effectors of NF-κB in Alzheimer's disease. *Journal of the neurological sciences* 366, pp. 127-134.

Shimazaki, T., Shingo, T. and Weiss, S. 2001. The ciliary neurotrophic factor/leukemia inhibitory factor/gp130 receptor complex operates in the maintenance of mammalian forebrain neural stem cells. *Journal of Neuroscience* 21(19), pp. 7642-7653.

Shrikant, P., Weber, E., Jilling, T. and Benveniste, E. N. 1995. Intercellular adhesion molecule-1 gene expression by glial cells. Differential mechanisms of inhibition by IL-10 and IL-6. *The Journal of Immunology* 155(3), pp. 1489-1501.

Siconolfi, L. B. and Seeds, N. W. 2001. Mice lacking tPA, uPA, or plasminogen genes showed delayed functional recovery after sciatic nerve crush. *Journal of Neuroscience* 21(12), pp. 4348-4355.

Şimşek, Ş., Çetin, İ., Çim, A. and Kaya, S. 2016. Elevated levels of tissue plasminogen activator and E-selectin in male children with autism spectrum disorder. *Autism Research* 9(12), pp. 1241-1247.

Sisodiya, S. M. et al. 2001. PAX6 haploinsufficiency causes cerebral malformation and olfactory dysfunction in humans. *Nature genetics* 28(3), pp. 214-216.

Skalicky, A. M. et al. 2015. The burden of subependymal giant cell astrocytomas associated with tuberous sclerosis complex: results of a patient and caregiver survey. *Journal of Child Neurology* 30(5), pp. 563-569.

Skupien, A. et al. 2014. CD44 regulates dendrite morphogenesis through Src tyrosine kinase-dependent positioning of the Golgi. *Journal of cell science* 127(23), pp. 5038-5051.

Smith, C. J. and Osborn, A. M. 2009. Advantages and limitations of quantitative PCR (Q-PCR)-based approaches in microbial ecology. *FEMS microbiology ecology* 67(1), pp. 6-20.

Sobue, K. et al. 1999. Induction of blood–brain barrier properties in immortalized bovine brain endothelial cells by astrocytic factors. *Neuroscience research* 35(2), pp. 155-164.

Sonoda, Y., Tooyama, I., Mukai, H., Maeda, K., Akiyama, H. and Kawamata, T. 2016. S6 kinase phosphorylated at T229 is involved in tau and actin pathologies in Alzheimer's disease. *Neuropathology* 36(4), pp. 325-332.

Sosunov, A. A., Wu, X., Weiner, H. L., Mikell, C. B., Goodman, R. R., Crino, P. D. and McKhann, G. M. 2008. Tuberous sclerosis: a primary pathology of astrocytes? *Epilepsia* 49, pp. 53-62.

Spooren, A., Kolmus, K., Laureys, G., Clinckers, R., De Keyser, J., Haegeman, G. and Gerlo, S. 2011. Interleukin-6, a mental cytokine. *Brain research reviews* 67(1-2), pp. 157-183.

Sretavan, D., Feng, L., Pure, E. and Reichardt, L. 1994. Embryonic neurons of the developing optic chiasm express L1 and CD44, cell surface molecules with opposing effects on retinal axon growth. *Neuron* 12(5), pp. 957-975.

St-Onge, L., Sosa-Pineda, B., Chowdhury, K., Mansouri, A. and Gruss, P. 1997. Pax6 is required for differentiation of glucagon-producing α-cells in mouse pancreas. *Nature* 387(6631), pp. 406-409.

Stemmer, K., Ellinger-Ziegelbauer, H., Ahr, H.-J. and Dietrich, D. R. 2007. Carcinogen-specific gene expression profiles in short-term treated Eker and wild-type rats indicative of pathways involved in renal tumorigenesis. *Cancer research* 67(9), pp. 4052-4068.

Stepanova, V. et al. 2017. Urokinase-type plasminogen activator (uPA) is critical for progression of tuberous sclerosis complex 2 (TSC2)-deficient tumors. *Journal of Biological Chemistry* 292(50), pp. 20528-20543.

Strojnik, T., Røsland, G. V., Sakariassen, P. O., Kavalar, R. and Lah, T. 2007. Neural stem cell markers, nestin and musashi proteins, in the progression of human glioma: correlation of nestin with prognosis of patient survival. *Surgical neurology* 68(2), pp. 133-143.

Su, L.-n., Song, X.-q., Wei, H.-p. and Yin, H.-f. 2017. Identification of neuron-related genes for cell therapy of neurological disorders by network analysis. *Journal of Zhejiang University-SCIENCE B* 18(2), pp. 172-182.

Sumi, Y., Dent, M., Owen, D., Seeley, P. and Morris, R. 1992. The expression of tissue and urokinase-type plasminogen activators in neural development suggests different modes of proteolytic involvement in neuronal growth. *Development* 116(3), pp. 625-637.

Sundberg, M. et al. 2018. Purkinje cells derived from TSC patients display hypoexcitability and synaptic deficits associated with reduced FMRP levels and reversed by rapamycin. *Molecular psychiatry* 23(11), pp. 2167-2183.

Swiech, L., Perycz, M., Malik, A. and Jaworski, J. 2008. Role of mTOR in physiology and pathology of the nervous system. *Biochimica et Biophysica Acta (BBA)-Proteins and Proteomics* 1784(1), pp. 116-132.

Tafer, H. 2018. *RNAxs Webserver*. Univie: Univie. Available at: http://rna.tbi.univie.ac.at/cgi-bin/RNAxs/RNAxs.cgi [Accessed.

Takahashi, K., Tanabe, K., Ohnuki, M., Narita, M., Ichisaka, T., Tomoda, K. and Yamanaka, S. 2007. Induction of pluripotent stem cells from adult human fibroblasts by defined factors. *Cell* 131(5), pp. 861-872.

Takahashi, S. 2011. Astroglial protective mechanisms against ROS under brain ischemia. *Rinsho shinkeigaku= Clinical neurology* 51(11), pp. 1032-1035.

Taneike, M. et al. 2016. mTOR hyperactivation by ablation of tuberous sclerosis complex 2 in the mouse heart induces cardiac dysfunction with the increased number of small mitochondria mediated through the down-regulation of autophagy. *PLoS One* 11(3), p. e0152628.

Taoufik, E. et al. 2011. Transmembrane tumour necrosis factor is neuroprotective and regulates experimental autoimmune encephalomyelitis via neuronal nuclear factor-κB. *Brain* 134(9), pp. 2722-2735.

Tarkowski, E., Blennow, K., Wallin, A. and Tarkowski, A. 1999. Intracerebral production of tumor necrosis factor-α, a local neuroprotective agent, in Alzheimer disease and vascular dementia. *Journal of clinical immunology* 19(4), pp. 223-230.

Tavazoie, S. F., Alvarez, V. A., Ridenour, D. A., Kwiatkowski, D. J. and Sabatini, B. L. 2005. Regulation of neuronal morphology and function by the tumor suppressors Tsc1 and Tsc2. *Nature neuroscience* 8(12), pp. 1727-1734.

Tee, A. R., Fingar, D. C., Manning, B. D., Kwiatkowski, D. J., Cantley, L. C. and Blenis, J. 2002. Tuberous sclerosis complex-1 and-2 gene products function together to inhibit mammalian

target of rapamycin (mTOR)-mediated downstream signaling. *Proceedings of the National Academy of Sciences* 99(21), pp. 13571-13576.

Terro, F., Esclaire, F., Yardin, C. and Hugon, J. 2000. N-methyl-D-aspartate receptor blockade enhances neuronal apoptosis induced by serum deprivation. *Neuroscience letters* 278(3), pp. 149-152.

Thal, D. R. 2012. The role of astrocytes in amyloid β-protein toxicity and clearance. *Experimental neurology* 236(1), pp. 1-5.

Thal, D. R. et al. 2010. Capillary cerebral amyloid angiopathy identifies a distinct APOE ε4-associated subtype of sporadic Alzheimer's disease. *Acta neuropathologica* 120(2), pp. 169-183.

Thien, A. et al. 2015. TSC1 activates TGF-β-Smad2/3 signaling in growth arrest and epithelial-to-mesenchymal transition. *Developmental cell* 32(5), pp. 617-630.

Torra, A. et al. 2018. Overexpression of TFEB drives a pleiotropic neurotrophic effect and prevents Parkinson's disease-related neurodegeneration. *Molecular Therapy* 26(6), pp. 1552-1567.

Townsend, M., Mehta, T. and Selkoe, D. J. 2007. Soluble Aβ inhibits specific signal transduction cascades common to the insulin receptor pathway. *Journal of Biological Chemistry*,

Trig, H., Trehu, E. and Atkins, M. 1994. Interleukin-6 as an anti-inflammatory cytokine: induction of circulating IL-1 receptor antagonist and soluble tumor necrosis factor receptor p55. *Blood* 83, pp. 113-118.

Tsirka, S. E., Gualandris, A., Amaral, D. G. and Strickland, S. 1995. Excitotoxin-induced neuronal degeneration and seizure are mediated by tissue plasminogen activator. *Nature* 377(6547), pp. 340-344.

Tucker, H. M., Kihiko-Ehmann, M. and Estus, S. 2002. Urokinase-type plasminogen activator inhibits amyloid-β neurotoxicity and fibrillogenesis via plasminogen. *Journal of neuroscience research* 70(2), pp. 249-255.

Tully, I. J. 2020. *Exploring the link between CHD2 mutations and double strand break repair in developing neurons.* Cardiff University.

Uberti, D., Cenini, G., Bonini, S., Barcikowska, M., Styczynska, M., Szybinska, A. and Memo, M. 2010. Increased CD44 gene expression in lymphocytes derived from Alzheimer disease patients. *Neurodegenerative Diseases* 7(1-3), pp. 143-147.

Ulich, T., Yin, S., Guo, K., Yi, E., Remick, D. and Del Castillo, J. 1991. Intratracheal injection of endotoxin and cytokines. II. Interleukin-6 and transforming growth factor beta inhibit acute inflammation. *The American journal of pathology* 138(5), p. 1097.

Unuma, K., Aki, T., Funakoshi, T., Hashimoto, K. and Uemura, K. 2015. Extrusion of mitochondrial contents from lipopolysaccharide-stimulated cells: Involvement of autophagy. *Autophagy* 11(9), pp. 1520-1536.

Van Eeghen, A. M. et al. 2013. Understanding relationships between autism, intelligence, and epilepsy: a cross-disorder approach. *Developmental Medicine & Child Neurology* 55(2), pp. 146-153.

Van Skike, C. E. and Galvan, V. 2018. A Perfect sTORm: The Role of the Mammalian Target of Rapamycin (mTOR) in Cerebrovascular Dysfunction of Alzheimer's Disease: A Mini-Review. *Gerontology* 64(3), pp. 205-211.

Van Slegtenhorst, M. et al. 1997. Identification of the tuberous sclerosis gene TSC1 on chromosome 9q34. *Science* 277(5327), pp. 805-808.

Veerhuis, R., Janssen, I., Hoozemans, J., De Groot, C., Hack, C. and Eikelenboom, P. 1998. Complement C1-inhibitor expression in Alzheimer's disease. *Acta neuropathologica* 96(3), pp. 287-296.

Vera, E., Bosco, N. and Studer, L. 2016. Generating late-onset human iPSC-based disease models by inducing neuronal age-related phenotypes through telomerase manipulation. *Cell reports* 17(4), pp. 1184-1192.

Verdier-Pinard, P. et al. 2009. Tubulin proteomics: towards breaking the code. *Analytical biochemistry* 384(2), p. 197.

Vereyken, E. J., Bajova, H., Chow, S., De Graan, P. N. and Gruol, D. L. 2007. Chronic interleukin-6 alters the level of synaptic proteins in hippocampus in culture and in vivo. *European Journal of Neuroscience* 25(12), pp. 3605-3616.

Verkhratsky, A. and Kirchhoff, F. 2007. Glutamate-mediated neuronal–glial transmission. *Journal of anatomy* 210(6), pp. 651-660.

Vernay, B., Koch, M., Vaccarino, F., Briscoe, J., Simeone, A., Kageyama, R. and Ang, S.-L. 2005. Otx2 regulates subtype specification and neurogenesis in the midbrain. *Journal of Neuroscience* 25(19), pp. 4856-4867.

Vezzani, A. and Viviani, B. 2015. Neuromodulatory properties of inflammatory cytokines and their impact on neuronal excitability. *Neuropharmacology* 96, pp. 70-82.

Vilchez, D. et al. 2007. Mechanism suppressing glycogen synthesis in neurons and its demise in progressive myoclonus epilepsy. *Nature neuroscience* 10(11), pp. 1407-1413.

Vogel, H., Butcher, E. and Picker, L. 1992. H-CAM expression in the human nervous system: evidence for a role in diverse glial interactions. *Journal of neurocytology* 21(5), pp. 363-373.

Volpato, V. et al. 2018. Reproducibility of molecular phenotypes after long-term differentiation to human iPSC-derived neurons: a multi-site omics study. *Stem cell reports* 11(4), pp. 897-911.

Volpato, V. and Webber, C. 2020. Addressing variability in iPSC-derived models of human disease: guidelines to promote reproducibility. *Disease models & mechanisms* 13(1), p. dmm042317.

Vukic, V. et al. 2009. Expression of inflammatory genes induced by beta-amyloid peptides in human brain endothelial cells and in Alzheimer's brain is mediated by the JNK-AP1 signaling pathway. *Neurobiology of disease* 34(1), pp. 95-106.

Walker, D. G., Lue, L.-F. and Beach, T. G. 2002. Increased expression of the urokinase plasminogen-activator receptor in amyloid β peptide-treated human brain microglia and in AD brains. *Brain research* 926(1-2), pp. 69-79.

Walsh, D. M. et al. 2002. Naturally secreted oligomers of amyloid β protein potently inhibit hippocampal long-term potentiation in vivo. *Nature* 416(6880), p. 535.

Waltereit, R., Welzl, H., Dichgans, J., Lipp, H. P., Schmidt, W. J. and Weller, M. 2006. Enhanced episodic-like memory and kindling epilepsy in a rat model of tuberous sclerosis. *Journal of neurochemistry* 96(2), pp. 407-413.

Wang, D. D. and Bordey, A. 2008. The astrocyte odyssey. *Progress in neurobiology* 86(4), pp. 342-367.

Wang, J. et al. 2021a. Interleukin-6 mediates PSAT1 expression and serine metabolism in TSC2-deficient cells. *Proceedings of the National Academy of Sciences* 118(39), p. e2101268118.

Wang, J. et al. 2022. FOXG1 as a Potential Therapeutic Target for Alzheimer's Disease with a Particular Focus on Cell Cycle Regulation. *Journal of Alzheimer's Disease* (Preprint), pp. 1-19.

Wang, L., Jin, G., Yu, H., Li, Q. and Yang, H. 2019a. Protective effect of Tenuifolin against Alzheimer's disease. *Neuroscience letters* 705, pp. 195-201.

Wang, L., Wang, J., Jin, T., Zhou, Y. and Chen, Q. 2018. FoxG1 facilitates proliferation and inhibits differentiation by downregulating FoxO/Smad signaling in glioblastoma. *Biochemical and biophysical research communications* 504(1), pp. 46-53.

Wang, Q. et al. 2019b. The CRISPR-cas13a gene-editing system induces collateral cleavage of RNA in glioma cells. *Advanced Science* 6(20), p. 1901299.

Wang, T., Lu, H., Li, D. and Huang, W. 2021b. Tgf-β1-mediated activation of serpine1 is involved in hemin-induced apoptotic and inflammatory injury in ht22 cells. *Neuropsychiatric Disease and Treatment* 17, p. 423.

Wang, W.-Y., Tan, M.-S., Yu, J.-T. and Tan, L. 2015. Role of pro-inflammatory cytokines released from microglia in Alzheimer's disease. *Annals of translational medicine* 3(10),

Watanabe, K. et al. 2007. A ROCK inhibitor permits survival of dissociated human embryonic stem cells. *Nature biotechnology* 25(6), p. 681.

Weichhart, T. et al. 2008. The TSC-mTOR signaling pathway regulates the innate inflammatory response. *Immunity* 29(4), pp. 565-577.

Weingarten, M. D., Lockwood, A. H., Hwo, S.-Y. and Kirschner, M. W. 1975. A protein factor essential for microtubule assembly. *Proceedings of the National Academy of Sciences* 72(5), pp. 1858-1862.

Wey, A., Cerdeno, V. M., Pleasure, D. and Knoepfler, P. S. 2010. c-and N-myc regulate neural precursor cell fate, cell cycle, and metabolism to direct cerebellar development. *The Cerebellum* 9(4), pp. 537-547.

White, R., Hua, Y., Scheithauer, B., Lynch, D. R., Petri Henske, E. and Crino, P. B. 2001. Selective alterations in glutamate and GABA receptor subunit mRNA expression in dysplastic neurons and giant cells of cortical tubers. *Annals of Neurology: Official Journal of the American Neurological Association and the Child Neurology Society* 49(1), pp. 67-78.

Williams, M. A., McKay, G. J., Carson, R., Craig, D., Silvestri, G. and Passmore, P. 2015. Age-Related Macular Degeneration–Associated Genes in Alzheimer Disease. *The American Journal of Geriatric Psychiatry* 23(12), pp. 1290-1296.

Wlodarczyk, J., Mukhina, I., Kaczmarek, L. and Dityatev, A. 2011. Extracellular matrix molecules, their receptors, and secreted proteases in synaptic plasticity. *Developmental neurobiology* 71(11), pp. 1040-1053.

Wolf, H. 2007. *Structural Neuroimaging Studies in Subjects with Mild Cognitive Impairment.*

Wolfe, D. M., Lee, J. h., Kumar, A., Lee, S., Orenstein, S. J. and Nixon, R. A. 2013. Autophagy failure in A lzheimer's disease and the role of defective lysosomal acidification. *European Journal of Neuroscience* 37(12), pp. 1949-1961.

Wong, M. and Crino, P. B. 2012. Tuberous sclerosis and epilepsy: role of astrocytes. *Glia* 60(8), pp. 1244-1250.

Wong, M. et al. 2003. Impaired glial glutamate transport in a mouse tuberous sclerosis epilepsy model. *Annals of neurology* 54(2), pp. 251-256.

Wong, P.-M., Puente, C., Ganley, I. G. and Jiang, X. 2013. The ULK1 complex: sensing nutrient signals for autophagy activation. *Autophagy* 9(2), pp. 124-137.

Wright, J. W. and Harding, J. W. 2015. The brain hepatocyte growth Factor/c-Met receptor system: A new target for the treatment of Alzheimer's disease. *Journal of Alzheimer's Disease* 45(4), pp. 985-1000.

Wu, F. et al. 2014. Urokinase-type plasminogen activator promotes dendritic spine recovery and improves neurological outcome following ischemic stroke. *Journal of Neuroscience* 34(43), pp. 14219-14232.

Wu, F. et al. 2013. Tissue-type plasminogen activator protects neurons from excitotoxin-induced cell death via activation of the ERK 1/2–CREB–ATF3 signaling pathway. *Molecular and Cellular Neuroscience* 52, pp. 9-19.

Wu, F. et al. 2012. Tissue-type plasminogen activator regulates the neuronal uptake of glucose in the ischemic brain. *Journal of Neuroscience* 32(29), pp. 9848-9858.

Wu, X., Sosunov, A. A., Tikoo, R., Weiner, H. L., Crino, P. D. and Mckhann, G. M. 2005. Glutamate Transport Is Impaired In The Human Tuberous Sclerosis Tissue: 3.016. *Epilepsia* 46, p. 279.

Wyss-Coray, T. et al. 2003. Adult mouse astrocytes degrade amyloid-β in vitro and in situ. *Nature medicine* 9(4), pp. 453-457.

Xing, Z., Gauldie, J., Cox, G., Baumann, H., Jordana, M., Lei, X.-F. and Achong, M. K. 1998. IL-6 is an antiinflammatory cytokine required for controlling local or systemic acute inflammatory responses. *The Journal of clinical investigation* 101(2), pp. 311-320.

Xu, Y. et al. 2021. TFEB regulates lysosomal exocytosis of tau and its loss of function exacerbates tau pathology and spreading. *Molecular psychiatry* 26(10), pp. 5925-5939.

Xue, X.-j. and Yuan, X.-b. 2010. Nestin is essential for mitogen-stimulated proliferation of neural progenitor cells. *Molecular and Cellular Neuroscience* 45(1), pp. 26-36.

Yamada, T., Kawamata, T., Walker, D. and McGeer, P. 1992. Vimentin immunoreactivity in normal and pathological human brain tissue. *Acta neuropathologica* 84(2), pp. 157-162.

Yamada, T., Tsubouchi, H., Daikuhara, Y., Prat, M., Comoglio, P., McGeer, P. and McGeer, E. 1994. Immunohistochemistry with antibodies to hepatocyte growth factor and its receptor protein (c-MET) in human brain tissues. *Brain research* 637(1-2), pp. 308-312.

Yamaguchi, F., Tsuchiya, M., Shimamoto, S., Fujimoto, T., Tokumitsu, H., Tokuda, M. and Kobayashi, R. 2016. Oxidative stress impairs the stimulatory effect of S100 proteins on protein phosphatase 5 activity. *The Tohoku journal of experimental medicine* 240(1), pp. 67-78.

Yang, F., Yang, L., Wataya-Kaneda, M., Yoshimura, T., Tanemura, A. and Katayama, I. 2018. Uncoupling of ER/Mitochondrial oxidative stress in mTORC1 hyperactivation-associated skin hypopigmentation. *Journal of Investigative Dermatology* 138(3), pp. 669-678.

Yasojima, K., Schwab, C., McGeer, E. G. and McGeer, P. L. 1999. Up-regulated production and activation of the complement system in Alzheimer's disease brain. *The American journal of pathology* 154(3), pp. 927-936.

Yates, S. C. et al. 2013. Dysfunction of the mTOR pathway is a risk factor for Alzheimer's disease. *Acta neuropathologica communications* 1(1), p. 3.

Yoshimura, T., Arimura, N., Kawano, Y., Kawabata, S., Wang, S. and Kaibuchi, K. 2006. Ras regulates neuronal polarity via the PI3-kinase/Akt/GSK-3β/CRMP-2 pathway. *Biochemical and biophysical research communications* 340(1), pp. 62-68.

Yoshimura, T., Kawano, Y., Arimura, N., Kawabata, S., Kikuchi, A. and Kaibuchi, K. 2005. GSK-3β regulates phosphorylation of CRMP-2 and neuronal polarity. *Cell* 120(1), pp. 137-149.

Yoshiyama, Y. et al. 2007. Synapse loss and microglial activation precede tangles in a P301S tauopathy mouse model. *Neuron* 53(3), pp. 337-351.

Yuizumi, N. et al. 2021. Maintenance of neural stem-progenitor cells by the lysosomal biosynthesis regulators TFEB and TFE3 in the embryonic mouse telencephalon. *Stem Cells* 39(7), pp. 929-944.

Zeng, L.-H., Bero, A. W., Zhang, B., Holtzman, D. M. and Wong, M. 2010. Modulation of astrocyte glutamate transporters decreases seizures in a mouse model of Tuberous Sclerosis Complex. *Neurobiology of disease* 37(3), pp. 764-771.

Zeng, L.-H. et al. 2007. Abnormal glutamate homeostasis and impaired synaptic plasticity and learning in a mouse model of tuberous sclerosis complex. *Neurobiology of disease* 28(2), pp. 184-196.

Zeng, L. H., Xu, L., Gutmann, D. H. and Wong, M. 2008. Rapamycin prevents epilepsy in a mouse model of tuberous sclerosis complex. *Annals of Neurology: Official Journal of the American Neurological Association and the Child Neurology Society* 63(4), pp. 444-453.

Zhang, C. et al. 2010. Amyloid-β production via cleavage of amyloid-β protein precursor is modulated by cell density. *Journal of Alzheimer's Disease* 22(2), pp. 683-694.

Zhang, H. H., Lipovsky, A. I., Dibble, C. C., Sahin, M. and Manning, B. D. 2006. S6K1 regulates GSK3 under conditions of mTOR-dependent feedback inhibition of Akt. *Molecular cell* 24(2), pp. 185-197.

Zhang, L., Feliciano, D. M., Huang, T., Zhang, S. and Bordey, A. 2016. Hypoxia-inducible factor-1a contributes to dendritic overgrowth in tuberous sclerosis. *Neuroscience letters* 612, pp. 43-47.

Zhang, P.-L., Levy, A. M., Ben-Simchon, L., Haggiag, S., Chebath, J. and Revel, M. 2007. Induction of neuronal and myelin-related gene expression by IL-6-receptor/IL-6: a study on embryonic dorsal root ganglia cells and isolated Schwann cells. *Experimental neurology* 208(2), pp. 285-296.

Zhang, Y., Gao, X., Saucedo, L. J., Ru, B., Edgar, B. A. and Pan, D. 2003. Rheb is a direct target of the tuberous sclerosis tumour suppressor proteins. *Nature cell biology* 5(6), p. 578.

Zhou, F.-Q. and Snider, W. D. 2005. GSK-3β and microtubule assembly in axons. *Science* 308(5719), pp. 211-214.

Zhou, Z., Peng, X., Insolera, R., Fink, D. J. and Mata, M. 2009. Interleukin-10 provides direct trophic support to neurons. *Journal of neurochemistry* 110(5), pp. 1617-1627.

Zhu, Y., Hilal, S., Chai, Y. L., Ikram, M. K., Venketasubramanian, N., Chen, C. P. and Lai, M. K. 2018. Serum hepatocyte growth factor is associated with small vessel disease in Alzheimer's dementia. *Frontiers in aging neuroscience* 10, p. 8.

Zhu, Z. and Huangfu, D. 2013. Human pluripotent stem cells: an emerging model in developmental biology. *Development* 140(4), pp. 705-717.

Zlokovic, B. V. 2008. The blood-brain barrier in health and chronic neurodegenerative disorders. *Neuron* 57(2), pp. 178-201.

Zois, C. E., Favaro, E. and Harris, A. L. 2014. Glycogen metabolism in cancer. *Biochemical pharmacology* 92(1), pp. 3-11.

Zucco, A. J., Dal Pozzo, V., Afinogenova, A., Hart, R. P., Devinsky, O. and D'Arcangelo, G. 2018. Neural progenitors derived from tuberous sclerosis complex patients exhibit attenuated PI3K/AKT signaling and delayed neuronal differentiation. *Molecular and Cellular Neuroscience* 92, pp. 149-163.

Zuckerman, L., Rehavi, M., Nachman, R. and Weiner, I. 2003. Immune activation during pregnancy in rats leads to a postpubertal emergence of disrupted latent inhibition, dopaminergic hyperfunction, and altered limbic morphology in the offspring: a novel neurodevelopmental model of schizophrenia. *Neuropsychopharmacology* 28(10), pp. 1778-1789.